GEORGIA INSTITUTE OF TECHNOLOGY
OFFICE OF CONTRACT ADMINISTRATION
SPONSORED PROJECT INITIATION

No action as of 8/1

Date: May 10, 1979

Project Title: Locating Voids Beneath Pavement Using Pulsed Electromagnetic Wave Techniques

Project No: A-2357

Project Director: Mr. John R. Moore Dr William J Stevenson

Sponsor: National Academy of Sciences; Washington, D. C. 20418

Agreement Period: From 4/2/79 Until ~~7/1/80~~ 5/1/81

Type Agreement: Contract No. HR 10-14(under National Cooperative Highway Research Program)

Amount: $99,850.00

Reports Required: Working Plan; Monthly Progress Schedule; Quarterly Progress Report; Publication Manuscripts/Reprints; Final Report

Sponsor Contact Person (s):

Technical Matters (Program Officer)
Mr. Harry A. Smith
NCHRP Projects Engineer
Transportation Research Board
National Academy of Sciences
2101 Constitution Ave., NW
Washington, D.C. 20418
Phone: (202)389-6741

Contractual Matters
(thru OCA)
Mr. Ronald R. Wiley
Contract Specialist
National Academy of Sciences
2101 Constitution Ave., NW
Washington, D. C. 20418
Phone: (202)389-6908

Defense Priority Rating: None

Assigned to: Radar Instrumentation Laboratory (School/Laboratory)

COPIES TO:

- Project Director
- Division Chief (EES)
- School/Laboratory Director
- Dean/Director—EES
- Accounting Office
- Procurement Office
- Security Coordinator (OCA) ✓
- Reports Coordinator (OCA)
- Library, Technical Reports Section
- EES Information Office
- EES Reports & Procedures
- Project File (OCA)
- Project Code (GTRI)
- Other

CA-3 (3/76)

GEORGIA INSTITUTE OF TECHNOLOGY
OFFICE OF CONTRACT ADMINISTRATION

SPONSORED PROJECT TERMINATION

Date: 7/24/81

Project Title: Locating Voids Beneath Pavement Using Pulsed Electromagnetic Wave Techniques

Project No: A-2357

Project Director: Dr. W. J. Steinway

Sponsor: National Academy of Science

Effective Termination Date: 5/1/81

Clearance of Accounting Charges: 5/1/81

Grant/Contract Closeout Actions Remaining:

- x Final Invoice and Closing Documents
- _ Final Fiscal Report
- x Final Report of Inventions
- x Govt. Property Inventory & Related Certificate
- _ Classified Material Certificate
- x Other Subcontract closeout

NOTE: Final voucher should show total costs less costs in excess of contract.

Assigned to: RAIL/RAD (School/Laboratory)

COPIES TO:

Administrative Coordinator
Research Property Management
Accounting Office
Procurement Office/EES Supply Services
Research Security Services
Reports Coordinator (OCA)
Suspense

Legal Services (OCA)
Library, Technical Reports
EES Research Public Relations (2)
Project File (OCA)
Other: _____

A-2357

INITIAL WORKING PLAN

Locating Voids Beneath Pavement Using Pulsed Electromagnetic Wave Techniques

J. R. Moore

May 1979

CONTRACT NO. NCHRP 10-14

Prepared for

Transportation Research Board
Washington, DC

Prepared by

Georgia Institute of Technology
Engineering Experiment Station
Atlanta, Georgia 30332

TABLE OF CONTENTS

Section	Title	Page
I.	Equipment Selection and Preparation	1
II.	Test Site Preparation	1
III.	Data Collection	6
IV.	Data Analysis Procedures	6
	a. Data Reduction	6
	b. Mathematical Model	8
	c. Selecting of Processing Algorithms	8
V.	Experimental Evaluation	8
	a. Performance Comparison	12
	b. Hardware Requirements	12

LIST OF FIGURES

Figure	Title	Page
1A.	Test Lane - Base - Top View	3
1B.	Test Lane - Base - Void Layout Nomenclature	3
2.	Void Layout Specifications	4
3A.	Slab - Top View	5
3B.	Slab - Side View	5
4.	Data Analysis and Experimental Evaluation Procedures	7
5.	Processing of Radar Data to Provide Temporal and Spectral Information	9
6.	Concrete Slab Environment Model	10
7A.	Multiple Reflections Between Concrete Slab Faces	11
7B.	Multiple Reflections Between Void Faces	11
8.	Ideal Processor Output for ½ Inch Voids Under Concrete Block With 24 Measurements Per Block	13

WORKING PLAN

I. Equipment Selection and Preparation

The experimental vehicular-mounted short-pulse radar system supplied by the U.S. Army primarily comprises three short-pulse receiver/transmitters, three wideband antennas, a storage and monitor oscilloscope mounted on a General Electric tractor (Model E-15). It has been designed as an experimental device to gather data on subsurface target characteristics. The unit will undergo a mechanical configuration modification to optimize its use with the proposed test site. The modification will require approximately 2 man-weeks.

The radar operates at a pulse repetition frequency (PRF) of five (5) MHz. To avoid mutual interference the output of the transmitter pulses are staggered so that each radar operates at a different time interval. This staggering is accomplished by shifting the phase of the 5 MHz signal to provide 0, 120^{0}, and 240^{0} outputs. A fourth 5 MHz output is provided which is again divided in frequency by a factor of 500 and used for synchronization of the range gates and staircase sweep generator. The phase shifted 5 MHz signals are sent to the receiver/transmitter modules where they are amplified and routed to the short pulse transmitter in which an approximately one nanosecond pulse is formed for transmission through the sampler unit and antenna.

Synchronization of the radar is provided by taking the 5 MHz signal and dividing down by a factor of 500 to produce a 10 kHz clock signal. This clock signal is used to step a staircase sweep generator which moves the sampling probe progressively in time. The received signal is sampled 50,000 times for each 10 ms sweep. By using the sampling receiver technique, a real-time waveform of approximately 1.0 nanosecond duration is displayed on the monitor scope in approximately 1.0 millisecond.

II. Test Site Preparation

From our experience with our previous programs, it was strongly felt that the measurements needed to be made under carefully controlled conditions which simulate the actual highway environment so that void size

estimates could be correlated with the physical measurement of the void. Also, the environmental parameters, void size and void thickness need to be variables in the correlation of the radar signal and actual void conditions. In order to achieve these conditions, a carefully constructed test site is needed. First, all construction must conform to standard road building techniques. This involves primarily the base thickness and composition, and the slab composition. Second, provisions must be made to vary the slab thickness, reinforcing, void size and thickness and base moisture levels. The proposed test site is illustrated in Figures 1, 2 and 3. The base is 12 feet wide by 76 feet long. It is a graded aggragate base conforming to section 815 of the Department of Transportation State of Georgia (DOT/SOG) Standard Specifications for Construction of Roads and Bridges, 1977 Edition. Pressed into its surface are voids of various sizes and depths per Figure 2. The top of Figure 1 is an overhead view of the base. Figure 2 shows the depths and relative locations of the voids for type A, B and type C locations. The void layout nomenclature on Figure 1 is summarized by the following examples.

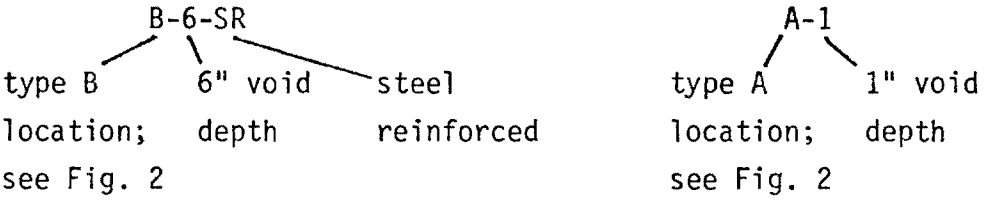

The base will be subcontracted to a local paving contractor. The cost of the 12' wide, 76' long base is anticipated at $3.8K. Time required to build the base is several weeks, which includes site grading and compacting. The concrete slab will also be subcontracted in conformity with section 430.05 of the DOT Standard Specifications in order to fully simulate actual road conditions. The anticipated cost of the slab production is $5.2K.

Half of the slab will be formed with steel reinforcing per DOT Standard Specifications for steel reinforced highway slabs to determine the extent of the interference caused by a conducting medium being present. Also, per Figure 3, doweled joints are simulated at one end of the slab.

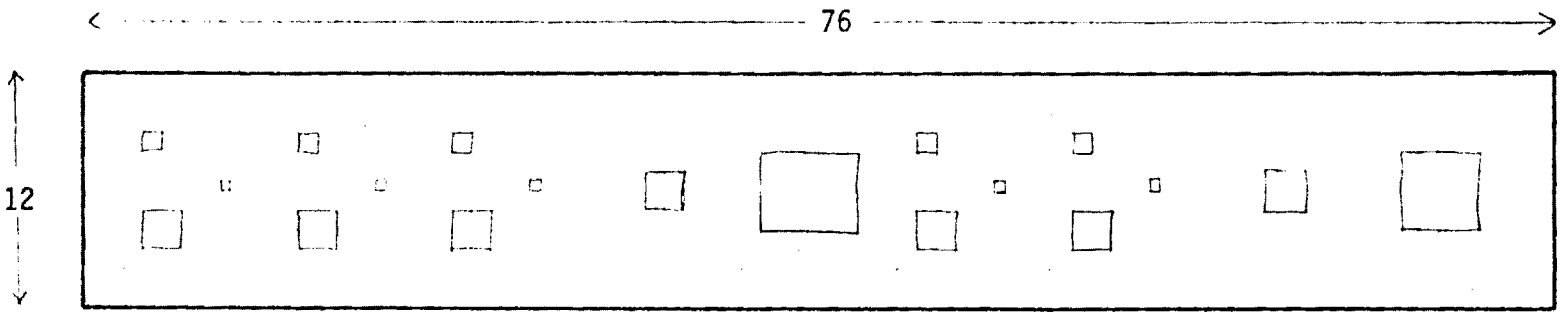

1A. Test Lane - Base - Top View

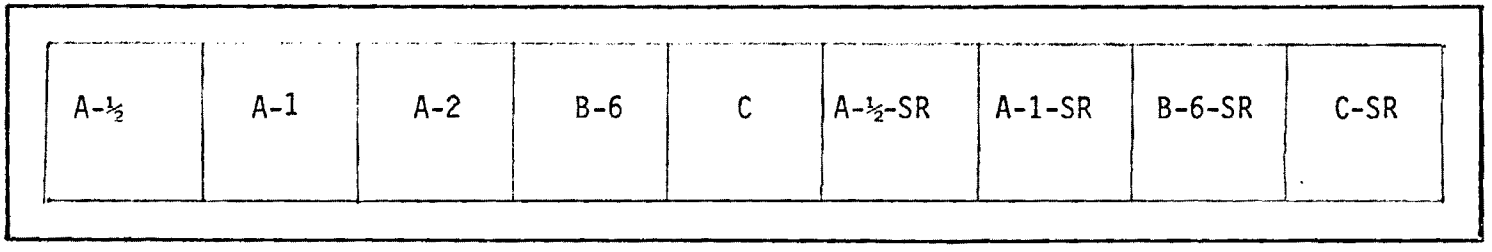

1B. Test Lane - Base - Void Layout Nomenclature

Note: All Dimensions in Feet, Scale is 1 Block Per Foot

Figure 1

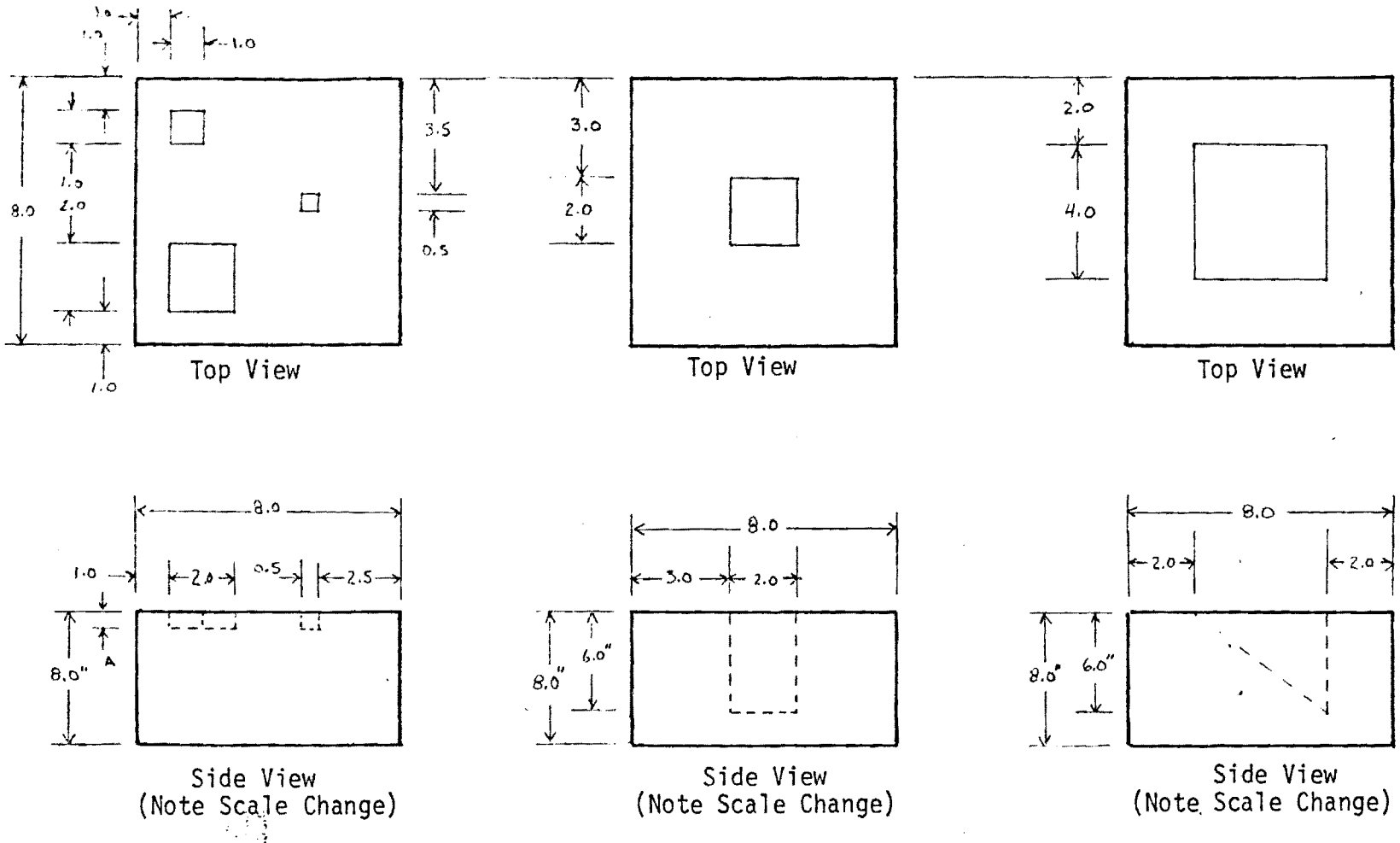

Note A: This Dimension is Specified by Dash Number

All Dimensions Are in Feet Except as Noted

Void Layout Specifications

Figure 2

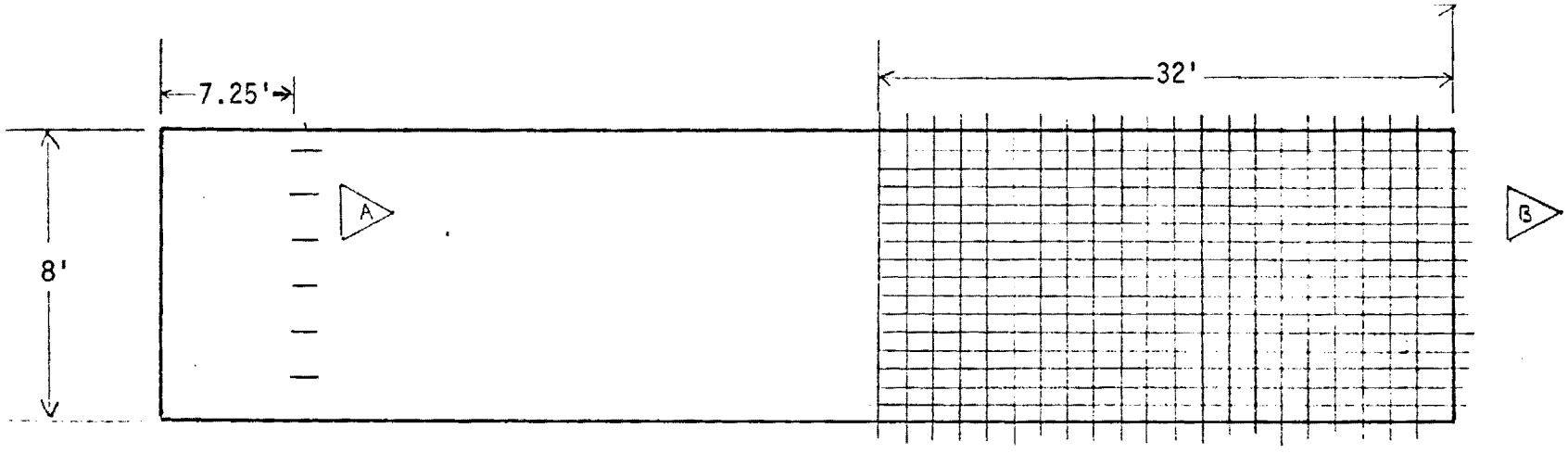

3A. Slab - Top View

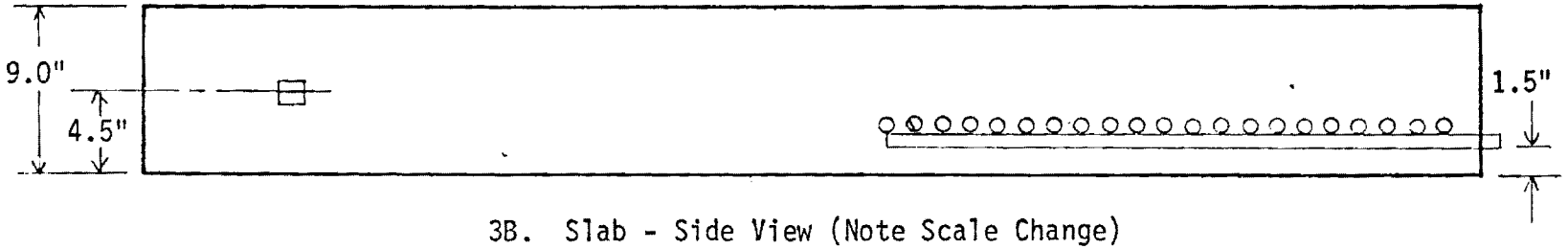

3B. Slab - Side View (Note Scale Change)

Figure 3

Notes:

A Dowel Bars 18" Long, 15" on Centers, 1.25" Dia. Height 4.5"

B Re-Bars Transverse: 5/8" Dia., 1'7" on Centers

Longitudinal: 7/8" Dia., 8" on Centers, Height 1.5"

All Dimensions in Feet Except as Noted

III. Data Collection

The data collection will consist of 2431 data points taken symmetrically on the slab using a 17 line x 143 line grid with the lines spaced 6 inches apart. This data will be recorded on magnetic tape for processing with the Cyber 74 university computer. The resulting matrix of data points will provide a "map" of the entire slab which will be compared to the known void locations and depths. In addition to the matrix described above, additional measurements are planned in a laboratory environment consisting of a mini-base and smaller concrete slabs. Some of the parameters to be varied under these conditions are: 1) concrete thickness, 2) base moisture, 3) base types, 4) water in voids, 5) irregular shaped voids. These measurements will be made as time, money and man-power permit. The effect of these variables on the "main test lane" data will be discussed in the final report.

The collection of the data will require approximately six months after the completion of the test site (see proposed time schedule).

IV. Data Analysis Procedures

The data analysis procedures will involve three subtasks. First, the measured data will be reduced to a form and format that is useable for analysis. Second, a mathematical model will be developed to allow an understanding of the environmental parameters of importance and the sensitivity of the radar data to these parameters. Third, candidate processing algorithms will be selected to process the collected data to provide identification of the location, size and shape of voids underneath pavements. The data analysis procedure that is planned is illustrated by the flow diagram in Figure 4.

a. Data Reduction

One of the objectives of the void measurement program is to develop algorithms to automatically process radar data in order to detect and measure voids under concrete highways. However, before selecting and testing candidate detection and measurement schemes, it is necessary to visually observe and compare the temporal and spectral responses for the various size

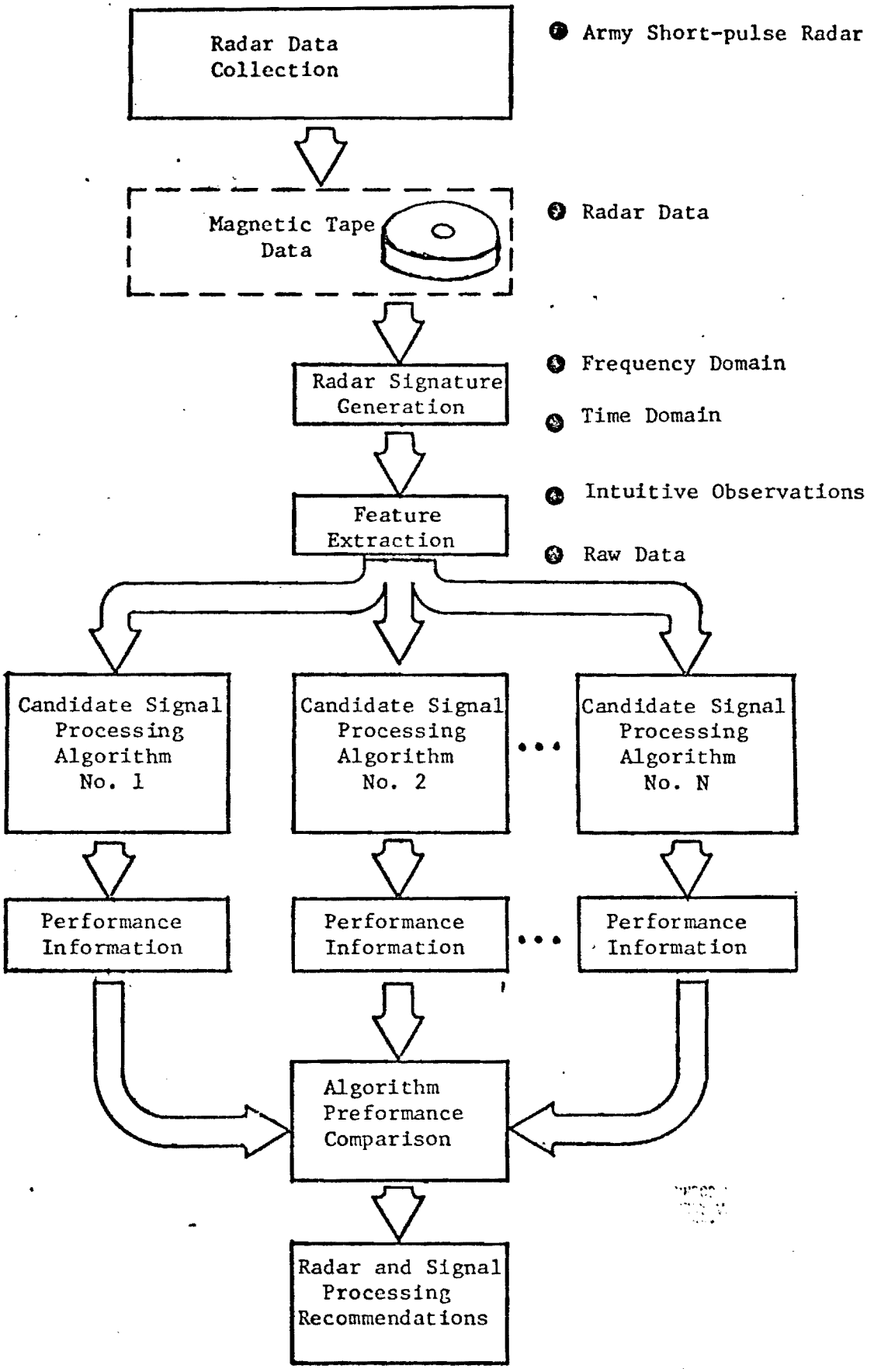

Figure 4. Data Analysis and Experimental Evaluation Procedures.

and shape voids sensed with the radar measurement system. To provide plots of the time and frequency responses, some of the data will be processed off-line with Georgia Tech's CYBER 74 computer as indicated in Figure 5. This figure shows the processing necessary to generate temporal and spectral plots of the short-pulse radar data.

As indicated in Figure 4, the spectral and temporal plots of the collected data will be studied to determine what radar signal return characteristics can be exploited to determine void size, shape and location. Some of the algorithms selected will be designed to respond to only those signal characteristics that appear exploitable. Other algorithms may be designed to use all of the raw data collected.

b. Mathematical Model

To assist in the design of the signal processing algorithms, the concrete slab, the road base, and environment will be mathematically modeled to determine how variations in the environmental parameters (i.e., void size, void fill, road base moisture, concrete moisture) effects the radar measurements (see Figure 6). A rudimentary model was developed under the Georgia State DOT research study. However, it needs to be refined to be more realistic. One of the effects that must be considered is multiple reflections a) between the concrete slab faces as shown in Figure 7(a), b) between the void faces as illustrated in Figure 7(b). The effect of these multiple reflections on the returning radar signal should be analyzed in order to properly interpret the measured data.

c. Selecting of Processing Algorithms

The spectral and temporal plots of the collected data along with the information obtained from the mathematical model will be scrutinized to determine what processing algorithms to consider. Several candidate algorithms will be selected.

V. Experimental Evaluation

Each processing algorithm selected will be implemented in software on the CYBER 74 general purpose computer. The collected data will be subjected to the selected algorithms and their performance will be compared. The best signal processing algorithm will be selected and the

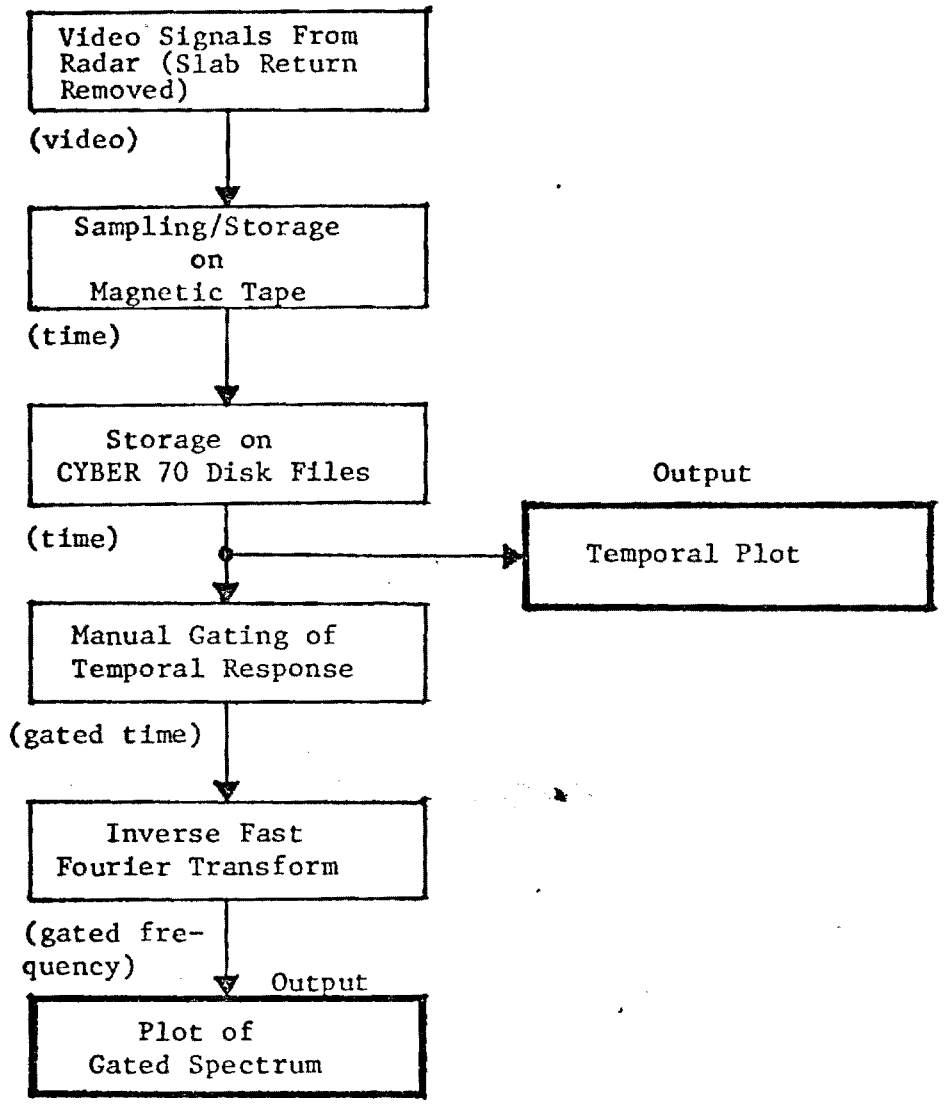

Figure 5. Processing of Radar Data to Provide Temporal and Spectral Information

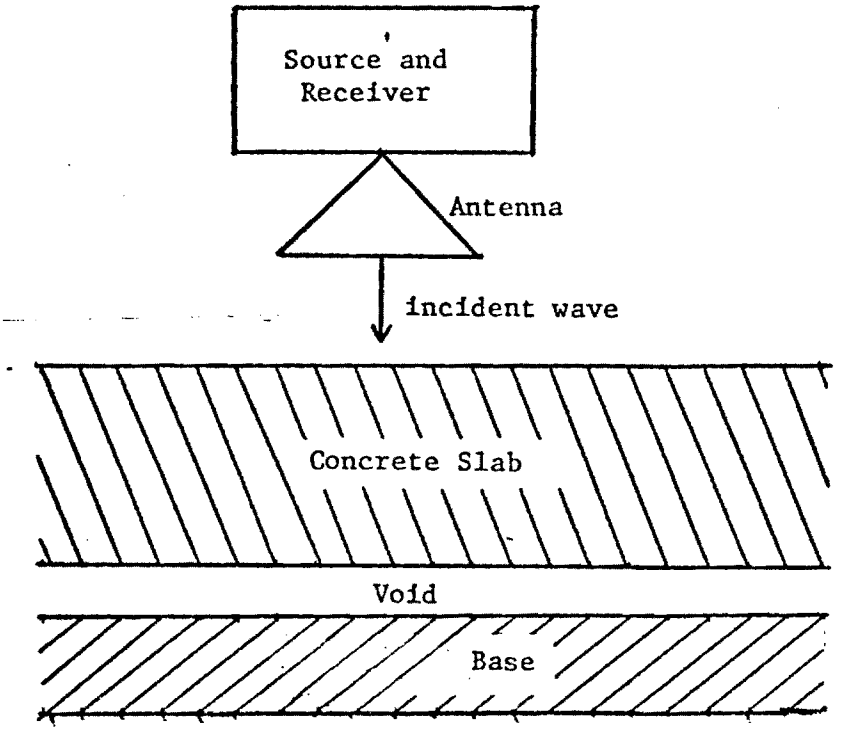

Figure 6. Concrete Slab Environment Model

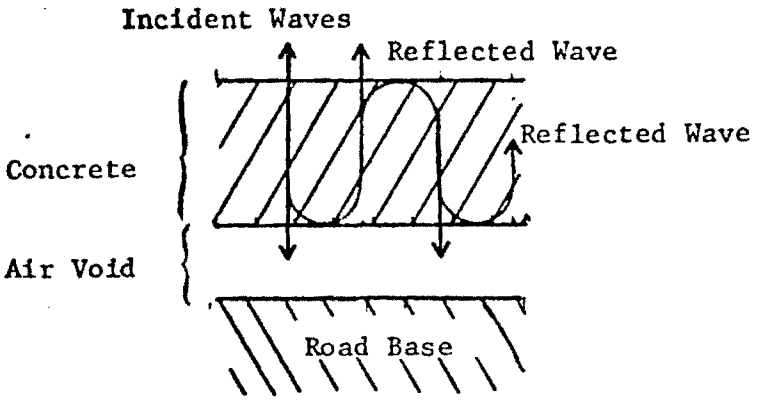

7A. Multiple Reflections Between Concrete Slab Faces.

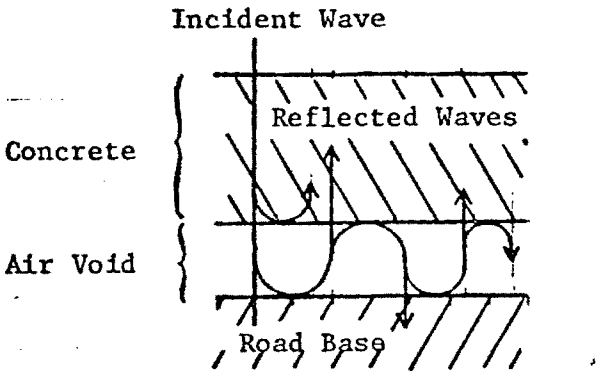

7B. Multiple Reflections Between Void Faces.

Figure 7

requirements for implementing that processor will be determined. In addition, the corresponding radar system requirements will be determined and recommended as indicated in Figure 4.

a. Performance Comparison

Figure 8 indicates one possible processor output. If only two rows of measurements are made across one of the test blocks in six inch steps as illustrated in Figure 8, then the processor would determine the void depth at each measurement position. The computer would plot the actual position of the voids below the test block and also superimpose on this plot the void depths obtained from the corresponding radar measurements. Figure 8 shows the computer plot obtained for a processor making 100% accurate void size estimates.

Each candidate processor algorithm will yield a different quality void size estimation. The algorithm performance will be compared by taking the difference between the estimate void size and the actual void size. The square of all of these differences will be summed over one test area to yield a measure of algorithm performance.

b. Hardware Requirements

After selecting the best processing algorithm, the implementation required to provide a viable void measurements system will be determined. Such a system might involve taking measurements with a short-pulse radar and recording them on magnetic tape in the field. The magnetic tape would then be taken to a central computing facility for processing. On the other hand, perhaps a "real-time" processor physically attached to the measurement radar would be feasible and advantageous. Locations of voids could be determined at the place of field measurement in almost real-time. The requirements for such a "real-time" processor will be developed.

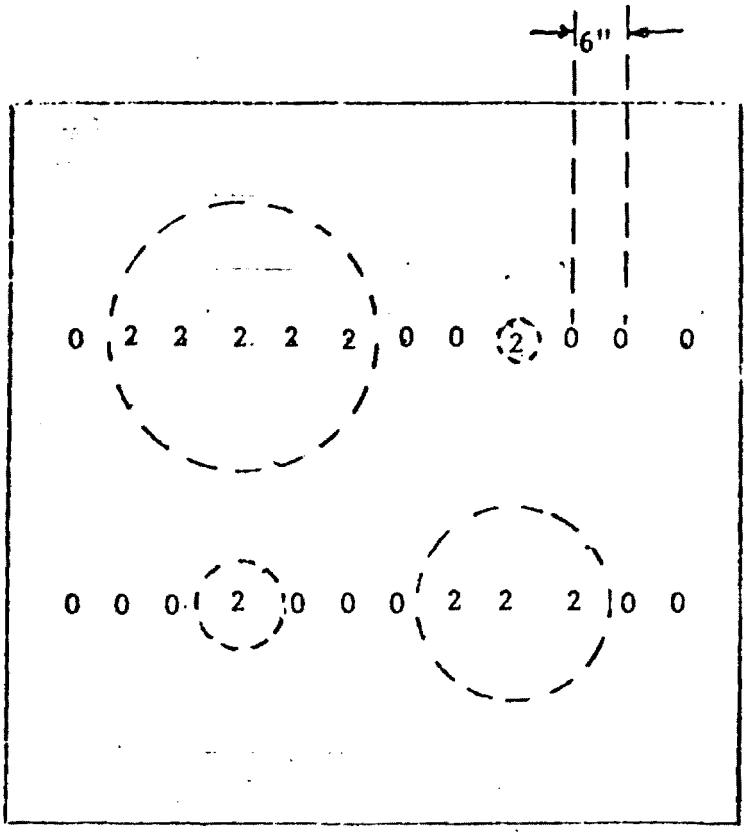

Code	Depth (inches)
0	0
1	1/4
2	2/4
3	3/4

Figure 8. Ideal Processor Output for ½ Inch Voids Under Concrete Block With 24 Measurements Per Block

NATIONAL COOPERATIVE HIGHWAY RESEARCH PROGRAM
TRANSPORTATION RESEARCH BOARD
NATIONAL RESEARCH COUNCIL

PROGRESS SCHEDULE

Project No. 10-14 Locating Voids Beneath Pavement Fy' 79 Month _____
h Agency Ga Tech - EES/RAIL
l Investigator John R. Moore - James D. Echard

RCH S	Research Task	1979 A	M	J	J	A	S	O	N	D	1980 J	F	M	A	M	J	ESTIMATED COMPLETION
	Equipment Select & Prep.	50	100														
	Test Track - Base Constr.		20	100													
	Test Track - Slab Constr.				50	100											
	Data Collection					20	40	60	80	100							
	Data Reduction						25	50	75	100							
	Develop Math Model						30	60	100								
	Algorithm Selection							25	50	75	100						
	Experimental Evaluation								25	50	75	100					
	Final Report											40	75			100	
L % TION		8	22	31	33	36	46	59	70	81	89	92	97	97	97	100	

FIG. A—OVERALL PROJECT SCHEDULE

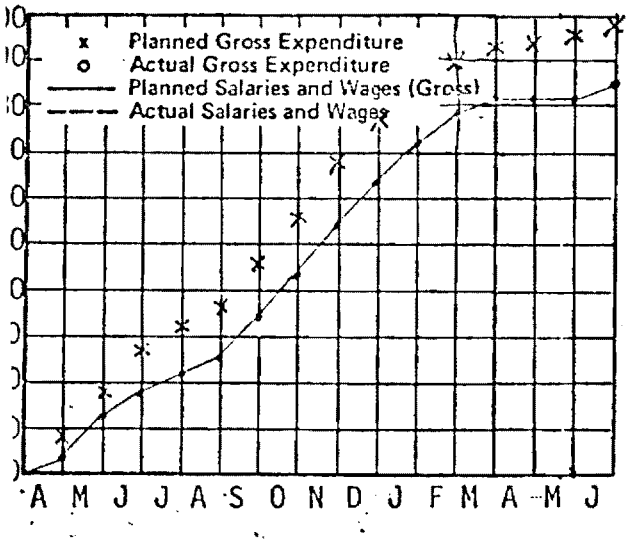

Months

FIG. B—CONTRACT FUNDS

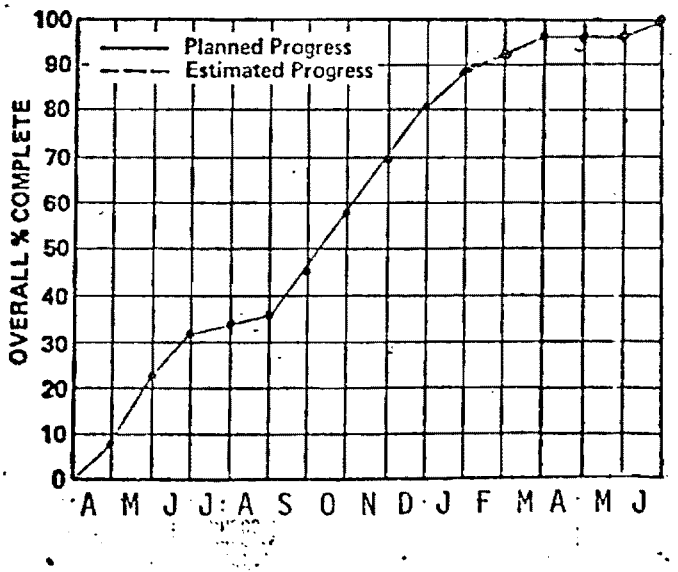

Months

FIG. C—CONTRACT PERIOD

Funds Expended %_____
Contract Amount $ 100,000
Expended this Month $_____
Total Exp. To Date $_____
Balance $_____

Time Expended %_____
Starting Date April 2, 1979
Completion Date June 30, 1980

Salaries and Wages Estimated This Month $_____
Salaries and Wages Spent This Month $_____

A-2357

QUARTERLY PROGRESS REPORT

to the

NATIONAL COOPERATIVE HIGHWAY RESEARCH PROGRAM

on Project

10 - 14

LOCATING VOIDS BENEATH PAVEMENT

for period

APRIL 1979 to JUNE 1979

from

GEORGIA INSTITUTE OF TECHNOLOGY - EES/RAIL

NATIONAL COOPERATIVE HIGHWAY RESEARCH PROGRAM
TRANSPORTATION RESEARCH BOARD
NATIONAL RESEARCH COUNCIL

PROGRESS SCHEDULE

Project No. 10-14 Locating Voids Beneath Pavement Fy' 79 Month June
h Agency Ga Tech - EES/RAIL
l Investigator John R. Moore

RCH S	Research Task	1979 A	M	J	J	A	S	O	N	D	1980 J	F	M	A	M	J	ESTIMATED % COMPLETION
	Equipment Select & Prep.	50	100														80
	Test Track - Base Constr.		20	100													15
	Test Track - Slab Constr.				50	100											
	Data Collection					20	40	60	80	100							
	Data Reduction						25	50	75	100							
	Develop Math Model						30	60	100								
	Algorithm Selection							25	50	75	100						
	Experimental Evaluation								25	50	75	100					
	Final Report											40	75			100	
L % TION		8	22	31	33	36	46	59	70	81	89	92	97	97	97	100	20

FIG. A–OVERALL PROJECT SCHEDULE

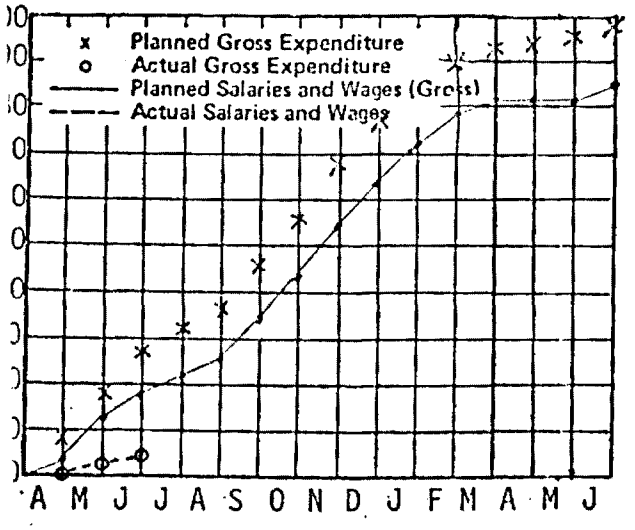

Months

FIG. B–CONTRACT FUNDS

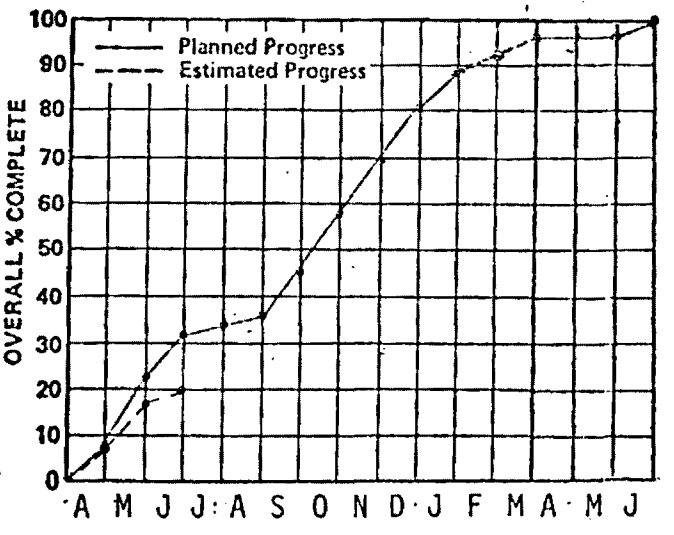

Months

FIG. C–CONTRACT PERIOD

Funds Expended	%	3,800
Contract Amount	$	100,000
Expended this Month	$	2,000
Total Exp. To Date	$	3,800
Balance	$	96,200

Time Expended %		20
Starting Date		April 2, 1979
Completion Date		June 30, 1980

Salaries and Wages Estimated This Month	$	6,950
Salaries and Wages Spent This Month	$	2,000
Accumulated Salaries and Wages To Date	$	3,800

QUARTERLY PROGRESS REPORT

Voids often develop over a period of years beneath portland cement concrete pavements at approaches to bridges and at other locations such as pavement joints due to pumping, consolidation, subsidence, and erosion of the support material from beneath the pavement. This loss of support results in pavement distress manifested by cracking, settlement, bumps, and depressions in the roadway that are rough and often hazardous to rapidly moving traffic. Maintenance activities and restoration of rideability of these distressed pavements are time consuming, costly, and disruptive to normal traffic movement. Such activities include patching, slabjacking, and replacement of pavement sections.

An ability to locate voids beneath portland cement concrete pavements by periodic nondestructive surveys would permit replacement of support material before the development of pavement distress and loss of structural qualities. Developments in recent years in the field of pulsed electromagnetic wave technology indicate good prospects for locating and defining the extent of voids beneath pavements by nondestructive methods.

The primary objective of this project is to determine the practicality of pulsed electromagnetic wave technology for locating voids beneath reinforced and nonreinforced portland cement concrete pavements up to 18 inches thick. Another objective is the identification or development of a data processing technique suitable for use with the equipment that can be operated by field personnel and that will provide information on the parameters of voids beneath pavements. It is further desired that the voids beneath pavements be defined with an accuracy of at least ± ½ inch in depth and ± 6 inches in horizontal dimension.

It is envisioned that accomplishment of the objectives will involve the following:

Task 1 - Equipment Selection and Preparation. Obtain pulsed electromagnetic wave equipment that shows promise for accuracy, reliability, and economical application for locating and defining voids beneath pavement slabs. The response signal for such equipment shall be capable of being recorded.

FIG. B—CONTRACT FUNDS

Funds Expended	% [illegible]
Contract Amount	$ [illegible]
Expended this Month	$ [illegible]
Total Exp. To Date	$ [illegible]
Balance	$ [illegible]

FIG. C—CONTRACT PERIOD

Months

Time Expended %	[illegible]
Starting Date	[illegible]
Completion Date	[illegible]

Salaries and Wages Estimated This Month $ [illegible]

Salaries and Wages Spent This Month $ [illegible]

Task 2 - Test Site Preparation. Build test lane with parameters as described in Task 3.

Task 3 - Data Collection. The radar measurements shall be conducted on portland cement pavement sections with thicknesses ranging from 6 inches to 18 inches, with and without reinforcing stell, and over pavement subbases with both high and low moisture levels. Further, there shall be voids of various sizes and shapes, both empty and filled with water, directly beneath the pavement sections.

Task 4 - Data Analysis Procedures. Develop data analysis procedures that will have as input the response signals from pulsed electromagnetic wave equipment and as the final output the identification of the location, size, and shape of voids beneath pavements.

Task 5 - Experimental Evaluation. Evaluate the void detection pulsed electromagnetic wave equipment and data analysis procedures with regard to accuracy, precision, reliability, limitations, operational characteristics, and environmental effects.

The major accomplishment of the quarter was to complete the specifications of the test lane via a conference with Mr. Harry Smith, Dr. Q. L. Robnett (Civil Engineering - Ga Tech), Mr. C. G. Neill (Research - Ga DOT), Dr. J. D. Echard and J. R. Moore (Ga Tech - EES/RAIL). The details of the test lane construction are included in the working plan. A secondary accomplishment of the quarter was the reconfiguration of the radar electronics. The electrical operation of the radar was not changed, however, the equipment was moved from the General Electric Tractor to a lab cart to facilitate: (1) transporation from storage to the test lane; (2) placement of equipment on the test lane (the concrete top surface will be some 20 inches above grade); (3) positioning of antenna for data collection. Efforts to subcontract the construction of the test lane are in progress. A statement of work describing the construction requirements, relationship between work to be done by Georgia Tech - EES/RAIL and the prospective subcontractor and the time table for these events has been completed and forwarded to the proper facilities for subcontract execution.

In the ensuing quarter, the test lane will be constructed, data collection will begin and preliminary data reduction will be accomplished. It is also planned that the development of a detailed math model of the void detection process using short pulse radar illumination will begin.

A-2357

QUARTERLY PROGRESS REPORT

to the

NATIONAL COOPERATIVE HIGHWAY RESEARCH PROGRAM

on Project

10-14

LOCATING VOIDS BENEATH PAVEMENT

for period

JULY 1979 to SEPT 1979

from

GIT-EES/RAIL

NATIONAL COOPERATIVE HIGHWAY RESEARCH PROGRAM
TRANSPORTATION RESEARCH BOARD
NATIONAL RESEARCH COUNCIL

PROGRESS SCHEDULE

Project No. 10-14 Locating Voids Beneath Pavement FY' 79 Month Sept.
Agency Ga Tech - EES/RAIL
Investigator John R. Moore

CH	Research Task	1979 A	M	J	J	A	S	O	N	D	1980 J	F	M	A	M	J	ESTIMATED % COMPLETION
	Equipment Select & Prep.	50	100														100
	Test Track - Base Constr.		20	100													100
	Test Track - Slab Constr.				50	100											100
	Data Collection					20	40	60	80	100							20
	Data Reduction						25	50	75	100							0
	Develop Math Model						30	60	100								0
	Algorithm Selection							25	50	75	100						0
	Experimental Evaluation								25	50	75	100					0
	Final Report											40	75			100	0
L % TION		8	22	31	33	36	46	59	70	81	89	92	97	97	97	100	37

FIG. A—OVERALL PROJECT SCHEDULE

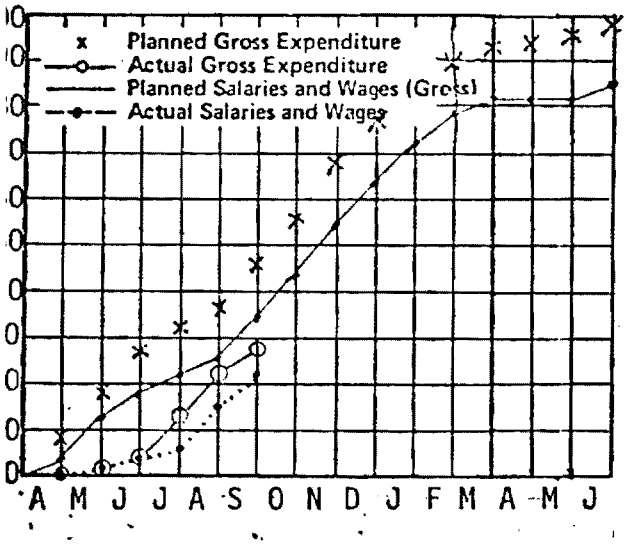

Months

FIG. B—CONTRACT FUNDS

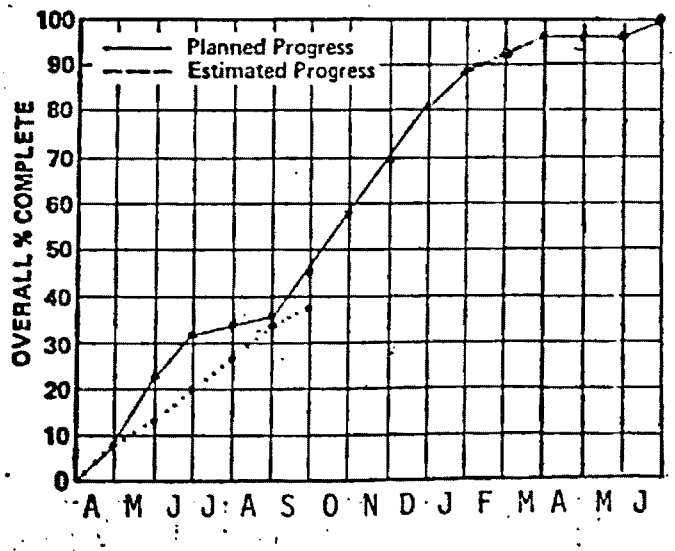

Months

FIG. C—CONTRACT PERIOD

Funds Expended	%	28
Contract Amount	$	100,000
Expended this Month	$	6,284
Total Exp. To Date	$	27,684
Balance	$	72,316

Time Expended %		40
Starting Date		April 2, 1979
Completion Date		June 30, 1980

Salaries and Wages Estimated This Month	$	7,738
Salaries and Wages Spent This Month	$	4,797
Accumulated Salaries and Wages To Date	$	20,297

QUARTERLY PROGRESS REPORT

Voids often develop over a period of years beneath portland cement concrete pavements at approaches to bridges and at other locations such as pavement joints due to pumping, consolidation, subsidence, and erosion of the support material from beneath the pavement. This loss of support results in pavement distress manifested by cracking, settlement, bumps, and depressions in the roadway that are rough and often hazardous to rapidly moving traffic. Maintenance activities and restoration of rideability of these distressed pavements are time consuming, costly, and disruptive to normal traffic movement. Such activities include patching, slabjacking, and replacement of pavement sections.

An ability to locate voids beneath portland cement concrete pavements by periodic nondestructive surveys would permit replacement of support material before the development of pavement distress and loss of structural qualities. Developments in recent years in the field of pulsed electromagnetic wave technology indicate good prospects for locating and defining the extent of voids beneath pavements by nondestructive methods.

The primary objective of this project is to determine the practicality of pulsed electromagnetic wave technology for locating voids beneath reinforced and nonreinforced portland cement concrete pavements up to 18 inches thick. Another objective is the identification or development of a data processing technique suitable for use with the equipment that can be operated by field personnel and that will provide information on the parameters of voids beneath pavements. It is further desired that the voids beneath pavements be defined with an accuracy of at least $\pm$ ½ inch in depth and $\pm$ 6 inches in horizontal dimension.

It is envisioned that accomplishment of the objectives will involve the following:

Task 1 - Equipment Selection and Preparation. Obtain pulsed electromagnetic wave equipment that shows promise for accuracy, reliability and economical application for locating and defining voids beneath pavement slabs. The response signal for such equipment shall be capable of being recorded.

Task 2 - Test Site Preparation. Build test lane with parameters as described in Task 3.

Task 3 - Data Collection. The radar measurements shall be conducted on portland cement pavement sections with thicknesses ranging from 6 inches to 18 inches, with and without reinforcing steel, and over pavement subbases with both high and low moisture levels. Further, there shall be voids of various sizes and shapes, both empty and filled with water, directly beneath the pavement sections.

Task 4 - Data Analysis Procedures. Develop data analysis procedures that will have as input the response signals from pulsed electromagnetic wave equipment and as the final output the identification of the location, size, and shape of voids beneath pavements.

Task 5 - Experimental Evaluation. Evaluate the void detection pulsed electromagnetic wave equipment and data analysis procedures with regard to accuracy, precision, reliability, limitations, operational characteristics, and environmental effects.

The major accomplishment of the quarter was to complete the test lane construction. The void layout pattern was photographed and recorded by survey prior to the pouring of the concrete. The construction was completed August 15, 1979, according to the plan and specifications outlined in the WORKING PLAN. Data collection began 28 days after the concrete pouring and the preliminary data are consistent with the expected results.

The next quarter's accomplishments will include finishing: the data collection task, the data reduction task, developing the math model, and partial algorithm evaluation. Included in the data collection task are the "lab measurements" to be made on three different base courses using reinforced and nonreinforced concrete slabs as outlined in the WORKING PLAN.

QUARTERLY PROGRESS REPORT

to the

NATIONAL COOPERATIVE HIGHWAY RESEARCH PROGRAM

on Project

10-14

LOCATING VOIDS BENEATH PAVEMENT

for period

January 1, 1980 to March 31, 1980

from

GIT-EES/RAIL

TRANSPORTATION RESEARCH BOARD
NATIONAL RESEARCH COUNCIL

PROGRESS SCHEDULE

RP Project No. 10-14 Locating Voids Beneath Pavement Fy' 79 Month _____
h Agency Ga Tech - EES/RAIL
pal Investigator J. D. Echard/W. J. Steinway

ARCH ES	Research Task	1979 A	M	J	J	A	S	O	N	D	1980 J	F	M	A	M	J	ESTIMATE COMPLETI
I	Equipment Select & Prep.	50	100														100
I	Test Track - Base Constr.		20	100													100
	Test Track - Slab Constr.				50	100											100
I	Data Collection					20	40	60	80	100							50
	Data Reduction						25	50	75	100							50
V	Develop Math Model						30	60	100								90
	Algorithm Selection							25	50	75	100						50
V	Experimental Evaluation								25	50	75	100					25
I	Final Report											40	75			100	0
ALL % LETION		8	22	31	33	36	46	59	70	81	89	92	97	97	97	100	70

FIG. A—OVERALL PROJECT SCHEDULE

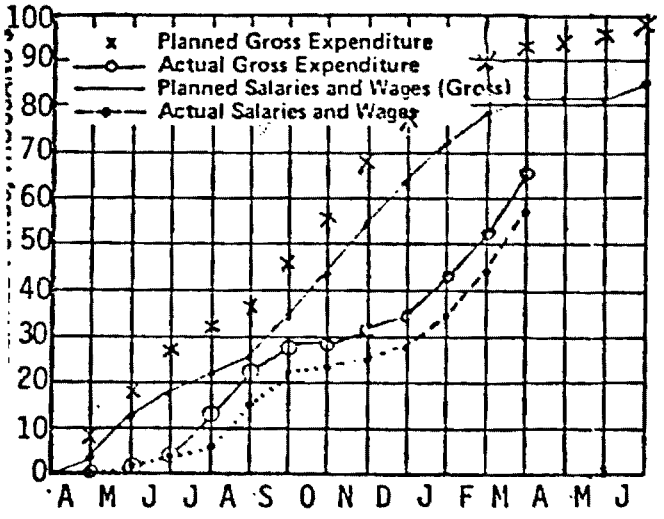

Months

FIG. B—CONTRACT FUNDS

Funds Expended	% 66%
Contract Amount	$ 99,672
Expended this Month	$ 8,000
Total Exp. To Date	$ 65,506
Balance	$ 34,166

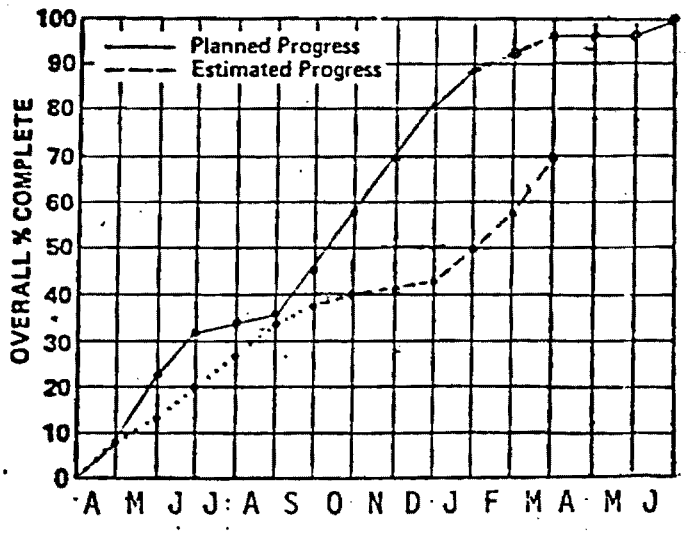

Months

FIG. C—CONTRACT PERIOD

Time Expended %	80%
Starting Date	April 2, 1979
Completion Date	June 30, 1980

Salaries and Wages Estimated This Month	$ 8,000
Salaries and Wages Spent This Month	$ -
Accumulated Salaries and Wages To Date	$ 56,532

QUARTERLY PROGRESS REPORT

Voids often develop over a period of years beneath portland cement concrete pavements at approaches to bridges and at other locations such as pavement joints due to pumping, consolidation, subsidence, and erosion of the support material from beneath the pavement. This loss of support results in pavement distress manifested by cracking, settlement, bumps, and depressions in the roadway that are rough and often hazardous to rapidly moving traffic. Maintenance activities and restoration of rideability of these distressed pavements are time consuming, costly, and disruptive to normal traffic movement. Such activities include patching, slabjacking, and replacement of pavement sections.

An ability to locate voids beneath portland cement concrete pavements by periodic non-destructive surveys would permit replacement of support material before the development of pavement distress and loss of structural qualities. Developments in recent years in the field of pulsed electromagnetic wave technology indicate good prospects for locating and defining the extent of voids beneath pavement by non-destructive methods.

The primary objective of this project is to determine the practicality of pulsed electromagnetic wave technology for locating voids beneath reinforced and non-reinforced portland cement concrete pavements up to 18 inches thick. Another objective is the identification or development of a data processing technique suitable for use with the equipment that can be operated by field personnel and that will provide information on the parameters of voids beneath pavements. It is further desired that the voids beneath pavements be defined with an accuracy of at least $\pm$ ½ inch in depth and $\pm$ 6 inches in horizontal dimension.

It is envisioned that accomplishment of the objectives will involve the following:

Task 1 - Equipment Selection and Preparation.

Obtain pulsed electromagnetic wave equipment that shows promise for accuracy, reliability and economical application for locating and defining voids beneath pavement slabs. The response signal for such equipment shall be capable of being recorded.

Two changes have been made to the system in the last quarter. The first was the rebuilding of the antenna boom structure making it more rigid. The second change, an addition to the system of an APPLE microcomputer, allows for processing of radar data in the field thereby shortening the time to record and process data.

Task 2 - Test Site Preparation.

Build test lane with parameters as described in Task 3.

This task is now complete. Four indoor test boxes containing base material were constructed. Base materials were asphalt, concrete, aggregate, and clay.

Task 3 - Data Collection.

The radar measurements shall be conducted on portland cement pavement sections with thickness ranging from 6 inches to 18 inches, with and without reinforcing steel, and over pavement subbases with both high and low moisture levels. Further, there shall be voids of various sizes and shapes, both empty and filled with water, directly beneath the pavement sections.

All the data on the indoor boxes under dry conditions, unreinforced and reinforced, has been taken. All data was taken against a calibrated reference. Data is yet to be taken on the indoor boxes under moist and wet conditions. When this is completed, measurements will begin on the outside roadway.

Task 4 - Data Analysis Procedures.

Develop data analysis procedures that will have as input the response signals from pulsed electromagnetic wave equipment and as the final output the identification of the location, size, and shape of voids beneath pavements.

Progress has been made in this area. Based upon the theoretical modeling thus far, two discriminates are being tested. For variations in size of small voids, there is primarily a change in amplitude of the return signal. For voids larger than approximately 4 inches, a time discriminate is used, measuring between negative and positive peaks. Measured data shows that these two discriminates overlap at 4 inches thus giving means to measure void sizes over a wide range. As a larger data base is developed verification of these discriminates is expected.

Task 5 - Experimental Evaluation.

Evaluate the void detection pulsed electromagnetic wave equipment and data analysis procedures with regard to accuracy, precision, reliability, limitations, operational characteristics, and environmental effects.

The experimental evaluation thus far has led to a modification in mounting the system and a change in calibration procedures. These mods have improved operational procedures and improved the accuracy of measurements.

Information on Outside Test Lane Construction

Two photographs have been attached to this report to help answer questions concerning the test lane construction. The photographs are of the outside test lane before concrete was poured and show the exposed styrofoam voids.

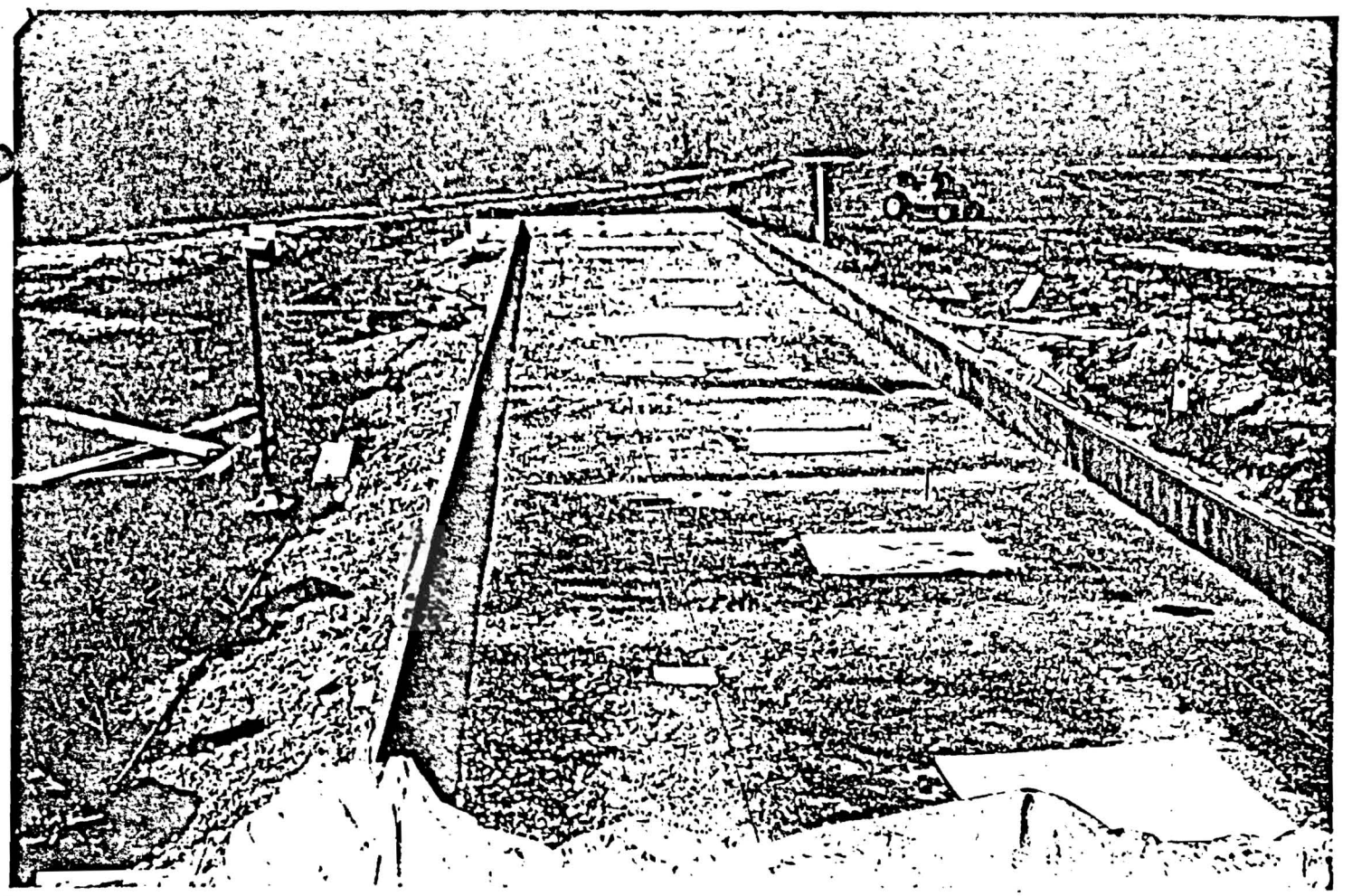

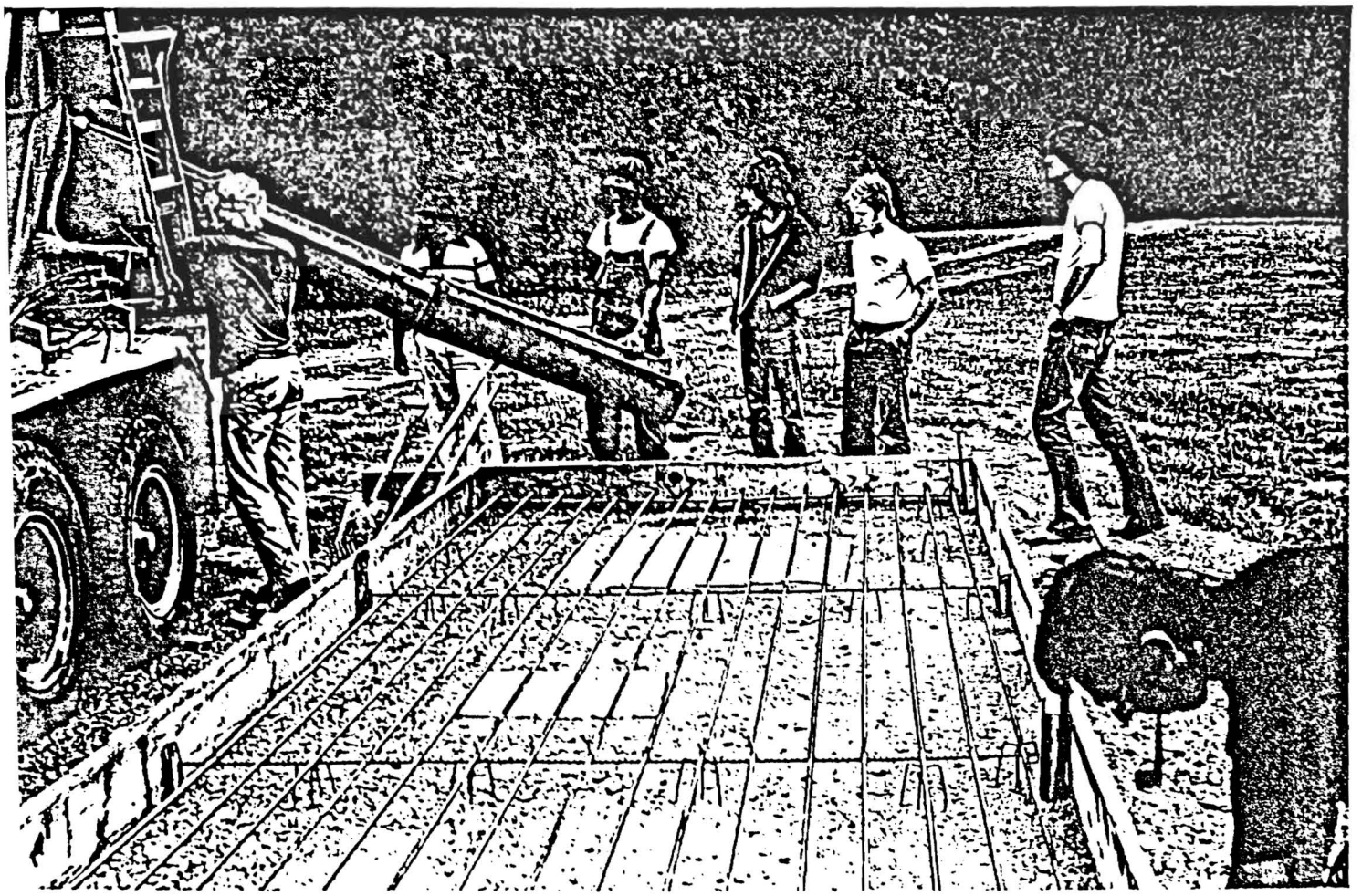

A-2357

QUARTERLY PROGRESS REPORT

to the

NATIONAL COOPERATIVE HIGHWAY RESEARCH PROGRAM

on Project

10-14

LOCATING VOIDS BENEATH PAVEMENT

for period

April 1, 1980 to June 30, 1980

from

GIT-EES/RAIL

NATIONAL COOPERATIVE HIGHWAY RESEARCH PROGRAM
TRANSPORTATION RESEARCH BOARD
NATIONAL RESEARCH COUNCIL

PROGRESS SCHEDULE

Project No. 10-14 Locating Voids Beneath Pavement Fy' 79 Month _____
h Agency Ga Tech - EES/RAIL
ıl Investigator _____

RCH S	Research Task	1979 A	M	J	J	A	S	O	N	D	1980 J	F	M	A	M	J	ESTIMATED % COMPLETION
	Equipment Select & Prep.	50	100														100
	Test Track - Base Constr.		20	100													100
	Test Track - Slab Constr.				50	100											100
	Data Collection					20	40	60	80	100							80
	Data Reduction						25	50	75	100							70
	Develop Math Model						30	60	100								100
	Algorithm Selection							25	50	75	100						100
	Experimental Evaluation								25	50	75	100					50
	Final Report											40	75			100	10
LL % ETION		8	22	31	33	36	46	59	70	81	89	92	97	97	97	100	80

FIG. A—OVERALL PROJECT SCHEDULE

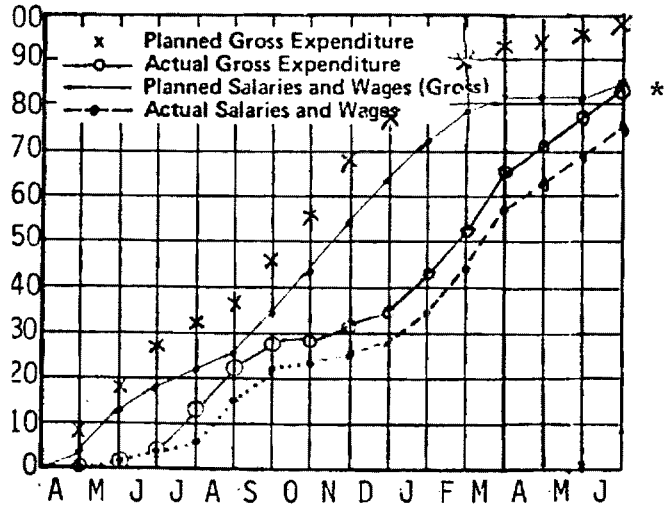

Months

FIG. B—CONTRACT FUNDS

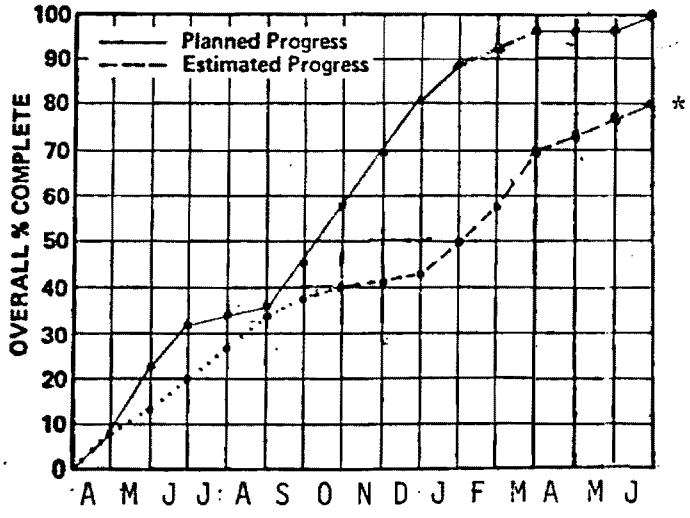

Months

FIG. C—CONTRACT PERIOD

Funds Expended	%	85
Contract Amount	$	99,672
Expended this Month	$	8,000
Total Exp. To Date	$	84,721
Balance	$	14,950

Time Expended %	80
Starting Date	April 2, 1979
Completion Date	Nov. 1, 1980

* Contract has been extended

Salaries and Wages Estimated This Month	$	8,000
Salaries and Wages Spent This Month	$	-
Accumulated Salaries and Wages To Date	$	74,200

QUARTERLY PROGRESS REPORT

Voids often develop over a period of years beneath portland cement concrete pavements at approaches to bridges and at other locations such as pavement joints due to pumping, consolidation, subsidence, and erosion of the support material from beneath the pavement. This loss of support results in pavement distress manifested by cracking, settlement, bumps, and depressions in the roadway that are rough and often hazardous to rapidly moving traffic. Maintenance activities and restoration of rideability of these distressed pavements are time consuming, costly, and disruptive to normal traffic movement. Such activities include patching, slabjacking, and replacement of pavement sections.

An ability to locate voids beneath portland cement concrete pavements by periodic non-destructive surveys would permit replacement of support material before the development of pavement distress and loss of structual qualities. Developments in recent years in the field of pulsed electromagnetic wave technology indicate good prospects for locating and defining the extent of voids beneath pavement by non-destructive methods.

The primary objective of this project is to determine the practicality of pulsed electromagnetic wave technology for locating voids beneath reinforced and non-reinforced portland cement concrete pavements up to 18 inches thick. Another objective is the identification or development of a data processing technique suitable for use with the equipment that can be operated by field personnel and that will provide information on the parameters of voids beneath pavements. It is further desired that voids beneath pavements be defined with an accuracy of at least $\pm$ ½ inch in depth and $\pm$ 6 inches in horizontal dimension.

It is envisioned that accomplishment of the objectives will involve the following:

Task 1 - Equipment Selection and Preparation.

Obtain pulsed electromagnetic wave equipment that shows promise for accuracy, reliability and economical application for locating and defining voids beneath pavement slabs. The response signal for such equipment shall be capable of being recorded.

Two changes have been made to the system in the last quarter. The first was the rebuilding of the antenna boom structure making it more rigid. The second change, an addition to the system of an APPLE microcomputer, allows for processing of radar data in the field thereby shortening the time to record and process data.

Task 2 - Test Site Preparation.

Build test lane with parameters as described in Task 3.

This task is now complete. Four indoor test boxes containing base material were constructed. Base materials were asphalt, concrete, aggregate, and clay.

Task 3 - Data Collection.

The radar measurements shall be conducted on portland cement pavement sections with thickens ranging from 6 inches to 18 inches, with and without reinforcing steel, and over pavement subbases with both high and low moisture levels. Further, there shall be voids of various sizes and shapes, both empty and filled with water, directly beneath the pavement sections.

All the data on the indoor boxes under dry, moist, and wet conditions, unreinforced and reinforced, has been taken. All data was taken against a calibrated reference. Measurements have begun on the outside roadway.

Task 4 - Data Analysis Procedures.

Develop data analysis procedures that will have as input the response signals from pulsed electromagnetic wave equipment and as the final output the identification of the location, size, and shape of voids beneath pavements.

Two discriminates based on theoretical modeling and verified on actual radar measurements have been chosen to form the final algorithum for void identification. For variations in size of small voids, there is primarily a change in amplitude of the return signal. For voids larger than approximately 4 inches, a time descriminate is used, measuring between negative and positive peaks. Measured data shows that these two discriminates overlap at 4 inches thus giving means to measure void sizes over a wide range.

Task 5 - Experimental Evaluation.

Evaluate the void detection pulsed electromagnetic wave equipment and data analysis procedures with regard to accuracy, precision, reliability, limitations, operational characteristics, and environmental effects.

The experimental evaluation thus far has led to a modification in mounting the system and a change in calibration procedures. These mods have improved operational procedures and improved the accuracy of measurements.

Current and Future Efforts

In the month of July the final outside test lane measurements will be made and the final report will be prepared.

A-2357

QUARTERLY PROGRESS REPORT

to the

NATIONAL COOPERATIVE HIGHWAY RESEARCH PROGRAM

on Project

10-14

LOCATING VOIDS BENEATH PAVEMENT

for period

July 1, 1980 to Oct. 31, 1980

from

GIT-EES/RAIL

NATIONAL COOPERATIVE HIGHWAY RESEARCH PROGRAM
TRANSPORTATION RESEARCH BOARD
NATIONAL RESEARCH COUNCIL

PROGRESS SCHEDULE

IP Project No. 10-14 Locating Voids Beneath Pavement Fy' 80 Month
ch Agency Ga Tech - EES/RAIL
ıal Investigator

ARCH ES	Research Task	1979 A	M	J	J	A	S	O	N	D	1980 J	F	M	A	M	J	ESTIMATED % COMPLETION
	Equipment Select & Prep.	50	100														100
	Test Track - Base Constr.		20	100													100
	Test Track - Slab Constr.				50	100											100
	Data Collection					20	40	60	80	100							100
	Data Reduction						25	50	75	100							100
	Develop Math Model						30	60	100								100
	Algorithm Selection							25	50	75	100						100
	Experimental Evaluation								25	50	75	100					100
	Final Report											40	75			100	100
LL % ETION		8	22	31	33	36	46	59	70	81	89	92	97	97	97	100	

FIG. A—OVERALL PROJECT SCHEDULE

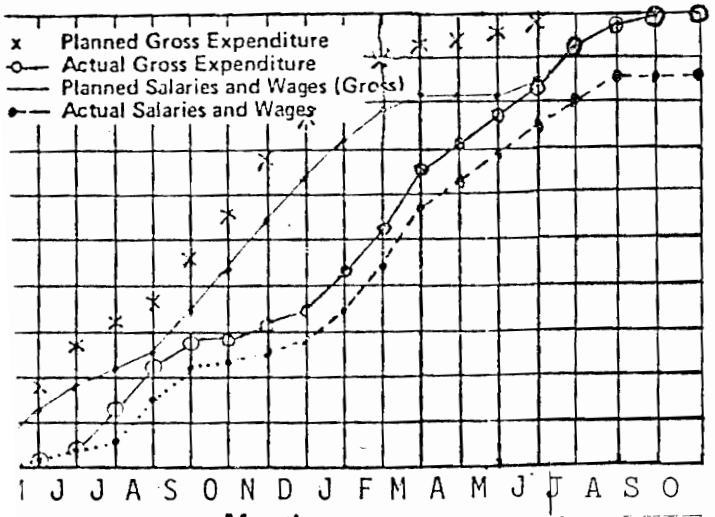

FIG. B—CONTRACT FUNDS

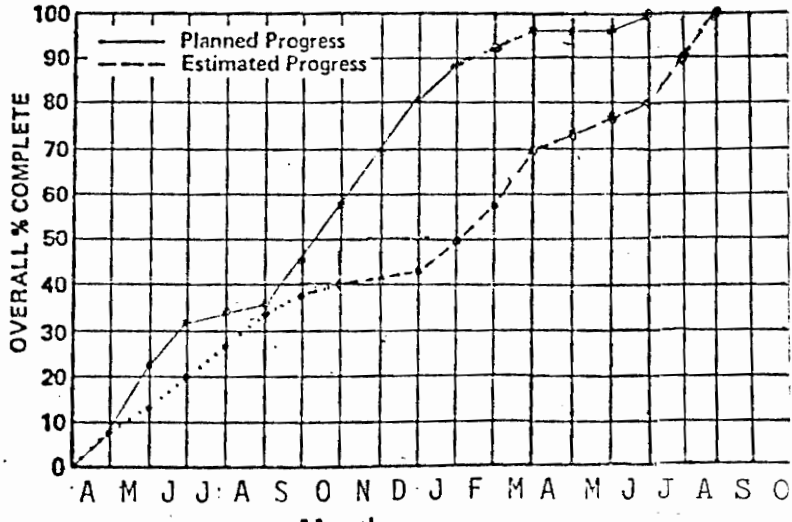

FIG. C—CONTRACT PERIOD

Funds Expended	%	100
Contract Amount	$	99,672
Expended this Month	$	-0.0
Total Exp. To Date	$	99,672
Balance	$	0.0

Time Expended %		100
Starting Date		April 2, 1979
Completion Date		Nov. 1, 1980

* Contract has been extended

Salaries and Wages Estimated This Month	$	-
Salaries and Wages Spent This Month	$	-
Accumulated Salaries and Wages To Date	$	99,672

QUARTERLY PROGRESS REPORT

Voids often develop over a period of years beneath portland cement concrete pavements at approaches to bridges and at other locations such as pavement joints due to pumping, consolidation, subsidence, and erosion of the support material from beneath the pavement. This loss of support results in pavement distress manifested by cracking, settlement, bumps, and depressions in the roadway that are rough and often hazardous to rapidly moving traffic. Maintenance activities and restoration of rideability of these distressed pavements are time consuming, costly, and disruptive to normal traffic movement. Such activities include patching, slabjacking, and replacement of pavement sections.

An ability to locate voids beneath portland cement concrete pavements by periodic non-destructive surveys would permit replacement of support material before the development of pavement distress and loss of structural qualities. Developments in recent years in the field of pulsed electromagnetic wave technology indicate good prospects for locating and defining the extent of voids beneath pavement by non-destructive methods.

The primary objective of this project is to determine the practicality of pulsed electromagnetic wave technology for locating voids beneath reinforced and non-reinforced portland cement concrete pavements up to 18 inches thick. Another objective is the identification or development of a data processing technique suitable for use with the equipment that can be operated by field personnel and that will provide information on the parameters of voids beneath pavements. It is further desired that voids beneath pavements be defined with an accuracy of at least $\pm$ 1/2 inch in depth and $\pm$ 6 inches in horizontal dimension.

It is envisioned that accomplishment of the objectives will involve the following:

Task 1 - Equipment Selection and Preparation

Obtain pulsed electromagnetic wave equipment that shows promise for accuracy, reliability and economical application for locating and defining voids beneath pavement slabs. The response signal for such equipment shall be capable of being recorded.

Two changes have been made to the system in the last quarter. The first was the rebuilding of the antenna boom structure making it more rigid. The second change, an addition to the system of an APPLE microcomputer, allows for processing of radar data in the field thereby shortening the time to record and process data.

Task 2 - Test Site Preparation

Build test lane with parameters as described in Task 3.

This task is now complete. Four indoor test boxes containing base material were constructed. Base materials were asphalt, concrete, aggregate, and clay.

Task 3 - Data Collection

The radar measurements have been conducted on portland cement pavement sections 9 inches thick, with and without reinforcing steel, and over pavement subbases with both high and low moisture levels. Further, there are voids of various sizes and shapes, both empty and filled with water, directly beneath the pavement sections.

All the data on the indoor boxes under dry, moist, and wet conditions, unreinforced and reinforced, has been taken. All data was taken against a calibrated reference. All data on the outside test lane has been taken at several temperatures.

Task 4 - Data Analysis Procedures

Develop data analysis procedures that will have as input the response signals from pulsed electromagnetic wave equipment and as the final output the identification of the location, size, and shape of voids beneath pavements.

Two discriminates based on theoretical modeling and verified on actual radar measurements have been chosen to form the final algorithm for void identification. For variations in size of small voids, there is primarily a change in amplitude of the return signal. For voids larger than approximately 3 inches, a time discriminate is used, measuring between negative and positive peaks. Measured data shows that these two discriminates overlap at 3 inches thus giving means to measure void sizes over a wide range.

Task 5 - Experimental Evaluation

Evaluate the void detection pulsed electromagnetic wave equipment and data analysis procedures with regard to accuracy, precision, reliability, limitations, operational characteristics, and environmental effects.

The experimental evaluation thus far has led to a modification in mounting the system and a change in calibration procedures. These mods have improved operational procedures and improved the accuracy of measurements.

The final report with appropriate modifications based on reviewers' comments is being compiled.

NATIONAL COOPERATIVE HIGHWAY RESEARCH PROGRAM
TRANSPORTATION RESEARCH BOARD
NATIONAL RESEARCH COUNCIL

A-2357

PROGRESS SCHEDULE

Project No. 10-14 Locating Voids Beneath Pavement Fy' 79 Month DECEMBER
Agency Ga Tech - EES/RAIL
Investigator John R. Moore

CH	Research Task	1979 A	M	J	J	A	S	O	N	D	1980 J	F	M	A	M	J	ESTIMATED % COMPLETION
	Equipment Select & Prep.	50	100														100
	Test Track - Base Constr.		20	100													100
	Test Track - Slab Constr.				50	100											100
	Data Collection					20	40	60	80	100							40
	Data Reduction						25	50	75	100							20
	Develop Math Model						30	60	100								95
	Algorithm Selection							25	50	75	100						50
	Experimental Evaluation								25	50	75	100					0
	Final Report											40	75			100	0
L % TION		8	22	31	33	36	46	59	70	81	89	92	97	97	97	100	52

FIG. A—OVERALL PROJECT SCHEDULE

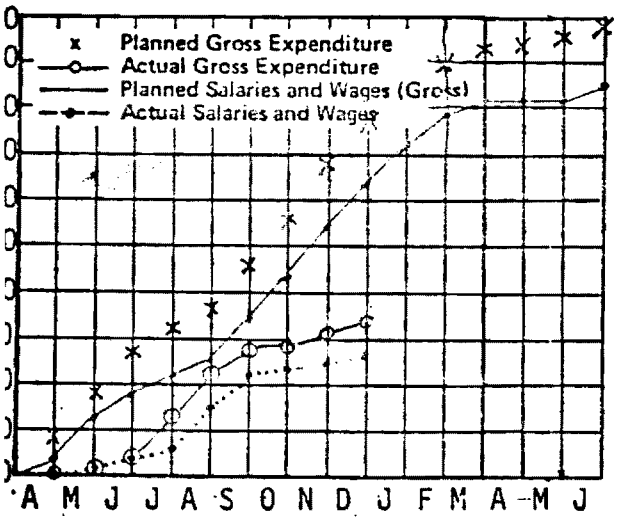

Months

FIG. B—CONTRACT FUNDS

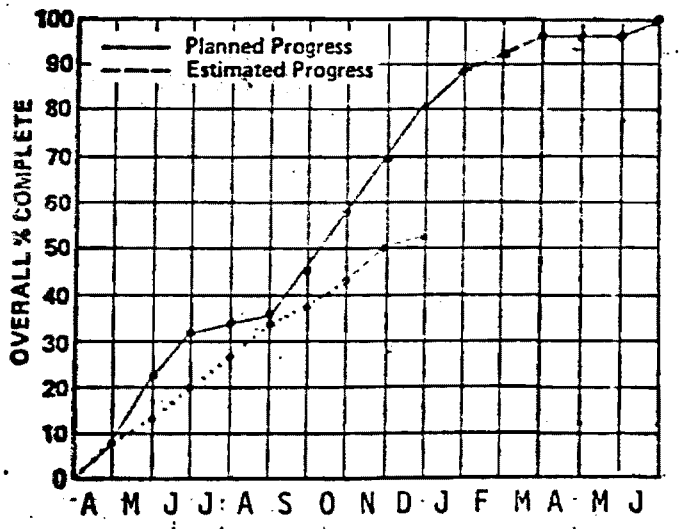

Months

FIG. C—CONTRACT PERIOD

Funds Expended	%	34	
Contract Amount	$	100,000	
Expended this Month	$	2,500	
Total Exp. To Date	$	33,684	
Balance	$	66,316	

Time Expended %		60
Starting Date		April 2, 1979
Completion Date		June 30, 1980

Salaries and Wages Estimated This Month	$	9,600
Salaries and Wages Spent This Month	$	2,500
Accumulated Salaries and Wages To Date	$	26,297

QUARTERLY PROGRESS REPORT

Voids often develop over a period of years beneath portland cement concrete pavements at approaches to bridges and at other locations such as pavement joints due to pumping, consolidation, subsidence, and erosion of the support material from beneath the pavement. This loss of support results in pavement distress manifested by cracking, settlement, bumps, and depressions in the roadway that are rough and often hazardous to rapidly moving traffic. Maintenance activities and restoration of rideability of these distressed pavements are time consuming, costly, and disruptive to normal traffic movement. Such activities include patching, slabjacking, and replacement of pavement sections.

An ability to locate voids beneath portland cement concrete pavements by periodic nondestructive surveys would permit replacement of support material before the development of pavement distress and loss of structural qualities. Developments in recent years in the field of pulsed electromagnetic wave technology indicate good prospects for locating and defining the extent of voids beneath pavement by nondestructive methods.

The primary objective of this project is to determine the practicality of pulsed electromagnetic wave technology for locating voids beneath reinforced and nonreinforced portland cement concrete pavements up to 18 inches thick. Another objective is the identification or development of a data processing technique suitable for use with the equipment that can be operated by field personnel and that will provide information on the parameters of voids beneath pavements. It is further desired that the voids beneath pavements be defined with an accuracy of at least $\pm$ ½ inch in depth and $\pm$ 6 inches in horizontal dimension.

It is envisioned that accomplishment of the objectives will involve the following:

Task 1 - Equipment Selection and Preparation. Obtain pulsed electromagnetic wave equipment that shows promise for accuracy, reliability and economical application for locating and defining voids beneath pavement slabs. The response signal for such equipment shall be capable of being recorded.

Task 2 - Test Site Preparation. Build test lane with parameters as described in Task 3.

Task 3 - Data Collection. The radar measurements shall be conducted on portland cement pavement sections with thickness ranging from 6 inches to 18 inches, with and without reinforcing steel, and over pavement subbases with both high and low moisture levels. Further, there shall be voids of various sizes and shapes, both empty and filled with water, directly beneath the pavement sections.

Task 4 - Data Analysis Procedures. Develop data analysis procedures that will have as input the response signals from pulsed electromagnetic wave equipment and as the final output the identification of the location, size, and shape of voids beneath pavements.

Task 5 - Experimental Evaluation. Evaluate the void detection pulsed electromagnetic wave equipment and data analysis procedures with regard to accuracy, precision, reliability, limitations, operational characteristics, and environmental effects.

The major accomplishment of the quarter was the construction of the inside laboratory measurement area. The three required base boxes were finished and some preliminary data taken. Weather and equipment problems slowed the collection of data and has resulted in the lag shown on the monthly progress reports. The equipment problems have been very costly in time due to long delivery times for a critical part in the receiver section. The replacement part and several spare parts have been on order for three or four weeks. Other tasks are proceeding on or near schedule. Next quarter's goals are the completion of data collection, development of the math model, and algorithm selection.

ENGINEERING EXPERIMENT STATION
GEORGIA INSTITUTE OF TECHNOLOGY • ATLANTA, GEORGIA 30332

March 17, 1981

National Academy of Sciences
2101 Constitution Avenue, NW
Washington, D. C. 20414

Attention: Ronald R. Wiley
Contract Specialist

Subject: Contract No. HR 10-14 Monthly Progress Schedules covering the period April 1979 through October 1980

Dear Mr. Wiley:

Enclosed is a progress schedule covering the entire term of the project, April 1979 through October 1980. This serves to satisfy the monthly progress schedule requirement for April 1979 through October 1980.

Respectfully submitted,

William J. Steinway
Project Director

APPROVED:

J. D. Echard, Chief
Radar Applications Division

Enclosure

NATIONAL COOPERATIVE HIGHWAY RESEARCH PROGRAM
TRANSPORTATION RESEARCH BOARD
NATIONAL RESEARCH COUNCIL

PROGRESS SCHEDULE

RP Project No. 10-14 Locating Voids Beneath Pavement Fy' 80 Month _____
rch Agency Ga Tech - EES/RAIL
pal Investigator _____

ARCH ES	Research Task	1979 A	M	J	J	A	S	O	N	D	1980 J	F	M	A	M	J	ESTIMATED % COMPLETION
I	Equipment Select & Prep.	50	100														100
I	Test Track - Base Constr.		20	100													100
	Test Track - Slab Constr.				50	100											100
	Data Collection					20	40	60	80	100							100
	Data Reduction						25	50	75	100							100
	Develop Math Model						30	60	100								100
	Algorithm Selection							25	50	75	100						100
	Experimental Evaluation								25	50	75	100					100
	Final Report											40	75			100	100
LL % ETION		8	22	31	33	36	46	59	70	81	89	92	97	97	97	100	

FIG. A–OVERALL PROJECT SCHEDULE

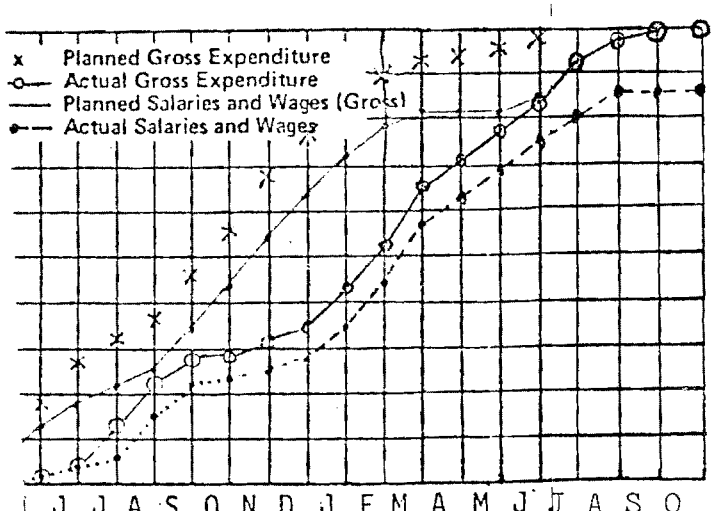

FIG. B–CONTRACT FUNDS

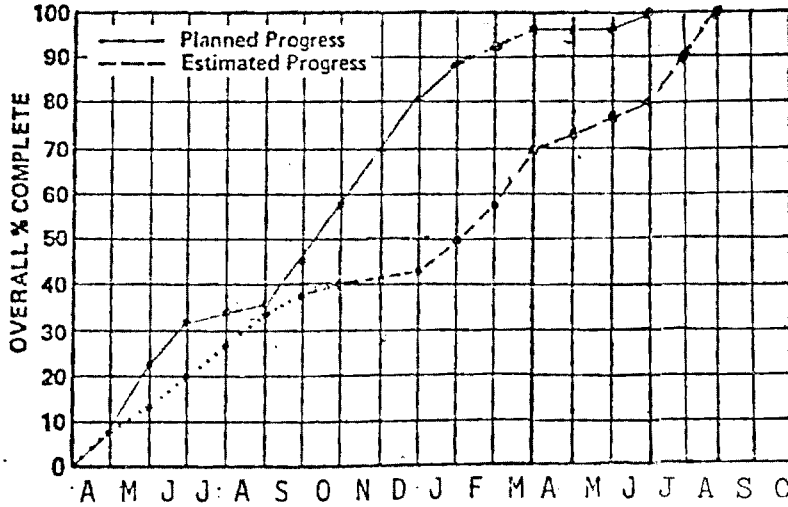

FIG. C–CONTRACT PERIOD

Funds Expended % 100
Contract Amount $ 99,672
Expended this Month $ -0.0
Total Exp. To Date $ 99,672
Balance $ 0.0

Time Expended % 100
Starting Date April 2, 1979
Completion Date Nov. 1, 1980
* Contract has been extended

Salaries and Wages Estimated This Month $ –
Salaries and Wages Spent This Month $ –
Accumulated Salaries and Wages To Date $ 99,672

TRANSPORTATION RESEARCH BOARD
NATIONAL RESEARCH COUNCIL

A-2357

PROGRESS SCHEDULE

Project No. 10-14 Locating Voids Beneath Pavement Fy' 79 Month April
Agency Ga Tech - EES/RAIL
Investigator John R. Moore - James A. Echard

CH	Research Task	1979 A	M	J	J	A	S	O	N	D	1980 J	F	M	A	M	J	ESTIMATED % COMPLETION
	Equipment Select & Prep.	50	100														50
	Test Track - Base Constr.		20	70													
	Test Track - Slab Constr.				50	100											
	Data Collection					20	40	60	80	100							
	Data Reduction						25	50	75	100							
	Develop Math Model						30	60	100								
	Algorithm Selection							25	50	75	100						
	Experimental Evaluation								25	50	75	100					
	Final Report											40	75			100	
L % TION		8	22	31	33	36	46	59	70	81	89	92	97	97	97	100	8

FIG. A—OVERALL PROJECT SCHEDULE

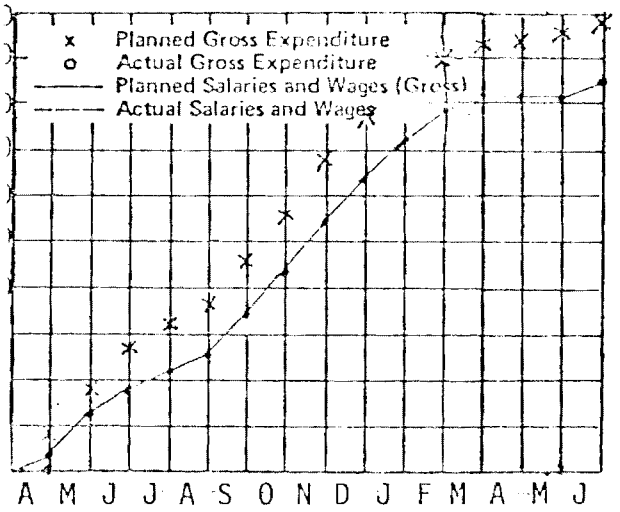

Months
FIG. B—CONTRACT FUNDS

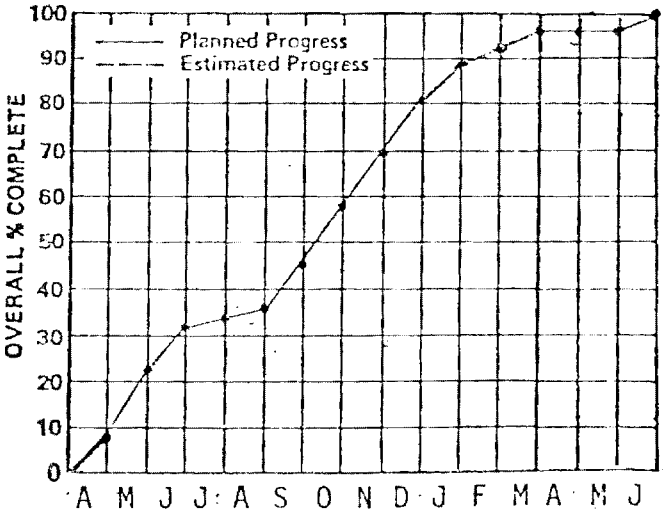

Months
FIG. C—CONTRACT PERIOD

Funds Expended	%	0
Contract Amount	$	100,000
Expended this Month	$	0
Total Exp. To Date	$	0
Balance	$	100,000

Time Expended %		7
Starting Date		April 2, 1979
Completion Date		June 30, 1980

Salaries and Wages Estimated This Month	$	2,000
Salaries and Wages Spent This Month	$	0
Accumulated Salaries and Wages To Date	$	0

NATIONAL COOPERATIVE HIGHWAY RESEARCH

TRANSPORTATION RESEARCH BOARD
NATIONAL RESEARCH COUNCIL

A-2357

PROGRESS SCHEDULE

Project No. 10-14 Locating Voids Beneath Pavement Fy' 79 Month MAY
Agency Ga Tech - EES/RAIL
Investigator John R. Moore & J. D. Echard

CH	Research Task	1979 A	M	J	J	A	S	O	N	D	1980 J	F	M	A	M	J	ESTIMATED % COMPLETION
	Equipment Select & Prep.	50	100														75
	Test Track - Base Constr.		20	100													15
	Test Track - Slab Constr.				50	100											
	Data Collection					20	40	60	80	100							
	Data Reduction						25	50	75	100							
	Develop Math Model						30	60	100								
	Algorithm Selection							25	50	75	100						
	Experimental Evaluation								25	50	75	100					
	Final Report											40	75			100	
% ION		8	22	31	33	36	46	59	70	81	89	92	97	97	97	100	18

FIG. A—OVERALL PROJECT SCHEDULE

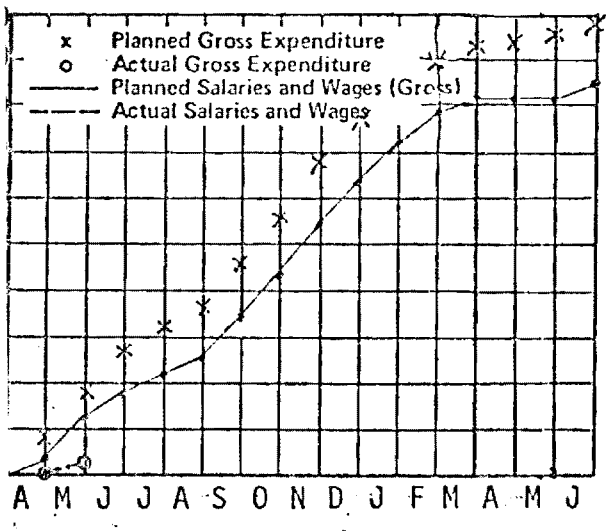

Months

FIG. B—CONTRACT FUNDS

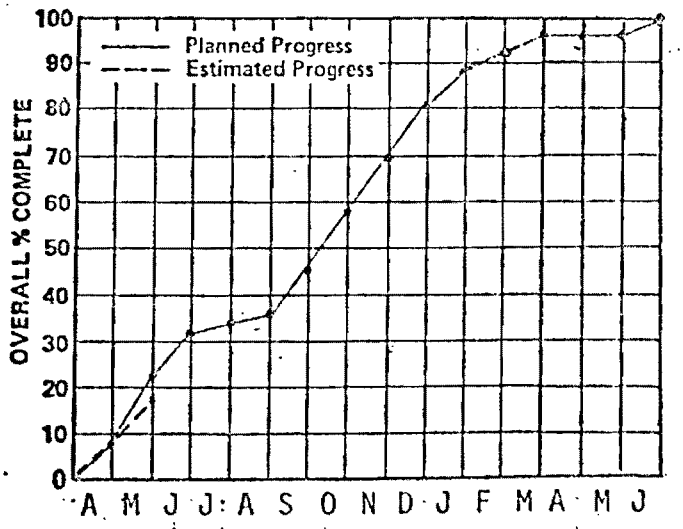

Months

FIG. C—CONTRACT PERIOD

Funds Expended	%	1,800
Contract Amount	$	100,000
Expended this Month	$	1,800
Total Exp. To Date	$	1,800
Balance	$	98,200

Time Expended %		13
Starting Date		April 2, 1979
Completion Date		June 30, 1980

Salaries and Wages Estimated This Month	$	3,470
Salaries and Wages Spent This Month	$	1,800
Accumulated Salaries and Wages To Date	$	1,800

TRANSPORTATION RESEARCH BOARD
NATIONAL RESEARCH COUNCIL

A-2357

PROGRESS SCHEDULE

Project No. 10-14 Locating Voids Beneath Pavement FY 79 Month July
Agency Ga Tech - EES/RAIL
Investigator John R. Moore

CH	Research Task	1979 A	M	J	J	A	S	O	N	D	1980 J	F	M	A	M	J	ESTIMATED % COMPLETION
	Equipment Select & Prep.	50	100														100
	Test Track - Base Constr.		20	100													70
	Test Track - Slab Constr.				50	100											30
	Data Collection					20	40	60	80	100							
	Data Reduction						25	50	75	100							
	Develop Math Model						30	60	100								
	Algorithm Selection							25	50	75	100						
	Experimental Evaluation								25	50	75	100					
	Final Report											40	75			100	
% ON		8	22	31	33	36	46	59	70	81	89	92	97	97	97	100	27

FIG. A—OVERALL PROJECT SCHEDULE

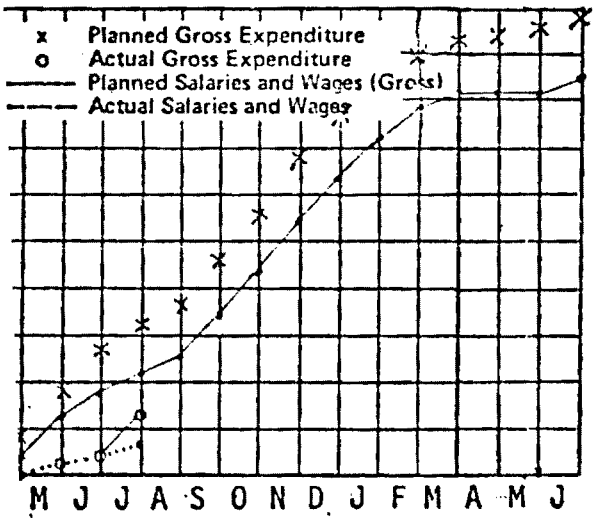

Months

FIG. B—CONTRACT FUNDS

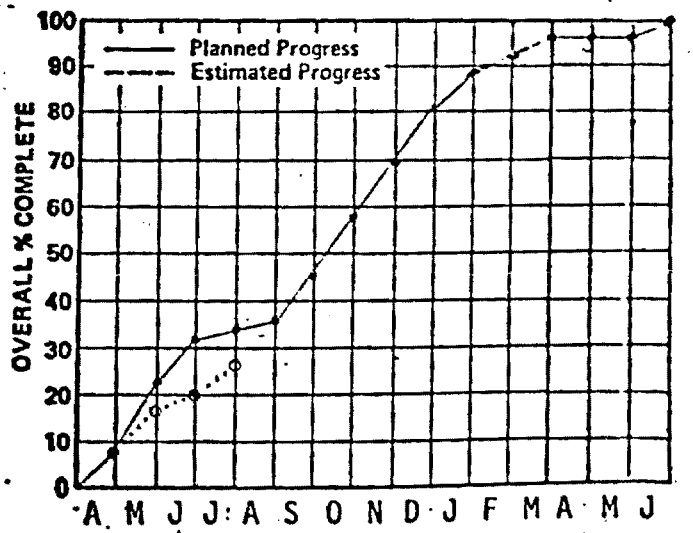

Months

FIG. C—CONTRACT PERIOD

Funds Expended	%	12
Contract Amount	$	100,000
Expended this Month	$	8,300
Total Exp. To Date	$	12,100
Balance	$	87,900

Time Expended %	27
Starting Date	April 2, 1979
Completion Date	June 30, 1980

Salaries and Wages Estimated This Month	$	4,340
Salaries and Wages Spent This Month	$	2,700
Accumulated Salaries and Wages To Date	$	6,500

NATIONAL COOPERATIVE HIGHWAY RESEARCH PROGRAM
TRANSPORTATION RESEARCH BOARD
NATIONAL RESEARCH COUNCIL

A-2357

PROGRESS SCHEDULE

P Project No. 10-14 Locating Voids Beneath Pavement Fy' 79 Month August
:h Agency Ga Tech - EES/RAIL
al Investigator John R. Moore

ARCH ES	Research Task	1979 A	M	J	J	A	S	O	N	D	1980 J	F	M	A	M	J	ESTIMATED % COMPLETION
	Equipment Select & Prep.	50	100														100
	Test Track - Base Constr.		20	100													100
	Test Track - Slab Constr.				50	100											100
	Data Collection					20	40	60	80	100							0
	Data Reduction						25	50	75	100							0
	Develop Math Model						30	60	100								
	Algorithm Selection							25	50	75	100						
	Experimental Evaluation								25	50	75	100					
	Final Report											40	75			100	
LL % ETION		8	22	31	33	36	46	59	70	81	89	92	97	97	97	100	34

FIG. A—OVERALL PROJECT SCHEDULE

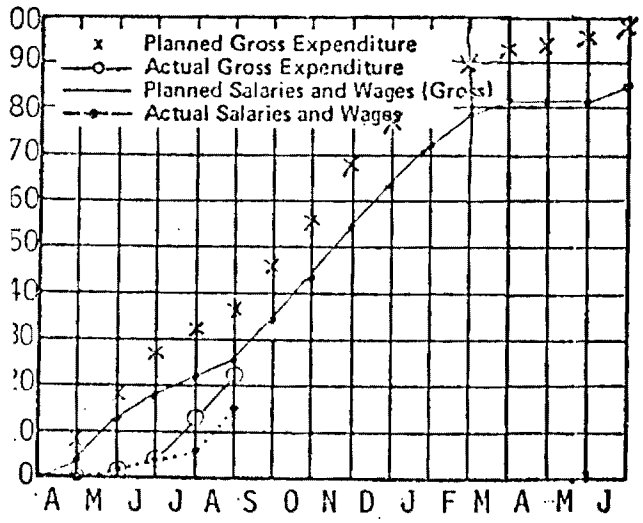

Months

FIG. B—CONTRACT FUNDS

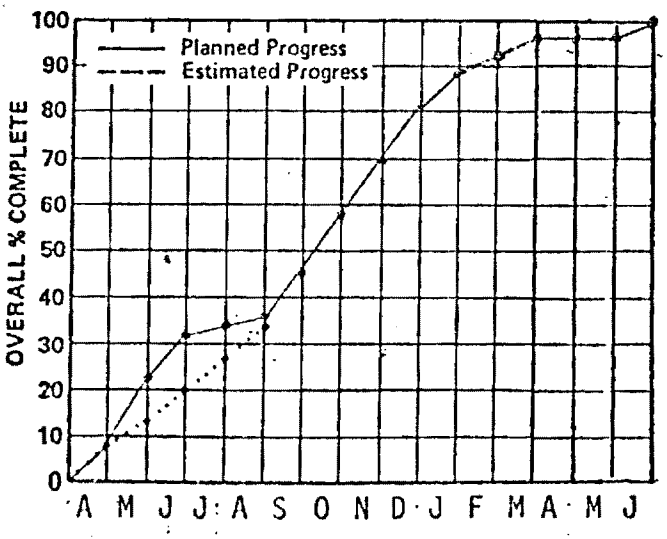

Months

FIG. C—CONTRACT PERIOD

Funds Expended	%	21
Contract Amount	$	100,000
Expended this Month	$	9,300
Total Exp. To Date	$	21,400
Balance	$	78,600

Time Expended %		33
Starting Date		April 2, 1979
Completion Date		June 30, 1980

Salaries and Wages Estimated This Month	$	9,179
Salaries and Wages Spent This Month	$	9,000
Accumulated Salaries and Wages To Date	$	15,500

NATIONAL COOPERATIVE HIGHWAY RESEARCH PROGRAM
TRANSPORTATION RESEARCH BOARD
NATIONAL RESEARCH COUNCIL

A-255

PROGRESS SCHEDULE

A2357

IP Project No. 10-14 Locating Voids Beneath Pavement Fy' 79 Month October
ch Agency Ga Tech - EES/RAIL
ıal Investigator John R. Moore

ARCH ES	Research Task	1979 A	M	J	J	A	S	O	N	D	1980 J	F	M	A	M	J	ESTIMATED COMPLETION
	Equipment Select & Prep.	50	100														100
	Test Track - Base Constr.		20	100													100
	Test Track - Slab Constr.				50	100											100
	Data Collection					20	40	60	80	100							40
	Data Reduction						25	50	75	100							0
	Develop Math Model						30	60	100								20
	Algorithm Selection							25	50	75	100						0
	Experimental Evaluation								25	50	75	100					0
	Final Report											40	75			100	0
LL % TION		8	22	31	33	36	46	59	70	81	89	92	97	97	97	100	43

FIG. A—OVERALL PROJECT SCHEDULE

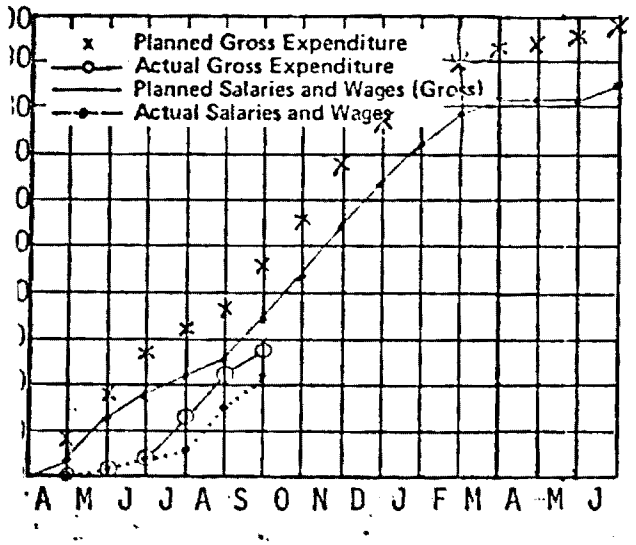

Months

FIG. B—CONTRACT FUNDS

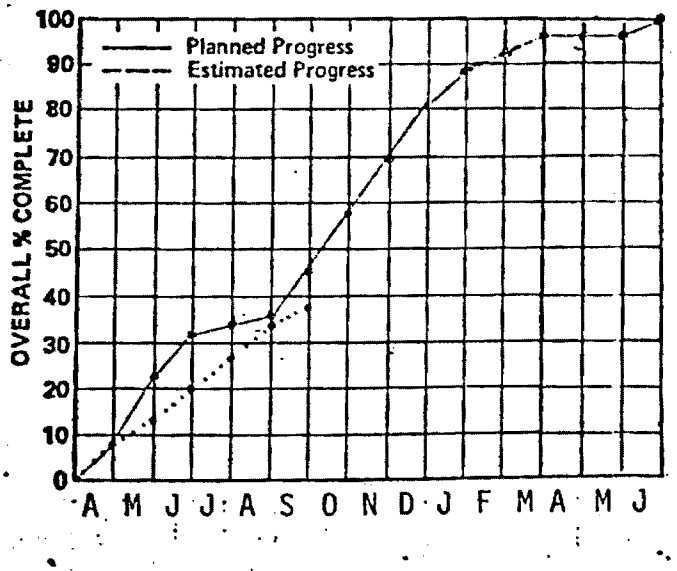

Months

FIG. C—CONTRACT PERIOD

Funds Expended	%	30
Contract Amount	$	100,000
Expended this Month	$	2,000
Total Exp. To Date	$	29,684
Balance	$	70,316

Time Expended %		47
Starting Date		April 2, 1979
Completion Date		June 30, 1980

Salaries and Wages Estimated This Month	$	9,136
Salaries and Wages Spent This Month	$	2,000
Accumulated Salaries and Wages To Date	$	22,297

NATIONAL COOPERATIVE HIGHWAY RESEARCH PROGRAM
TRANSPORTATION RESEARCH BOARD
NATIONAL RESEARCH COUNCIL

PROGRESS SCHEDULE

Project No. 10-14 Locating Voids Beneath Pavement Fy' 79 Month NOV
h Agency Ga Tech - EES/RAIL
il Investigator John R. Moore

RCH S	Research Task	1979 A	M	J	J	A	S	O	N	D	1980 J	F	M	A	M	J	ESTIMATED % COMPLETION
	Equipment Select & Prep.	50	100														100
	Test Track - Base Constr.		20	100													100
	Test Track - Slab Constr.				50	100											100
	Data Collection					20	40	60	80	100							40
	Data Reduction						25	50	75	100							20
	Develop Math Model						30	60	100								80
	Algorithm Selection							25	50	75	100						25
	Experimental Evaluation								25	50	75	100					0
	Final Report											40	75			100	0
L % TION		8	22	31	33	36	46	59	70	81	89	92	97	97	97	100	50

FIG. A—OVERALL PROJECT SCHEDULE

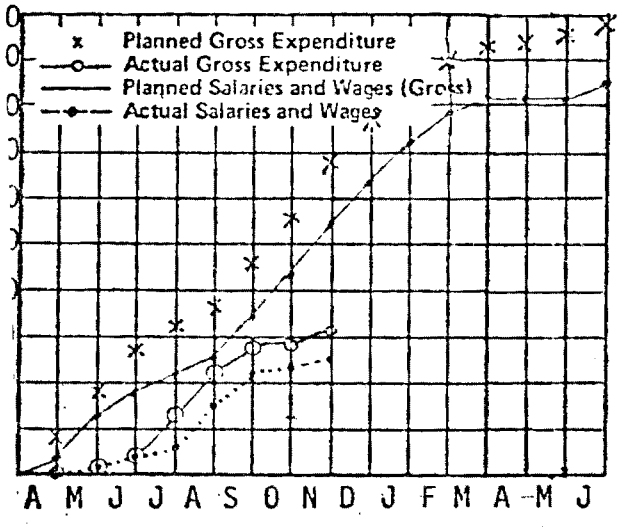

Months

FIG. B—CONTRACT FUNDS

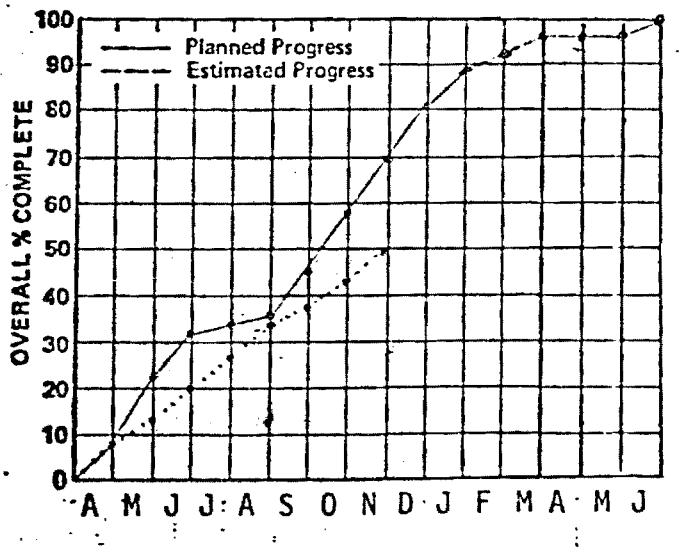

Months

FIG. C—CONTRACT PERIOD

Funds Expended	%	31	Time Expended % 53
Contract Amount	$	100,000	Starting Date April 2, 1979
Expended this Month	$	1,500	Completion Date June 30, 1980
Total Exp. To Date	$	31,184	
Balance	$	68,816	

Salaries and Wages Estimated This Month	$	11,272
Salaries and Wages Spent This Month	$	1,500
Accumulated Salaries and Wages To Date	$	23,797

A-2357

LOCATING VOIDS BENEATH PAVEMENT USING PULSED ELECTROMAGNETIC WAVES

FINAL REPORT

Prepared for

National Cooperative Highway Research Program

Transportation Research Board

National Research Council

W. J. Steinway, J. D. Echard, C. M. Luke

Georgia Institute of Technology

Engineering Experiment Station

Atlanta, Georgia 30067

GT/EES Project A-2357

April 1981

Acknowledgement

This work was sponsored by the American Association of State Highway and Transportation Officials, in cooperation with the Federal Highway Administration, and was conducted in the National Cooperative Highway Research Program which is administered by the Transportation Research Board of the National Research Council.

Disclaimer

LOCATING VOIDS BENEATH PAVEMENT USING PULSED ELECTROMAGNETIC WAVES

FINAL REPORT

Prepared for

National Cooperative Highway Research Program

Transportation Research Board

National Research Council

W. J. Steinway, J. D. Echard, C. M. Luke

Georgia Institute of Technology

Engineering Experiment Station

Atlanta, Georgia 30067

GT/EES Project A-2357

April 1981

TABLE OF CONTENTS

LIST OF FIGURES..... iv

LIST OF TABLES..... viii

ACKNOWLEDGEMENTS..... ix

ABSTRACT..... x

SUMMARY..... 1

CHAPTER 1 INTRODUCTION AND RESEARCH APPROACH..... 3

CHAPTER 2 FINDINGS AND INTERPRETATION..... 5

- Measurement and Processing Equipment..... 5
- Theoretical Modeling..... 10
- Signal Processing..... 12
- Laboratory Measurements..... 17
- Test Lane Measurements..... 21
- Operational Equipment Considerations..... 22

CHAPTER 3 CONCLUSIONS AND SUGGESTED RESEARCH..... 30

APPENDIX A MEASUREMENT AND PROCESSING EQUIPMENT..... A-1

APPENDIX B THEORETICAL MODELING..... B-1

APPENDIX C SIGNAL PROCESSING C-1

APPENDIX D LABORATORY MEASUREMENTS..... D-1

APPENDIX E TEST LANE MEASUREMENTS..... E-1

APPENDIX F SOFTWARE..... F-1

LIST OF FIGURES

FIGURE		PAGE
1	Block diagram of measurement system.....	6
2	Photograph of measurement system.....	7
3	Illustrative signal return.....	9
4	Simulated signal returns; void sizes 0" to 8.5".....	11
5	Amplitude variation of signal returns.....	13
6	Time difference variation of signal returns.....	14
7	Graphical representation of discrimination algorithm.....	16
8	Laboratory measurement configuration.....	19
9	Synthetic display of measurement results.....	20
10	Test lane and measurement equipment.....	23
11	Test lane void layout.....	25
12	Test lane measurements.....	25
A-1	Radar block diagram.....	A-3
A-2	Periodic sampling.....	A-6
A-3	Sequential sampling.....	A-8
B-1	Concrete slab and environment.....	B-2
B-2	Behavior of EM waves at a dielectric boundary.....	B-2
B-3	Behavior of EM waves at air/concrete and concrete/soil boundaries.....	B-5
B-4	Behavior of EM waves at concrete/air and air/soil boundaries.....	B-7
B-5(a)	Multiple reflections between slab faces.....	B-9

LIST OF FIGURES (continued)

FIGURE		PAGE
B-5(b)	Multiple reflections between void faces	B-9
B-6	Theoretical radar time responses	B-11
B-7	Amplitude of positive peak versus void size	B-13
B-8	Amplitude of negative peak versus void size	B-13
B-9	Time difference versus void size	B-13
B-10	Amplitude of peak for various types of read passes	B-13
B-11	Radar environment	B-16
B-12	Void signal	B-16
B-13	Temporal and spectral responses of transmitted wavelength	B-20
B-14	Loss tangents	B-22
B-15	Relative dielectric constants	B-22
B-16	Two-way attenuation	B-23
C-1	Synthetic display for measurements	C-8
D-1	Calibration fixture	D-4
D-2	Laboratory measurements, non-reinforced pavement concrete base	D-5
D-3	Laboratory measurements, non-reinforced pavement clay base	D-6
D-4	Laboratory measurements, non-reinforced pavement, aggregate base	D-7
D-5	Laboratory measurements, non-reinforced pavement, asphalt base	D-8

LIST OF FIGURES (continued)

FIGURE		PAGE
D-6	Laboratory measurements, reinforced pavement, concrete base	D-9
D-7	Laboratory measurements, reinforced pavement, clay base	D-10
D-8	Laboratory measurements, reinforced pavement, aggregate base	D-11
D-9	Laboratory measurements, reinforced pavement, asphalt base	D-12
D-10	Synthetic display measurements for concrete	D-15
D-11	Synthetic display measurements for aggregate	D-16
D-12	Synthetic display measurements for clay	D-17
D-13	Measurements with wet concrete base	D-21
D-14	Measurements with wet clay base	D-22
D-15	Void location simulation: wet base	D-23
D-16	Measurements: void partially filled with water	D-25
E-1	Plan of reinforcing bars and dowel bars	E-3
E-2	Reinforcing bar layout	E-4
E-3	Chair supports	E-5
E-4	Void layout	E-6
E-5	Photograph of test lane layout	E-8
E-6	Photograph of test lane during concrete pouring	E-8
E-7	Schematic diagram of measurements path	E-10
E-8	Test lane measurements, Set #1, 90°F	E-11

LIST OF FIGURES (continued)

FIGURE		PAGE
E-9	Test lane measurements, Set #1, 32°F.....	E-12
E-10	Test lane measurements, Set#1, 48°F.....	E-13
F-1	Basic diagrams.....	F-7
F-2	Main program.....	F-8
F-3	Void processing and plot.....	F-9
F-4	Get data.....	F-10

LIST OF TABLES

TABLE		PAGE
1	Void Size Estimates	26
D-1	Results Summary for Concrete Base	D-18
D-2	Results Summary for Aggregate Base	D-19
D-3	Results Summary for Clay Base	D-20
D-4	Laboratory Attenuation Measurements	D-26
E-1	Void Sizes	E-7
E-2	Attenuation Comparison	E-15
E-3	Results Summary for Test Lane 32°F, 48°F	E-16
F-1	Software Code Listing	F-2
F-2	Variables and Memory Locations	F-11
F-3	Code Locations	F-12

ACKNOWLEDGEMENT

The research reported herein was performed under NCHRP Project HR-10-14 by the Georgia Institute of Technology Engineering Experiment Station.

William J. Steinway - Senior Research Engineer, Jim D. Echard - Principle Research Engineer, and Charles M. Luke - Research Engineer were the principal investigators. Other contributors include Quentin L. Robnett - Assistant Professor in the Civil Engineering Department and John R. Moore - former Research Engineer at the Engineering Experiment Station, now with Radio Corporation of America.

ABSTRACT

This report documents and presents the results of a study to determine the feasibility of using pulsed electromagnetic wave technology for locating and sizing voids beneath reinforced and nonreinforced concrete pavements. The data processing techniques developed can be implemented on equipment operated by field personnel to provide information for void depth and sizing to ± 1/2 inch and spatial location within ± 6 inches. A very short pulse radar directly connected to a microcomputer was chosen as the equipment necessary to obtain measurements. This equipment has the required accuracy and reliability, and is a cost effective solution for the void locating problem. The radar provides a signal return from voids that has unique characteristics that can be examined to provide information regarding the location, depth, and size of the void. The microcomputer provides a means of real-time processing to extract the information from the radar signal return and record the results. Theoretical modeling of signal returns from voids led to suitable techniques for locating and sizing voids beneath the pavement. Analysis and application of these techniques to radar measurements verified the theoretical predictions that radar can be used to determine the location size, and shape of actual voids.

Measurements using pavement 9" thick were made inside a laboratory controlled environment for void sizes from 0" to 8.5" in 1/2" increments, over base materials of concrete, aggregate, asphalt and concrete stabilized clay. Outside measurements were made on a specially

constructed "highway specification" test lane with built-in calibrated voids.

Measurements verified the feasibility of using pulsed electromagnetic wave radar equipment along with appropriate signal processing techniques to locate, and size voids in real-time on the highway in a nondestructive manner.

SUMMARY

Pulsed electromagnetic wave technology has been shown to be very useful for locating and sizing voids beneath reinforced and nonreinforced concrete pavement. Specific signal processing techniques have been developed that provide the field personnel with information for void detection; spatial location to within ± 6 inches, and sizing to ±0.5 inches. The signal processing techniques were implemented on a microcomputer system so that the results can be displayed on a video unit, permenantly stored on magnetic diskettes, and printed directly on paper for permanent hard-copy.

Experimental evaluation of the pulsed electromagnetic wave equipment and signal processing techniques for void detction and sizing was accomplished under laboratory controlled conditions. The equipment accuracy, precision, reliability, limitations, and operational characteristics were evaluated using 9 inch thick sections of reinforced and nonreinforced concrete pavement containing calibrated voids and base materials of concrete asphalt, aggregate, and concrete stabilized clay. Void sizes from 0" to 8.5" in 0.5" increments were measured under laboratory controlled conditions including several moisture levels.

Additional measurements were made on a specially constructed outdoor concrete pavement test lane, 72 feet long by 8 feet wide by 9 inches thick. Calibrated voids of various shapes and sizes were surveyed in-place before concrete was poured, and reinforcing steel was implanted in one-half of the test lane. Initial measurements made at 100°F

temperature enabled trained operators to detect voids but the magnitude of the signal return was not large enough for the microprocessor algorithms to detect and size the voids. This lack of signal strength was attributed to the moisture content and temperature conditions under which the measurements were made. Succeeding measurements made at temperatures in the range from 32°F to 70°F yielded excellent estimates of void location and size. the signal processing algorithms, making use of both amplitude ratios and time differences with respect to reference calibrations, have been verified to perform as designed.

Future suggested research includes continuing measurements, both in the laboratory and outside, to more fully substantiate the effects of temperature and moisture. Measurements should be made when temperatures are as high of 100°F to below freezing, in 5-10°F intervals. A full set of measurements so that seasonal temperature/moisture cycles can be taken into account would require tests over a period of 9-12 months, and establish exact limitations on the equipment operation. An engineering design study should be conducted to establish specifications and cost estimates for a fully ruggedized void location and sizing system for highways.

CHAPTER ONE

INTRODUCTION AND RESEARCH APPROACH

An ability to locate voids beneath portland cement concrete pavements by periodic nondestructive surveys would permit replacement of support material before the development of pavement distress and loss of structural qualities. The primary objective of NCHRP Project HR-10-14 is to determine the practicality of using pulsed electromagnetic wave technology for locating voids beneath reinforced and nonreinforced portland cement concrete pavements up to 18 inches thick. Another objective is the identification or development of data processing techniques suitable for use with equipment that can be operated by field personnel and provide information on the parameters of voids beneath the pavement.

Initial work on this project was directed towards obtaining the pulsed electromagnetic wave equipment that showed promise for accuracy, reliability and economical application for locating and defining voids beneath pavement slabs. The research approach included a examination of existing pulsed electromagnetic wave equipment, signal processing hardware, and recording devices.

After this initial work, attention was concentrated on the development of data analysis algorithms for processing the response signals from the pulsed electromagnetic wave equipment to enable identification of the location, size, and shape of voids beneath pavements. The first step was to construct a mathematical model for the pavement/void/base configuration and a mathematical model for the eletromagnetic wave equipment. The

two models were then combined and used to predict response signal characteristics. This theoretical model was used as an aid to developing data processing algorithms that can be used to locate and identify void shape, size, and depth beneath pavements.

The final task on this project was the experimental evaluation of the void detection pulsed electromagnetic wave equipment and data analysis procedures with regard to accuracy, precision, reliability, limitations, operational characteristics, and environmental effects. Measurements were made in two phases. The first measurement phase was conducted under laboratory controlled conditions using sections of concrete pavement, 9 inches thick with and without reinforcing steel, over various types of base materials, with both low and high moisture levels. In addition, voids were of various sizes, both empty and filled with water. The second measurement phase was conducted using a specially constructed outdoor test lane, 72 feet long and 8 feet wide, of 9 inch thick concrete over an aggregate base. Calibrated voids of various sizes, were surveyed in-place before concrete was poured and reinforcing steel was placed in one-half of the test lane.

The basic report includes only a brief description of the electromagnetic wave equipment, the data analysis procedures, and the results and interpretation of the measurements made in the laboratory and on the outside test lane. The details of the work are presented in separate appendices covering the electromagnetic wave equipment selected, the theoretical modeling, signal processing algorithms, laboratory measurements and results, and test lane construction, measurements, and results.

CHAPTER TWO

FINDINGS AND INTERPRETATION

Measurement and Processing Equipment

The electromagnetic wave equipment chosen for measurements on this project was a very short pulse radar. This radar has the required accuracy and reliability and can be economically constructed. The characteristics of the radar signal response from pavement containing voids will allow signal processing algorithms to recognize small variations related to void detection and identification.

The equipment includes output devices that clearly display results in easily interpreted symbols and is mounted on a moveable platform. The system is totally portable and can be operated by a semi-skilled person. A microcomputer is used to control two output devices: a video screen display and a line-printer. The radar signal response from the pavement/void is processed in an "on-line" fashion by the microcomputer to extract information useable by the field personnel in determining void location, depth, size and shape. Permanent recording of the radar signals is available automatically via magnetic disks attached to the microcomputer. Measurement results for void detection are presented on the video monitor and the line-printer.

The radar system and the microcomputer were mounted on a cart that can be pushed to most locations for measurement purposes. A complete description of the radar hardware and the microcomputer is given in Appendix A. Figure 1 is a block diagram of the system, and Figure 2 is a photograph of the equipment mounted on the cart.

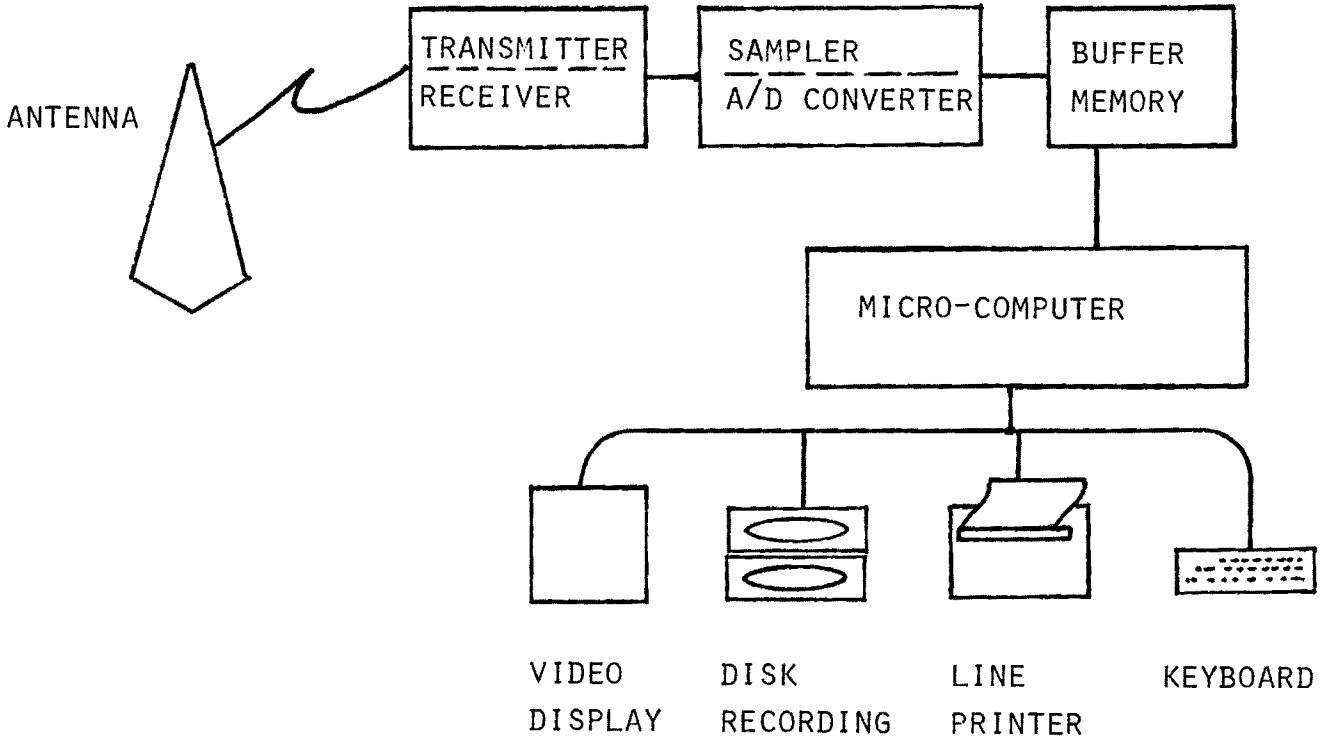

FIGURE 1

BLOCK DIAGRAM OF MEASUREMENT SYSTEM

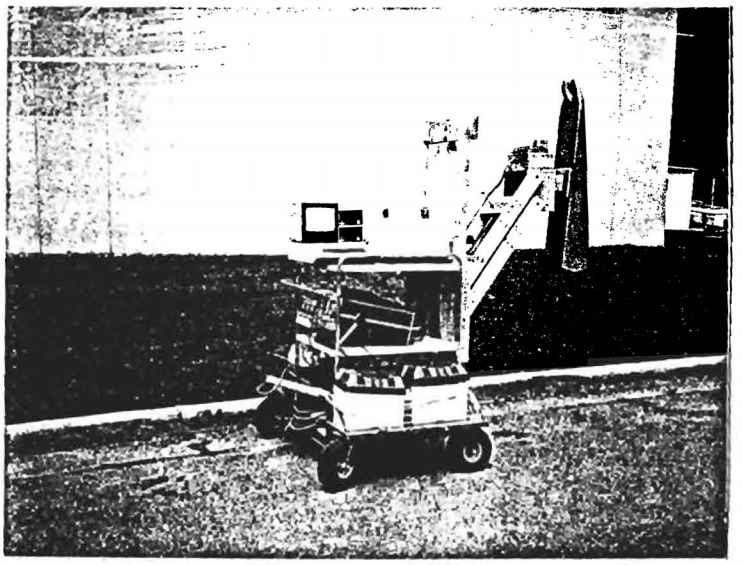

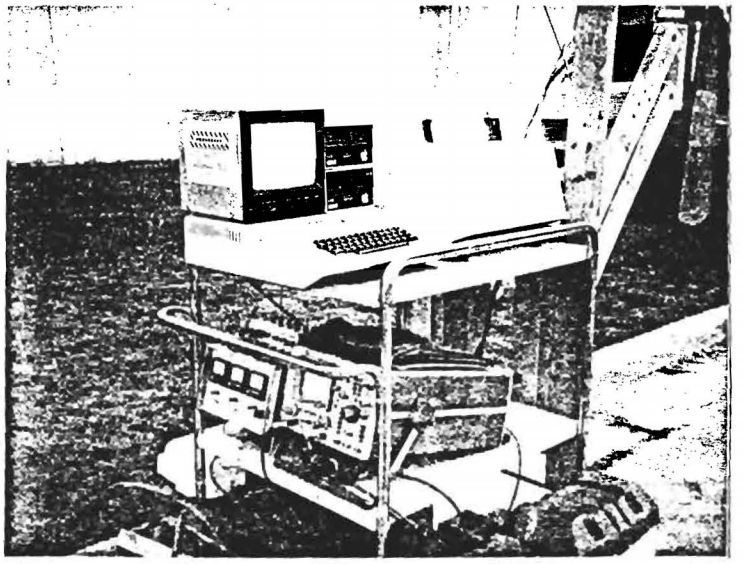

FIGURE 2

PHOTOGRAPH OF MEASUREMENT SYSTEM

It is emphasized that the system described and used by the researchers for this study is not a fully operational highway version, the equipment has not been ruggedized. Measurements provided by the radar equipment and the algorithms programmed on the microcomputer are identical to those desired in an operational system.

A typical return signal waveform from concrete pavement with a void beneath is represented in Figure 3. It is instructive to examine this in detail. The transmitted pulse is a single "sinewave" cycle of approximately 1 nanosecond in time. It travels through a coaxial cable and is connected to the antenna. The connector on the antenna causes a small reflection to be observed in the signal return. The signal travels through the horn type antenna cavity and enters the air medium. The antenna itself is not perfectly matched to the air, thus another reflection occurs at the end of the antenna. This reflection tends to be very distorted and large in amplitude. The signal that is propagated in air strikes the surface of the concrete, and only a very small amount penetrates. The majority is reflected, and appears as a replica of the transmitted pulse. Of the signal that does penetrate, some energy will be reflected by each subsequent interface. In the case of a "no void" situation a single small return will be present from the pavement/base interface. In the case of a "void" existing, two signals will be present. The time of occurance and amplitude of those signals are the important parameters for void location and size determination.

In the data measurements presented in this report only the time interval of the signal return around which a void typically will occur is processed and displayed (or plotted).

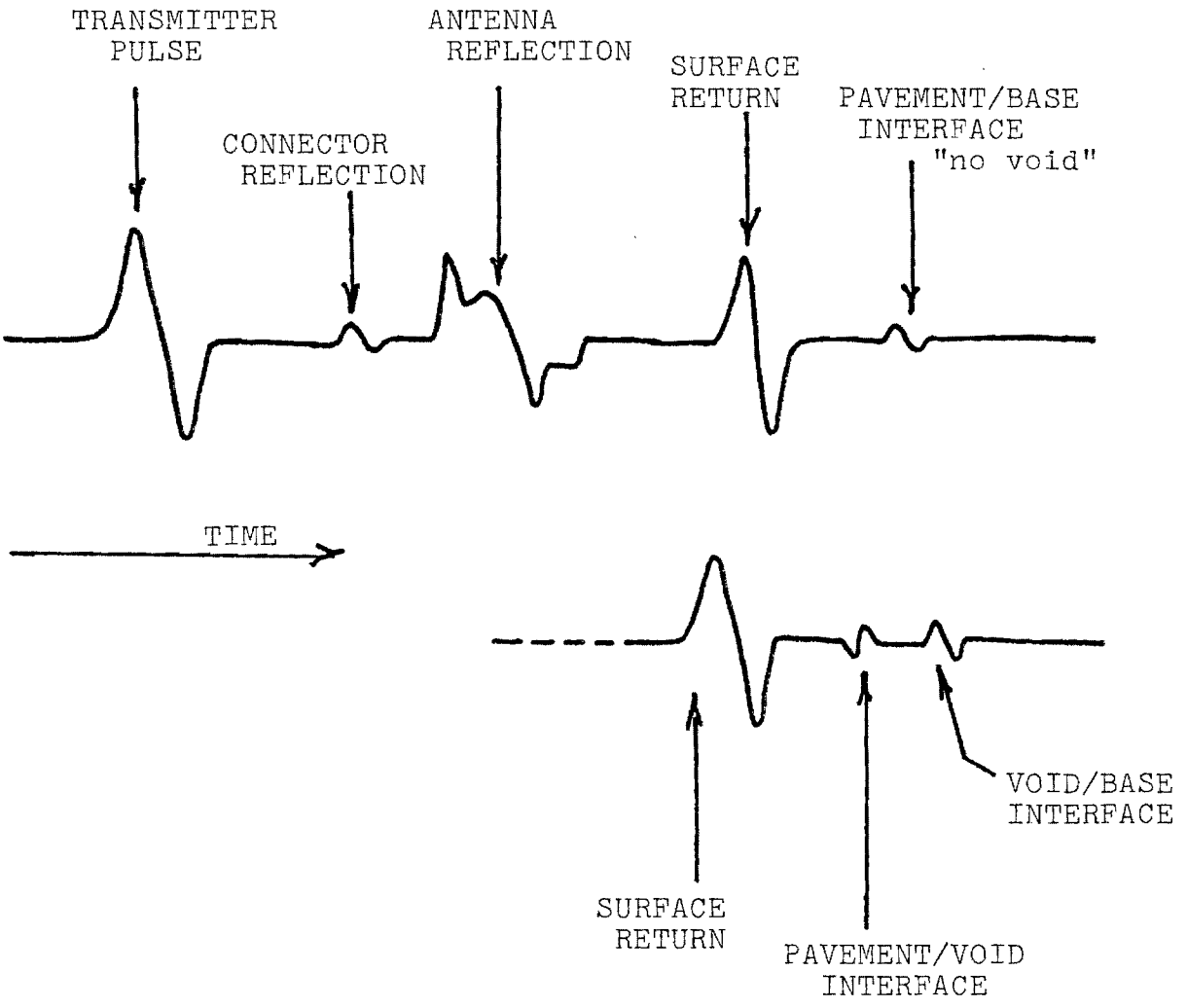

FIGURE 3

ILLUSTRATIVE SIGNAL RETURN

Theoretical Modeling

The development of a theoretical signal model was essential to the understanding of the problem of making measurements of voids under pavement via radar. Transmission line theory provided the means for the modeling solution; the details are given in Appendix B. The mathematical algorithms derived from the study were programmed on the microprocessor, and many simulated data sets were generated.

The simulated data sets were analyzed to extract signal characteristics unique to the void detection and identification process. In this process two important discriminants were identified, and provide the theoretical basis for the signal processing techniques. For voids less than two and one half to three inches, there is primarily a change in the amplitude of the return signal. For voids larger than this a time difference measurement is used; that is measuring the time difference between the negative and positive peaks of the return signals from the void interfaces.

Figure 4 illustrates a set of simulated signal return from voids ranging in size from 0" to 8.5" in 0.5" increments.

The set of signal returns is plotted only around the actual time of void occurance. At time t=0 is the surface of the pavement. The return that occurs at approximately 2 nanoseconds in time in traces 0.5" to 8.5" is the reflection from the bottom of the pavement/top of void air space interface, and is an inverted version of the transmitted signal. The part of the signal that occurs at a varying time from 2.3 ns to 3.5 ns is the return from the air/base interface. Where the two signals inter-

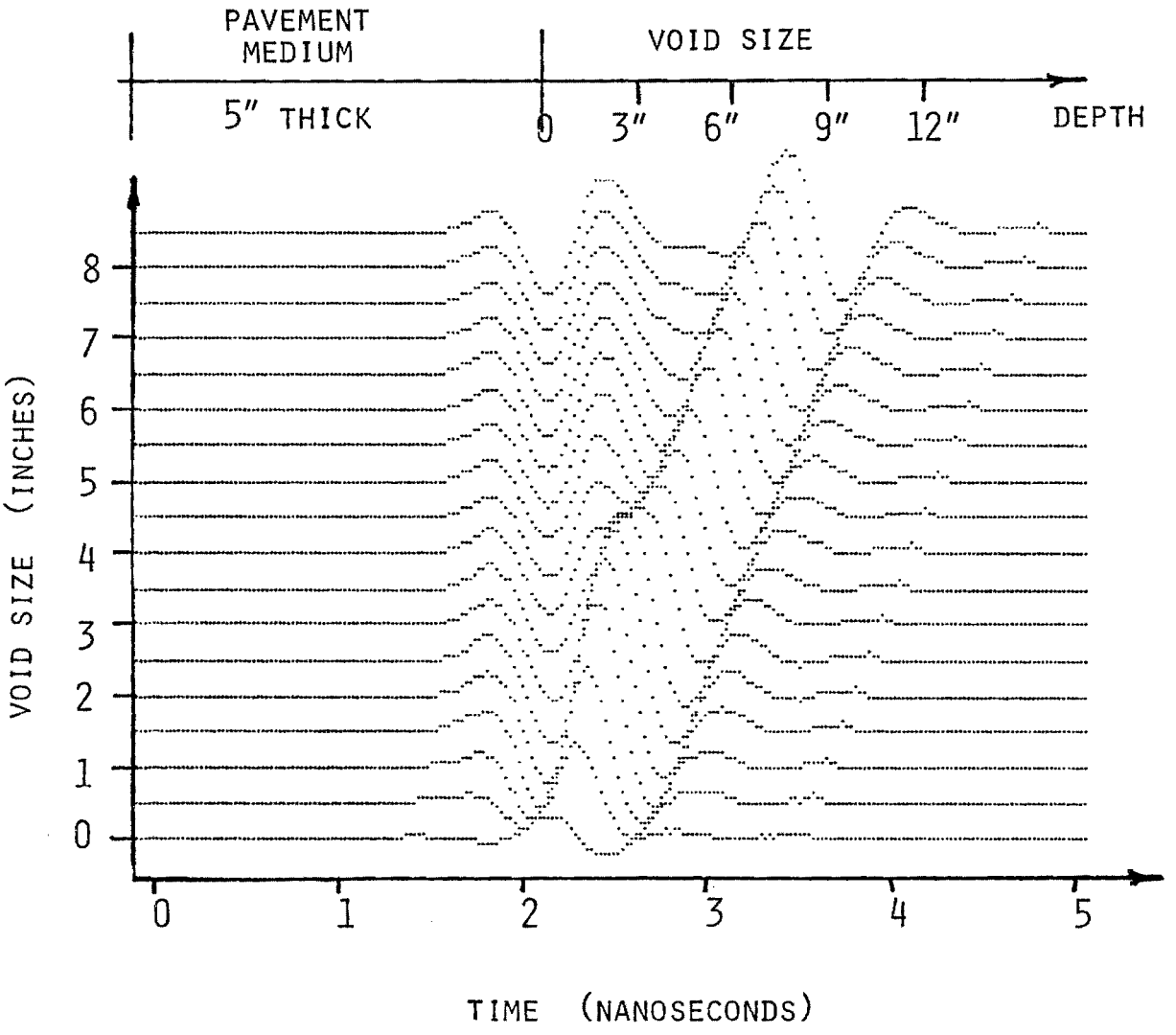

FIGURE 4

SIMULATED SIGNAL RETURNS

fere with each other, void sizes 0.5" to approximately 3", an amplitude variation is visible. Beyond 3" the time difference is the key indicator of void size.

The time scale for the data is linearly related to depth, but will be segmented dependent upon the dielectric constant through which the signal is propagating. In Figure 4, a depth scale is indicated at the top of the plot and is divided into two parts. The first part represents the time/ depth scale through a medium with $\varepsilon = 6$. The second part is scaled with respect to air, $\varepsilon = 1$ for the void area. Thus, concrete thickness can be read directly as can void size, with the two readings added to give depth to the base. Beyond the air/base reflection the air time calibration is not valid. With this segmented time/depth relation in mind the plots in this report will be simply labeled in time only (nanoseconds), with the realization that in air/void areas, 1 nanosecond equals 5.9 inches.

If the variations of the time and amplitude are plotted versus void size Figures 5 and 6 result. In Figure 5 the important area of the amplitude variation occurs between 0" and 2.5" where a monotonically increasing relationship is evident. The time difference plot of Figure 6 illustrates a linear relationship with void size from approximately 3" and greater.

Signal Processing

The analog signal processing begins with detection of the large signal return from the top surface of the concrete. A timing window is started when the top surface of the concrete is detected and stopped

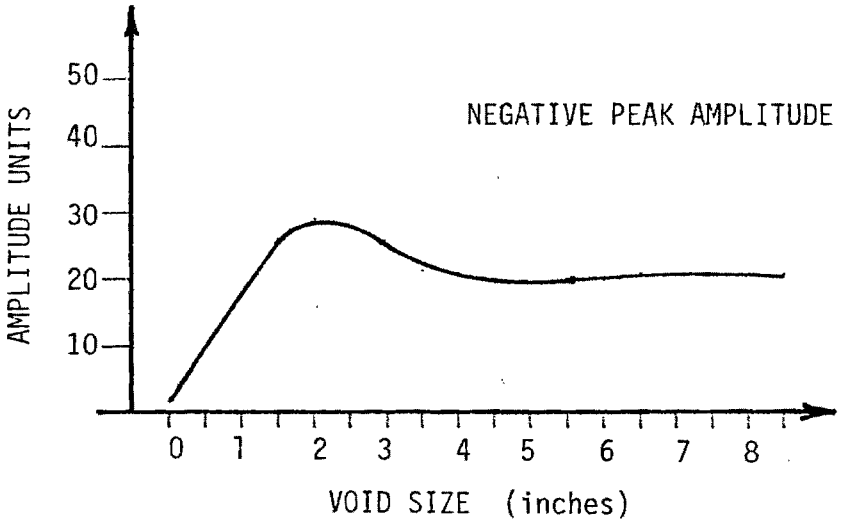

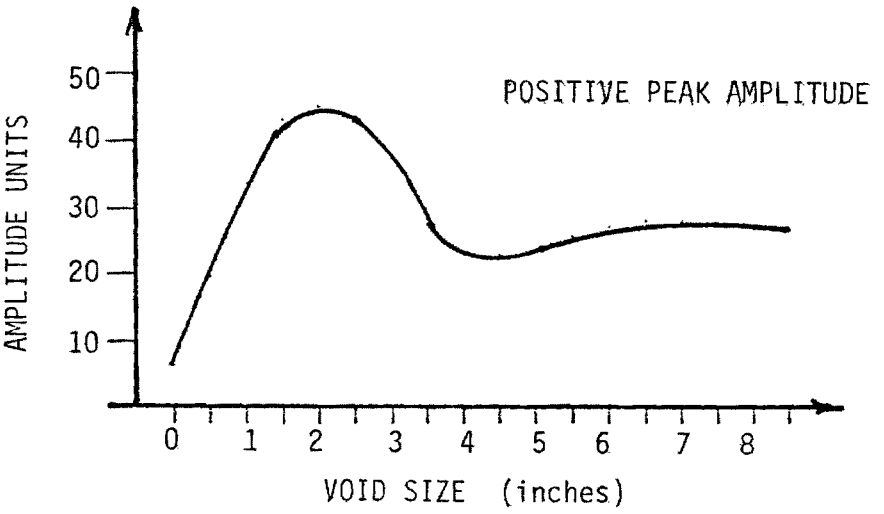

FIGURE 5

AMPLITUDE VARIATIONS OF SIGNAL RETURNS

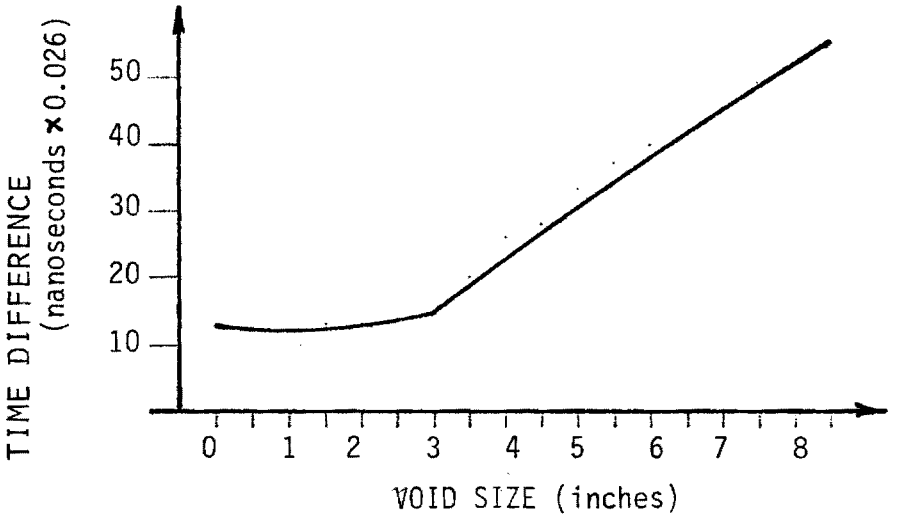

FIGURE 6

TIME DIFFERENCE VARIATION OF SIGNAL RETURNS

after approximately twenty nanoseconds has elasped. The signal response during the timing window represents the return from typical concrete pavement and the base material to a depth of at least 24 inches. A portion of this signal, from the pavement surface to approximately 12 inches depth is then digitized by an analog-to-digital converter and stored in a digital buffer that is accessible by the microprocessor. The actual measurement process is controlled by the operator via microprocessor commands; the operator can position the equipment over the area to be tested and designate when a measurement is to be made.

The digital signal processing algorithms were synthesized from information provided by the theoretical modeling study. The specific discriminants used are the time between the negative and positive peaks, and the amplitudes of those peaks. The computer algorithms search through the electromagnetic return signal and identify minimum and maximum values and their time of occurrance. If the amplitude exceeds a minimum threshold and time differences fall within prescribed bounds then a void is said to exist. The time discriminant is then examined to determine if the void size is greater than or less than three inches. If the void is less than three inches, the amplitude is employed to obtain the void size estimate. If the void size is greater than three inches then a time difference is used to directly gauge void size.

A graphical representation of the void sizing algorithm is given in Figure 7. In the first part of the algorithm the void size is based upon the ratio of the negative peak to a calibration number. This number is determined by the operator during a set of preliminary calibration measurements. The procedure for calibration involves finding sections of

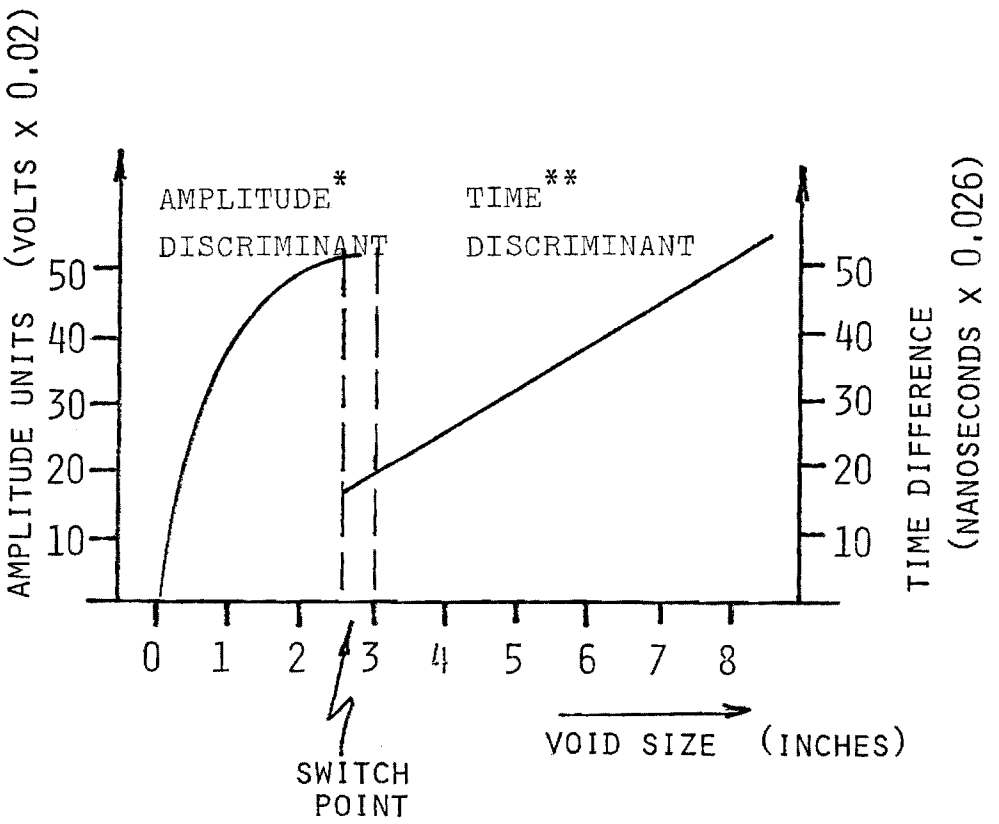

*AMPLITUDE: void size = $(6/\pi)\ \sin^{-1}\left(\frac{\text{amplitude peak}}{\text{calibration \#}}\right)$

**TIME: void size = 0.026 x 5.9014402 x time units

FIGURE 7

GRAPHICAL REPRESENTATION OF DISCRIMINATION ALGORITHM

pavement where voids are not likely to exist and making measurements. The signal return accepted for calibration at that time is used as a reference during the remainder of the measurements. The second part of the void sizing algorithm makes use of the time difference between the negative and positive peak signal returns from the concrete/void interface and void/ base interface respectively. At approximately 3" and greater these signals have a time difference that is directly proportional to the void size. Appendix C covers the details of the signal processing.

The next step in the signal processing is to present the results on the visual display. Microcomputer software was developed to display the signal return from a particular measurement, whether or not a void exists, and the size of the void if it exists. The information is also automatically saved for future use and can be typed out on a line printer for permanent recording. Various options were also incorporated to permit permanent visual recording of the signal waveform on magnetic disk. Post processing software was developed to display a sequence of measurements and send the plot to the line-printer for permanent recording. All of the plots of signal waveforms in this report were generated or processed by the microcomputer and subsequently plotted on the line printer.

Laboratory Measurements

The experimental evaluation of the void detection pulsed electromagnetic wave equipment and signal processing algorithms was accomplished in two phases. The objective was to evaluate the accuracy, precision,

reliability, limitations, operational characteristics, and environmental characteristics of the equipment and processing algorithms. The first phase was conducted inside a laboratory under controlled environmental conditions. Test sections of concrete pavement approximately 43 inches by 43 inches by 9 inches thick, both reinforced and nonreinforced, were used. These test sections were placed over base materials of concrete asphalt, aggregate, and cement stabilized clay. Measurements were made as the moisture levels for the pavement section as well as the base material were varied. Voids were simulated by elevating the pavement section a measured amount above the base material. Figure 8 is a photograph of a pavement section over the clay base, a 4" void is visible. Measurements were made for void sizes ranging from 0" to 8.5" in 0.5" increments. These measurements are illustrated in Appendix D. Some measurements were made for simulated voids partially filled with water. The findings indicate a definite agreement with the theory as to the variation in amplitude of the positive and negative peaks and in the time differential of the peaks. Thus, the discriminates from the theoretical considerations were verified. In addition, the measurements provided the basis verifying and refining the theoretical model.

As an example of the results achieved, Figure 9 is an representation of what the operator would see on the visual display after processing a set of measurements as given by Figure 4. A brief explaination of this figure is given here; the reader is referred to Appendix C for further details. The horizontal axis represents a series of sequential measurements; in the case illustrated, 18 measurements have been made. The vertical axis is calibrated in inches and information about the signal

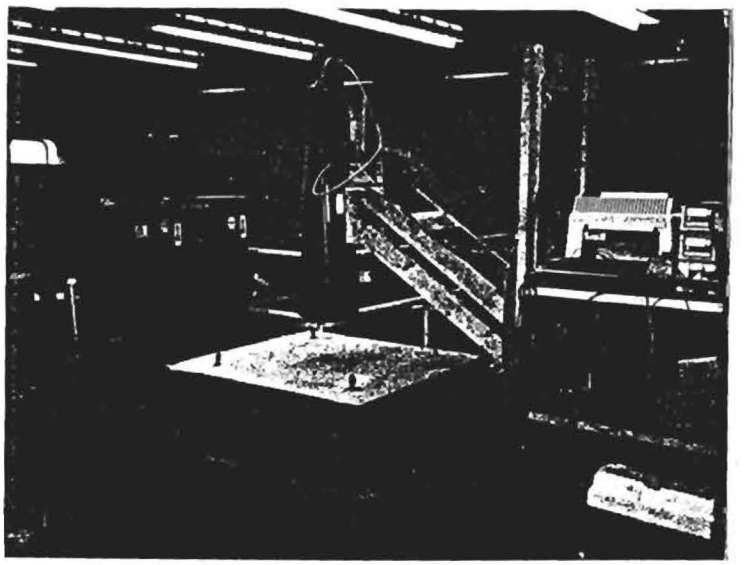

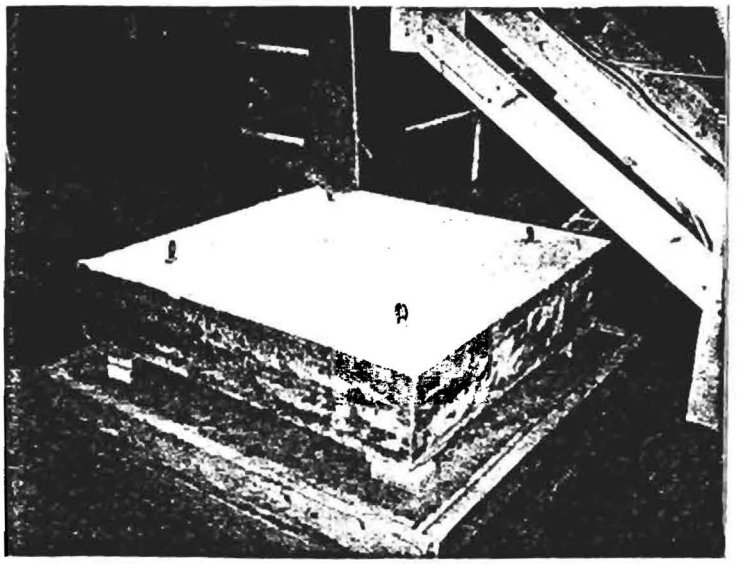

FIGURE 8

LABORATORY MEASUREMENT CONFIGURATION

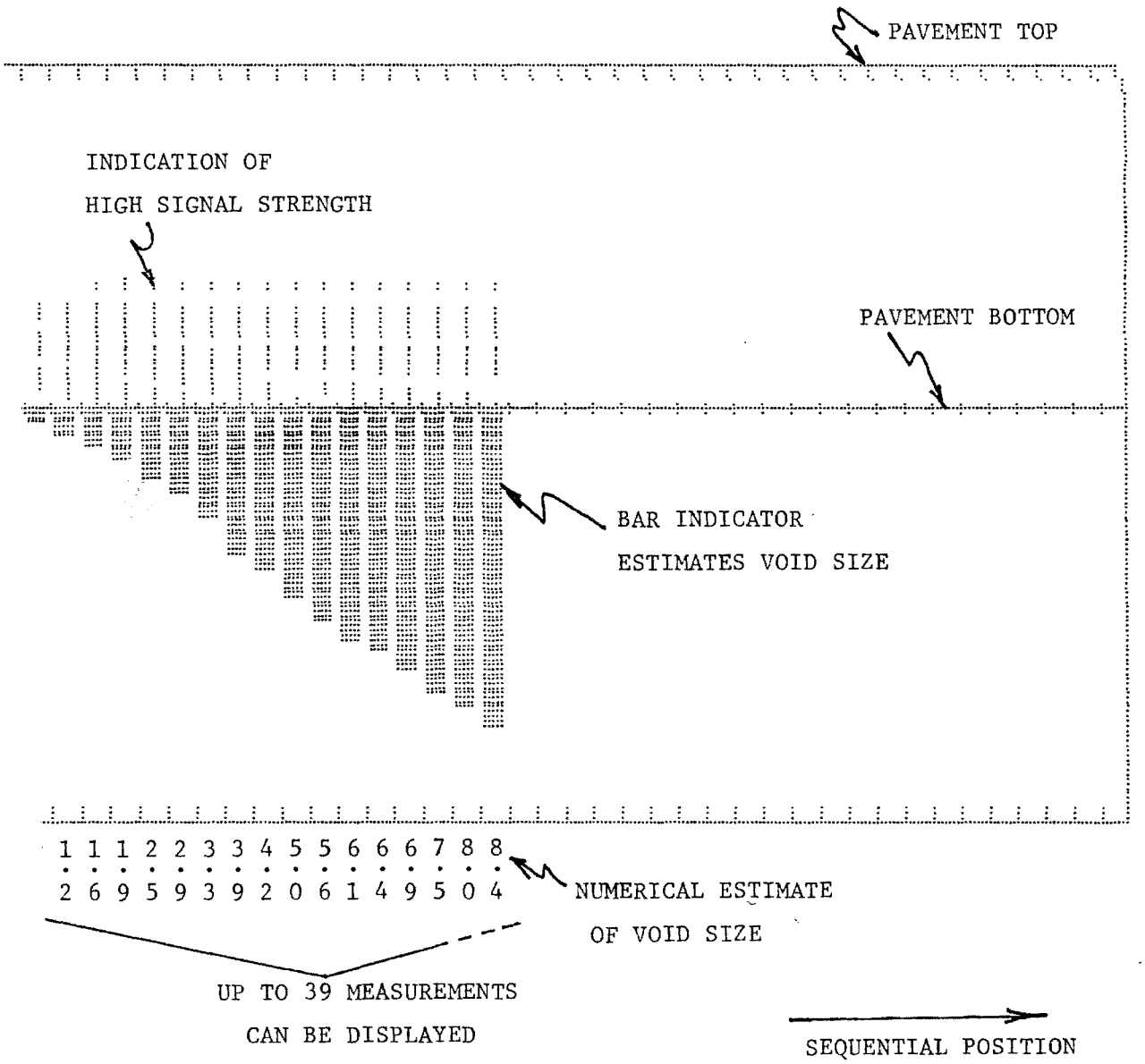

POSITION #	1	2	3	4	5	6	7	8	9	10	11	12	13	14	15	16	17	18
VOID SIZE	0	0.5	1.0	1.5	2.0	2.5	3.0	3.5	4.0	4.5	5.0	5.5	6.0	6.5	7.0	7.5	8.0	8.5
ESTIMATE	0	0.6	1.2	1.6	1.9	2.5	2.9	3.3	3.9	4.2	5.0	5.6	6.1	6.4	6.9	7.5	8.0	8.4

ERRORS: MEAN = -0.028", standard deviation = 0.123"

FIGURE 9

SYNTHETIC DISPLAY OF MEASUREMENT RESULTS

return and a void if detected and sized is represented. The estimated size for the void is represented two ways; one, by the length of a vertical bar and two, by the numbers read vertically downward at the bottom of the plot. The distance from the top of the plot to the horizontal line where the void bars begin represents the concrete pavement, below the line is base material. The narrow vertical lines visible above the void size bars represent areas of the signal return where the amplitude exceeds a threshold value. Currently this value is set just above the clutter or noise in the signal return, thus only the strongest signals are displayed.

As indicated by the void bars, this is a sequence of increasing size voids, and follows the signal sequence given in Figure 4. The signals were generated by simulation for voids of 0" to 8.5" in 0.5" increments. The estimated sizes, via the algorithms, are summarized below the plot. The mean and standard deviation for these estimates is $\mu = -0.028"$, $\sigma = 0.123"$. Additional plots are given in Appendix D for actual measurements on several base types.

Test Lane Measurements

The second phase of the experimental evaluation was conducted on a specially constructed outdoor "test lane" which is representative of a section of concrete highway. The test lane measures 72 feet long, 8 feet wide, and 9 inches thick. The test lane was constructed according to the Georgia Department of Transportation specifications using portland cement concrete over aggregate base. Calibrated voids of various sizes and shapes were surveyed in place before the concrete was poured. In one

half of the test lane reinforcing steel was used. The voids were created by shaped pieces of lightweight foam, the foam itself being virtually invisible to the electromagnetic signal.

Figure 10 is a photograph of the measurement equipment on the test lane and Figure 11 gives an approximate layout for the voids beneath the pavement and the reinforcing bars in the pavement. Exact measurements resulting from the survey of the test lane are given in Appendix E. Measurements on the test lane were made over the wide temperature range of 32°F to 100°F which had a definite influence on the results of the signal processing algorithms. Moisture is also a critical element that can affect performance. Initially when measurements were made during the summer at temperatures around 90°F, void indications were visible only to a trained operator. The microprocessor processings algorithms were not capable of the performance desired. Measurements subsequently made during the Fall and Winter seasons at temperatures down to 32°F, produced excellent results.

Figure 12, presented in the format of Figure 9, is the result of a set of processed measurements taken every 6" along a path through the center of voids as indicated in Figure 11. The void sizes that were estimated by the processing algorithms are given both on the figure, as the would be seen by the operator, and in Table 1. The results of Table 1 indicate void size estimates with a $\mu = 0.09"$ and $\sigma = 0.46"$.

Operational Equipment Considerations

Several factors must be considered if this system is to be built for field operation. They include the efficient coverage over an actual highway and modifications for environmental conditions.

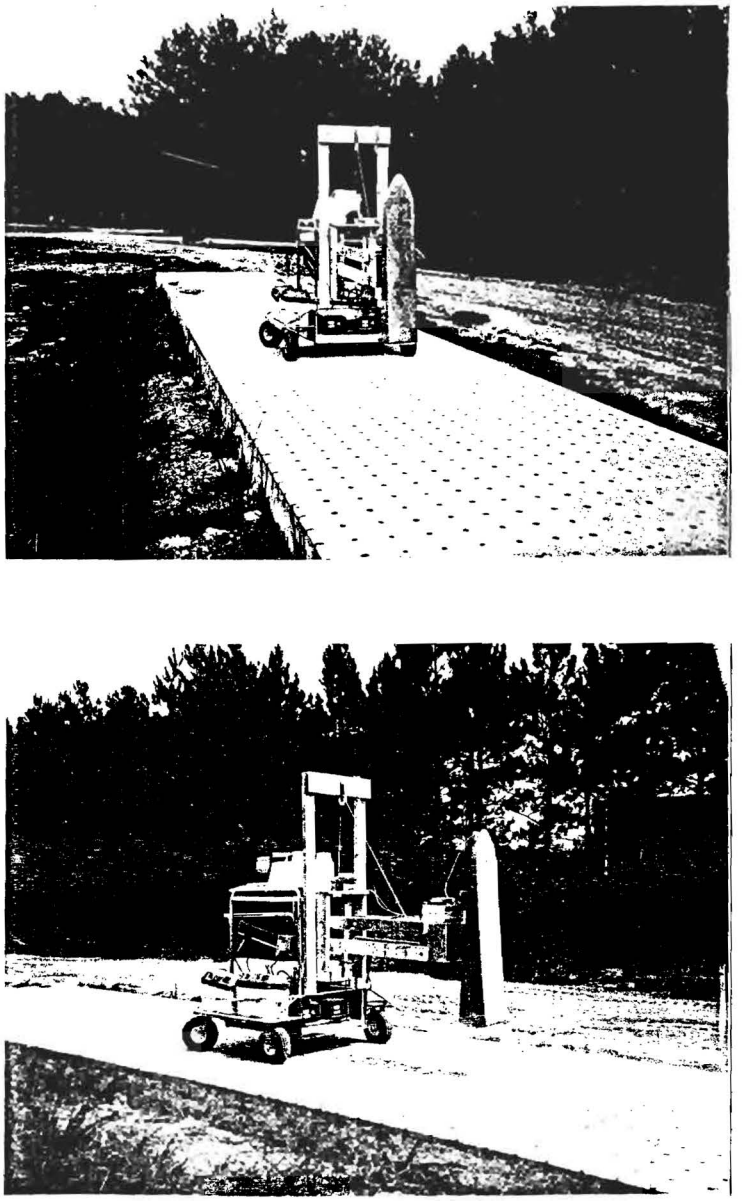

FIGURE 10

TEST LANE AND MEASUREMENT EQUIPMENT

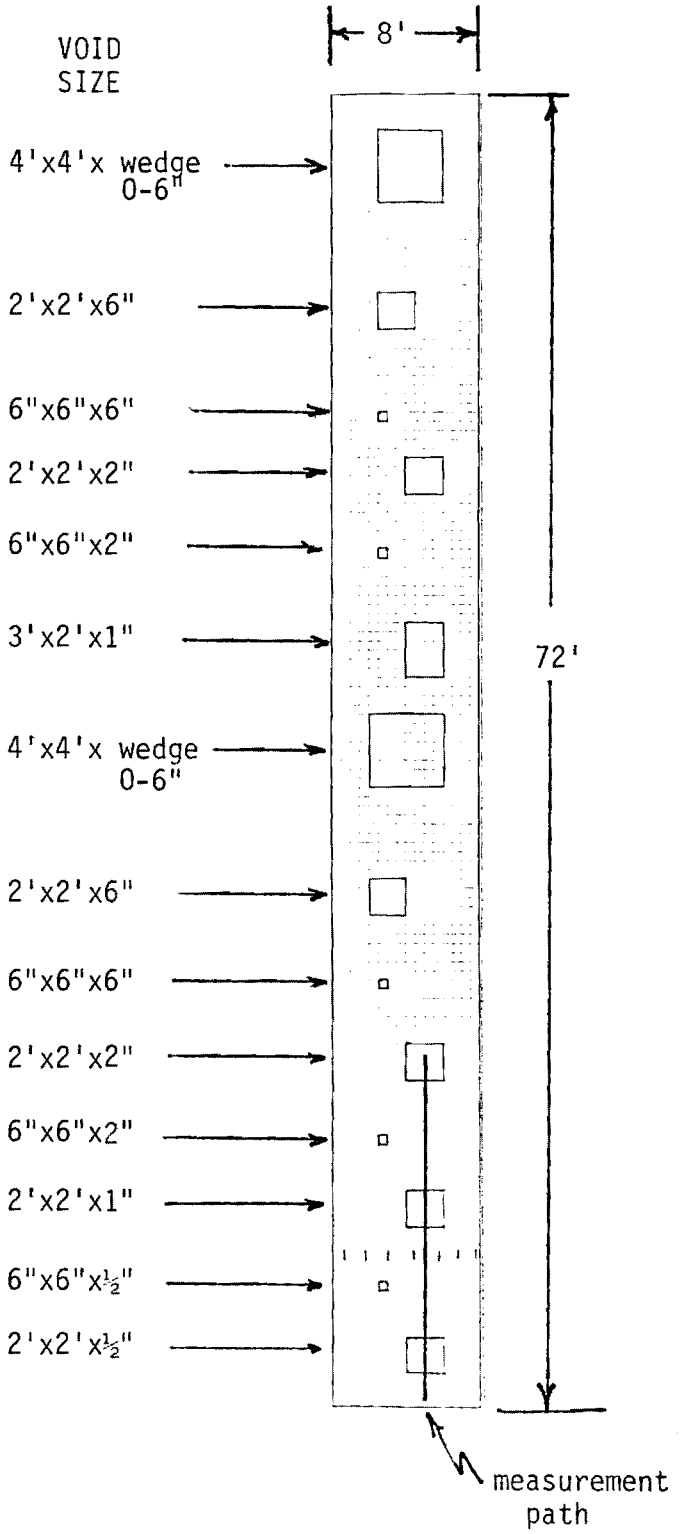

FIGURE 11

TEST LANE VOID CONFIGURATION

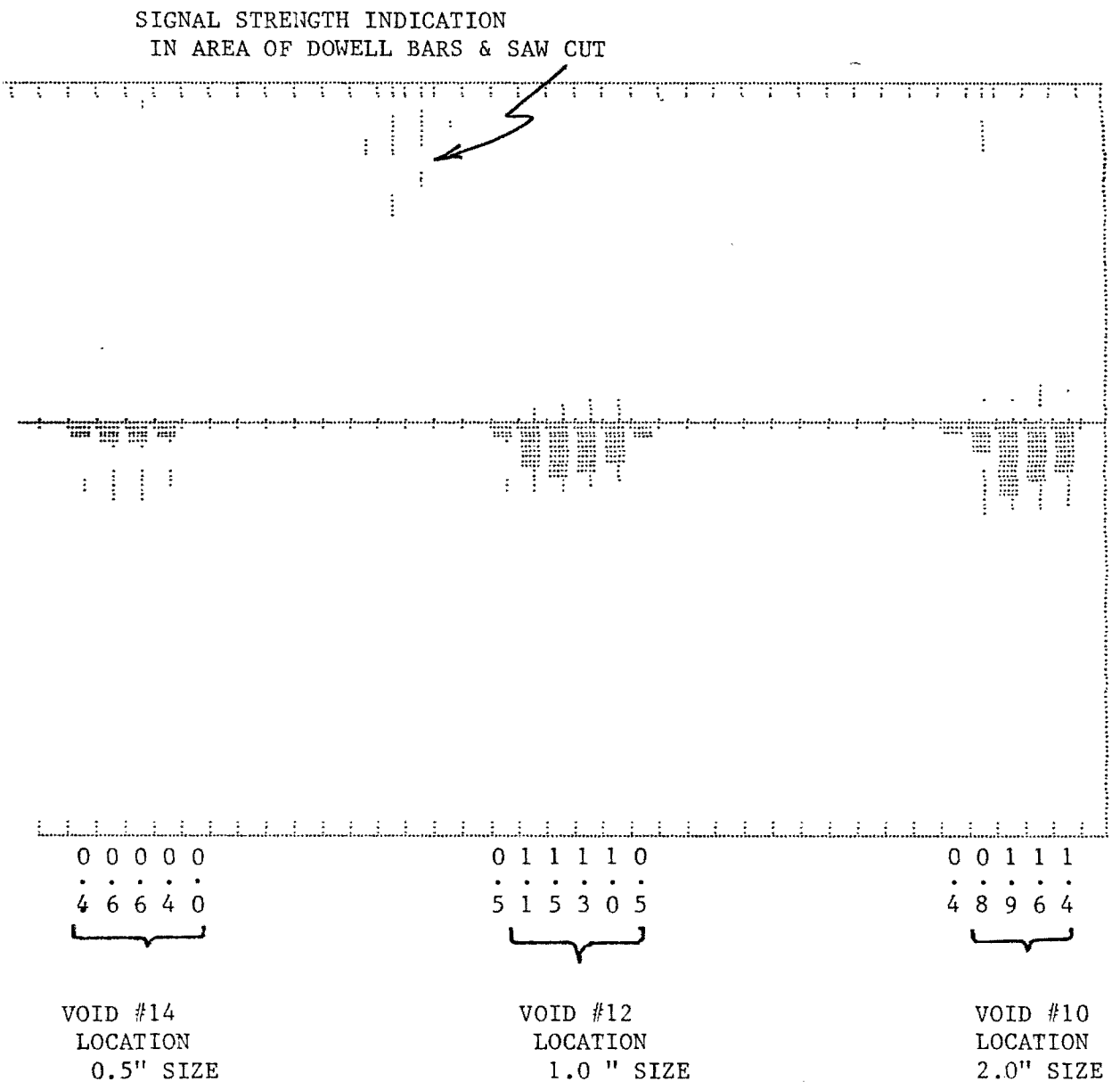

FIGURE 12

TEST LANE MEASUREMENTS

TABLE 1

VOID SIZE ESTIMATES*

VOID #	TEST LANE POSITION	ACTUAL VOID SIZE	VOID SIZE ESTIMATE	SIZE ERROR	POSITION ERROR
14	70.'	0.5	.4	-.1	0
14	69.5'	0.5	.6	+.1	0
14	69.'	0.5	.6	+.1	0
14	68.5'	0.5	.4	-.1	0
14	68.0'	0.5	.0	-.5	.0
12	62.5'	0.	.5	+.5	-6.
12	62.'	1.0	1.1	+.1	0
12	61.5'	1.0	1.5	+.5	0
12	61.'	1.0	1.3	+.3	0
12	60.5'	1.0	1.0	0.	0
12	60.'	1.0	0.5	-.5	0
10	54.5'	0.	.4	+.4	-6
10	54.'	2.	.8	-1.2	0
10	53.5'	2.	1.9	-.1	0
10	53.'	2.	1.6	-.4	0
10	52.5'	2.	1.4	-.6	0

SUMMARY: $\bar{X} = -0.09"$
$\sigma = 0.46"$

*Except for void# and position, the data are in inches.

Speed of highway coverage. The current radar unit has an effective signal (or pulse) per second output of 50 PPS. If one reading every six inches is used as a criterion, then the unit has the capability of covering 25 feet/ second or 17.1 miles/hour. Thus, the radar unit itself has a reasonable coverage/speed capability. The microprocessor is currently configured as a demonstration unit and processes only about one signal return every 5 seconds. Indeed, even if efficiently written software code were used it is doubtful that any acceptable speed could be produced. Thus, a new faster processor unit must be implemented. Identical operations to that used by the researchers would be programmed, the only difference would be speed of processing. Processors exist on the market today that have the desired capability.

Width of highway coverage. Currently the antenna in use is effective over not more than a 2 foot width (±1 one foot). It is noted that the characteristics are slightly different in the length direction for an effective coverage of ±6 inches. To completely cover a single highway lane at one time would require the use of multiple antennas. There appears to be no mechanical equipment problem posed by the mounting of multiple antennas in a side-by-side configuration. There would be electrical considerations. The antennas would have to be sequentially pulsed with energy and some of the signal background characteristics might change due to coupling of energy into adjacent antennas. It is thought at this time by the researchers that the electrical changes pose no problem in interpreting the signal return from a void. The speed of highway coverage would remain the same (17.1 mph maximum) with multiple antennas.

Environmental factors. As currently configured the equipment is an experimental measurements system. None of the hardware has been exposed to, nor was it expected to be, the rigors of highway use day after day. Both the radar unit and the microprocesser must be re-packaged for that purpose. The actual re-packaging of the equipment to withstand highway conditions, including environmental factors such as rain, snow, heat, etc...., does not pose any technical challenges. With the presupposition of this type of equipment availability the electrical characteristics remain unchanged. The basic signal representation would be identical to what is presented in this report. It has been indicated by the researchers that spurious reflections can be a problem and must be minimized. The operational equipment configuration, especially if multiple antennas are used, is critical if minimum reflection is to be realized. Techniques for this task exist and make the final operational hardware realizable with a minimum of additional experimentation.

With the existing experimental measurements system some attempt was made to minimize these spurious reflections by simply eliminating causes. That is, objects were not allowed in the vicinity (±6') of the antenna while measurements were being made.

As a proof of concept demonstration, absorbing material was placed around the antenna at a stand-off distance of 2 feet. This simple technique provided a significant reduction of unwarranted reflections. This technique would definitely be used in an operational system.

Temperature and Moisture. Although temperature and moisture are considered environmental factors, they have been singled out as having a critical effect upon the signal characteristics. In fact, it appears at

this time that if the temperature/moisture levels are to high, the equipment cannot be operated. This is the prime area that more study must be directed towards, if an operational system is desired. Theoretical analysis indicates that attenuation of the electromagnetic signal varies with total moisture content and temperature. From the curves given in the theoretical material in Appendix B, for 75°F temperature and 10% moisture, the attenuation is about 5 to 10 times as great as it would be for a temperature of 14°F and the same moisture level. Specific attenuation measurements were made both in the laboratory and on the test lane to verify that high temperature measurement problems on the test lane are related to the moisture-temperature combination. Under the same moisture conditions, attenuation for measurements on the outside test lane at 100°F was a factor of 4 greater than attenuation for laboratory measurements at 78°F. Clearly, the effects of a high temperature is a higher attenuation level and decrease in signal strength to a point where the microprocessor algorithms cannot detect and size the void.

Reliability. Over the period of this research effort, the radar and microcomputer have been extremely reliable. Only minimal repairs and maintenance have been necessary. Highway use would require fastening components firmly to support structures that are then shock-mounted to maintain high reliability.

CHAPTER THREE

CONCLUSIONS AND SUGGESTED RESEARCH

The electromagnetic wave equipment chosen for the void detection and size measurement program provided excellent results. The signal response from the radar has the sensitivity and accuracy to allow signal processing algorithms to be applied and identify small variations related to the void detection problem. The equipment itself can be economically constructed and is suitable for highway operation with a minimum of modifications.

The microcomputer connected to the radar processed the signal returns in an on-line mode and presented the results on a video monitor as well as a line-printer for a permanent copy. Magnetic disk provided permanent recording of the actual signal returns.

The system mounted on the moveable cart provided the portability needed for this research project. The system was configured to be operated by field personnel with a minimum amount of skill required.

Further research for the equipment should consist of methods of protection from the environment, and shock and virbration mounting. The microcomputer for application to rapid highway measurements should be updated for faster processing.

The theoretical modeling provided during this research project was complete for the understanding of the void detection and sizing problem. It provided the basis for development of the discriminants necessary for the algorithm development. The theory also provided the

preliminary background for the attenuation effects of moisture and temperature.

A combination of analog and digital signal processing provided the timing signals necessary for the extraction of the portion of the radar signal return corresponding to the possible locations of a void. Digital signal processing algorithms were developed for detecting and sizing the voids. The results provided the capability for spatial void location to ±6 inches and depth sizing up to 8.5 inches with a standard deviation of the error of less than 0.5 inches. Calibration of the measurement process is easily accomplished by field personnel.

The laboratory measurements provided a controlled environment for studying the radar signal interactions with voids. Verification of the discriminants developed in the theoretical modeling was provided by the controlled measurements. Several typical base materials under various moisture levels were measured. Void sizes from 0 inches to 8.5 inches in 0.5 inch increments were measured, and an extensive data base was accumulated for future use. Suggested future measurements should include special processing to show that the thickness of the concrete pavement and its dielectric constant can be estimated. Present measurements give an indication that this can be accomplished.

The test lane measurements provided an opportunity to obtain data from a set of known calibrated voids under concrete pavement that closely simulated an actual highway situation. Measurements were made over a wide temperature range and results indicate that at high temperatures, 100°F, a large attenuation of the electromagnetic signal occurs. Measurements made at less than 70°F resulted in excellent void location and

sizing estimates. This result definitly indicates that environmental conditions, especially high temperature, limit the measurement capability. Thus, the optimum time to make measurements could be during the winter season, at low temperatures, when the attenuation is minimized. Further research is suggested into the effects of temperature on the signal strength. Both laboratory and actual highway measurements should be made to more fully substantiate current available measurements and modeling information.

Overall suggestions for further research include preliminary design of an operational high-speed processing system, additional measurements in the laboratory and on the test lane on a continuing basis to completely document the effects of temperature, and actual highway measurements to verify effectiveness of the processing algorithms.

APPENDIX A

MEASUREMENT AND PROCESSING EQUIPMENT

As a result of research, the electromagnetic wave equipment chosen most suitable for measurements on this project was a very short pulse "radar." This radar has the required accuracy and reliability and can be economically constructed. The signal response from the radar has the characteristics that will allow signal processing algorithms to recognize small variations related to void detection and identification.

In order to have a totally portable system capable of being operated by a semi-skilled person the equipment must have output devices that clearly display results in easily interpreted symbols and be mounted on a moveable platform. To satisfy the first requirement a microcomputer was used with video screen display and a line-printer for output. The signal response from the radar equipment is then processed in an "on-line" fashion by the microcomputer and provides information to the field personnel for void location, depth, size and shape. Permanent recording of the radar signals is available automatically via magnetic disks attached to the microcomputer. Results for void detection are not only available on the video monitor but can be printed on the line-printer.

To satisfy the portable requirement, the radar system and the microcomputer were mounted on a cart that can be pushed to most locations for measurement purposes. The complete description of the radar hardware and the micro-computer is given in the following.

Electromagnetic Wave Equipment

The requirements for void detection and sizing necessitate the use of equipment of very high time resolution and usability at short distances from the medium being measured. This translates into a requirement for an extremely short pulse of energy to be generated by the equipment. In order to actually transmit this energy into the medium a wide-bandwidth, low loss, matched antenna must be used. The return signal from the medium being measured enters the antenna and must be detected. This requires a sensitive wide-bandwidth receiver.

The radar that satisfies these requirements and is used in these tests is an adaptation of the Vehicle-Mounted Mine Detection Radar developed by the Calspan Corporation, Buffalo, New York, for the U.S. Army (MERADCOM, Ft. Belvoir, Virginia). The radar transmits pulses consisting of one cycle at one gigahertz (GHz), i.e., a one nanosecond pulse width. Since one cycle of 1 GHz is a transient type of signal, we need a bandwidth as much as 2 GHz to prevent distortions of the signal. For our system, this bandwidth is required only in the transmitter, antenna, and sampler. The wide bandwidth is not needed for the video sections because the periodic, real-time return signal is sampled and reconstructed at a much lower frequency. Figure A-1 is a block diagram of the system, and the following paragraphs describe the blocks in detail.

Timing Generator

The timing for the system is derived from a 15 MHz crystal controlled oscillator. This signal is divided down to produce all gating and trigger waveforms needed in the radar. In particular, the timing

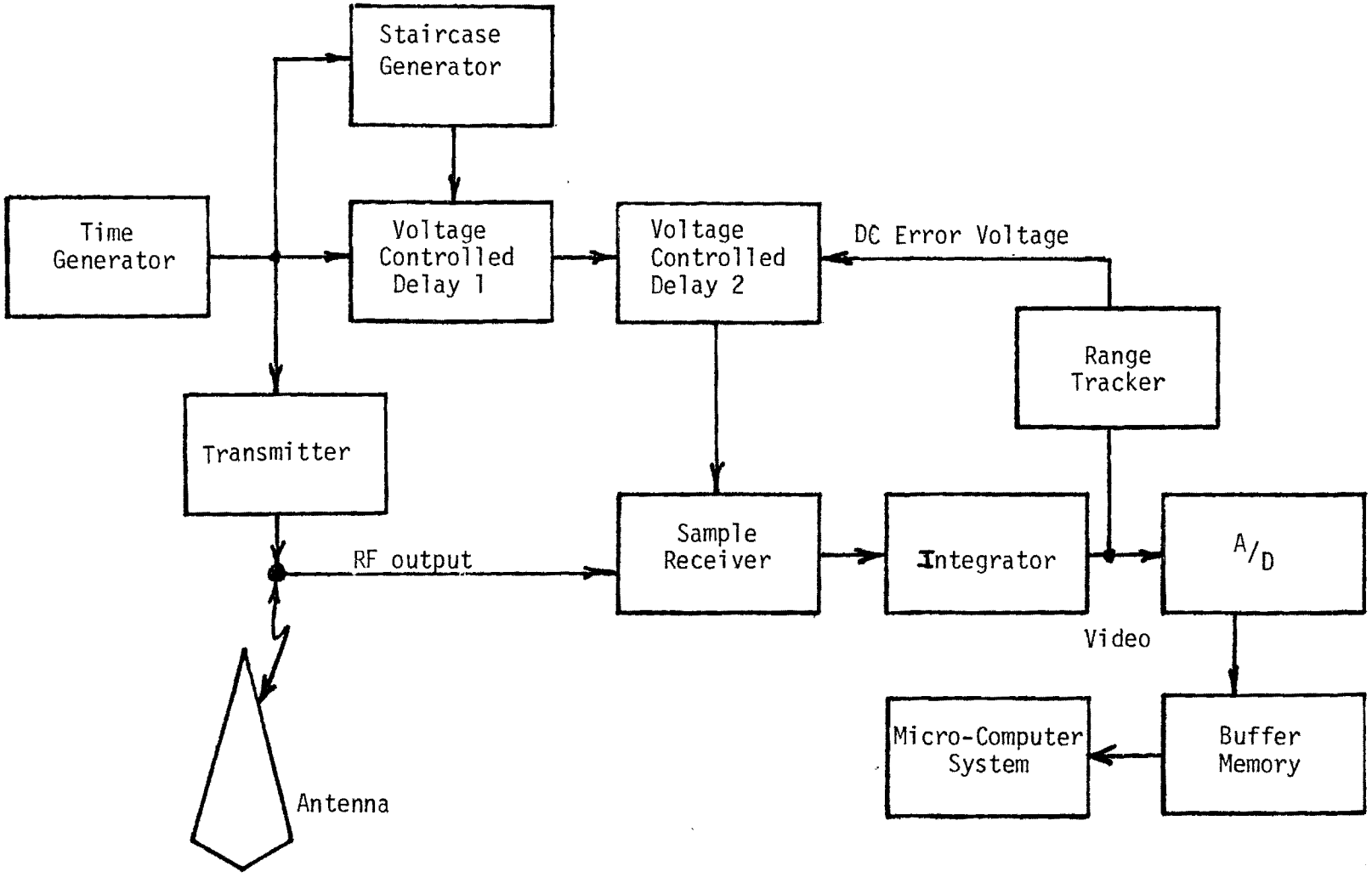

FIGURE A-1

RADAR BLOCK DIAGRAM

generator produces the 5 MHz signal that establishes the radar pulse repetition frequency (how many pulses per second are transmitted).

Transmitter

The transmitter can be divided into a short-pulse driver and avalanche pulse generator. The drive consists of a snap-off, step recovery diode that generates a transition across a coaxial pulse forming network, thereby generating a short transition pulse. Amplification is then achieved by a transistor operated in the avalanche mode for high speed switching. This transistor output goes directly to the antenna.

Antenna

The antenna is of broadband design, working over the range from 200 MHz to 2 GHz in frequency. To obtain the low frequency response, a TEM (transverse electromagnetic) horn was used which is not limited by low frequency. To maintain the required wide bandwidth, the plates of the horn are flared and exponentially tapered with resistive card loading on the ends. Because of this, there is little reflection of energy from the antenna into the receiver. In other words, the antenna has a very low voltage-standing-wave-ratio and most of the energy is transmitted into the medium.

Sample Receiver

The returning signal is sampled by a Schottky barrier diode that is strobed by a snap off, step-recovery diode at a 5 MHz rate. The periodicity of the received waveform allows us to take individual samples

from pulse to pulse in order to reconstruct the waveform over a longer time period, thereby decreasing the bandwidth requirements on the video and digital subsystems as given in Figure A-2. To have samples at times differing from the transmit pulse, the 5 MHz signal to the sampler is delayed by voltage controlled delay lines 1 and 2. The control voltage for delay line 1 is a staircase waveform of 200 steps. Each voltage step causes the sample strobe to occur later on the waveform than the previous sample strobe. Because there are 200 steps, we sample at 200 positions across our real-time waveform. At each of these 200 positions we take 450 samples and then perform intergration to increase the signal-to-noise ratio. Each voltage step moves the sample strobe out 92.5 picoseconds in range. Since there are 200 steps, the width of our sample window is 200 X 92.5 ps = 18.5 nanoseconds. Comparing real-time waveforms to reconstructed waveforms, 18.5 nanoseconds of real time corresponds to 18 milliseconds in reconstructed time. The position of the sample window in range is controlled by delay line 2, via a voltage from the range tracker.

Range Tracker

The main function of the range tracker is to establish a fixed time reference position for the surface return. Once this is established, all other video is referenced to this time. Video cannot be referenced to the transmit pulse because of the varying antenna height above the ground. If it were, the position in time of the void return would vary making detection difficult. The range tracker locks on the surface by applying an error voltage to delay line 2 that keeps the leading edge of

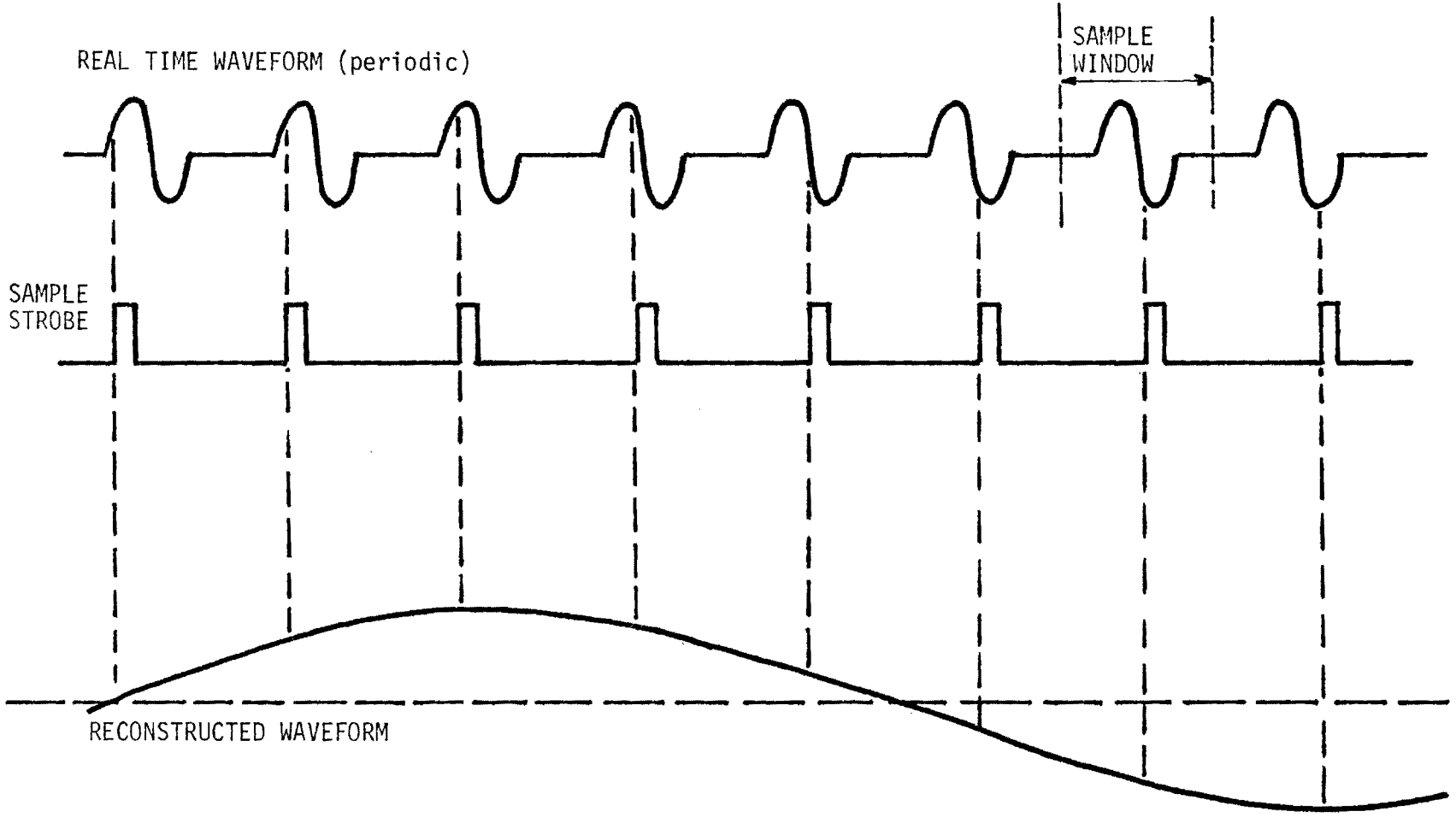

FIGURE A-2

PERIODIC SAMPLING (SINGLE SAMPLE/POSITION)

the sample window locked to a point slightly behind the surface return. The void always remains at the same position within the window regardless of antenna height.

Analog-to-Digital Converter with Buffer Storage

The video information must first be converted into a digital format before it can be processed by the computer. That is the purpose of the analog-to-digital converter. Figure A-3 illustrates sequential sampling that is used with the converter. The waveform can be represented by samples taken over one cycle of the video waveform. The video is sampled and in real time, each sample is converted to a digital word and stored in a buffer memory. Both loading and unloading of the buffer are under computer software control.

Micro-Computer

The micro-computer chosen for the void detection system was built by APPLE Computer, Inc., Cupertino, California and consists of the following components.

(1) Main Computer

48,000 words of random access memory

Keyboard interface

BASIC and PASCAL language systems

(2) Video Display

9" black and white

text and graphics modes of display

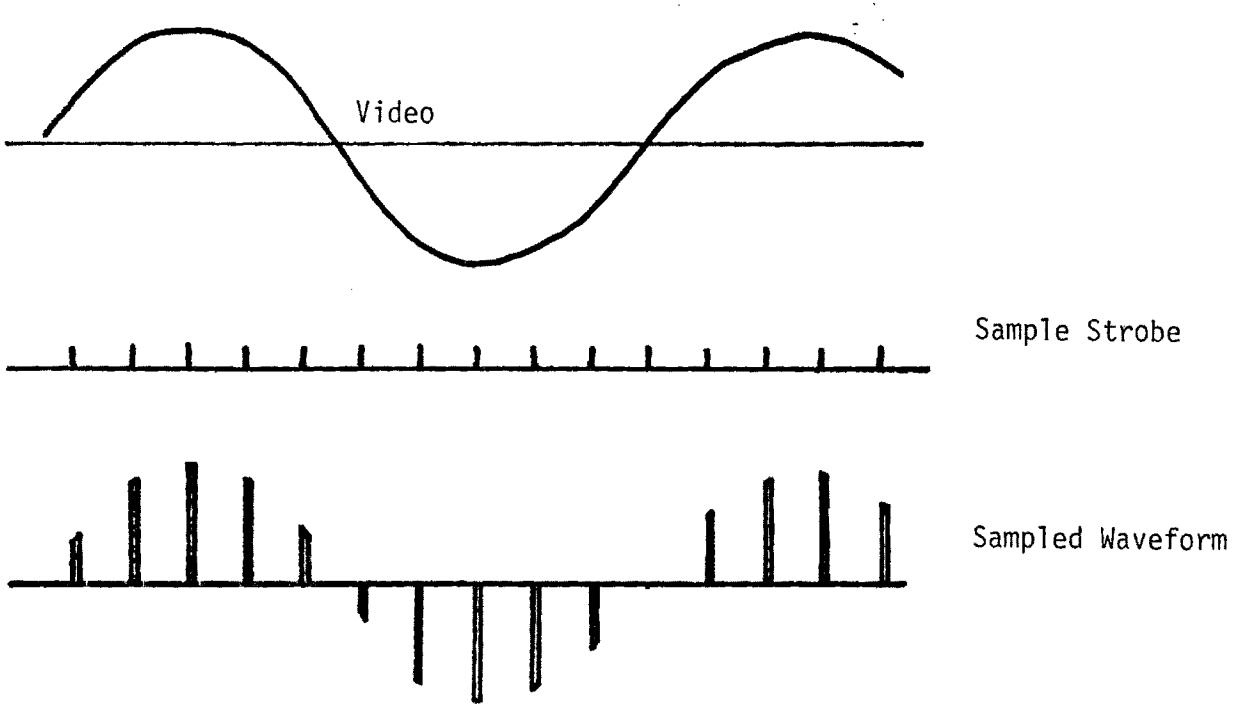

FIGURE A-3

SEQUENTIAL SAMPLING

(3) Two Mini-Floppy Disk Drives

5" floppy diskettes

102,000 words of storage each diskette

3 Interface Cards

Radar interface - digitizes radar data

Communications interface-transfers data to/from the CYBER facility Printer interface - line printer communication

(4) Printer

Capable of printing out data/program listings or graphics (plots),

All the plots of actual or simulated data presented in this report were generated on the printer.

REFERENCES FOR HARDWARE SPECIFICATION

1. "Antennas and Pulsers for a Vehicular-Mounted Mine Detector (U)," CALSPAN Report #MA-5366-E-1, M. E. Bechtel and A. V. Alongi, September 1974

2. Discrimiator and Display for Vehicular-Mounted Mine-Detector Radar (U)," CALSPAN Report #MA-5366-E-2, M. E. Bechtel and A. V. Alongi, June 1976

APPENDIX B

THEORETICAL MODELING

A theoretical mathematical model has been developed for a concrete slab, an air void and an underlying base material to evaluate their effect on impinging radar electromagnetic (EM) waves. These theoretical results can then be compared to the measurements taken with the short-pulse radar to assist in interpreting the measured results. This section describes the details of the mathematical model development and the theoretical effects of void size, spurious reflections, and concrete attenuation on the reflected EM waves.

Mathematical Model

The model of a concrete slab and its surrounding environment is shown in Figure B-1. The model was deliberately kept simplistic so that describing mathematics are tractable. The source and receiver of the electromagnetic (EM) waves are located above the slab and the waves are directed into the slab by an appropriate antenna. The EM waves are reflected by the slab surface and dielectric discontinuities beneath the slab surface. If there is no void beneath the slab, then the only dielectric discontinuity beneath the slab surface will be at the concrete-soil interface and the incident EM waves will be reflected from it. If a void does exist, there will be two dielectric discontinuities beneath the slab surface; the concrete-void interface and the void-soil boundary. Each of these boundaries will reflect the incident EM waves.

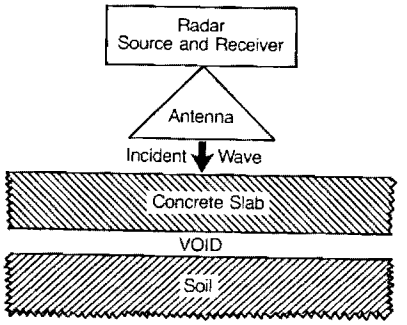

FIGURE B-1. CONCRETE SLAB AND ENVIRONMENT.

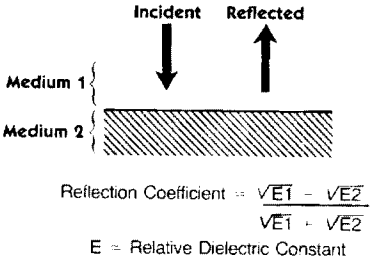

FIGURE B-2. BEHAVIOR OF EM WAVES AT A DIELECTRIC BOUNDARY.

Consider for a moment the behavior of electromagnetic waves at the boundary between two media as illustrated in Figure B-2. The reflection coefficient, ρ, at the boundary is given by

$$\rho = \frac{n_2 - n_1}{n_2 + n_1} \qquad \text{(B-1)}$$

where n_1 and n_2 are the wave impedance of medium 1 and 2, respectively. For a perfect conductor, the wave impedance is zero; for a non-conducting, non-ferrous medium such as dry soil or concrete, the wave impedance is

$$n = \frac{\mu_o}{\varepsilon} \qquad \text{(B-2)}$$

where μ_o is the magnetic permittivity of space, and ε is the dielectric constant of the medium. If the wave impedance for free space (air) is denoted by

$$n_o = \frac{\mu_o}{\varepsilon_o} \qquad \text{(B-3)}$$

then equations (1) and (2) above may be written as

$$n = \frac{n_o}{\varepsilon_r} \tag{B-4}$$

and

$$\rho = \frac{\varepsilon_{r1} - \varepsilon_{r2}}{\varepsilon_{r1} + \varepsilon_{r2}} \tag{B-5}$$

where ε_r is the relative dielectric constant of the medium. Note that if medium 1 has a smaller relative dielectric constant than medium 2, then ρ has a negative value. On the other hand, if medium 1 has a larger relative dielectric constant than medium 2, then ρ is positive.

Consider the situation where a void is not present beneath the concrete slab as illustrated in Figure B-3. Also, assume the transmitted pulse (the amplitude variation of the EM waves with time) is of the shape shown in the same figure. How should the radar returns from the air-concrete and the concrete-soil interfaces appear? The concrete has a dielectric constant greater than that of air; thus, ρ at the air-concrete interface has a negative value. If the soil is moist, its dielectric constant will be greater than that of concrete and ρ at the concrete-soil interface will also be negative. Thus, the radar return will appear as shown in Figure B-3. Assuming the concrete-soil boundary is far enough below the slab surface so the two reflected pulses do not overlap, each of the returns should appear as the inverse of the transmitted waveform as illustrated. If the soil is very dry, its dielectric constant may be smaller than that of concrete. Then the radar return from the concrete-soil boundary will be the same polarity as the transmitted waveform.

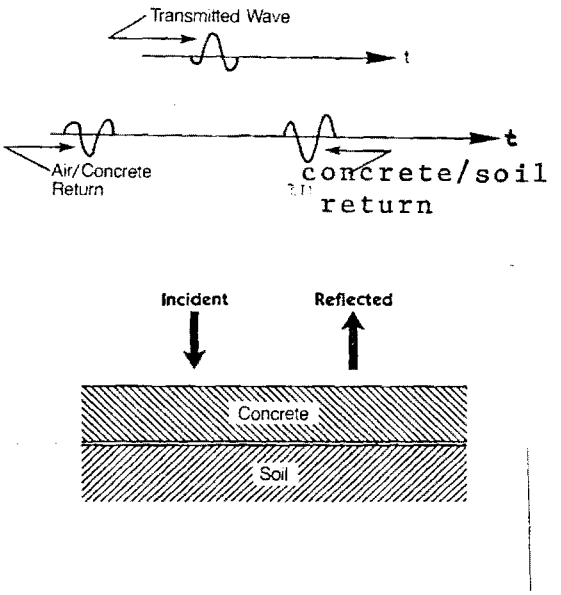

FIGURE B-3. BEHAVIOR OF EM WAVES AT AIR/CONCRETE AND CONCRETE/SOIL BOUNDARIES.

Extending this simplified analysis to the case where a void (air gap) between the concrete slab and the soil base does exist, the reflected EM waves (radar returns) are as shown in Figure B-4. Since the dielectric constant of concrete is greater than that of air, the reflection coefficient at the concrete-void interface is positive. However, the reflection coefficient at the void-soil interface is negative. Thus, the reflected pulses from these two boundaries are of different polarities as shown.

The time separation between the pulses from the top and bottom of the void is proportional to the size of the void in the direction of the incident EM wave propagation. Since the radar is positioned so the incident EM waves travel perpendicular to the concrete slab surface, the time separation between pulses is proportional to the void thickness. The relationship between an air void thickness, d, and pulse separation is as follows:

$$\text{pulse separation} = \frac{2d}{C}$$

$$\text{PS (nanoseconds)} = \frac{d \text{ (inches)}}{5.9} \qquad \text{(B-6)}$$

where $C = 118.0288 \times 10^{8}$ inches/second.

The radar that was used in this measurement program has a pulse length of about one nanosecond. Thus, the void thickness must be greater

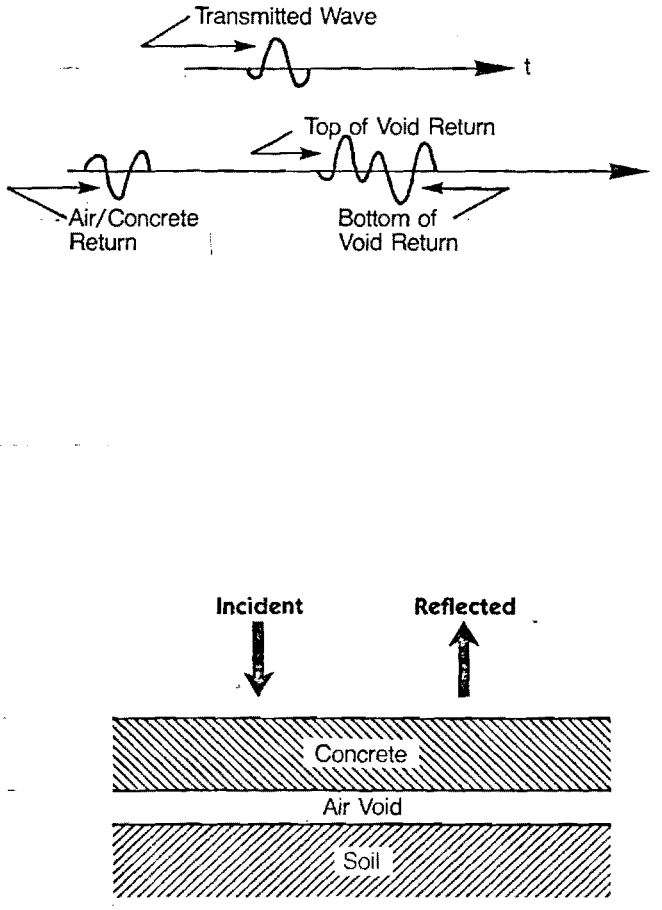

FIGURE B-4. BEHAVIOR OF EM WAVES AT CONCRETE/AIR AND AIR/SOIL BOUNDARIES.

than 5.9 inches if the reflected radar pulses from the concrete-void and void-soil interfaces are not to overlap in time. Most of the voids expected are much smaller than 5.9 inches. Thus, the radar returns from the top and bottom of the void will overlap. Since the two pulses are of different polarities, they will tend to subtract, producing a particular pulse shape that may be much different than the ones shown in Figure B-4. In addition, the amplitude of the composite pulse will vary depending on the time separation between the two pulses. The amplitude will tend to be proportional to the time separation and, hence the void thickness. This is one property of the radar return that can be utilized to estimate void thickness.

Another consideration that complicates the prediction of what one should expect the radar return to be is multiple reflections as illustrated in Figure B-5. In Figure B-5(a), multiple reflection of the EM waves between the top and bottom faces of the concrete slab is shown. Some of the incident radar energy is reflected back and forth between faces. Each time, some of the energy is returned towards the radar receiver yielding a returning pulse of energy. However, if the distance between the concrete slab faces is greater than

$$5.9/\sqrt{\varepsilon_{concrete}}$$

inches or approximately 2.4 inches for dry concrete, the pulses do not overlap, and each reflection is easily identifiable.

Multiple reflections between the air void faces as illustrated in Figure B-5(b) combine and must be considered, however. Since the

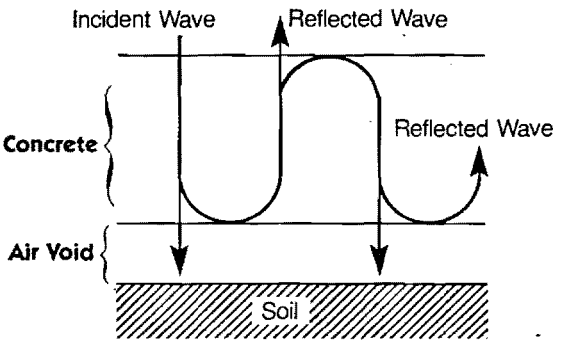

(a). MULTIPLE REFLECTIONS BETWEEN SLAB FACES.

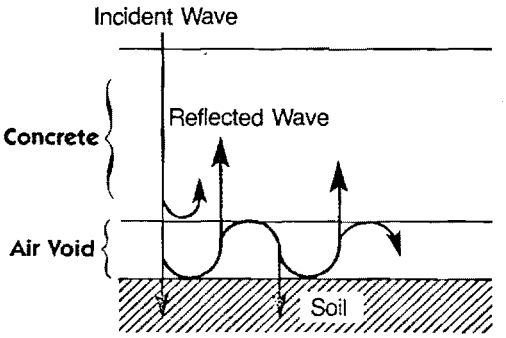

(b). MULTIPLE REFLECTIONS BETWEEN VOID FACES.

FIGURE B-5. MULTIPLE REFLECTIONS BETWEEN SLAB FACES AND BETWEEN VOID FACES.

distance between air void faces is much less than 5.9 inches, the pulse returns resulting from multiple reflections do overlap and each contributes to the composite pulse return. The individual contribution can be calculated. Also, each succeeding reflection is smaller than the preceeding one. Thus, only a finite number of reflections need to be considered.

Effect of Void Size

An approximate mathematical expression for the composite radar return, s(t), due to single and multiple (3) bounces between void faces is as follows:

$$s(t) = \rho_1 X(t) + \rho_2(1-\rho_1^2)\, X(t+\tau) + \rho_1\, \rho_2^2\, (1-\rho_1^2)\, X(t+2\tau)$$

$$+ \rho_1^2\, \rho_2^3\, (1-\rho_1^2)\, X(t+\tau) \qquad \text{(B-7)}$$

where:

$X(t)$ = transmitted pulse,

ρ_1 = reflection coefficient at the concrete-void interface,

ρ_2 = reflection coefficient at the void-soil interface, and

τ = time delay the radar pulse experiences in traveling across the void and back.

This expression was programmed on a digital computer and the composite reflected waveform calculated and plotted. The radar return pulses are as shown in Figure B-6. In this figure, void thickness was

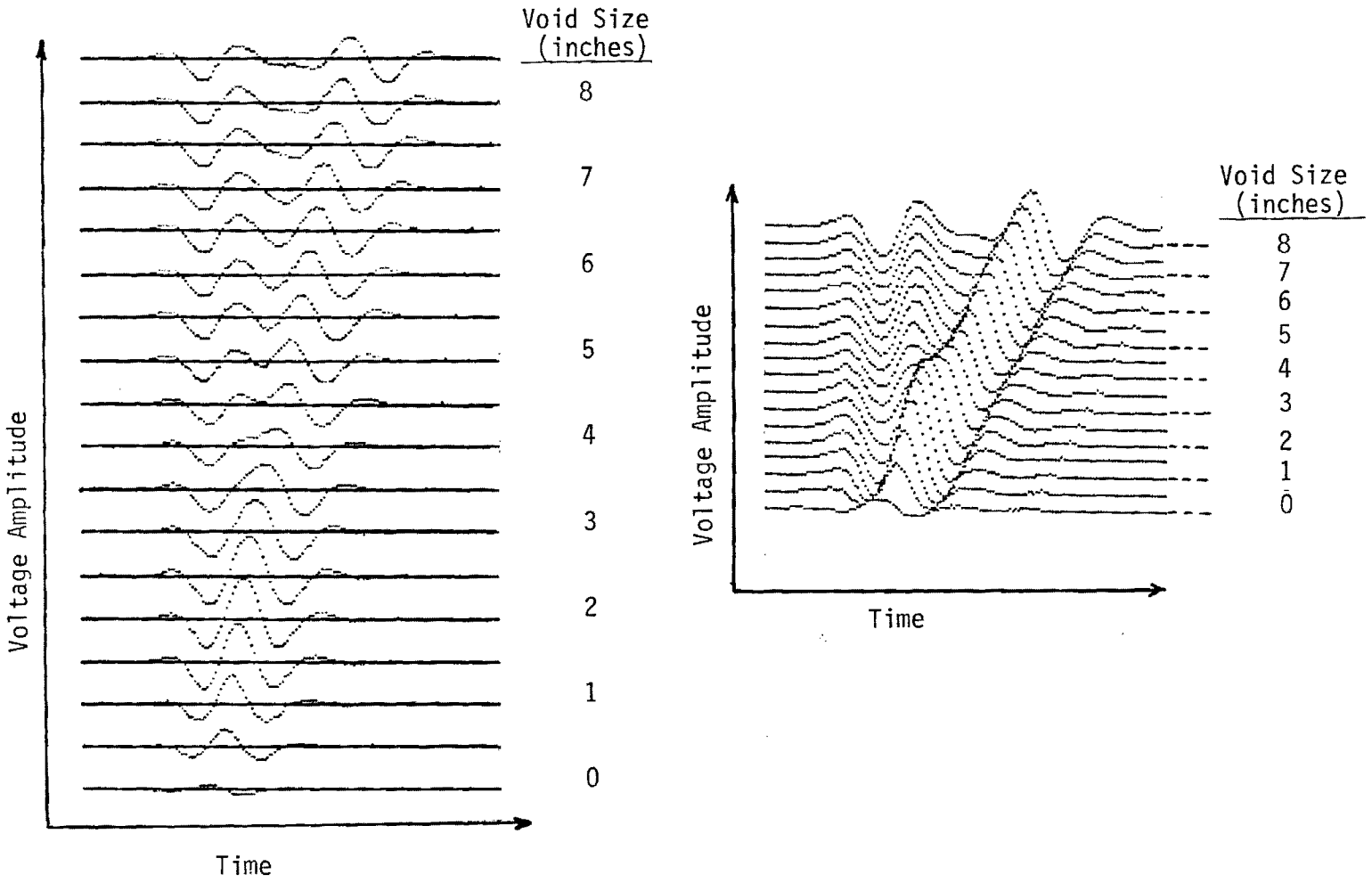

FIGURE B-6

THEORETICAL RADAR TIME RESPONSES OF AIR VOIDS UNDER HIGHWAY CONCRETE SLAB FOR VARIOUS VOID SIZES. RELATIVE DIELECTRIC CONSTANT OF CONCRETE AND ROAD BASE EQUAL 6 AND 12, RESPECTIVELY. IDENTICAL TIME RESPONSES ARE SHOWN IN TWO PLOT FORMATS.

varied and soil dielectric constant was selected to approximately match the measured data. The concrete relative dielectric constant for dry concrete was determined by radar measurements to be about 6.0.

Upon examining the plots shown in Figure B-6, one notes that both the negative and positive peaks of the reflected EM wave increase in magnitude as the void size increases. However, when the void size is larger than about two inches, the peak amplitude of the returning EM wave starts to diminish. For void sizes of three inches and larger, the pulse amplitude appears to be independent of void size. This behavior of the returning EM waves can be explained by realizing that void sizes of three inches or greater produce returning pulses that tend to be non-overlapping and, thus, signal interference does not occur. The amplitude of the positive peak is plotted in Figure B-7 as a function of void size in inches. Note that the amplitude of the positive peak varies in almost linear fashion for void sizes less than two inches. For void sizes between two and three inches, the amplitude of the peak starts to decrease, and for void sizes three inches or larger the amplitude is somewhat independent of void size. The amplitude of the negative peak as a function of void size is plotted in Figure B-8. Note that the behavior of the negative peak is very similar to that of the positive peak just described.

Another measure of void size is the time separation between the EM reflection from the top of the air void and the EM reflection from the bottom of the air void. A plot of the separation between the largest positive going peak and the largest negative going peak as a function of void size is shown in Figure B-9. In this figure, note that the time

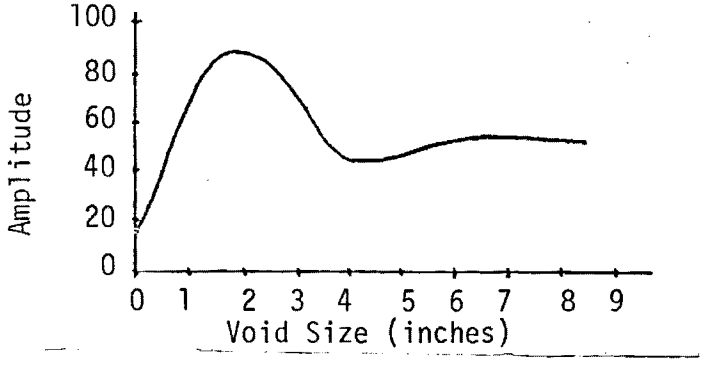

FIGURE B-7. AMPLITUDE OF POSITIVE PEAK VERSUS VOID SIZE.

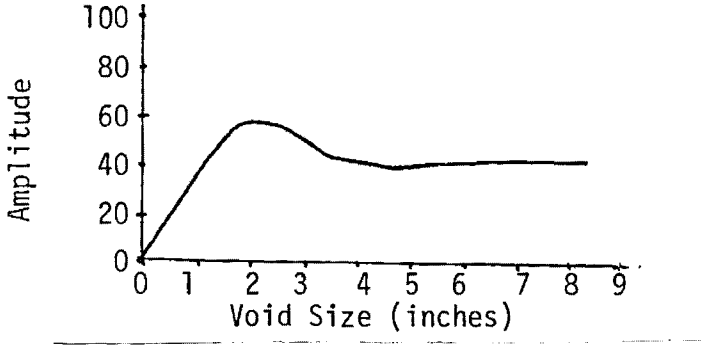

FIGURE B-8. AMPLITUDE OF NEGATIVE PEAK VERSUS VOID SIZE.

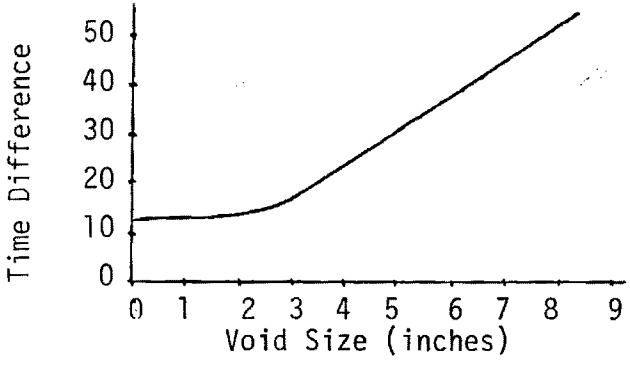

FIGURE B-9. TIME DIFFERENCE VERSUS VOID SIZE.

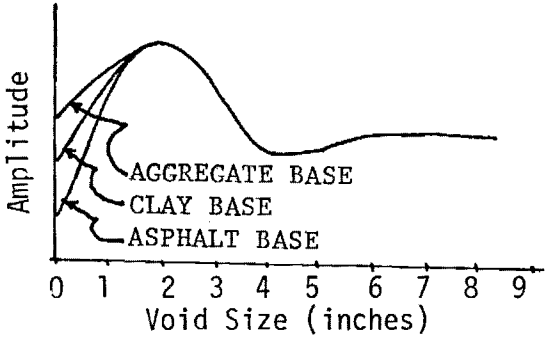

FIGURE B-10. AMPLITUDE OF PEAK FOR VARIOUS TYPES OF ROAD BASES.

separation between these two pulses varies linearly with void size only for void sizes of three inches or larger. For void sizes less than three inches, there is virtually no change in the time difference as a function of void size. Thus one concludes from Figures B-7 through B-9 that the pulse amplitude can be used to estimate void size for voids of two inches or less and that the time separation between returning pulses can be used to estimate void sizes of three inches or more. However, it appears that void sizes between two and three inches presents a problem. There is a slight slope to the curve in Figure B-9 for void sizes less than three inches. It may be that one can use the combination of the curve in B-9 with the curves in B-7 and B-8 to estimate void sizes between two and three inches.

The initial value of the amplitude plots shown in Figures B-7 and B-8 changes with the type of road base. This variation or change is illustrated in Figure B-10 for three different types of road bases. Note that only the portion of the curve for void sizes of two inches or less changes with road base type. The net effect is that the proportionality constant between the pulse amplitude and the void size changes with road base type. If the road base type is known a priori then one can select the proper proportionality constant and estimate void size based on the amplitude of the returning EM pulse. Road base type does not have any effect upon the estimation of void sizes of larger than three inches because the time separation between the returning pulses is not a function of this variable, but is dependent only upon the air void size.

Effects of Spurious Reflections

In any radar system, there are spurious reflections which can mask the signals of interest. In the short pulse radar system utilized on this project, the interference resulting from spurious reflections limits the performance of the system. To recognize radar returns from air voids underneath concrete slabs, the returns must be large enough to exceed the interference level caused by reflections. To understand this limitation, it is important to know why these spurious reflections are generated and what steps one may take to reduce them. In Figure B-11, the short pulse radar is shown in its environment. As indicated, the transmitter/receiver is attached to an antenna which is suspended in the air above a highway concrete slab. The transmitter/receiver is connected to a cable via a connecter and the cable is attached to the antenna via a connecter. Connecter joints in this cable create spurious reflections. Likewise, the interface between the antenna and the air represents a discontinuity and radar reflections are generated. In addition to the concrete slab and road base, other discontinuities which generate reflections are obstacles that are laterally displaced from the radar; for example, the mobile cart upon which the radar is mounted. Other obstacles which might generate spurious reflections are personnel in the vicinity of the radar or perhaps nearby vehicles and other such obstacles.

The time that it takes a electromagnetic pulse to traverse an electrical circuit such as a cable or antenna is equal to the physical length of the circuit divided by the velocity of the electromagnetic wave within the circuit. For microwave cables, the velocity of EM waves is approxi-

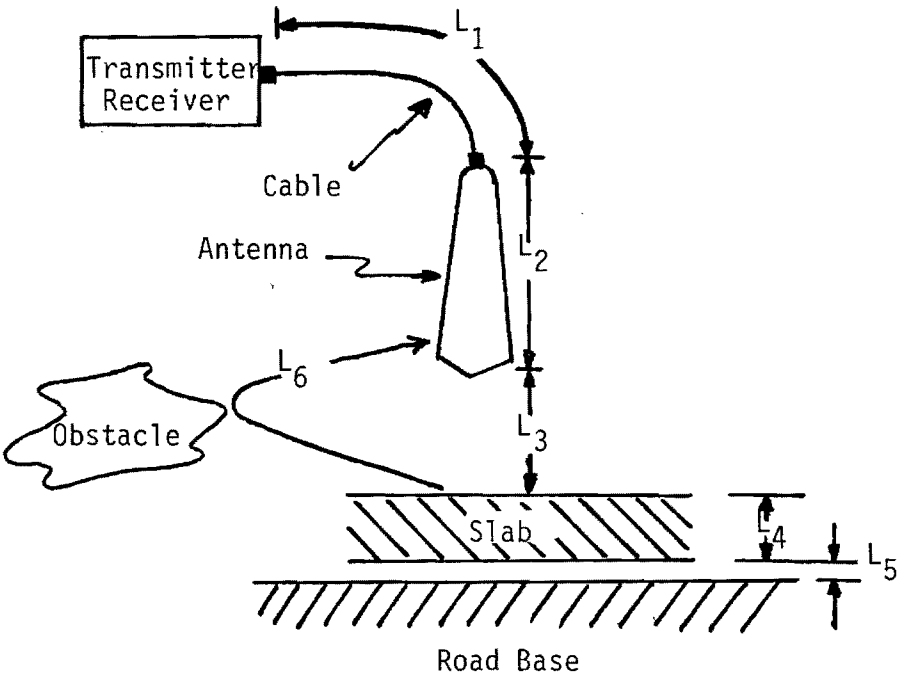

FIGURE B-11. RADAR ENVIRONMENT. ELECTRICAL LENGTHS OF VARIOUS EM WAVE PATHS.

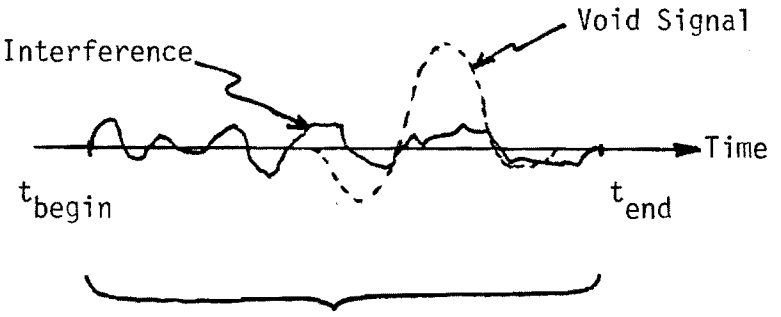

FIGURE B-12. VOID SIGNAL IN THE PRESENCE OF INTERFERENCE CAUSED BY SPURIOUR REFLECTIONS.

mately the speed of light. Thus the time it makes waves to travel from one end of the cable to the other is its physical length divided by the speed of light. The velocity of EM waves through an antenna structure, such as the one used with the short pulse radar, is much slower than the speed of light. The exact delay time through the antenna is not known, but is considerably more than that associated with its length. Of course, the transit time of EM waves through air is equal to the distance they travel divided by the speed of light. The transit time through concrete depends upon the amount of moisture in the concrete. The dielectric constant of dry concrete at these frequencies is approximately six. Thus, the time it takes electromagnetic waves to traverse one direction in the concrete slab is the thickness of the slab divided by the velocity of the waves through the slab. The velocity of EM waves through concrete is approximately the speed of light divided by the square root of the relative dielectric constant.

The reflections in the antenna cable places an attenuated replica of the slab return at about the same time as the void return, thus interfering with the void return. Other paths that provide interferring signals in the time period of interest are suggested in Figure B-11. In Figure B-12, the presence of interference caused by spurious reflections is illustrated by the solid curve and the signal that one might expect from a void is indicated by the dashed line. It is fairly obvious that if the void return is attenuated and is small, then one might have difficulty in distinguishing it from the interference signals. Thus, it is necessary that the void amplitude be several times larger than the largest interference signal amplitude in order to differentiate between

the two. The ratio of these two signals is called the signal to interference ratio (SIR). The SIR should be at least four or greater in order to properly detect the presence of an air void. In the next section of this appendix the sources of signal attenuation will be addressed. As will be indicated in that section, the major source of attenuation only attenuates the void signal and does not have much of an effect on the interference level. Thus the void signal may be reduced in size comparable to that of the interference level.

Effects of Attenuation

The effects of attenuation on the void return signal is three-fold. As mentioned previously, the attenuation reduces the returning signal relative to the interference level and thus the SIR may be insufficient for proper void detection. Another effect of attenuation is to lengthen the pulse so as to distort the return signal. A third effect is to reduce the peak to peak amplitude of the returning signal and thus make it difficult to estimate the size of the void based on amplitude. Because of these reasons, it is important to understand the effects of attenuation and how it comes about and under what conditions it exists. In this section attenuation factors for various types of materials as a function of moisture will be reviewed and presented.

The major source of attenuation in this application is the concrete slab positioned on the road base. Radar return signals from beneath the road base are not of interest. Thus, in this discussion, attenuation characteristics of the concrete block is of paramount importance. Unfortunately, very little information on the attenuation characteristics of

cement or concrete at the frequency of the short pulse radar seems to be available. However, some inferences can be made based on existing data.

Attenuation characteristics of materials are very much dependent on the frequency of the electromagnetic energy impinging on it. Therefore, a discussion of the radar frequency of operation is necessary. The temporal signal generated by the radar transmitter is approximately that illustrated in Figure B-13 (a). The frequency spectrum of this transmitted signal is calculated to be that shown in Figure B-13 (b). The antenna frequency characterics will modify this spectrum somewhat. However, since the antenna is very wideband, it does not significantly alter the spectrum shown. Most of the energy in the transmitted signal is located between the "one-half power" frequencies. These frequencies are defined where the voltage spectrum is down 0.707 from the peak value. For the spectrum shown, these frequencies are approximately 0.4 and 1.2 GHz with a mean of about 0.8 GHz. Thus, the attenuation characteristics of concrete over this frequency band is of major interest.

The attenuation of EM waves in a dieletric material is given by

$$\text{Attn} = e^{-\alpha x} \qquad \text{(B-8)}$$

with

$$\alpha = (2\pi f/c) \sqrt{\epsilon_r} \tan \delta$$

f = frequency

c = velocity of light

ϵ_r = the relative dielectric constant,

$\tan \delta$ = the loss targent, and

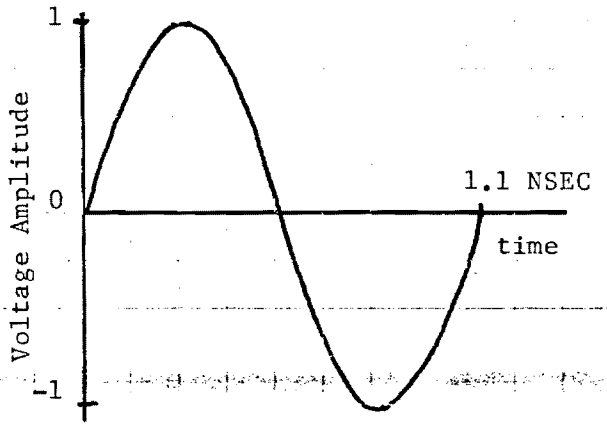

(a) Transmitted Temporal Waveform

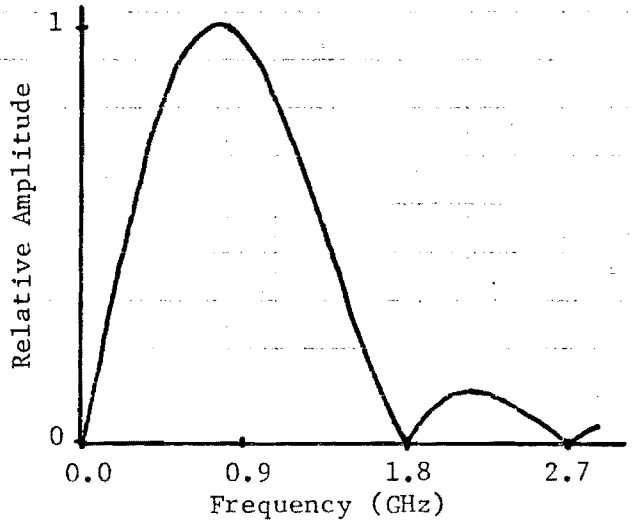

(b) Transmitted Waveform Voltage Spectrum

Figure B-13. Temporal and Spectral Responses of Transmitted Waveform.

x = the distance EM waves travel through the dielectric material.

The attenuation in dB per inch of two-way travel is given by

$$\text{Attn (dB/inch)} = 2.31 \times 10^{-9} \, f \, \varepsilon_r \tan \delta \qquad \text{(B-9)}$$

with the terms as defined above. Thus, there are two dielectric properties that contribute to a material's attenuation characteristics: the relative dielectric constant and the loss tangent. Tables of these two characteristics for a large variety of materials exist. (2) (3) (4). However, usually they are given for widely separated discrete frequencies, e.g., 0.3 and 3.0 GHz. The value of these parameters between these frequencies appears not to be available for many materials. Dielectric properties for a few materials have been measured in the frequency range of interest over a continuous range of frequencies. For example, the relative dielectric constant and loss tangent of Goodrich Clay has been measured and is given in Figures B-14 and B-15 for two different temperatures. Similiar information for concrete over a range of temperatures and moisture conditions is highly desirable, but apparently not available. One paper (4) discusses concrete and cement but not in the frequency range of interest for this application. The dielectric constant and loss tangent for a frequency of 3.0 GHz (λ = 10cm) is indicated in Figures B-14 and B-15 by an asterisk. The corresponding two way attenuation has been calculated utilizing the information in Figures B-14 and B-15 and is given in Figure B-16. Note that the signal attenuation value shown for hardened cement is about half that of clay at 3.0 GHz. Whether this is true at all frequencies is not known.

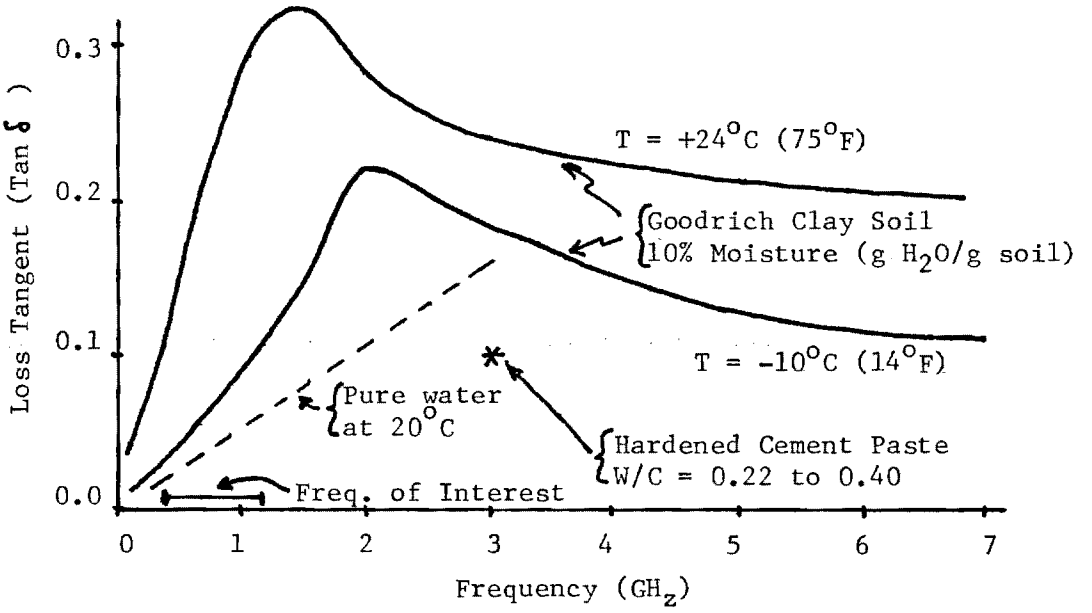

Figure B-14. Loss Tangent of Goodrich Clay, Water and Hardened Cement Paste.

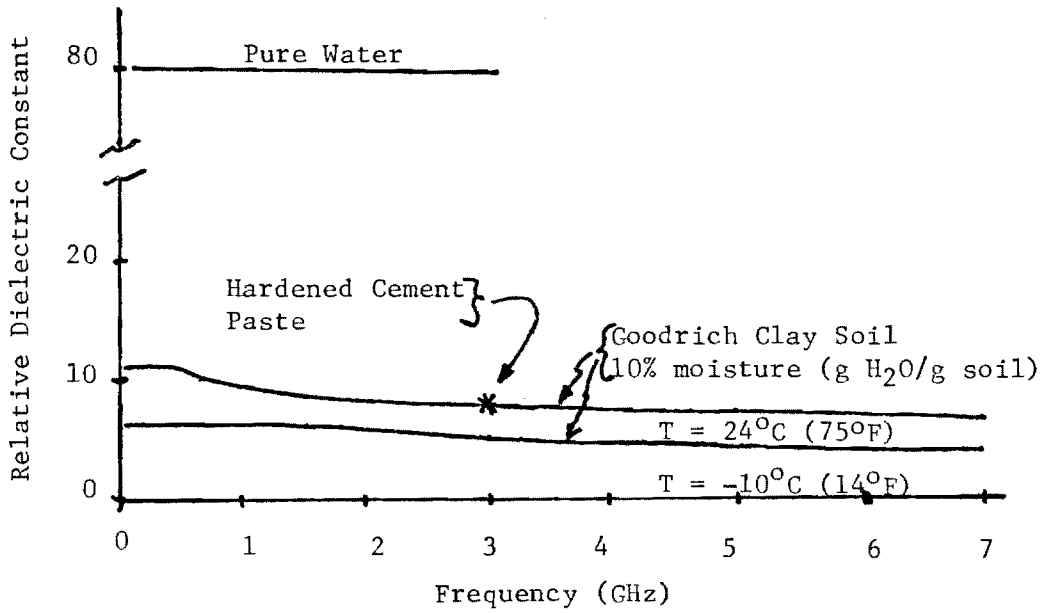

Figure B-15. Relative Dielectric Constant of Clay, Water and Hardened Cement Paste

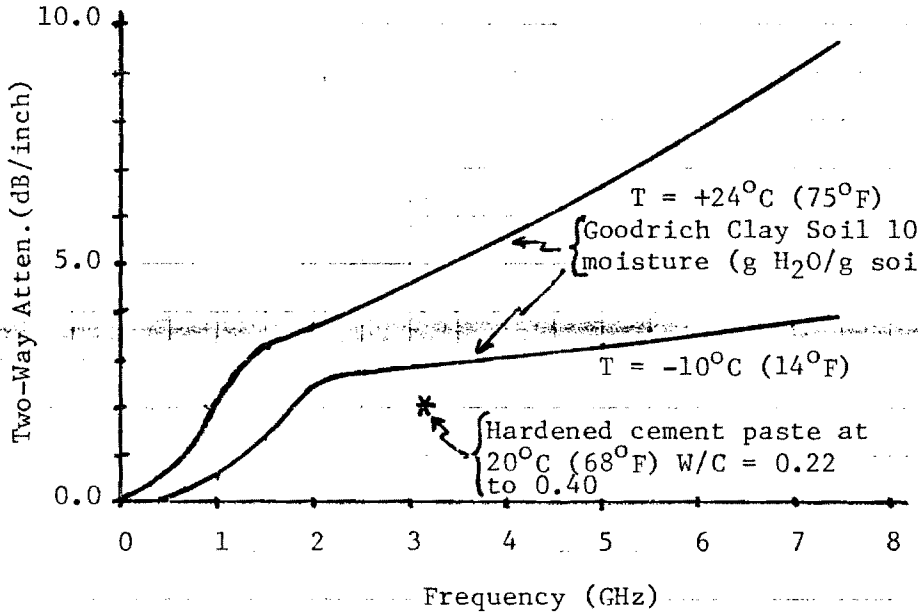

Figure B-16. Two-Way Attenuation Versus Frequency For Goodrich Clay Soil with 10% Moisture (g H_2O/g soil) at Two Temperatures. Attenuation For Hardened Cement Paste At 3GHz Is Indicated By Asterisk.

Hoekstra and Delaney (3) indicate that many types of soils are characterized by a "dielectric relaxation" at certain frequencies. The dielectric constant decreases with increasing frequency and the dielectric loss factor (loss tangent) goes through a maximum at a certain frequency. They indicate that the relaxation observed can be attributed to the presence of bound water in soils. In comparing the relaxation of water in bulk and soil water, it is observed that the frequency of maximum dielectric loss in soils is displaced to a much lower frequency than in bulk water; typically between 0.3 to 1 GHz for soil water compared to 22 GHz for bulk water. Also, the frequency of maximum loss is dependent on temperature. These effects are clearly illustrated by the curves shown in Figures B-14 and B-15 for the Goodrich Clay. In general, lower temperature yields a lower attenuation and a higher frequency of maximum loss. Apparently, the so-called "bound water" consists of a thin layer of water molecules intimately bonded to polar sites in the host medium. This bonding reduces the rotational polarizability of the water molecules and thus lowers their relaxation frequency (5).

It is suspected by the authors of this report that the same effects of moisture on concrete can be observed. In summary, there is more information on moist soils than on moist concrete at the frequencies of interest. For the purpose of this discussion on theory, it will henceforth be assumed that moist concrete behaves in the same manner as moist Goodrich Clay. It is also postulated that concrete at lower temperatures (e.g. freezing) will exhibit considerably lower attenuation in the same manner as moist Goodrich Clay. This observation becomes significant when trying to interpret some of the measured data collected on this project.

The effect of the attenuation on the radar return from an air void under a concrete slab is threefold as indicated earlier. First, the signal to interference ratio (SIR) is reduced. For example, the signal attenuation through a 10 inch slab of concrete with the loss characteristic postulated in Figure B-16 is about 8 dB at 24°c (one half the value for clay at 0.8 GHz). If the moisture content is reduced or if the temperature is reduced, this loss decreases dramatically. For example, if the temperature is below freezing, the attenuation through 10 inches of material is about 2 dB. If the concrete is relatively dry, the attenuation has been observed by the authors at much smaller values. As indicated earlier, most of the interference signals do not travel through the concrete slab, and therefore, do not experience this attenuation. Thus, the attenuation being discussed directly reduces the SIR, and thereby reduces the ability to distinguish void signals from interference signals.

Another effect of attenuation is to corrupt the estimation of void size if the void is less than 3 inches where peak signal values are used in the estimation. For larger void sizes, the attenuation does not directly effect the estimation.

A third effect of attenuation on the radar return from an air void is to distort the shape of the returning signal, making it more difficult to recognize. In Figure B-16, note that high frequencies in the band of interest are attenuated more than low frequencies. Thus, the spectrum of the radar return is distorted causing the radar signal itself to be changed. The general effect is to make the spectrum narrower in bandwidth and, thus, make the radar returning signal of longer time dura-

tion. However, this effect is not as serious as the attenuation of signal amplitude. The signal is likely to be attenuated below the interference level before any major distortion of signal shape can be observed.

APPENDIX B

REFERENCES

(1) Ramo, S. and Whinney, J. R., Fields and Waves in Modern Radio, John Wiley and Sons, Inc., N. Y., 1960 pp 270-292.

(2) Von Hippel, Arthur R., Editor, Dielectric Materials and Applications, The M.I.T. Press, Cambridge, Mass.

(3) Hoekstra, P. and Delaney, A., "Dielectric Properties of Soils at UHF and Microwave Frequencies", Journal of Geophysical Research, Volume 79, No. 11, April 10, 1974, pp 1699-1708.

(4) Hasted, J. B., and Shah, M. A., "Microwave Absorption by Water in Building Materials", Brit, J. Appl. Phys., Volume 15, 1964, pp 825-836.

(5) Herrick, David L., An Intrusive Slotted Cylinder Antenna Array for Subsurface Moisture Profiling, Ph.D. Disertation, Montana State University, 1979., Univ. Microfilms International, Ann Arbor, Mich.

APPENDIX C

SIGNAL PROCESSING

Analog/Digital Hardware Processing

The analog signal processing involves the detection of the large signal return from the top of the surface of the pavement. This is accomplished by a electronic hardware section called the "range tracker". Once the time of the surface return is established all other video timing is referenced to that point for the hardware functions. This has been done so that small random movements of antenna height above the ground do not affect the signal return timing for void detection. With the top of the pavement surface established as a fixed time reference voids will appear within a fixed time interval after the reference time.

From this reference point a timing "window" is initiated. The signal is allowed to pass through for subsequent processing for approximately 20 nano-seconds ($20X10^{-9}$ seconds), relating to an equivalent distance in air of approximately ten feet. This time (20 nanoseconds) in a medium such as concrete, $\varepsilon = 6$, is modified by the dielectric constant so that approximately 4 feet is available for processing. It is noted that this is only a result of timing conditions in the analog processor. The radar signal return before application of the window represents a distance of approximately 100 feet in air, or 30 feet in average soil. With the analog signal windowing applied, the available depth is limited.

A portion of the analog signal in this timing window is then digitized by an analog-to digital converter and stored in a digital buffer memory. The buffer memory is accessed by the micro-computer under program control, thus the signal return is now represented by a set of numbers that can be further processed by the software program in the micro-computer. The actual time at which a set of samples is digitized and put into the micro-computer memory is under direct operator control. A command is issued to the micro-computer by the operator and the sampling process is initiated. Thus, the operator can position the radar equipment over the specific area to be tested and designate when a measurement is to be made. The amount of signal currently digitized and stored is approximately equivalent to a two-foot depth.

Digital Software Signal Processing

Any manipulation of the radar signal return can be construed as "signal processing". Thus, everything that occurs within the micro-computer related to the signal falls in this category and needs explanation. For this reason this section has been divided into two parts; the first detailing the signal processing related to the theory of finding and sizing voids; the second describing secondary manipulations of the signal return. These secondary manipulations do not extract information but include such processing functions as display and storage of the signal. The following is a listing of the processing described in both parts.

Part one:

(1) Calibrate signal return using reference waveform.

(2) Identification of local minimums and maximums in the signal return.

(3) Locate the smallest minimum and largest maximum and test for "threshold" crossing.

(4) Test for time difference between the selected smallest/largest peaks; estimate void size if time discriminate is applicable.

(5) Test for amplitude values; estimate void size using amplitude.

Part two:

(1) Data transfer from buffer memory to micro-computer memory.

(2) Data transfer from micro-computer memory to magnetic disk memory.

(3) Data display and plot on the video unit.

(4) Data print-out on the line-printer.

Part One

(1) The signal return from the concrete/base media has a significant amount of interference or clutter amplitude perturbations. In an attempt to "normalize" or remove the interference a "reference" signal return is recorded from an area where no void is likely to exist. This reference is subtracted directly from all subsequent measurements. Only perturbations from the reference signal are thus processed for void location and sizing. The clutter perturbations remain essentially fixed over the extent of the concrete pavement. Changes occur in going from a non-reinforced section to a reinforced section, if thickness changes drastically, or temperature/moisture content vary significantly. In these cases, a new reference signal must be recorded.

(2) The identification of the minimum and maximum peaks of the signal return is the first step in void detection. As indicated in the theoretical modeling there is a reflection from the bottom of the pavement/void interface and another reflection from the void/base interface. The size of the void determines the timing of the two signal reflections. Even under no void conditions there will exist a signal reflection if the base material is not identical to the pavement material, but this should be minimal due to the subtraction of the reference. A sequential search is made through the signal and all local minimum/maximum values are stored along with their time of occurrence.

(3) From the theoretical modeling it is known that if a void is present a large negative amplitude peak occurs first followed by a large positive amplitude peak. As a result, the algorithm initially searches through the list of minimum values and picks the largest negative amplitude as the candidate. Then the algorithm searches for the largest positive peak occurring after the negative amplitude occurrence. The resulting output is now the amplitude and time of occurrence for the largest negative peak and the largest positive peak following the negative peak occurrence. The amplitudes are then compared to a minimum acceptable amplitude called the "threshold". If the values fall below this threshold there is a high probability that the minimum/maximum pair chosen does not represent the location of a void. This threshold value has been computed based upon laboratory measurements to give reliable void detection and identification of size.

(4) As described in the theoretical modeling, the time differential between the identified peaks is a measure of void size, especially for

voids larger than three inches. Thus the algorithm checks this time differential. If the value exceeds the nominal value for a three inch void then the void is sized by that time differential. If the time is less than the nominal value for a three inch void the determination of void size is passed on to the amplitude discrimination. For actual signal returns from voids there is a minimum value for the time differential, and the algorithm checks to see that the minimum is exceeded. This prevents random noise spikes from being detected as voids.

The time between data samples being processed is 0.026 nanoseconds. In terms of the time difference in these units, the void size is estimated by

$$\text{Void Size (inches)} = (0.026)\cdot(5.9014402)\cdot\text{time difference}$$

with the constraint that the time difference is greater than 19 time units or data samples. This establishes the switch point at 3".

(5) Based on the theoretical modeling and with calibration biases developed during laboratory measurements, the amplitude discrimination algorithm looks at the negative peak values to size a void less than three inches. Experience with laboratory measurements has shown that the negative peak value yields the best results.

In terms of the amplitude units in the microcomputer for the data samples, the void size is estimated by

$$\text{Void Size (inches)} = \frac{6}{\pi}\sin^{-1}\left[\frac{\text{Peak Negative Amplitude}}{\text{Calibration Number}}\right]$$

with the constraint that the time difference is less than or equal to 19 time units.

Part Two

(1) The signal return that has been digitized by the analog-to-digital converters has been stored in a temporary buffer memory. The digitizer samples the signal return every 0.013 nanoseconds. In concrete, this is approximately equivalent to 0.03 inches. This memory is not easily used for normal micro-computer operations and a special retrieval algorithm was written so that the signal data is accessible. The algorithm transfers up to 512 8-bit binary words from the buffer memory to the computer memory.

(2) At the option of the operator signal returns can be automatically transferred from micro-computer memory and stored on permanent magnetic diskettes. The algorithm transfers up to 512 8-bit binary words from micro-computer memory to disk.

For the detection/sizing of voids it was determined that only a sampling of every other point was needed to accurately represent the signal return. In addition, the total length of 512 points was deemed unnecessary since the area or time for a signal return from a void should appear much sooner than the 400th point. Thus, every other point, for the first 440 points, was chosen for transfer, making the total of 220 points available. This represents approximately 1.15 feet of depth in concrete. When 9 inches of concrete is assumed, the signal return is composed of a portion through the concrete and the remainder through the void (air). The resulting signal return processed (220 points) thus

represents 9 inches of concrete and approximately 12 inches of void possible below the concrete - a total depth of just under 2 feet. It is important to realize that this is simply a function of user chosen parameters. If thicker concrete pavement is involved or more depth is desired, only timing parameter changes are necessary. No limitations are placed on the signal processing or void sizing algorithms because of the chosen timing parameters.

(3) Several display options are available to the operator at any time during the data processing sequence. The first is the actual digitized signal return. The second is the numerical information about the minimum/maximum amplitudes and time difference values of the signal. The third is the "synthetic" void location and sizing display, which is the primary information display for the operator. This display illustrates both numerically and graphically the void location and size results for each measurement. The display is labeled "synthetic" because of the representative graphical indications of concrete pavement thickness and void size. Figure C-1 illustrates the display with annotations for explanation. The results obtained from the signal processing through the amplitude/time discriminate algorithms are directly illustrated on the display.

(4) At any point in the measurement process, a permanent hard-copy of the results can be obtained. All the necessary data has been stored on magnetic disk and can also be printed at any time in the future. The software programs involved can plot 220 points for a single return and the multiple option can plot up to seventeen returns on the same video display and obtain a hard-copy.

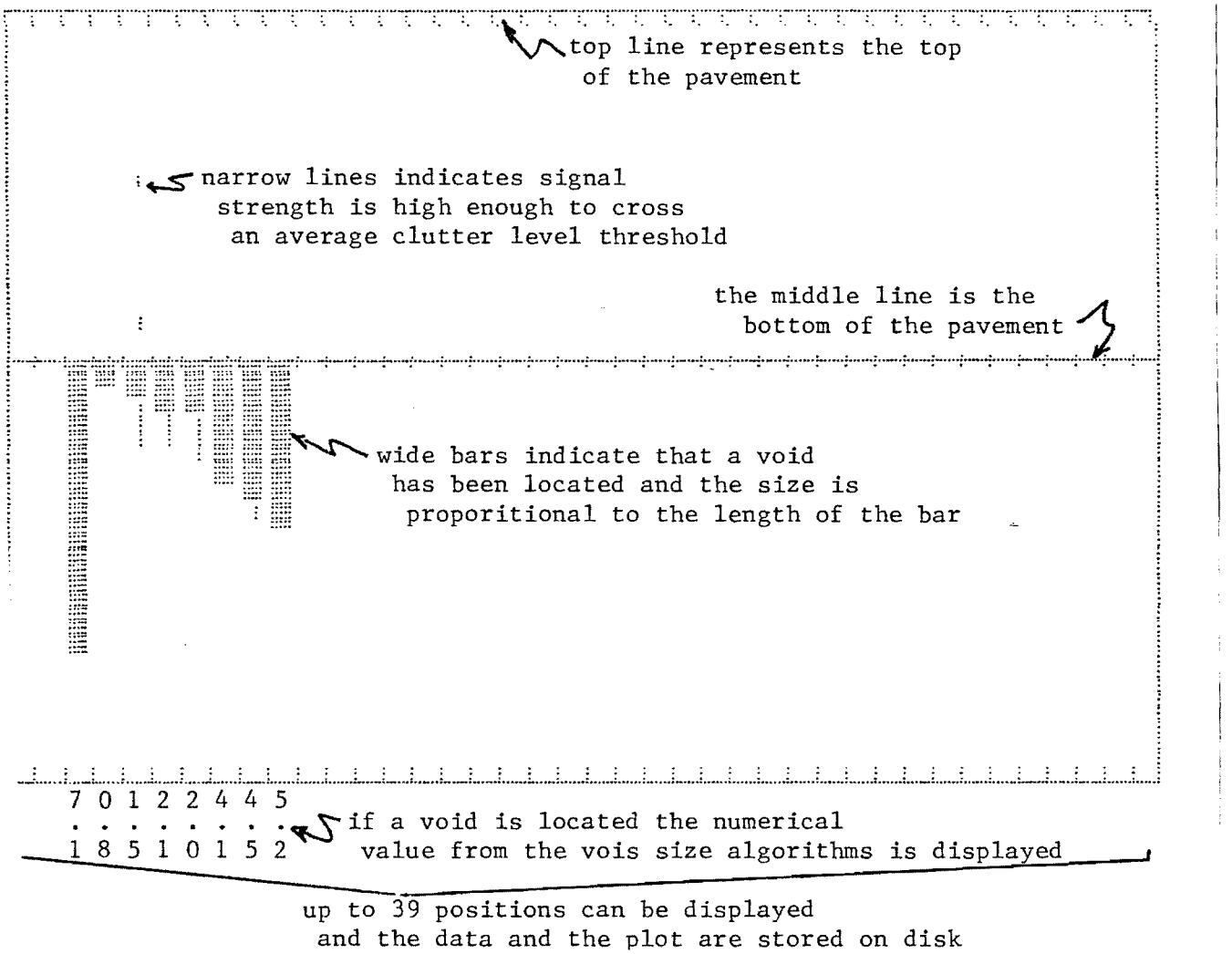

FIGURE C-1

SYNTHETIC DISPLAY

APPENDIX D

LABORATORY MEASUREMENTS

The experimental evaluation of the void detection pulsed electromagnetic wave equipment and signal processing algorithms was accomplished in two phases. The objective of the experimental evaluation being to quantify the accuracy, precision, reliability, limitations, operational characteristics and environmental characteristics of the equipment and processing algorithms. The first phase was conducted inside a laboratory under controlled environmental conditions. Test sections of concrete pavement approximately 43 inches by 43 inches by 9 inches thick, both reinforced and nonreinforced, were used. These test sections were placed over base materials of concrete, asphalt, aggregate, and concrete stabilized clay and measurements were made. Moisture levels were varied both for the concrete top section as well as the base material. Voids were simulated by elevating the top concrete section a measured amount above the base material.

Actual measurements were made for void sizes 0" to 8.5" in 0.5" increments. Some measurements were made simulating voids filled with water. The findings indicate a definite agreement with the theory as to the variation in amplitude of the positive and negative peaks and in the time differential of the peaks. Thus, the discriminates from the theoretical considerations were verified. In addition, the measurements provided the basis for calibration of the theoretical modeling. The calibration involves a bias for differing base materials.

In the following paragraphs the details of the laboratory measurements and results are given. The design and construction of the test sections of concrete pavement, base sections, the methods used to obtain voids between the pavement and base sections, and methods for calibration are detailed. Extensive plots are included covering all measurements made, including non-reinforced and reinforced concrete sections. The analysis of the measurements and the resulting tables for void sizing are included.

Pavement and Base Description

Four base forms were constructed from wood, all with dimensions of 43" by 43" by 12". The base forms were filled with concrete (12 inches deep), asphalt (8 inches deep), aggregate (10 inches deep), and concrete stabilized clay (12 inches deep). Three pavement forms were constructed from wood, all with inside dimensions of 43" by 43" by 9". These forms were all filled with concrete, one having reinforcing steel. So that the pavement sections could be moved easily, eye bolts were included in the corners. A hoist was also constructed to accomodate the movement of the concrete pavement sections. All materials and construction methods followed as close as possible State of Georgia Construction specifications.

Void Simulation

Measurements were made by placing one of the concrete pavement sections on top of a selected base section. Voids were created by elevating the top section using exact sized wood blocks. The wooden

blocks themselves do not interfere with the radar signal return from the voids. A complete set of wooden blocks were made such that voids from 0.5" to 8.5" in 0.5" increments could be created.

Calibration

The pulsed electromagnetic wave equipment must be adjusted at the beginning of each day to insure that a consistent set of measurements can be obtained from day to day. In addition, fine tuning might be required if there is a large temperature changes during the measurement time period. To make this calibration as easy as possible a calibration test fixture was constructed. Figure D-1 illustrates the configuration for this fixture. The fixture contains special light weight absorbing foam and a metal plate. The foam absorbs some of the electromagnetic energy, thus, decreasing the return from the metal plate. This calibration fixture is very light weight and provided a consistent reference for the equipment. So that a very consistent set of measurements could be obtained in the laboratory controlled conditions, the calibration fixture was used as a check between each void size change. This procedure is not necessary under normal operating conditions, only an initial calibration is needed.

Plotted Measurements

Figure D-2 to D-5 illustrate the results of measurements for void sizes 0" to 8.5" in 0.5" increments over all four types of base materials. The concrete pavement section used did not contain reinforcing steel. Figures D-6 to D-9 illustrate the same measurements of voids using the steel reinforced pavement section.

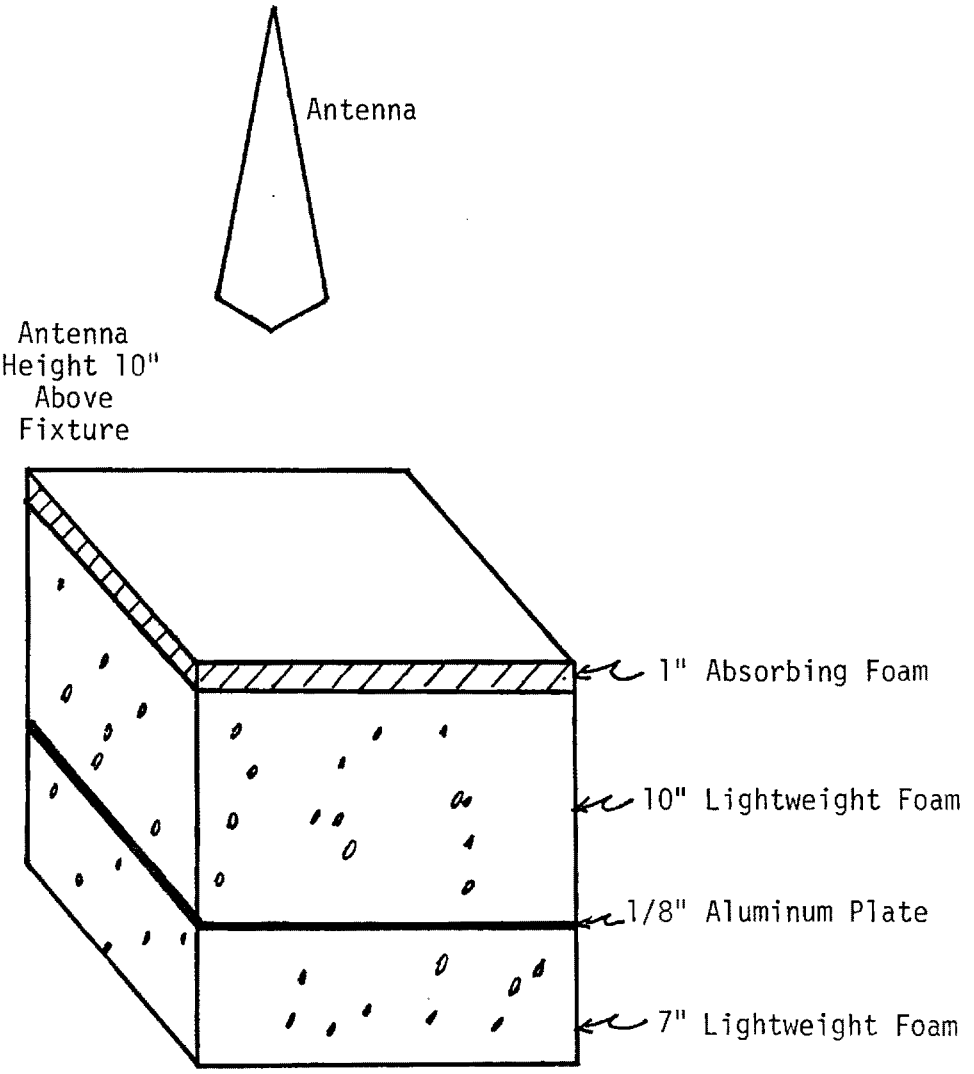

Overall Dimensions: 18" x 18" x 18"

FIGURE D-1. CALIBRATION FIXTURE.

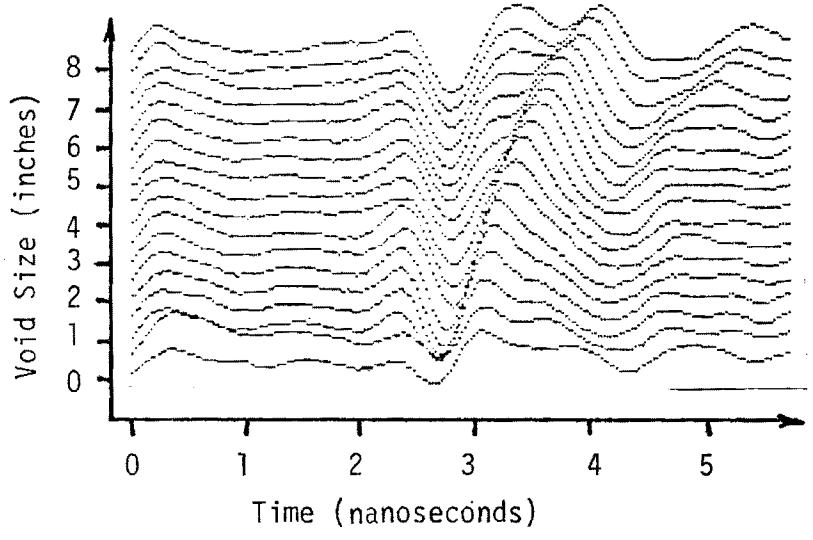

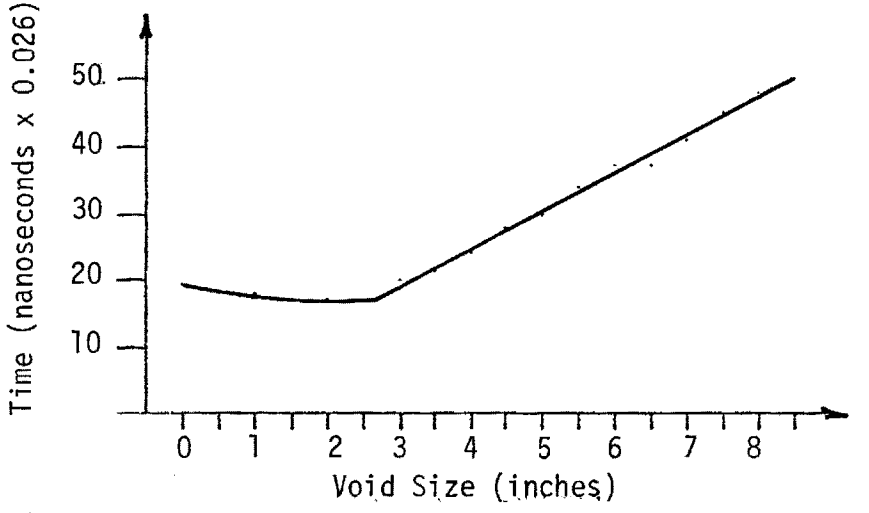

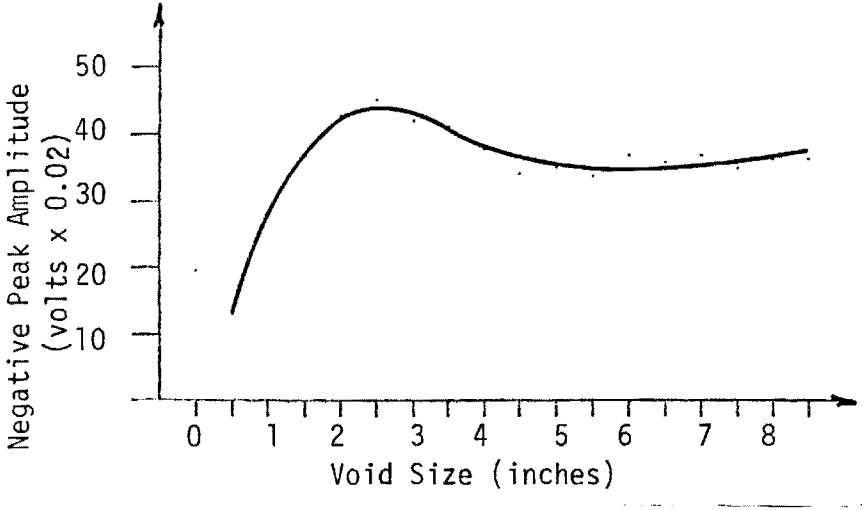

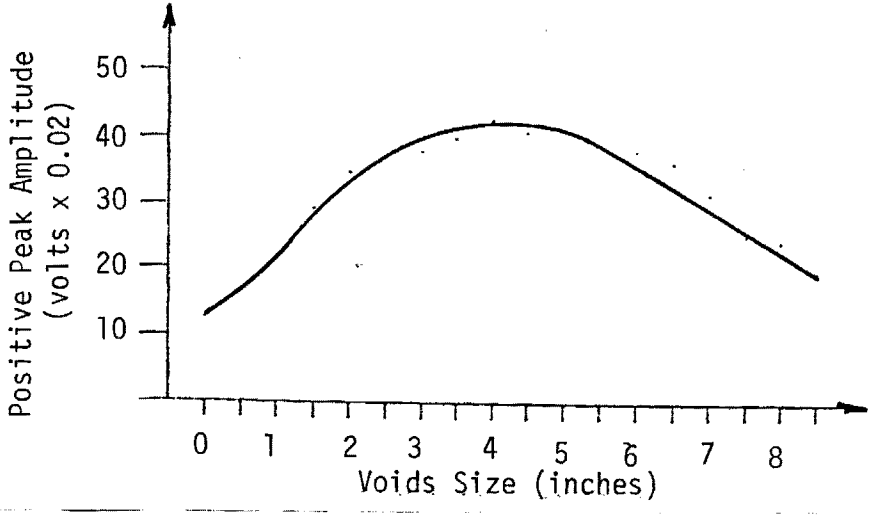

FIGURE D-2

LABORATORY MEASUREMENTS, NON-REINFORCED PAVEMENT, CONCRETE BASE

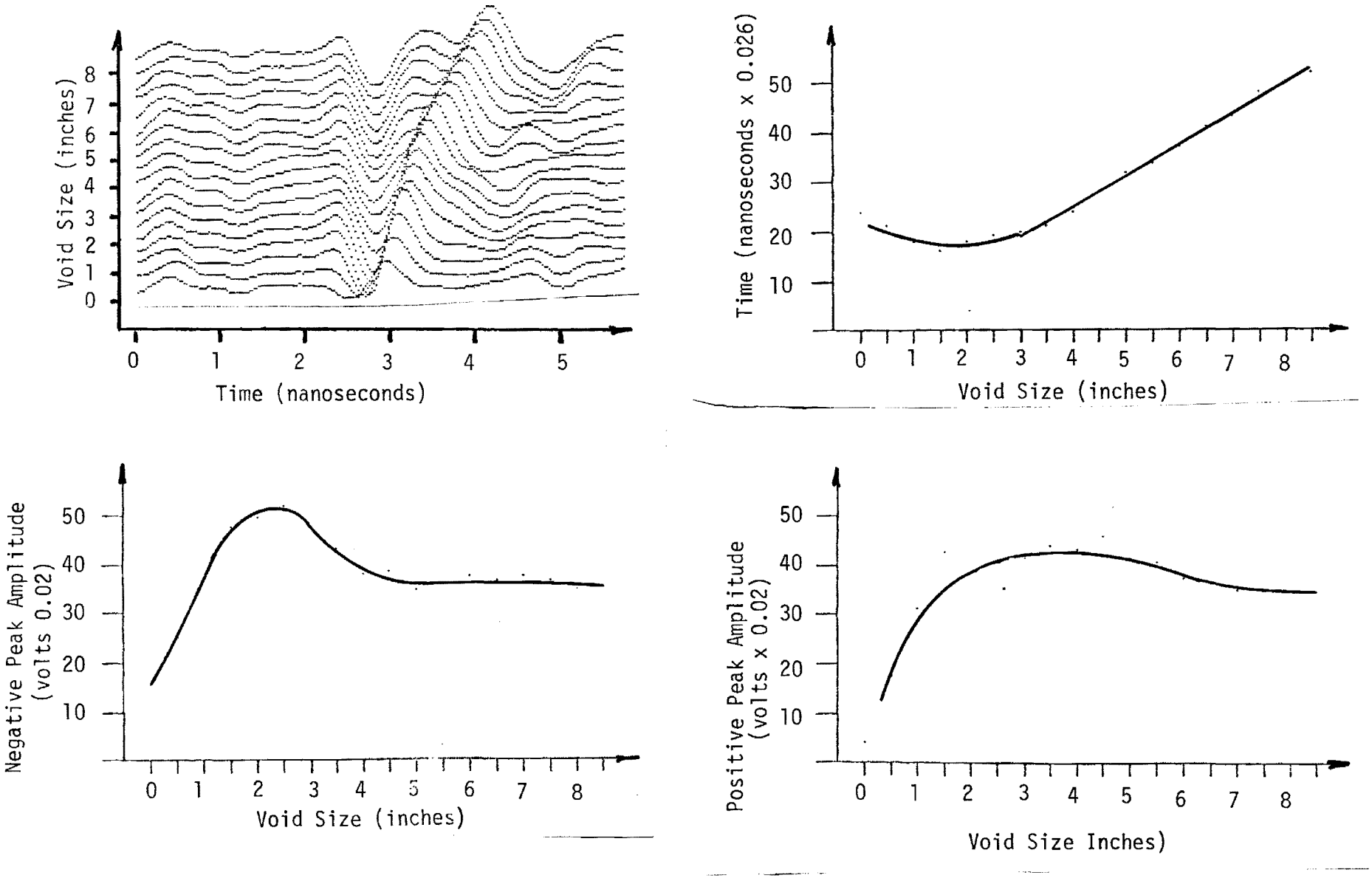

FIGURE D-3

LABORATORY MEASUREMENTS, NON-REINFORCED PAVEMENT, CLAY BASE

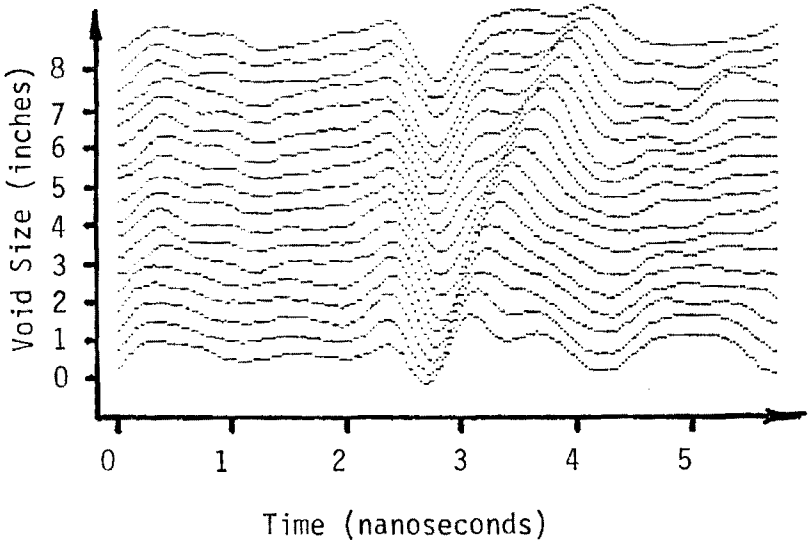

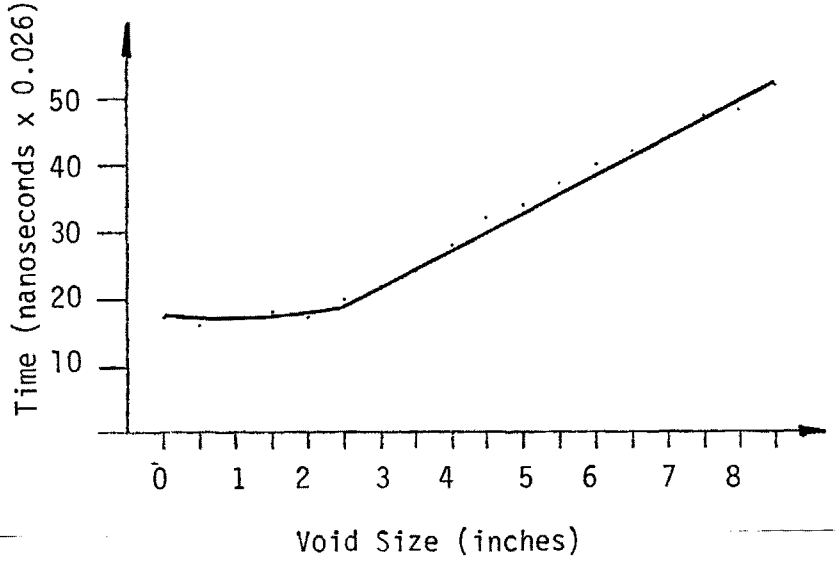

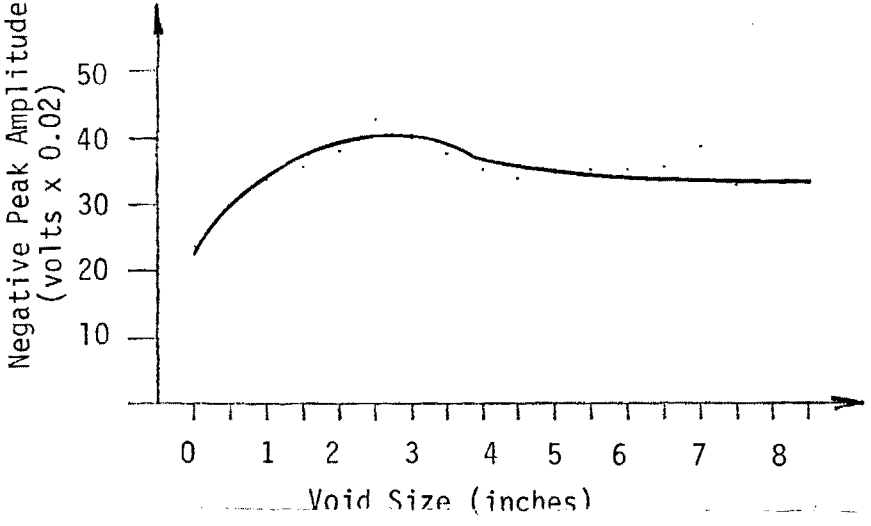

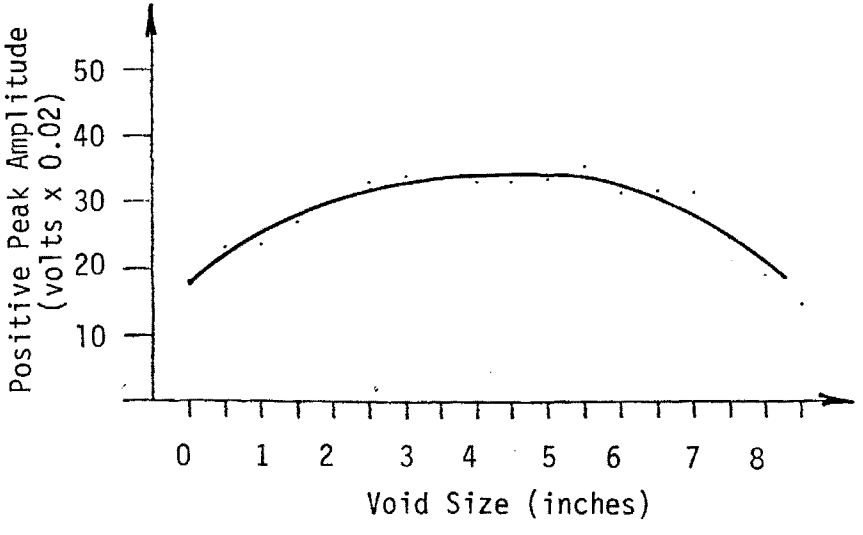

FIGURE D-4

LABORATORY MEASUREMENTS, NON-REINFORCED PAVEMENT, AGGREGATE BASE

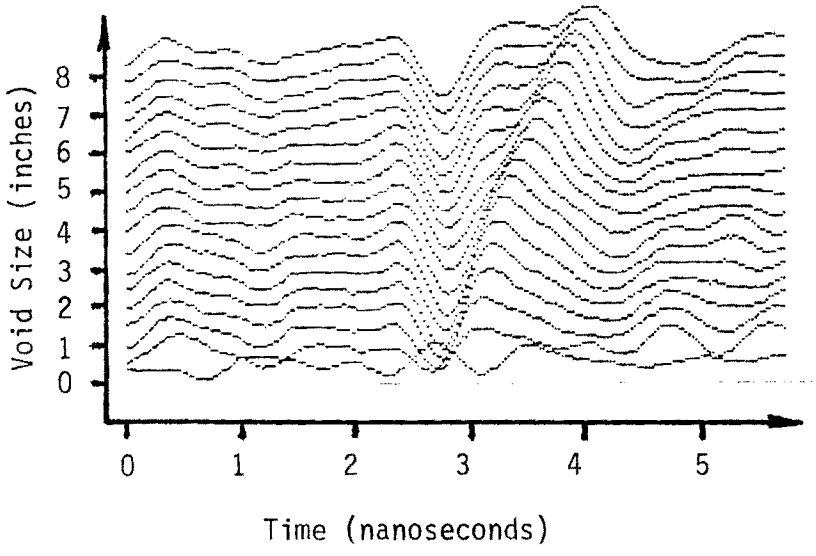

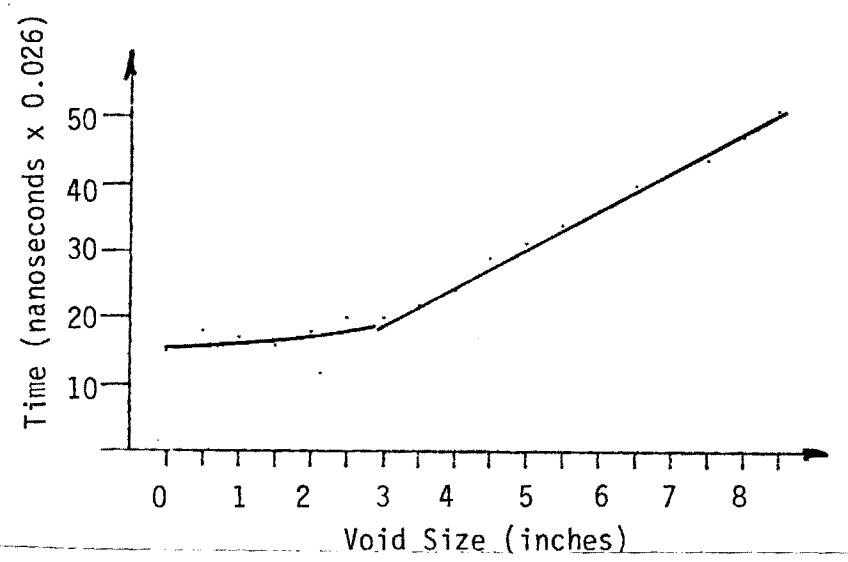

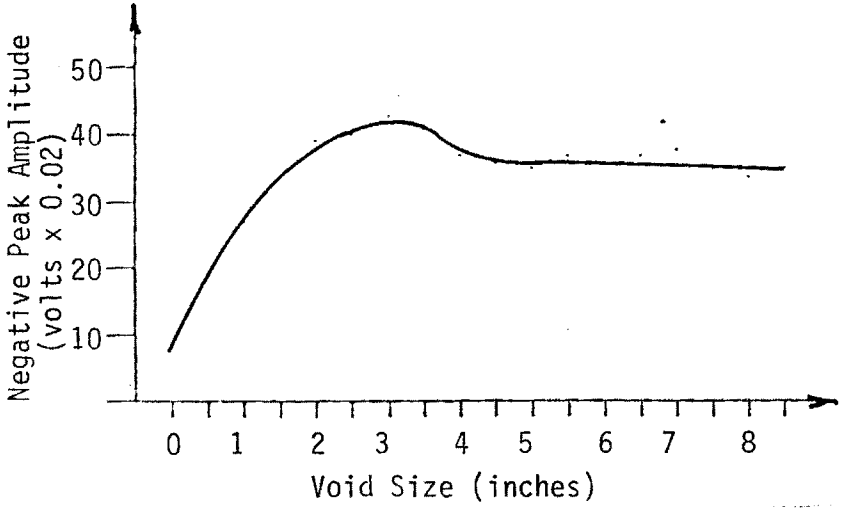

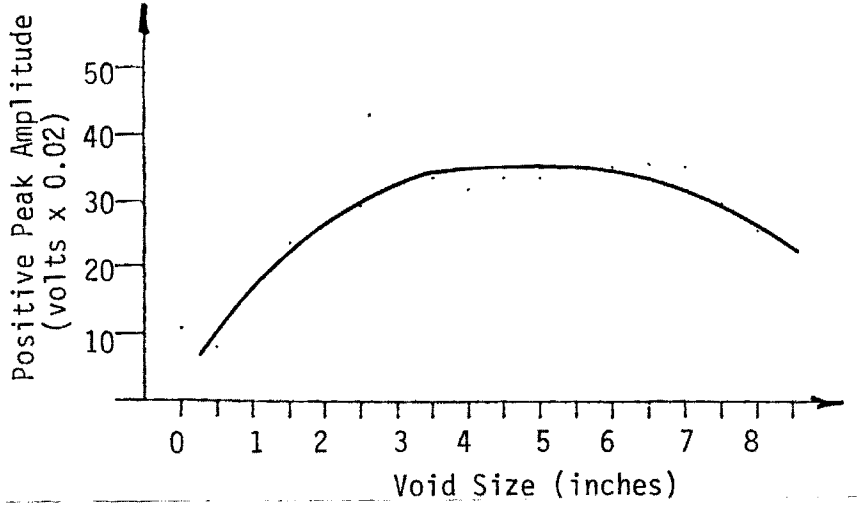

FIGURE D-5

LABORATORY MEASUREMENTS, NON-REINFORCED PAVEMENT, ASPHALT BASE

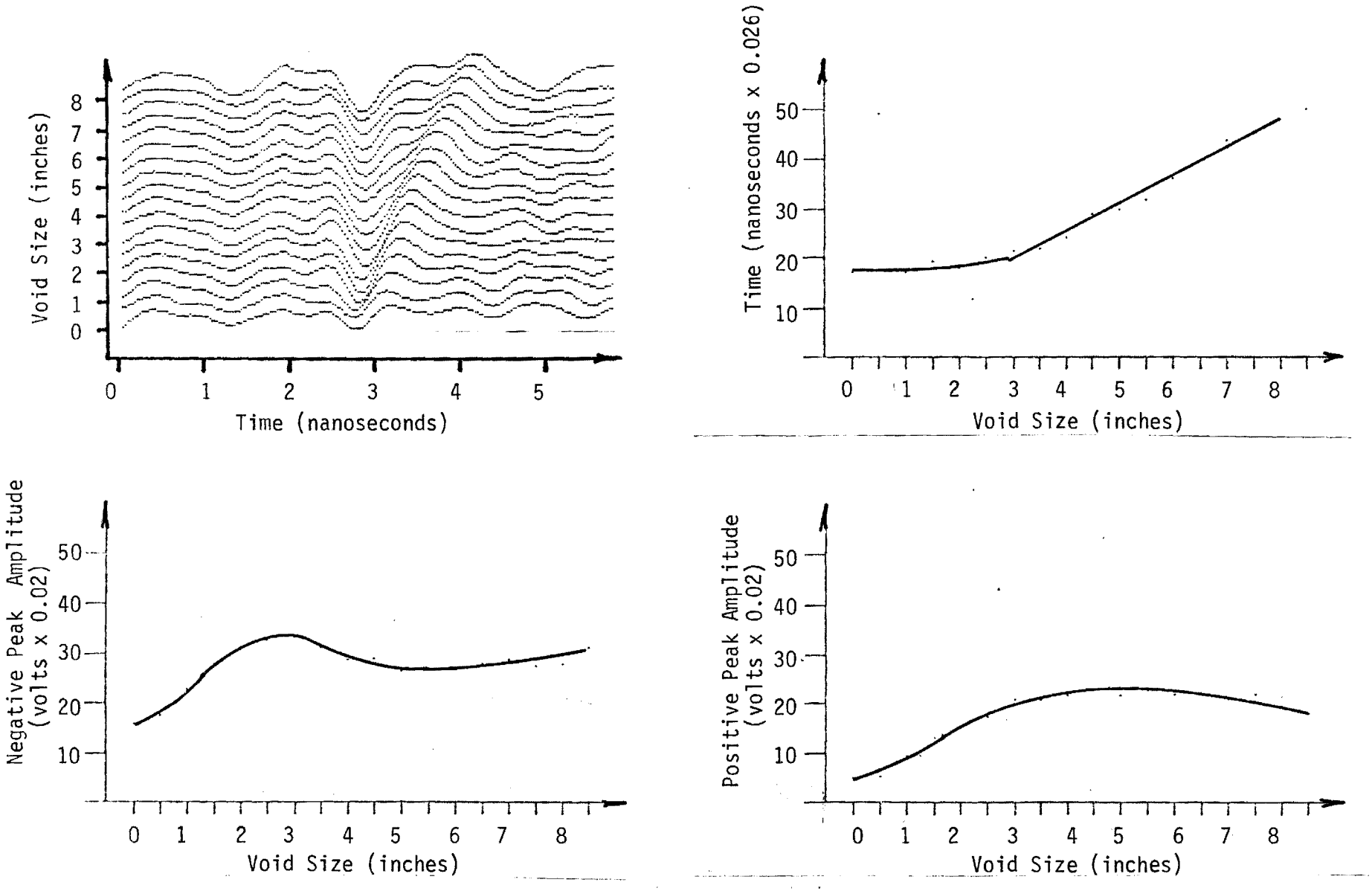

FIGURE D-6

LABORATORY MEASUREMENTS, REINFORCED PAVEMENT, CONCRETE BASE

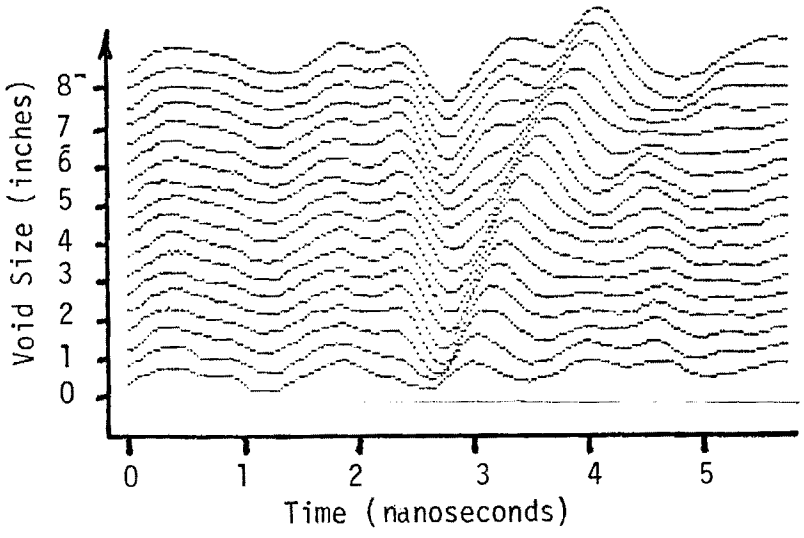

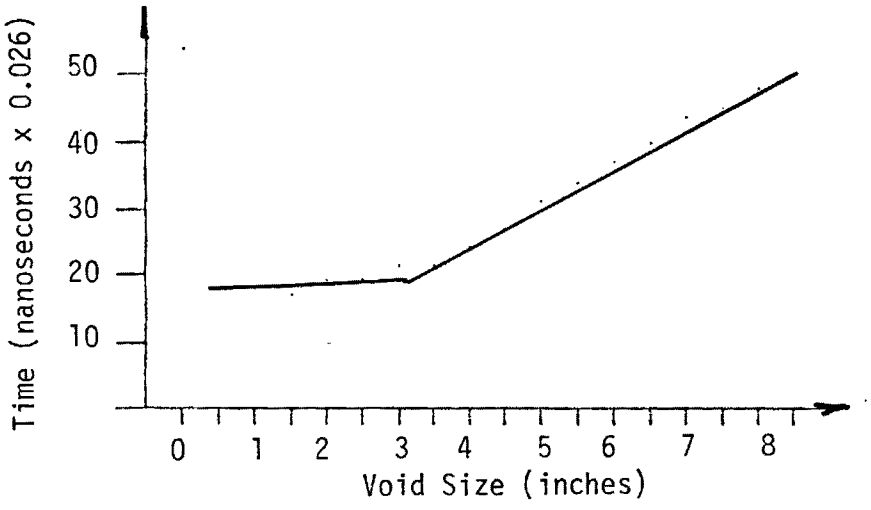

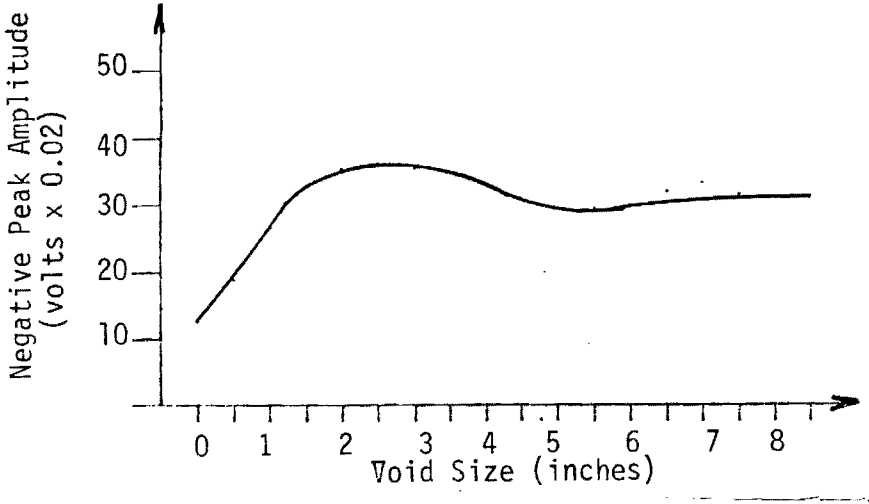

FIGURE D-7

LABORATORY MEASUREMENTS, REINFORCED PAVEMENT, CLAY BASE

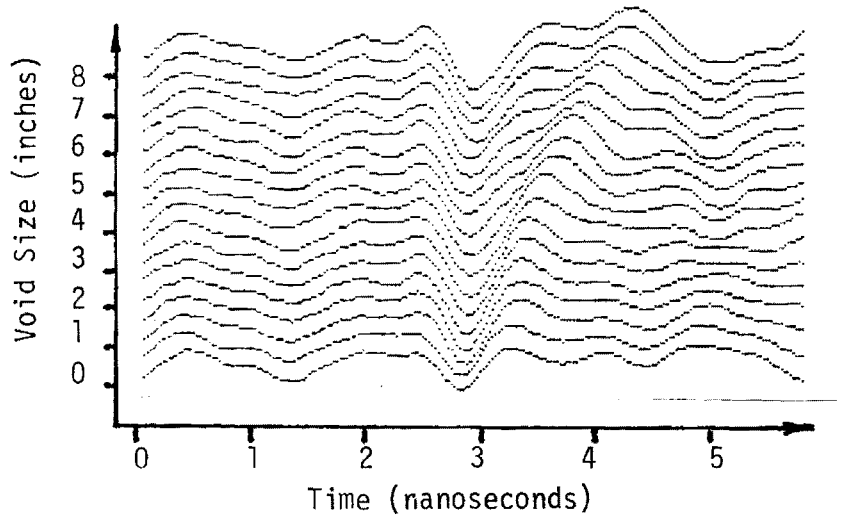

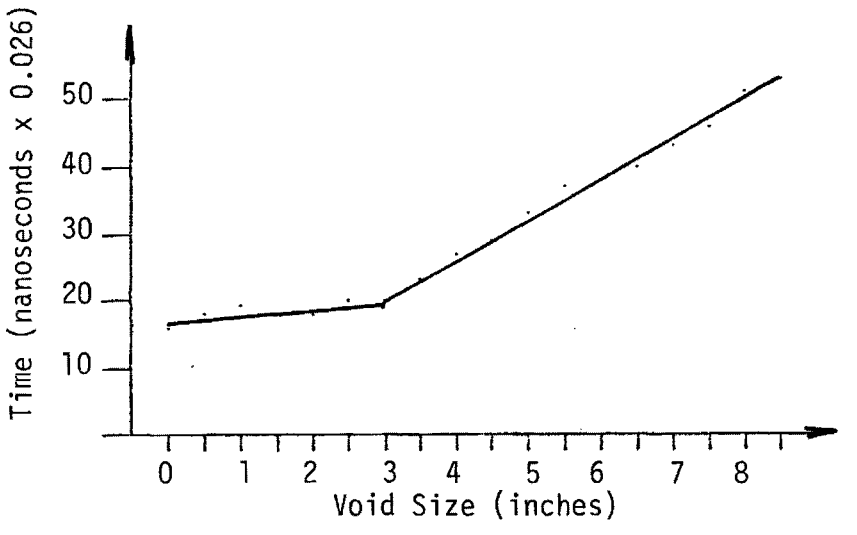

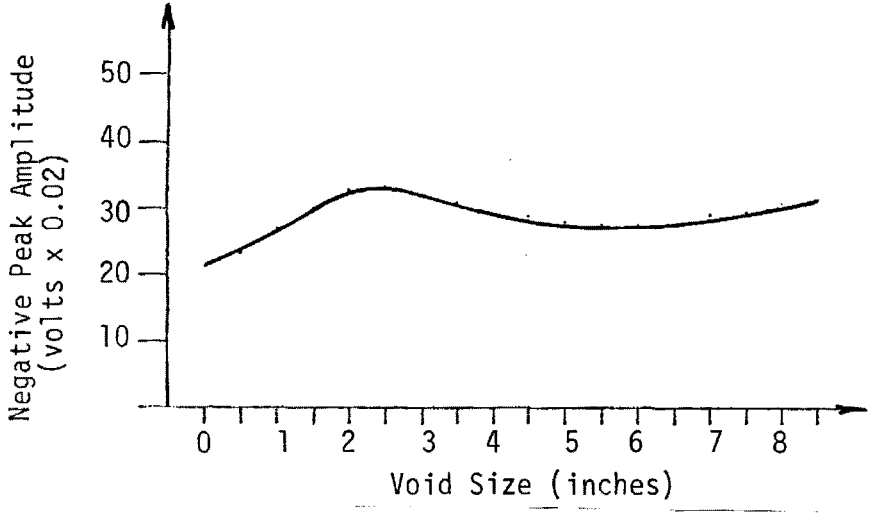

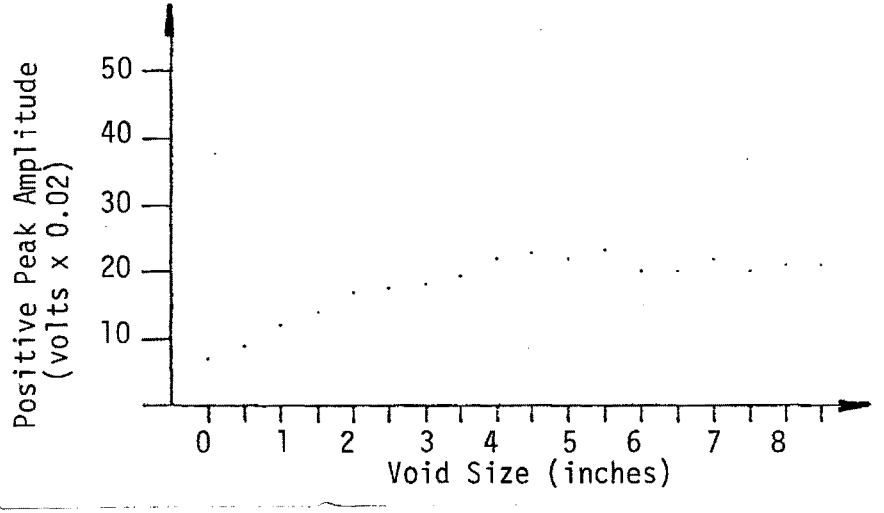

FIGURE D-8

LABORATORY MEASUREMENTS, REINFORCED PAVEMENT, AGGREGATE BASE.

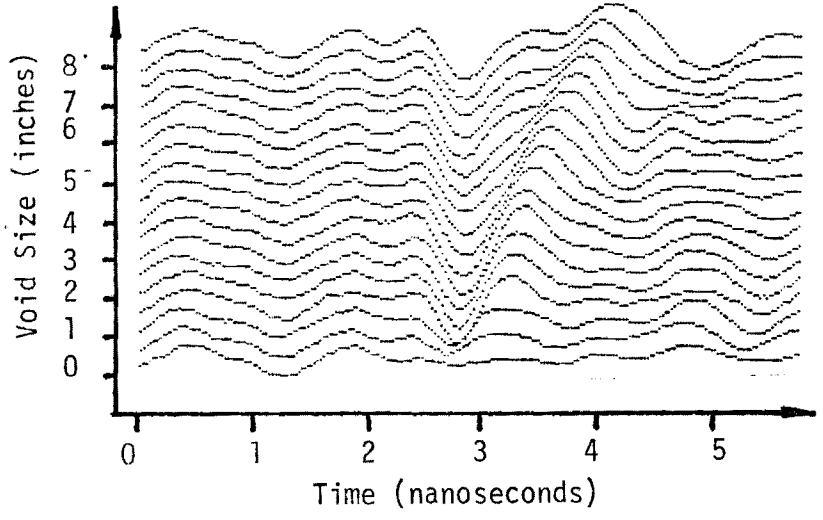

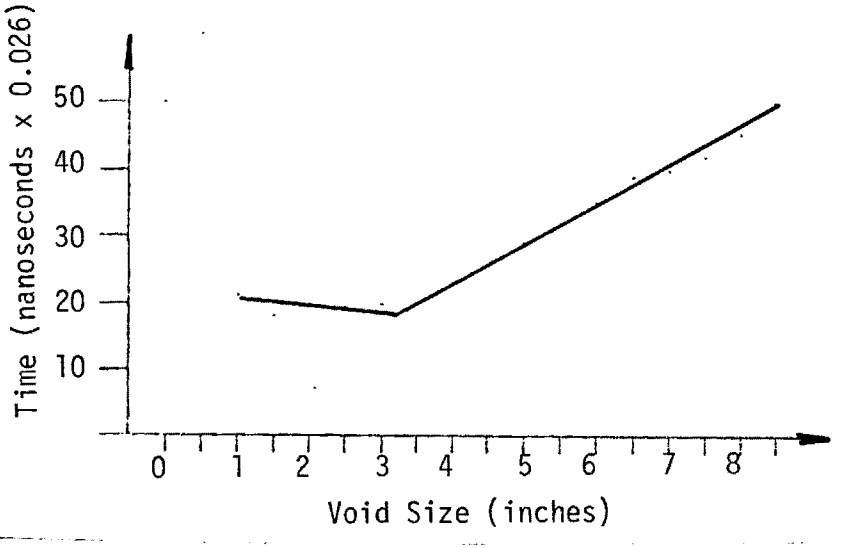

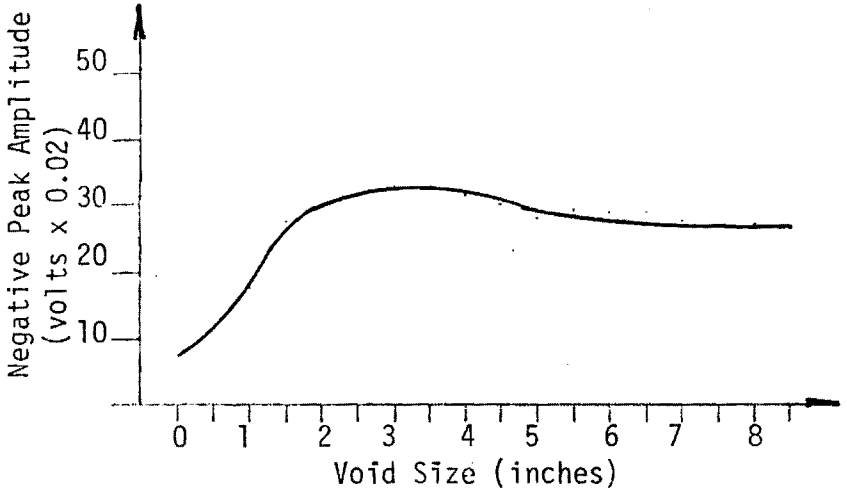

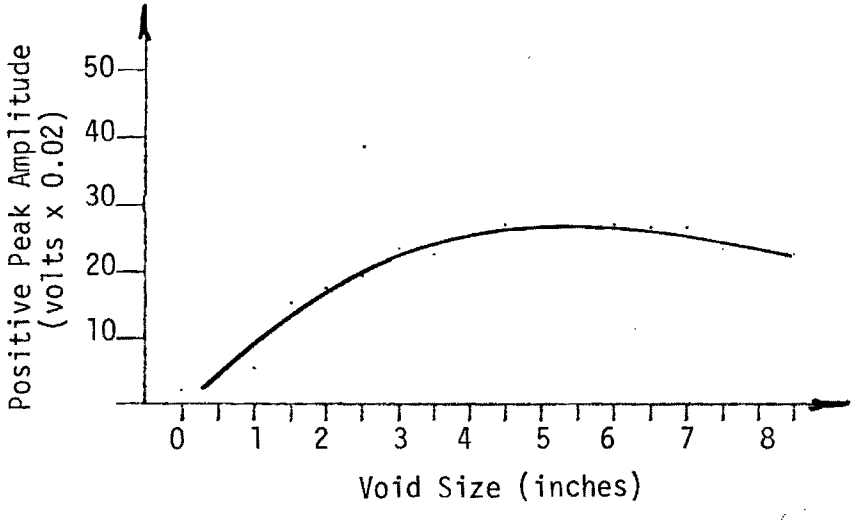

FIGURE D-9

LABORATORY MEASUREMENTS, REINFORCED PAVEMENT, ASPHALT BASE.

Each figure has four associated plots. The first in each is a sequence of signal returns for the void sizes 0" to 8.5", in 0.5" increments, with each signal return sequentially offset up the page for clarity. This type of plot facilitates comparisons between signals as the void size increases. By examination the differences in the signals become evident, especially the time deviation of the most positive amplitude peak. The second plot is of the time difference actually measured by the micro-computer between the largest negative amplitude peak and the largest positive amplitude peak. By examination it can be seen that this curve follows the theoretical modeling quite accurately. Similarly it can be seen that in the neighborhood of three inches a slope change occurs. It is in this area of a steeper slope that reliable void sizing can be accomplished. The remaining two plots illustrate the largest negative amplitude peak value and the largest positive amplitude peak value respectively. These plots also follow the theory very closely, the steepest slope occurring in the void size areas less than three inches.

In all cases, the plots with and without reinforcing steel can be compared in the area of the void and be found to be almost identical. This clearly indicates that the reinforcing steel has only a minimal effect on the signal response from the void and is not a potential problem area. There is a difference in the signal returns in the area where the steel rod occurs. This result indicates that the electromagnetic wave equipment can definitely detect and locate reinforcing steel.

In all of the above measurements, the pavement sections and the base material were kept as dry as possible, being exposed only to inside laboratory temperatures and humidity levels. Voids themselves were kept

empty. This set of measurements represents an excellent verification of the theoretical modeling. The data for the cases of concrete, aggregate and clay base materials were put through the signal processing software for void location and sizing. The results are illustrated in Figures D-10, D-11, and D-12 for the synthetic displays in each case. In Tables D-1, D-2, and D-3, the results are tabulated along with a mean and standard deviation computation for the error in estimation of void size.

Figure D-13 and D-14 are plots of signal returns from selected void sizes for wet concrete and clay base sections. Two moisture levels were used, the second being considered very wet, and by comparison no significant signal changes are observed. In addition, comparison with the dry measurements yielded no significant differences. For this set of measurements it is important to remember that only the base materials were wet. When the top pavement sections have a higher moisture level attenuation of the signal results. It is concluded that as long as the high moisture levels are confined to the base materials no degradation in performance for locating and sizing voids beneath pavement occurs.

Figure D-15 plots signal returns for the situation indicated in the diagram. For this case, the void was represented by a 12" by 12" by 2" thick piece of foam set in the aggregate base material under soaking wet conditions. The pavement section on top did not have reinforcing steel. The measurements plotted were made by sequentially moving the equipment across the block in 2" increments. This situation simulates the location of a typical void under highway pavement with wet base conditions. The indication is that the signal returns decrease in strength at the edges of the void. At greater than 4 inches from the edge of the void, the signal no longer indicates a void.

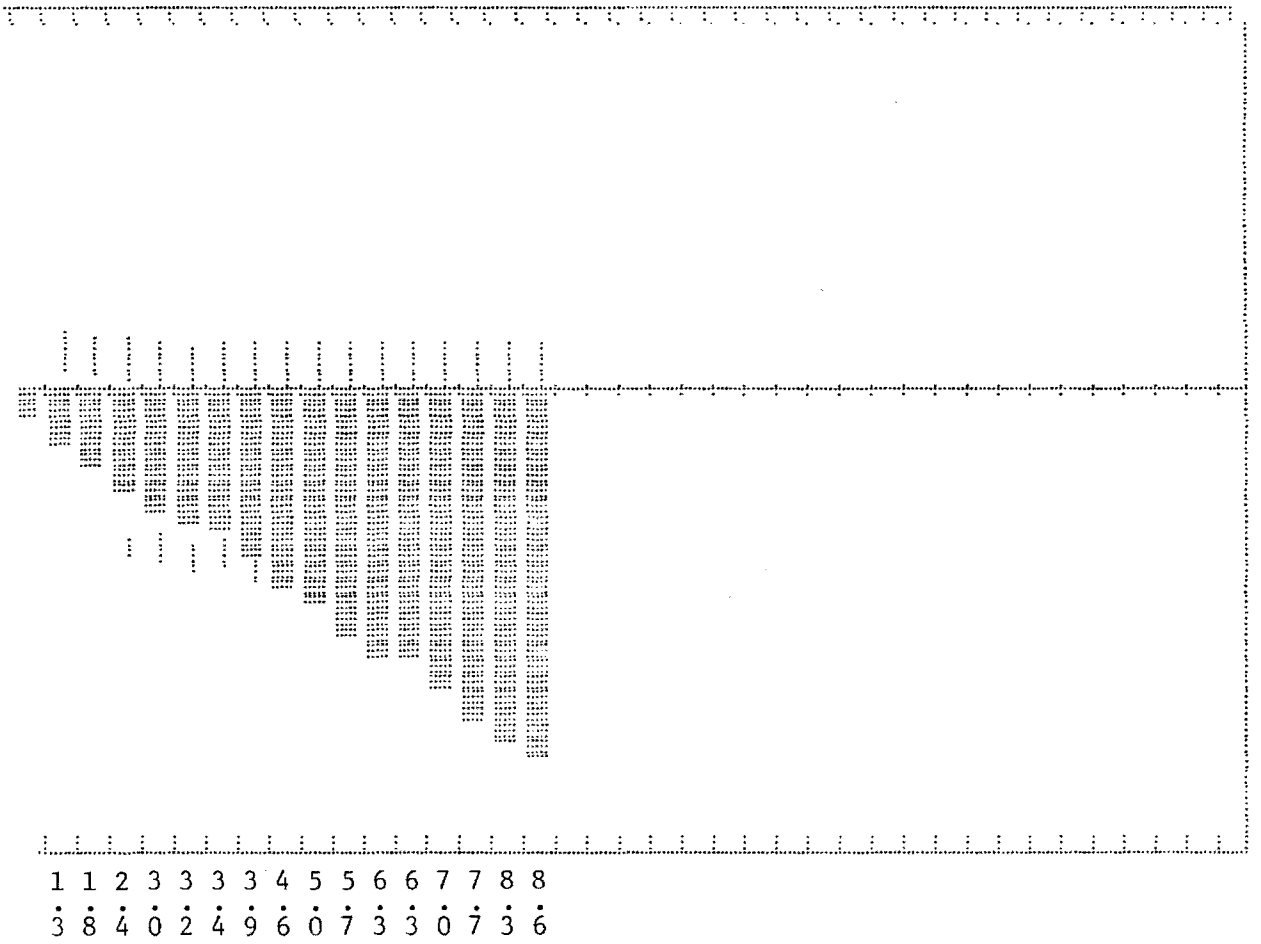

FIGURE D-10

SYNTHETIC DISPLAY MEASUREMENTS FOR CONCRETE BASE

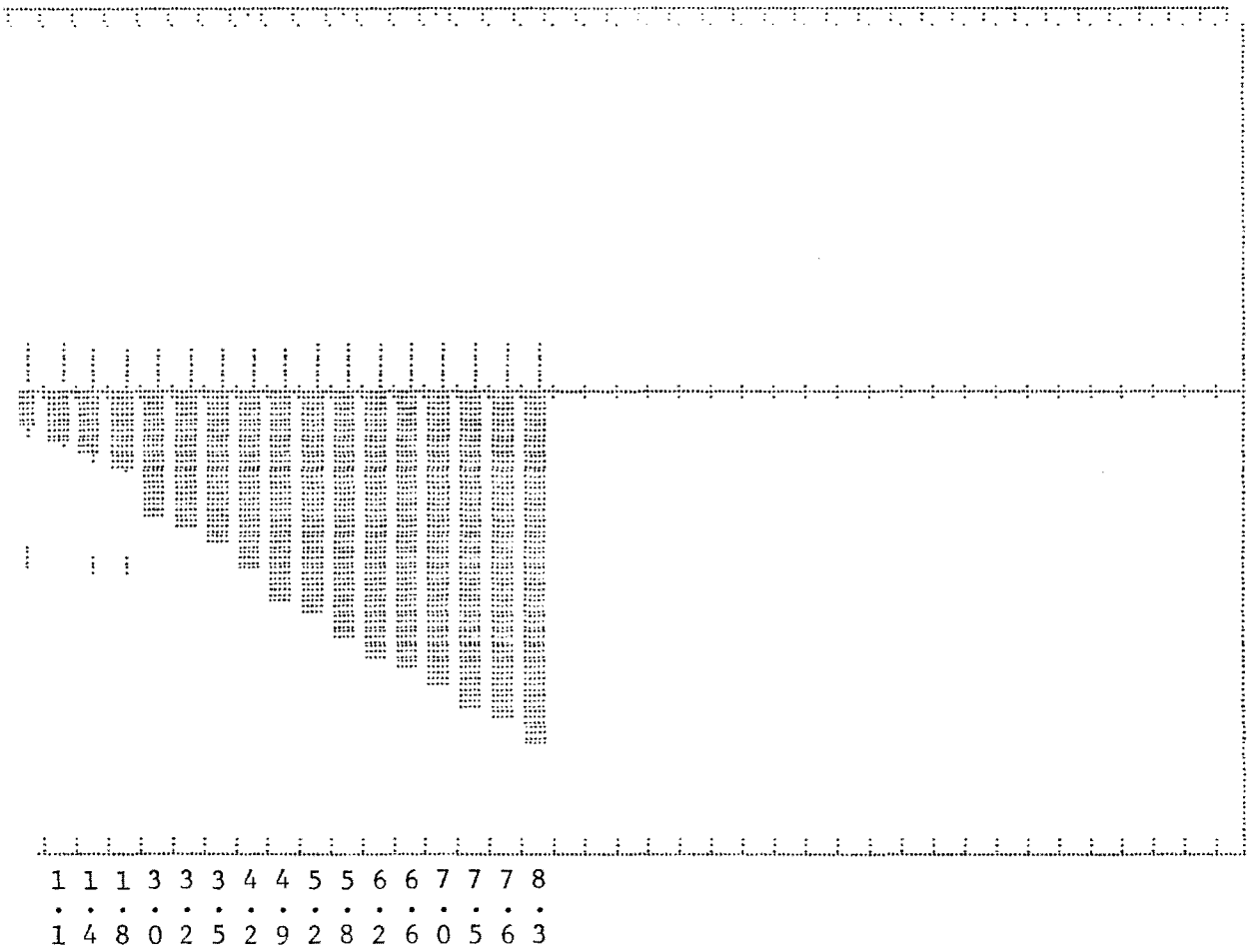

FIGURE D-11

SYNTHETIC DISPLAY MEASUREMENTS FOR AGGREGRATE BASE

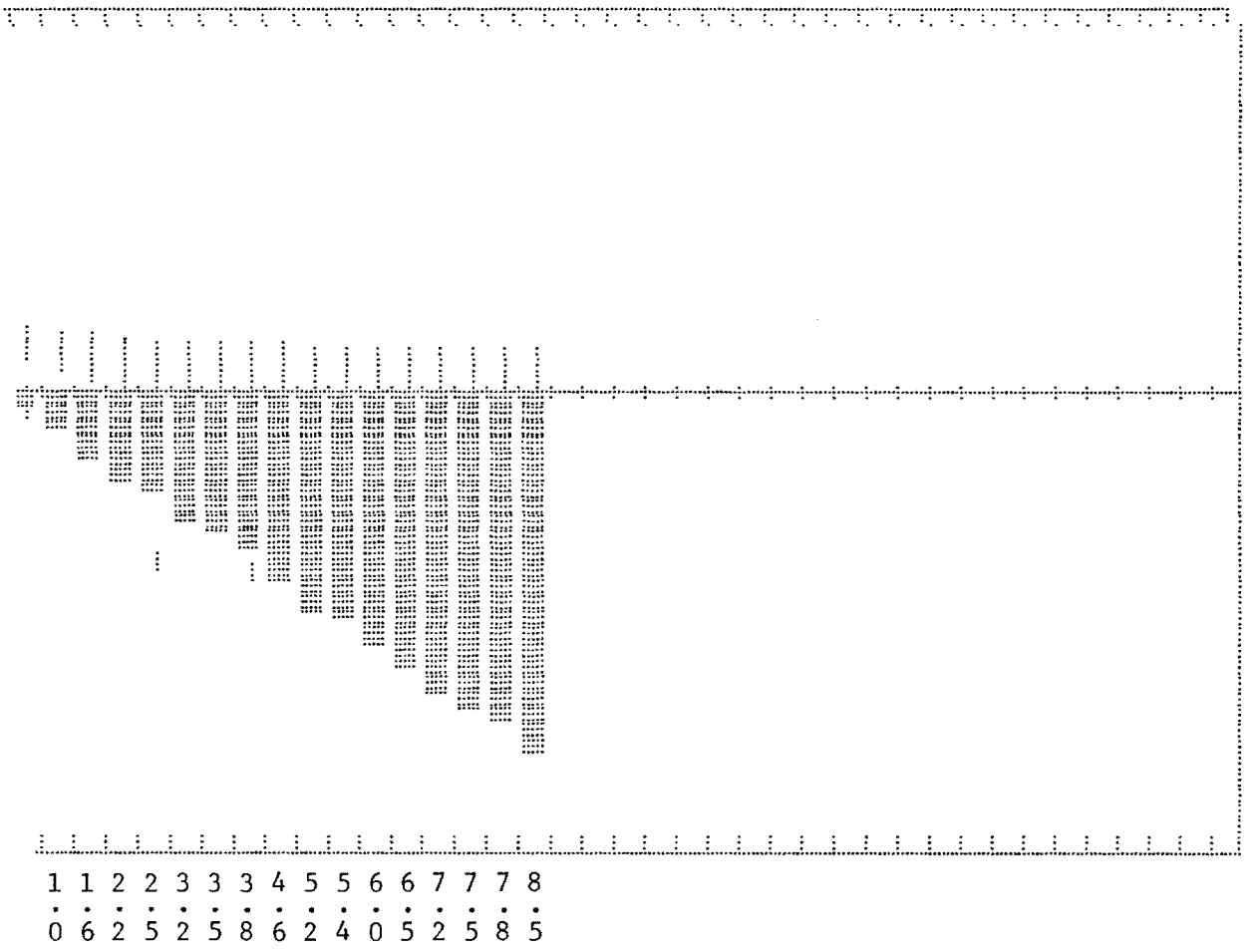

FIGURE D-12

SYNTHETIC DISPLAY MEASUREMENTS FOR CLAY BASE

TABLE D-1

RESULTS SUMMARY FOR CONCRETE

Error: $\mu = 0.14"$, $\sigma = 0.18"$

POSITION #	VOID SIZE	ESTIMATE	ERROR
1	0.0	0.1	+.1
2	0.5	0.6	+.3
3	1.0	1.3	+.3
4	1.5	1.8	+.3
5	2.0	2.4	+.4
6	2.5	3.0	+.5
7	3.0	3.2	+.2
8	3.5	3.4	-.1
9	4.0	3.9	-.1
10	4.5	4.6	+.1
11	5.0	5.0	+.0
12	5.5	5.7	+.2
13	6.0	6.3	+.3
14	6.5	6.3	-.2
15	7.0	7.0	+.0
16	7.5	7.7	+.2
17	8.0	8.3	+.3
18	8.5	8.6	+.1

TABLE D-2

RESULTS SUMARY FOR AGGREGATE

Error: $\mu = 0.09"$, $\sigma = 0.23"$

POSITION #	VOID SIZE	ESTIMATE	ERROR
1	0.0	0.1	+.1
2	0.5	0.8	+.3
3	1.0	1.1	+.1
4	1.5	1.4	-.1
5	2.0	1.8	-.2
6	2.5	3.0	+.5
7	3.0	3.2	+.2
8	3.5	3.5	+.0
9	4.0	4.2	+.2
10	4.5	4.9	+.4
11	5.0	5.2	+.2
12	5.5	5.8	+.3
13	6.0	6.2	+.2
14	6.5	6.6	+.1
15	7.0	7.0	+.0
16	7.5	7.5	+.0
17	8.0	7.6	-.4
18	8.5	8.3	-.2

TABLE D-3

RESULTS SUMMARY FOR CLAY

Error: $\mu = 0.02"$, $\sigma = 0.13"$

POSITION #	VOID SIZE	ESTIMATE	ERROR
1	0.0	0.0	+.0
2	0.5	0.4	-.1
3	1.0	1.0	+.0
4	1.5	1.6	+.1
5	2.0	2.2	+.2
6	2.5	2.5	+.0
7	3.0	3.2	+.2
8	3.5	3.5	-.0
9	4.0	3.8	-.2
10	4.5	4.6	+.1
11	5.0	5.2	+.2
12	5.5	5.4	-.1
13	6.0	6.0	+.0
14	6.5	6.5	-.0
15	7.0	7.2	+.2
16	7.5	7.5	+.0
17	8.0	7.8	-.2
18	8.5	8.5	+.0

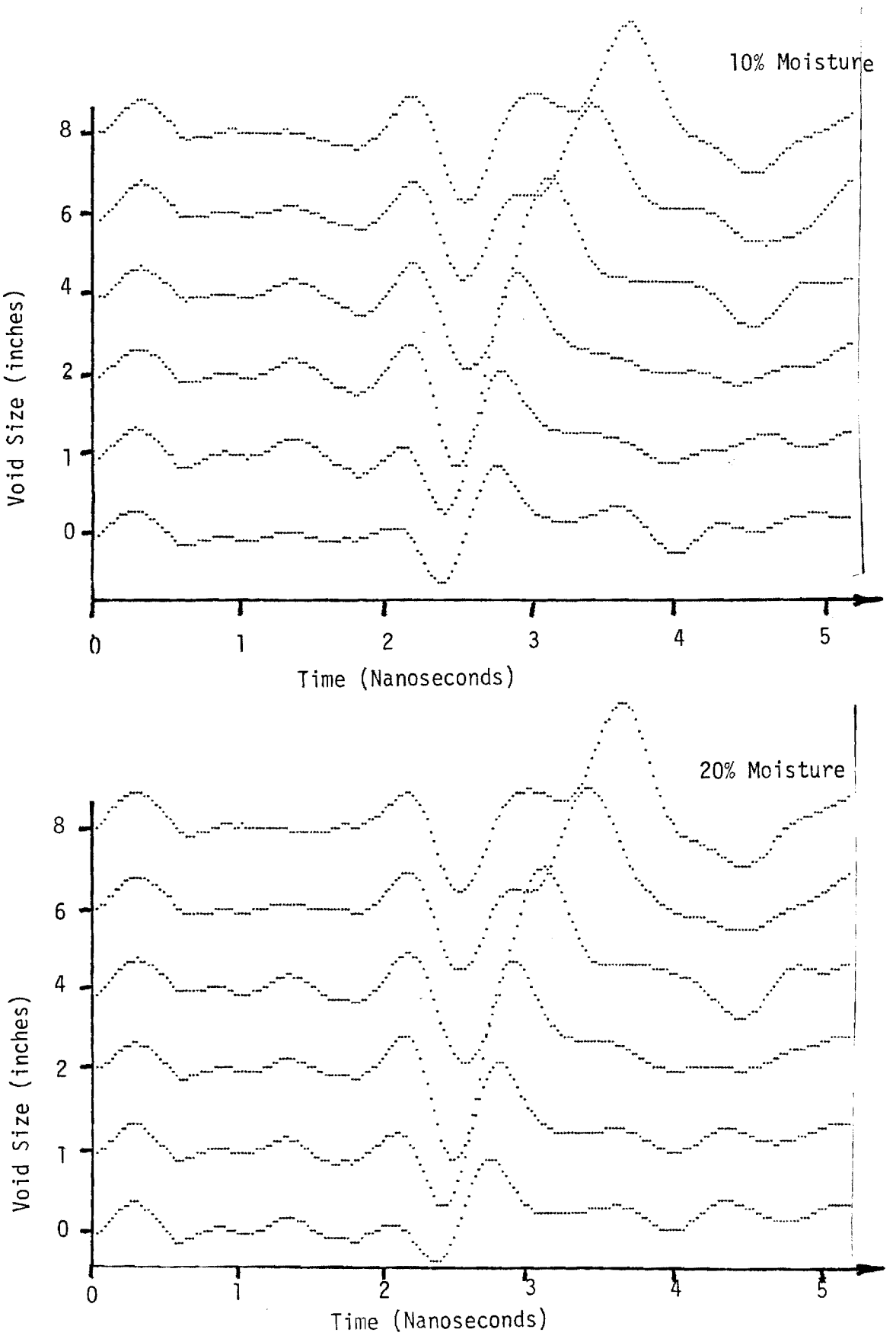

FIGURE D-13

MEASUREMENTS WITH WET CONCRETE BASE

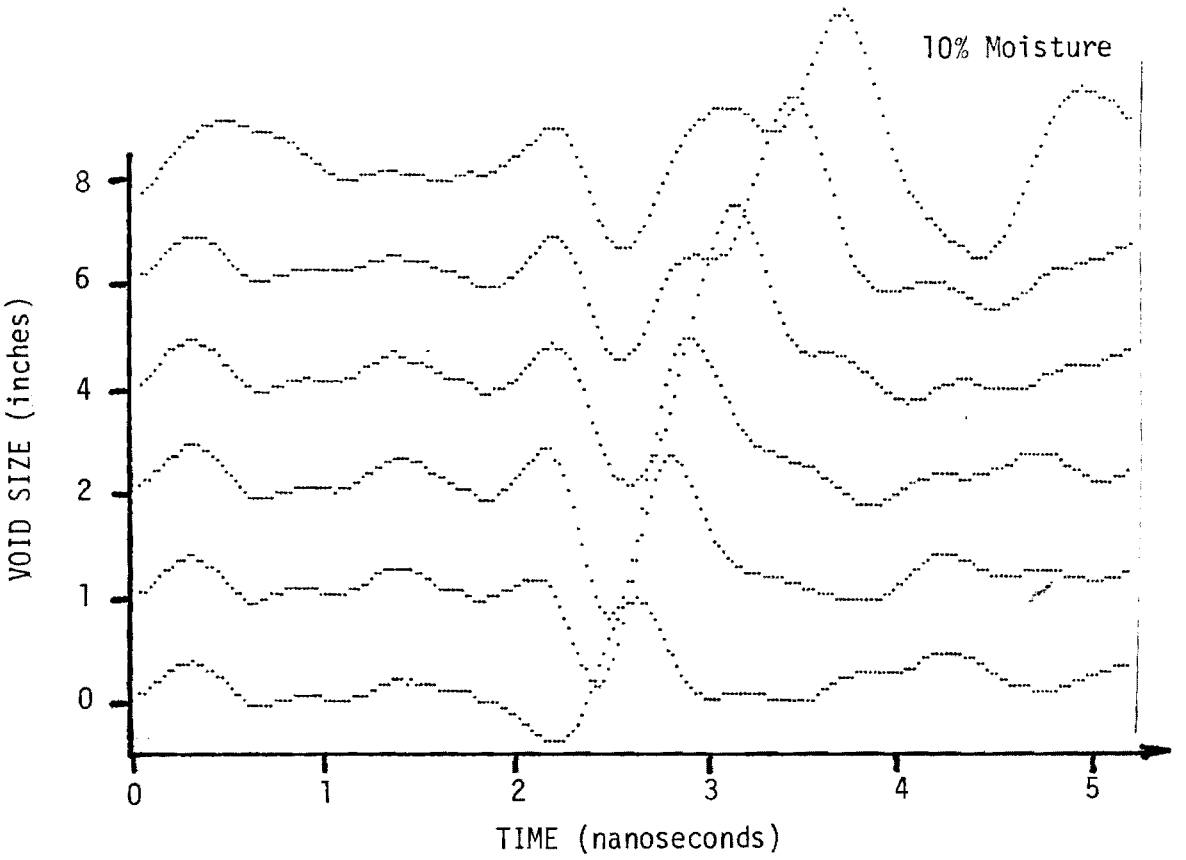

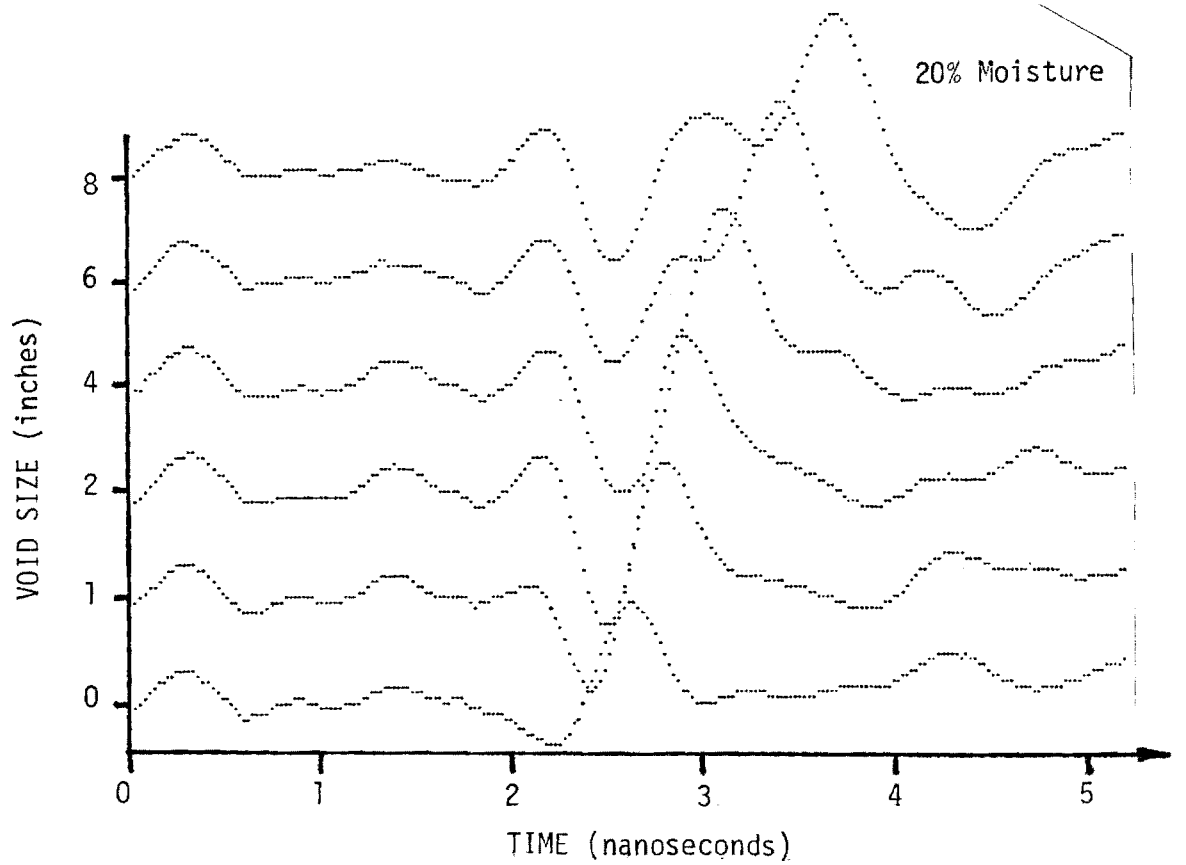

FIGURE D-14

MEASUREMENTS WITH WET CLAY BASE

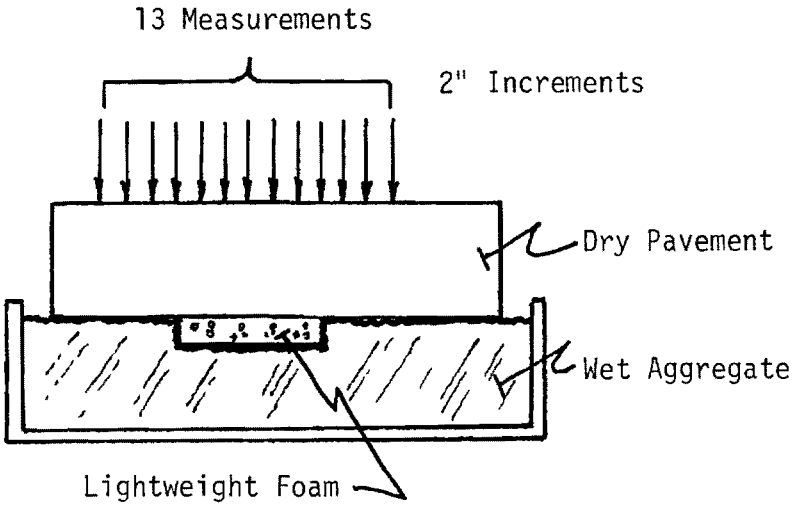

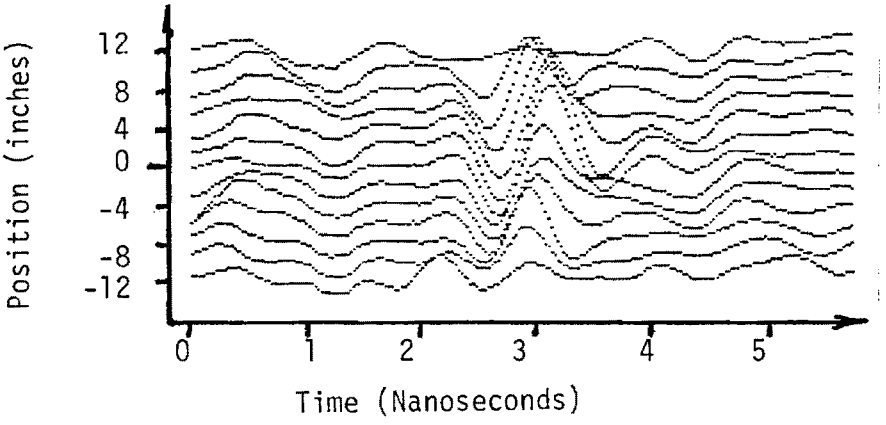

FIGURE D-15 VOID LOCATION SIMULATION: WET BASE.

Figure D-16 illustrates measurements of a selected set of void sizes with one-half inch of water filling the bottom of the void. The base material was clay and the pavement section did not contain reinforcing steel. The water itself has a very high reflection coefficient, thus a larger magnitude return is observed for the positive peak. Also, since more energy is reflected, less is transmitted through the water and the top of the clay base is not obviously visible. The table included in Figure D-16 list the time and amplitude discrimination results for these measurements. As indicated by the table, the discrimination algorithm was in error by -0.5" for void size, exactly the depth of the water. This result is expected since the large return from the water masks the true void bottom. Only if a void is totally filled with water is it possible to obtain a return from the bottom, thus making a void size estimate possible.

All measurements inside the laboratory thus far have been with dry concrete pavement sections. In order to obtain background data on the effects of moist pavement conditions, one of the sections was heavily soaked with water. Table D-4 summarizes the results of attenuation measurements made for both wet and dry cement sections. The units of comparison are decibels; if a value of 10 dB attenuation is observed, only one-tenth of the signal strength is available. The wet block clearly attenuates the signal a significant amount, and in some cases would eliminate the possibility of seeing voids. Another measure of system performance is the amount of signal strength returned from a void as compared to the noise or miscellaneous signal returns. Measurements of this have indicated a ratio of 20 dB or approximately 100 times

NON-REINFORCED PAVEMENT
CLAY BASE

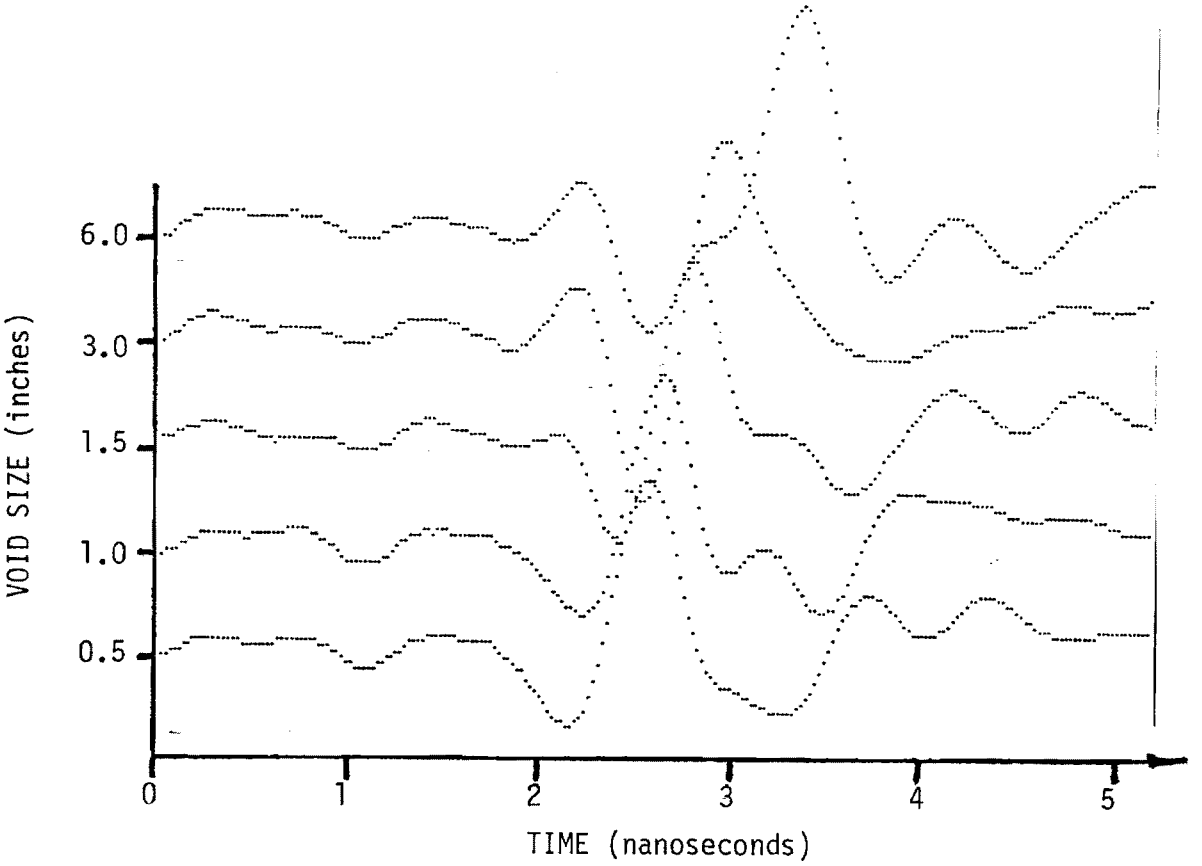

VOID FILLED WITH 0.5 INCHES WATER

ACTUAL VOID SIZE	DISCRIMINATION ALGORITHM RESULT
0.5"	0.1"
1.0"	0.55"
1.5"	1.3"
3.0"	2.6"
6.0"	5.4"

FIGURE D-16

MEASUREMENTS: VOID PARTIALLY FILLED WITH WATER

TABLE D-4

LABORATORY ATTENUATION MEASUREMENTS*

PAVEMENT	MOISTURE	ATTENUATION	SIGNAL-TO-INTERFERENCE RATIO
Dry Non-reinforced	5%	14 dB	12 dB
Dry Reinforced	5%	15 dB	10 dB
Wet Non-reinforced	11%	20 dB	7 dB

*78°F.

greater signal than noise is possible under dry conditions. Significant attenuation will decrease this ratio and the minimum ratio that the micro-computer signal processing algorithms can produce reliable results with is approximately 8-10 dB.

APPENDIX E

TEST LANE MEASUREMENTS

The second phase of the experimental evaulation was conducted on a specially constructed outdoor "Test Lane" which is representative of a section of cement highway. The test lane measures 72 feet long, 8 feet wide and 9 inches thick. Georgia Department of Transportation specifications were used in its construction; concrete over aggregate base. Surveyed in place before concrete was poured were calibrated voids of various sizes and shapes. In one-half of the test lane reinforcing steel was used. The voids were created by shaped pieces of light weight foam, the foam itself being virtually invisible to the electromagnetic signal emitted.

Several sets of measurements were made over the test lane with the main variable being temperature. Initial measurements were made at 100°F and results were very poor. Voids were visible; that is they could be located, but only by the trained operator. The magnitude of the signal return was not large enough for the micro-processor to be able to positively detect. This lack of signal strength is directly attributable to the moisture content in the concrete. The attenuation of the electromagnetic signal varies with total moisture content and temperature.

Later measurements made at temperatures from 32°F to 70°F produced signal levels that resulted in void location and sizing via the microprocessor algorithms. Results verify the discriminates developed.

In the following paragraphs the details of the test lane construction, which includes a description of the voids and how they were created, is given. The measurements made on the test lane are illustrated and results discussed. Conclusions regarding the effects of moisture and temperature are given and future research and measurements are suggested.

Test Lane Construction

The test lane pavement is 72 feet long by 8 feet wide by 9 inches thick concrete, built in accordance with Section 430 of the State of Georgia Specification for Concrete Highways. The base material is graded aggregate, 8 inches thick, again following the Georgia Specification. Reinforcing steel bars were included in one-half of the test lane pavement and small dowell bars were placed in the pavement section without reinforcing steel. Figure E-1 to E-3 are drawings of the reinforcing steel bar and dowell bar positions, the method used to support the bars, and locations for all steel bars are as indicated.

To create the voids under the pavement surface, calibrated holes were dug and pieces of light weight foam were layed into the aggregate. The foam itself is invisible to the electromagnetic energy, and is used to keep the void areas intact during the pouring of the slab. The top surface of the foam was level with the top surface of the aggregate. Figure E-4 illustrates the results of a survey of the void layout and Table E-1 gives the details of the void sizes. Figure E-5 and E-6 are photographs taken during the construction phases of the test lane.

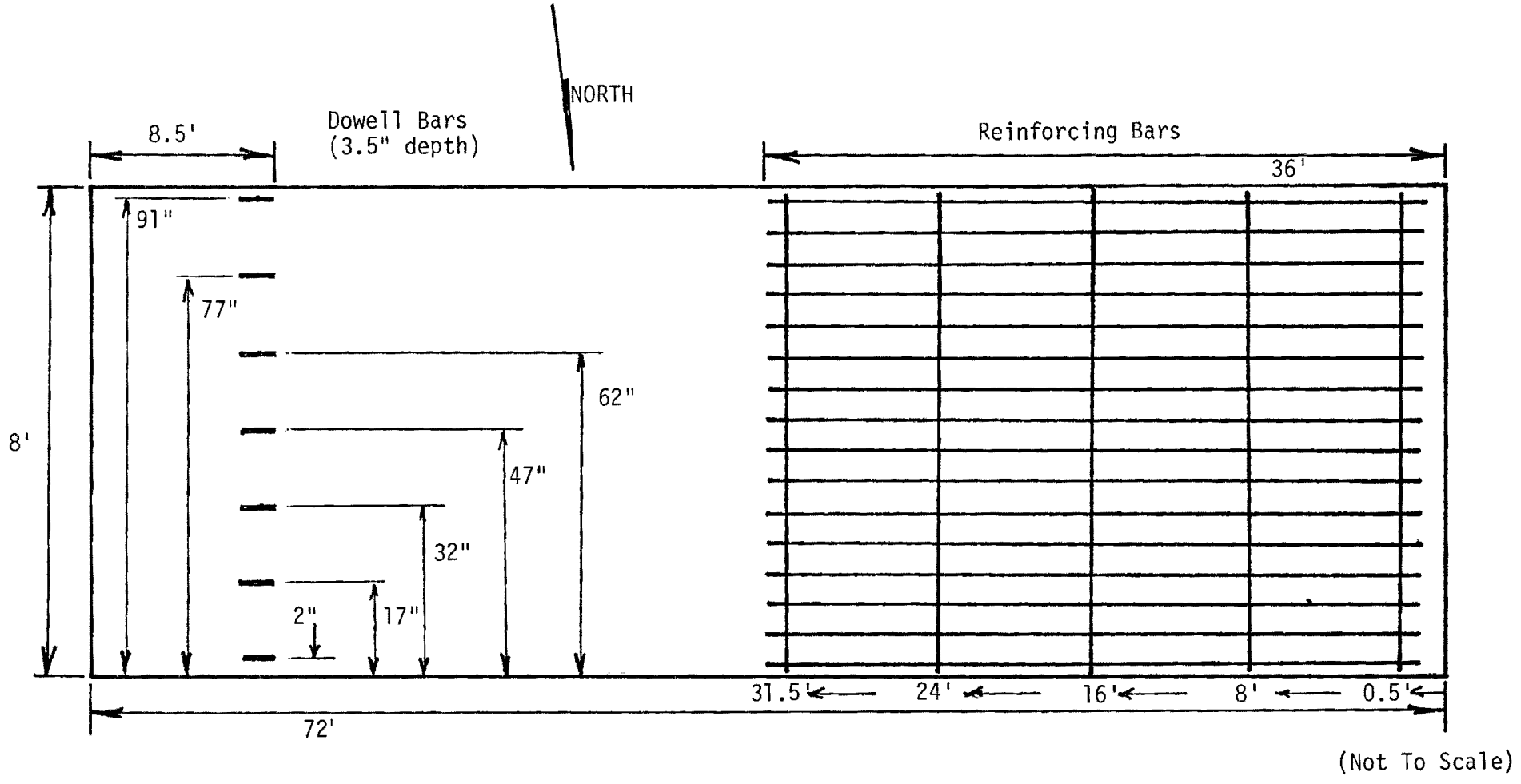

FIGURE E-1. PLAN OF REINFORCING BARS AND DOWELL BARS.

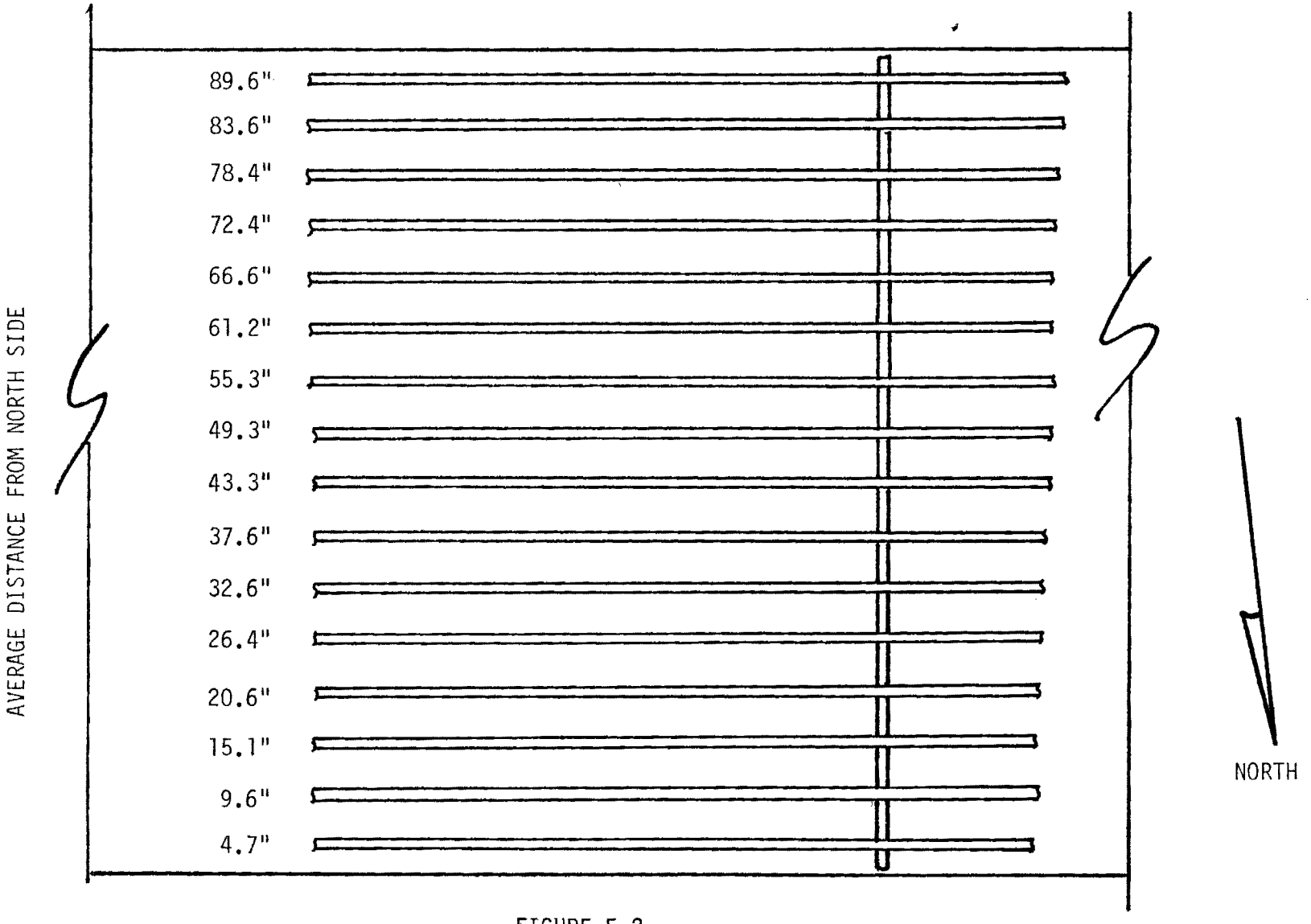

FIGURE E-2

REINFORCING BAR LAYOUT

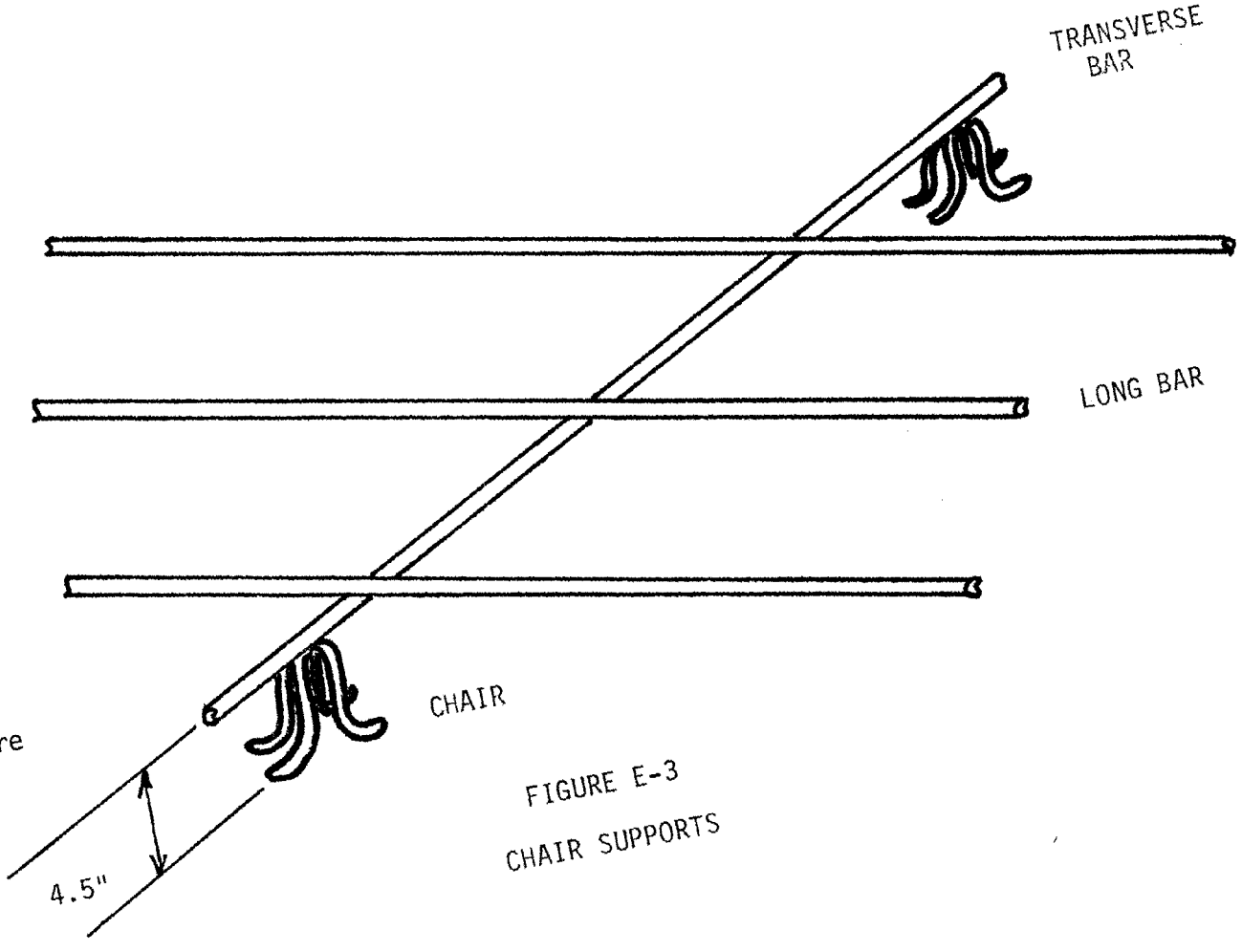

NOTE:

Chairs were placed at random

FIGURE E-3

CHAIR SUPPORTS

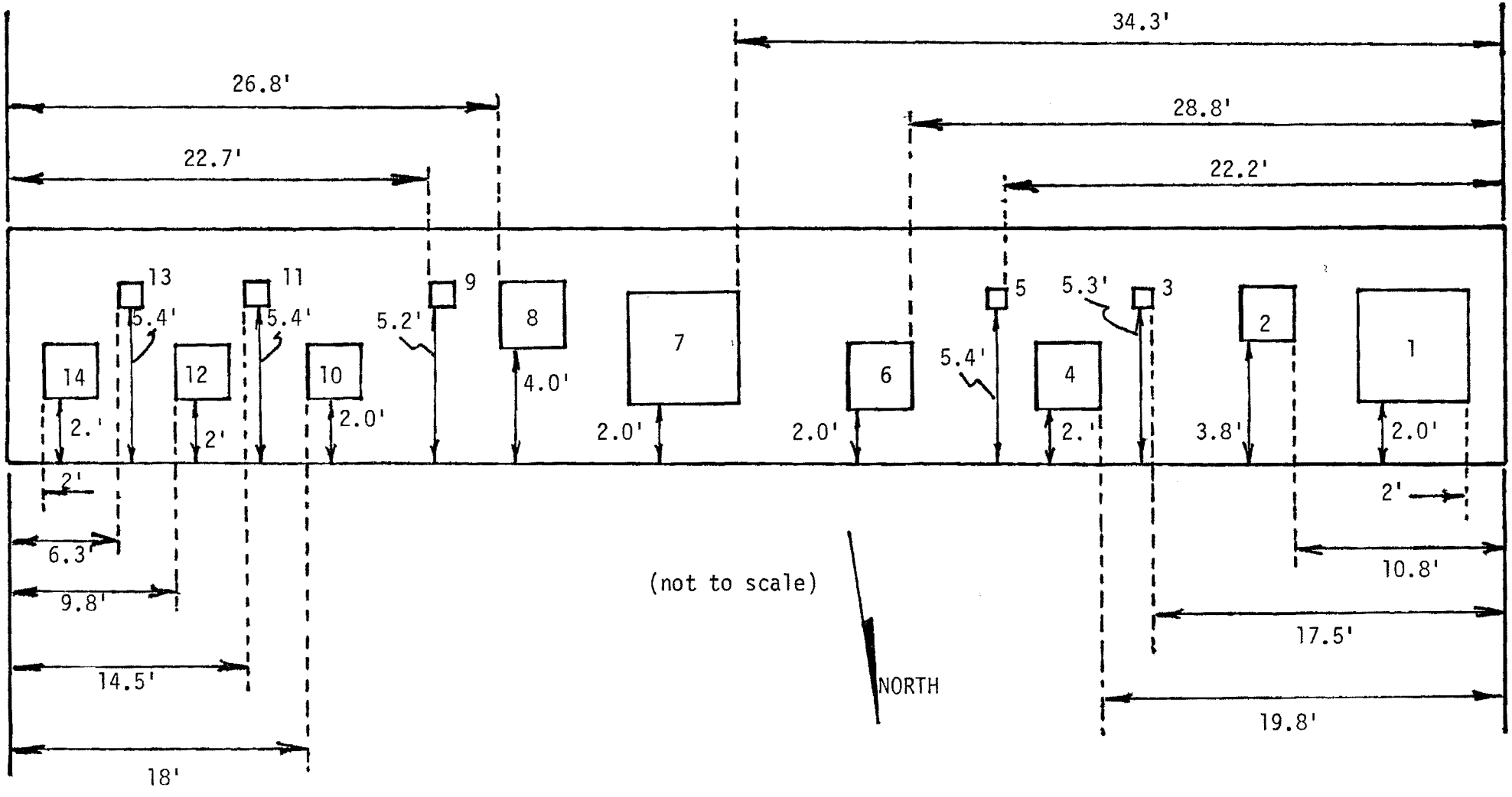

FIGURE E-4

VOID LAYOUT

TABLE E-1

VOID SIZES

VOID NUMBER	LENGTH (in)	WIDTH (in)	VOID SIZE (in)
1	48	48	wedge, 0-6
2	24	24	6
3	6	6	6
4	24	24	2
5	6	6	2
6	36	24	1
7	48	48	wedge, 0-6
8	24	24	6
9	6	6	6
10	24	24	2
11	6	6	2
12	24	24	1
13	6	6	½
14	24	24	½

FIGURE E-5

PHOTOGRAPH OF TEST LANE LAYOUT

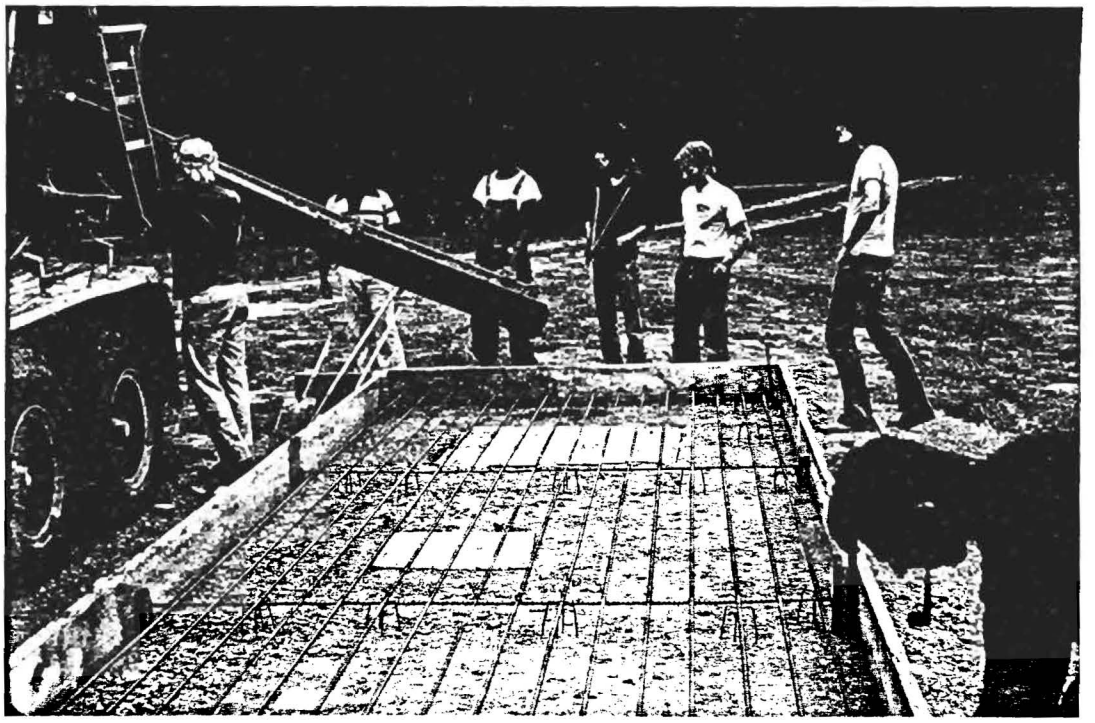

FIGURE E-6

PHOTOGRAPH OF TEST LANE DURING CONCRETE POURING

Test Lane Measurements

To facilitate the making of measurements, markings (small dots) were painted over the entire surface of the pavement in a 6 inch square grid. This insured the repeatibility of positioning of the measurements as well as a method for cataloging measurement positions.

Figure E-7 is a schematic diagram of measurements illustrated in Figures E-8, E-9, and E-10. Figure E-8 is a plot of a sequential set of measurements for the position Set #1 indicated on the schematic diagram. These measurements were made at a temperature of 90°F. By visual inspection the void areas can be located. It is noted that the large return approximately one-third of the distance up the plot and close to the surface point in time, is the signal return from a saw-cut/dowell bar combination in the pavement. The saw-cut over the dowell bars was made so that its effect on the signal return could be gaged. Although the void areas can be located by the trained operator, the micro-computer algorithm has difficulty recognizing the signal response. The lack of signal strength reduces the probability of detecting and correctly sizing a void. Many sets of measurements such as these were made at temperatures from 85°F to 100°F with the same results.

The lack of signal strength returned from the void is directly attributable to the moisture content in the concrete. But the moisture itself is not the key factor in the signal attenuation problem. More importantly is the temperature-moisture combination. From the information given in Appendix B with respect to attenuation, there can be a factor of 10 difference, in the attenuation between temperatures of 40°F and 90°F.

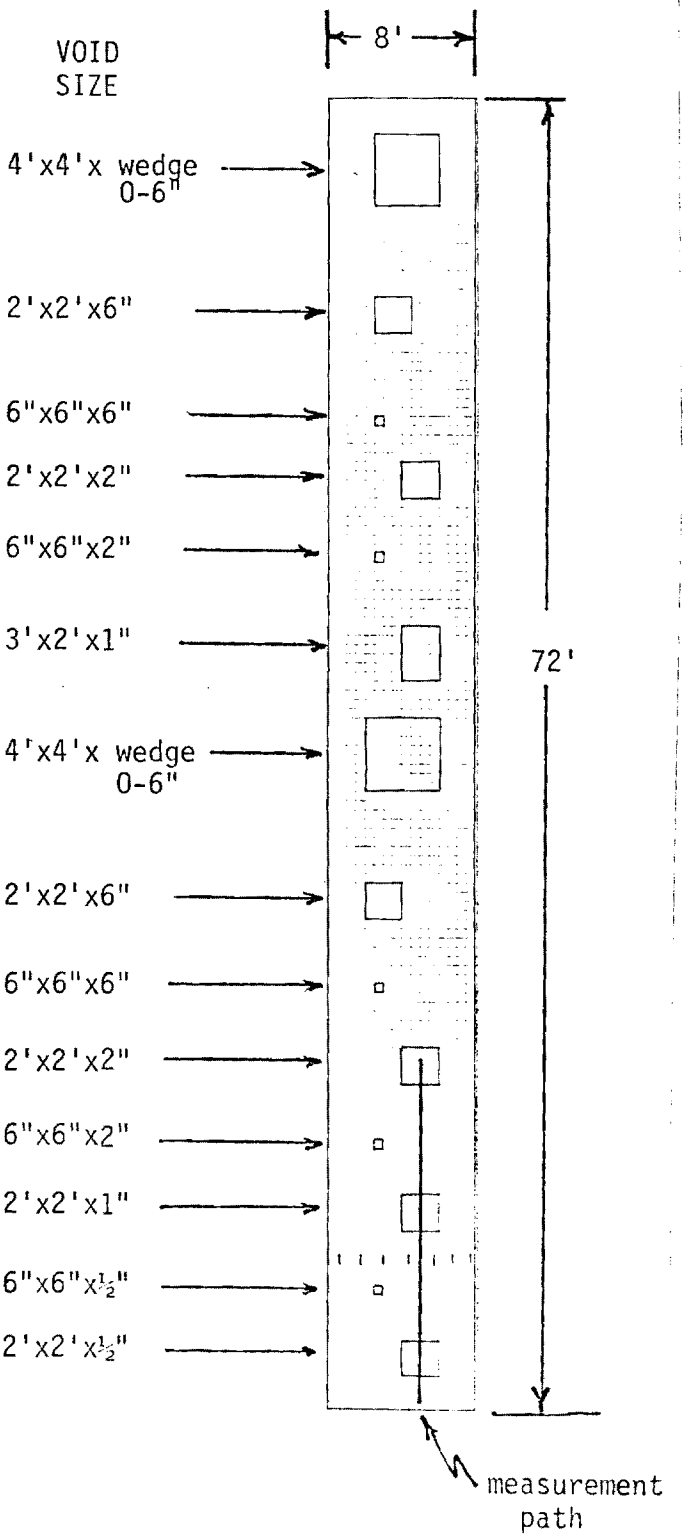

FIGURE E-7

SCHEMATIC DIAGRAM FOR MEASUREMENTS PATH

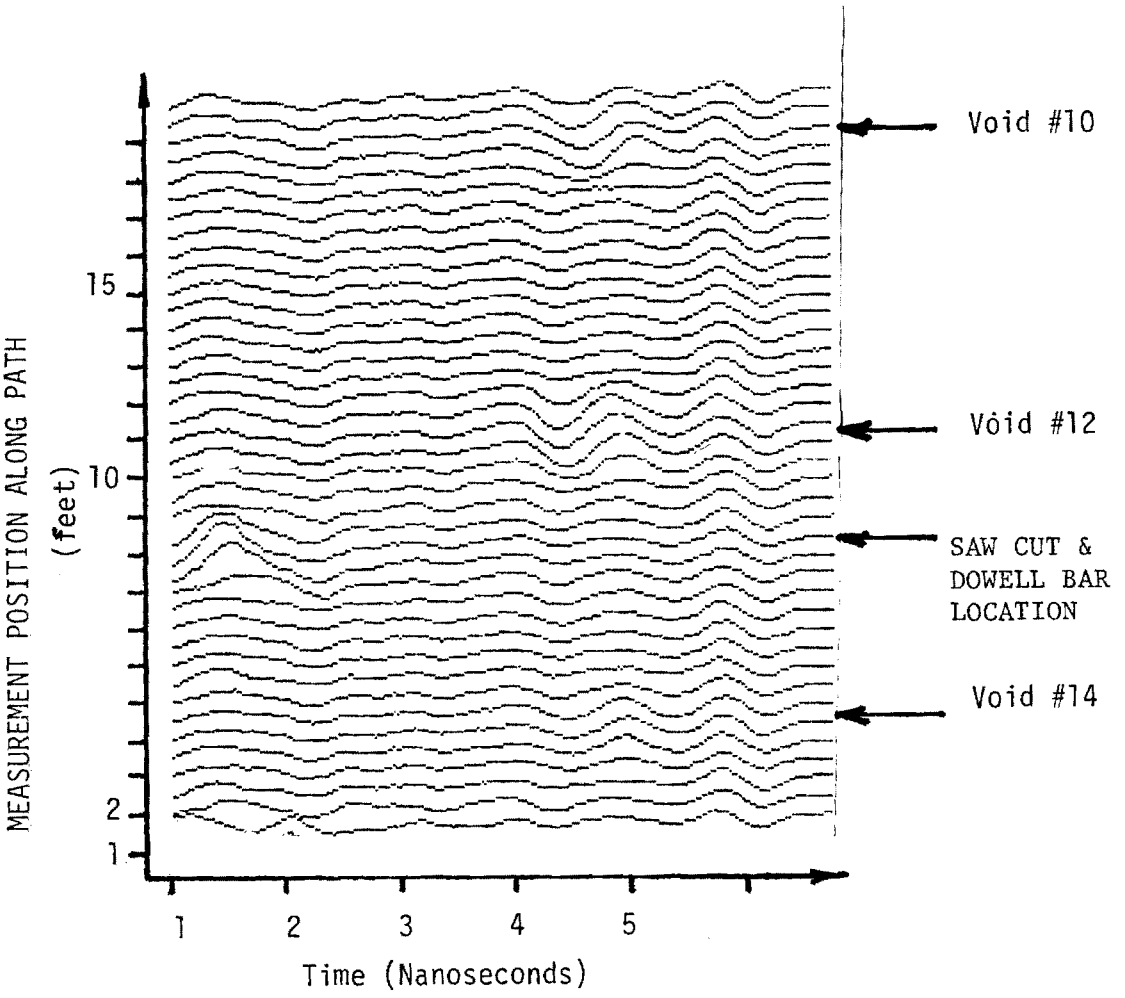

FIGURE E-8

TEST LANE MEASUREMENTS SET #1, 90°F

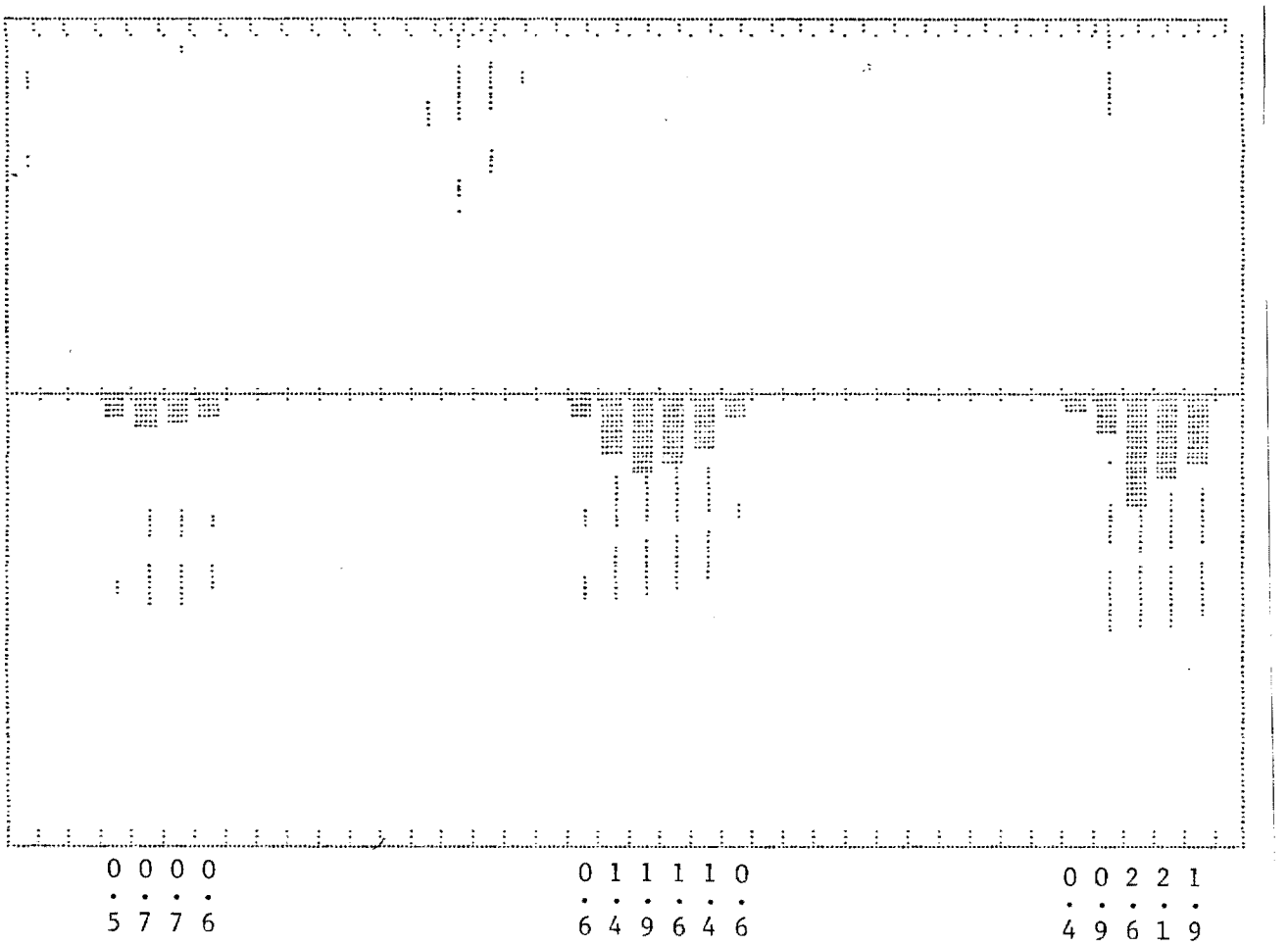

FIGURE E-9

TEST LANE MEASUREMENTS SET #1, 32°F

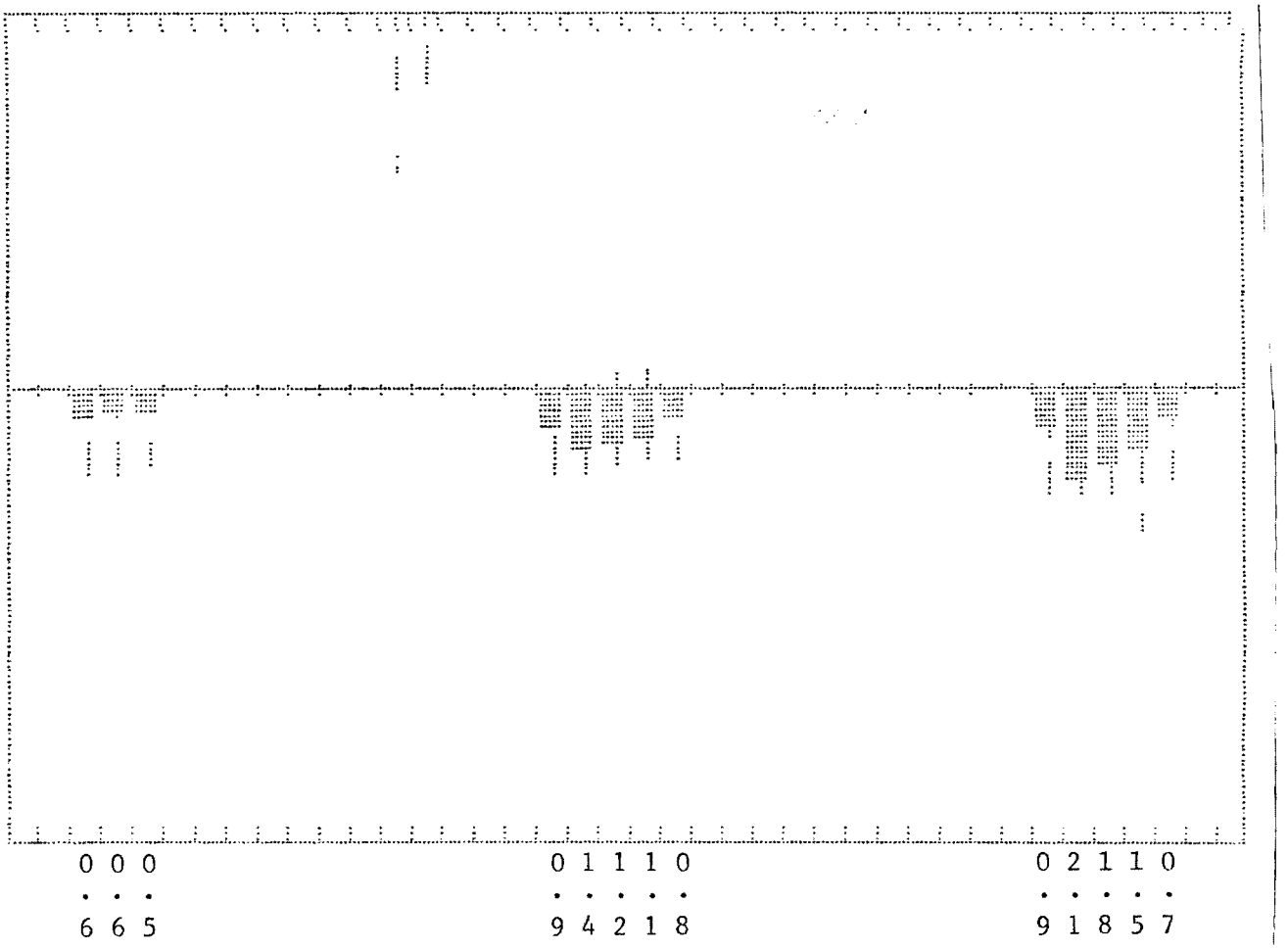

FIGURE E-10

TEST LANE MEASUREMENTS SET #1, 50°F

In order to verify that the problem with the test lane measurements are related to the moisture-temperature combination, specific attenuation measurements were made. Table E-2 illustrates the measurement configuration with the accompanying table listing the results. The return signals from a metal plate with and without a section of pavement over the metal plate were compared. The difference in signal levels relates directly to the attenuation of the pavement. Laboratory measurements were made using a dry reinforced block, a dry non-reinforced block, and a set non-reinforced block all at a temperature of 78°F. Outside test lane measurements were made at a temperature of 100°F. The metal plate was inserted under the edge of the test lane by first digging out the base material slightly. As the table indicates there is a 12 dB (factor of ~ 16) increase in attenuation for the outside test lane measurements over that of the dry non-reinforced laboratory measurements. A better comparison of the effects of temperature only is to compare the wet laboratory measurement with the outside test lane measurement. For this case the moisture levels in both pavement sctions were very close. The resulting attenuation difference is 6 dB (factor of 4). Clearly the effects of a high temperature is a higher attenuation level and decrease in signal strength to a point where the micro-computer algorithms cannot detect and size the void.

Figures E-9 and E-10 illustrate the results for processing measurements made at temperatures of 32°F and 50°F. As is clearly indicated, a much different conclusion is drawn with respect to the validity of the location and sizing algorithms. Summary statistics are given in Table E-3.

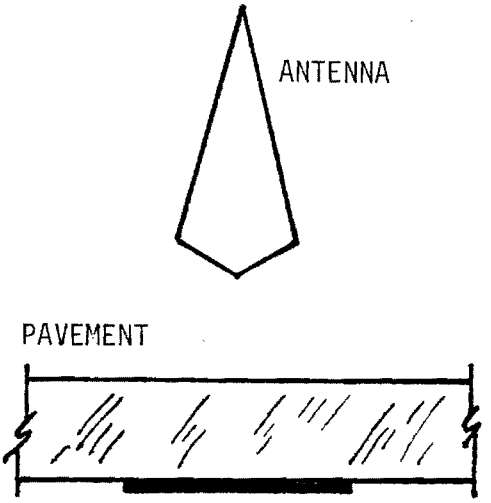

PAVEMENT	TEMPERATURE	MOISTURE	ATTENUATION*	SIR*
Dry non-reinforced	78°F	5%	14 dB	12 dB
Dry reinforced	78°F	5%	15 dB	10 dB
Wet non-reinforced	78°F	11%	20 dB	7 dB
TEST LANE	92°F	9%	26 dB	1 dB

* $dB = 10 \times LOG_{10}(\text{signal ratio})$

TABLE E-2

ATTENUATION COMPARISON

TABLE E-3

RESULTS SUMMARY FOR TEST LANE, 32°F AND 50°F

VOID SIZE	ESTIMATE	ERROR
0.5"	0.5	0.0
0.5"	0.7	0.6
0.5"	0.7	0.5
0.5"	0.6	0.5
0.5"	0.	0.0
0.0"	0.6	0.0
1.0	1.4	0.9
1.0	1.9	2.5
1.0	1.6	2.3
1.0	1.4	2.2
1.0	0.6	0.8
0.0	0.4	0.9
2.0	0.9	2.1
2.0	2.6	1.8
2.0	2.1	1.5
2.0	1.9	0.7

Further research is suggested into the effects of temperature on signal strength. Both laboratory and outside measurements should be made to more fully substantiate currently available measurements and modeling information. Actual highway measurements should be made to verify the signal processing discrimination algorithms effectiveness under typically varying road conditions.

APPENDIX F

SOFTWARE

This appendix contains a listing of the software code implemented in the APPLE II PLUS microprocessor. The code is written in BASIC language for the most part, interspersed with machine language commands. It must be noted that this code is processor specific. Following the code is a flow chart linking identified pieces of code. Included after the flow chart is a definition of variables.

TABLE F-1

SOFTWARE CODE LISTING

```
21  POKE 33,40
25  LOMEM: 102 * 256
40  PRINT  CHR$ (4);"NOMON C,I,O": TEXT : HOME
50  GOTO 2000: REM  MAIN PROGRAM
99  REM DISK I/O
100  PRINT D$;"OPEN ";FL$;DA$;SI;",D2": RETURN : REM OPEN-FILE
110  PRINT D$;"CLOSE ";FL$;DA$;SI: RETURN : REM  CLOSE-FILE
120  PRINT D$;"READ ";FL$;DA$;SI: RETURN : REM  READ-FILE
130  PRINT D$;"WRITE ";FL$;DA$;SI: RETURN : REM  WRITE-FILE
140  GOSUB 100: GOSUB 120: RETURN : REM  OPEN-READ
141  GOSUB 100: GOSUB 130: RETURN : REM  OPEN-WRITE
148  REM
149  REM TEXT/HIRES, PG 1/2 TOGGLES
150 T1 = 0:T2 = 0
152  GET A$:A =  ASC (A$)
153 A1 =  NOT (A = 88 OR A = 90 OR A = 84 OR A = 71 OR A = 49 OR A = 50)
154  IF A = 90 THEN T1 = T1 + 1
155  IF A = 88 THEN T2 = T2 + 1
156  IF A = 71 THEN T1 = 1
157  IF A = 84 THEN T1 = 0
158  IF A = 49 OR A = 50 THEN T2 = A - 49
159  IF A1 THEN T1 = 0:T2 = 0
170 T1 = (T1 / 2 -  INT (T1 / 2)) * 2
171 T2 = (T2 / 2 -  INT (T2 / 2)) * 2
175  POKE  - 16304 + (1 - T1),0
180  POKE  - 16302 + (1 - T2),0
185  POKE  - 16300 + T2,0
190  POKE  - 16298 + T1,0
195  IF  NOT A1 THEN 152
197  RETURN
198  REM
199  REM  VERTICAL $,LINES 21-24
200  IF A < 0 THEN  INVERSE
205 A =  ABS (A): POKE  - 16300,0
210  HTAB TB: VTAB 21: PRINT  INT (A / 10)
220  HTAB TB: PRINT  INT (A -  INT (A / 10) * 10)
230  HTAB TB: PRINT "."
240  HTAB TB: PRINT  INT ((A -  INT (A)) * 10);: VTAB 20: PRINT
245  NORMAL
250  RETURN
299  REM
300  REM GET A/D, AD=-1,0,1
305 MM = DT: IF AD = 0 THEN MM = BS
310  IF DS THEN  PRINT : PRINT D$;"BLOAD ";FL$;DA$;SI;",A";MM
315  IF DS THEN 350
325 I =  PEEK (49328): REM  A/D
330  POKE MEMMOV + 9,MM / 256: POKE MEMMOV + 24,MM / 256
340  CALL MEMMOV
350  POKE SUBTRCT + 4,DT / 256: POKE SUBTRCT + 7,BS / 256: POKE SUBTRCT + 12,SB /
 256
355  IF AD = 1 THEN  CALL SUBTRCT
360 MM = SB: IF AD = 0 THEN MM = BS
365  GOSUB 500: REM PLOT REF
375  IF A$ = "N" THEN 1300
385  RETURN
399  REM
400  REM  WAIT FOR KEY
```

TABLE F-1 (continued)

```
401  POKE  - 16368,0
402  IF  PEEK ( - 16384) < 128 THEN 402
403  RETURN
498  REM
499  REM SIG-PLOT
500  HCOLOR= 3:C1 = 220 / NP:C2 = 150 / 255
505  HGR2
520  FOR I = 1 TO NP
530 PX = C1 * (I - 1)
535 PY = C2 *  PEEK (MM + I)
540  HPLOT PX,PY
550  NEXT I
560 PX = 240
565  HPLOT PX,1 TO PX,150
580 PY = 75
585  HPLOT 230,PY TO 250,PY
587  GOSUB 150
590  RETURN
598  REM
599  REM MIN/MAX VOID-DET.
600 DM =  - 1000:DN = 1000:NN = NP - 20:TH = 10
605 XF = 0:NF = 1
610  FOR I = 50 TO NN
620 DA% = 127 -  PEEK (SB + I)
630  IF DN < DA% THEN 650
640 DN = DA%:IE = I
650  NEXT I
655  IF  ABS (127 -  PEEK (SB + IE)) < TH THEN NF = 0
660  FOR I = IE TO NN
670 DA% = 127 -  PEEK (SB + I)
675  IF DM > DA% THEN 690
680 DM = DA%:IM = I:XF = 1
690  NEXT I
700  IF  ABS (127 -  PEEK (SB + IM)) < TH THEN XF = 0
710 VD = NF AND XF
713  VTAB 15: PRINT  SPC( 75)
715  VTAB 15: HTAB 1: PRINT "MIN=";DN;"MAX=";DM;"   DELTA=";IM - IE
716  HTAB 1: PRINT "AT  ";IE;"AT  ";IM
720  RETURN
799  REM
800  REM SAVE SIGNATURES
805  VTAB 1: PRINT
810  PRINT D$;"BSAVE ";FL$;DA$;SI$;",A";SB$;",L";NP + 1
820  RETURN
898  REM
899  REM TIME-DIFF DET.
900 VD = 0
910  IF ((IM - IE) > 10 AND (IM - IE) < 70) THEN VD = 1
920  RETURN
999  REM
1000  REM QUERY-START
1010  TEXT : HOME
1011  PRINT "  VOID DETECTION PROGRAM"
1012  PRINT " "
1013  PRINT "  GEORGIA INSTITUTE OF TECHNOLOGY"
1014  PRINT " "
1015  PRINT "  ENGINEERING EXPERIMENT STATION"
1016  PRINT " "; PRINT " "
1020  PRINT "OLD,NEW DATA OR QUIT? (O,N,Q) ": GET A$: PRINT
1025  IF A$ = "Q" THEN  GOTO 12000
1030  IF  NOT (A$ = "O" OR A$ = "N") THEN 1010
1040 DS = 0: IF A$ = "O" THEN DS = 1
1050  PRINT "WHAT FILE NAME FOR DATA SETS?"
1051  INPUT "(UP TO 15 CHARS)-";FL$: PRINT
1052  IF FL$ = "" THEN  GOTO 1010
1060  IF DS THEN  INPUT "DATE DATA WAS SAVED? ";DA$
```

TABLE F-1 (continued)

```
1070  IF  NOT DS THEN  INPUT "TODAY'S DATE? ";DA$
1071  IF DA$ = "" THEN  GOTO 1010
1150  HOME
1160  IF DS THEN SI = 127: GOSUB 140: REM  OPEN-READ
1170  INPUT "THICKNESS OF CEMENT? (INCHES) ";CL
1180  IF DS THEN  GOSUB 110:SI = 1: REM  CLOSE-FILE
1185  IF DS THEN 1290
1190 SI = 127: GOSUB 141: REM OPEN-WRITE
1200  PRINT CL
1210  GOSUB 110: REM  CLOSE-FILE
1220 SI = 1
1290  RETURN
1298  REM
1299  REM  GET REF.
1300  TEXT : HOME
1302  PRINT
1303  IF DS THEN  INPUT " # FOR CAL. SIGNATURE  ";SI
1310  IF  NOT DS THEN  PRINT "POSITION RADAR FOR CAL. INPUT"
1360  PRINT " ": PRINT "    HIT SPACE BAR"
1370  PRINT "TO GET REFERENCE SIGNATURE"
1371  PRINT " "
1372  PRINT "---SPACE BAR ACCEPT---"
1373  PRINT "---N = REJECT, SAMPLE AGAIN"
1380  GOSUB 400: POKE  - 16368,0
1385 AD = 0: IF  NOT DS THEN SI = 0
1390  GOSUB 300
1410 MM = BS: IF  NOT DS THEN  GOSUB 800: REM SAVE
1420  RETURN
1498  REM
1499  REM DRAW-GRID
1500  HGR : TEXT : HOME : GOSUB 6000: GET A$
1505  HCOLOR= 3: VTAB 20: POKE 230,32
1510  HPLOT 0,0 TO 279,0
1511  HPLOT  TO 279,159
1512  HPLOT  TO 0,159
1513  HPLOT  TO 0,0
1520  HPLOT 0,CL * 8 TO 279,CL * 8
1540  FOR I = 0 TO 273 STEP 7
1545  HPLOT I,158 TO I,156
1546  HPLOT I,1 TO I,3
1547  HPLOT I,CL * 8 - 1 TO I,CL * 8 + 1
1550  NEXT I
1570  RETURN
1599  REM
1600  REM GET-VOID
1605  GOSUB 6000
1610  FOR DC = 1 TO 39
1630   IF A$ = "0" THEN  GOTO 1300
1650 AD = 1:SI = DC: GOSUB 300
1665 MM = DT: IF  NOT DS THEN  GOSUB 800: REM SAVE
1670  GOSUB 600
1680  IF  NOT VD THEN 1745
1690  GOSUB 900
1700  IF  NOT VD THEN 1745
1710  IF (IM - IE) > 21 THEN VS = 3. + 5.5 * ((IM - IE) - 21.) / 32.
1720  IF (IM - IE) <  = 21 THEN  GOSUB 2000
1721  PRINT D$;"OPEN";FL$;DA$;"DATA,L30,D2": REM    OPEN DATA FILE
1722 ID = ID + 1
1723  FOR KD = 1 TO 5
1724  PRINT D$;"WRITE";FL$;DA$;"DATA,R";(ID - 2) * 5 + KD + 1
1725  IF KD = 1 THEN  PRINT DN
1726  IF KD = 2 THEN  PRINT IE
1727  IF KD = 3 THEN  PRINT DM
1728  IF KD = 4 THEN  PRINT IM
1729  IF KD = 5 THEN  PRINT VS
1730  NEXT KD
```

TABLE F-1 (continued)

```
1737  PRINT D$;"CLOSE";FL$;DA$;"DATA": REM   CLOSE DATA FILE
1738 TB = DC:A = VS: GOSUB 200
1740 TB = DC - 1: GOSUB 1900
1745 TC = 30: REM     THRESHOLD AT 30
1750  POKE  - 16297,0: POKE  - 16300,0: POKE  - 16301,0: POKE  - 16304,0
1755  VTAB 21: HTAB DC + 1: POKE 230,32
1760  FOR I = 1 TO NP
1765  HCOLOR= 3
1770  IF  ABS ( PEEK (SB + I) - 127) > TC THEN  HPLOT (DC - 1) * 7 + 4,I * 140 /
220
1780  NEXT I
1787  GOSUB 4000
1790  NEXT DC
1793  GOSUB 1800
1795  RETURN
1798  REM
1799  REM EXIT
1800  TEXT : VTAB 18: HTAB 1: FLASH
1810  PRINT "SAVE PLOT? (Y,N) ";
1811  NORMAL : GET A$
1820  IF A$ <  > "Y" THEN  GOTO 1840
1825  PRINT
1830  PRINT D$;"BSAVE ";FL$;DA$;"PLT N=";DC - 1;",A$2000,L$1FFF"
1835  PRINT D$;"BSAVE";FL$;DA$;"TEXT,A$400,L$400"
1840  PRINT
1841  PRINT D$;"OPEN";FL$;DA$;"DATA,L30,D2": REM     OPEN DATA FILE
1842  PRINT D$;"WRITE";FL$;DA$;"DATA,R1": REM   WRITE TO REC 1 THE # OF REC.
1843  PRINT ID
1844  PRINT D$;"CLOSE";FL$;DA$;"DATA": REM   CLOSE DATA FILE
1845  GOTO 12000
1850  END
1899  REM
1900  REM  V-PLOT
1904  TEXT
1905  POKE  - 16297,0: POKE  - 16300,0: POKE  - 16301,0: POKE  - 16304,0: VTAB 19
: HTAB 1: POKE 230,32
1910  FOR I = 1 TO VS * 8
1920  HPLOT TB * 7 + 1,CL * 8 + I TO TB * 7 + 5,CL * 8 + I
1930  NEXT I
1950  RETURN
1998  REM
1999  REM MAIN PROGRAM
2000  REM  INSERT CODE HERE TO
2001  REM  ALLOW CHOICE OF RUN
2002  REM  OR LOOK AT DOCUMENTATION
2100  GOSUB 10000: REM  INIT
2150  GOSUB 11000: REM  LOAD ML-ROUTINES
2200  GOSUB 1000: REM  QUERY-START
2250  GOSUB 1300: REM  GET-REF
2300  GOSUB 1500: REM  DRAW-GRID
2400  GOSUB 1600: REM  GET-VOID
2450  GOTO 2200: REM  NEW RUN, START OVER
3000  REM VOID-SIZE, AMPL.
3010 DA =  PEEK (SB + IE) - 127
3020 AG = (DA - 45) / 40.
3021  IF AG >  = 1. THEN AG = .9999
3024 VS = 1.91 *  ATN (AG /  SQR (1 - AG * AG))
3100  RETURN
4000 T1 = 1:T2 = 0: GOSUB 152
4010  IF A <  > ASC ("N") THEN  RETURN
4015 TB = DC - 1
4020  HCOLOR= 0: GOSUB 1900
4030 A = (DC - 1) * 7 + 4
4040  HPLOT A,1 TO A,160
4050  GOSUB 1505
4055  FOR I = 21 TO 24: VTAB I: HTAB DC: PRINT " ";: NEXT I
```

TABLE F-1 (continued)

```
4056  VTAB 18: PRINT
4060 DC = DC - 1
4100  RETURN
6000  VTAB 1
6001  INVERSE : PRINT "CAL. DATA";
6005  NORMAL : PRINT " N = NO"
6006  PRINT "           ANY OTHER = ACCEPT": PRINT
6010  INVERSE : PRINT "VOID DATA"
6015  NORMAL : PRINT " COMANDS:"
6020  PRINT "     Q =QUIT    N =DO NOT ACCEPT"
6030  PRINT "     T =TEXT    G =GRAPHICS"
6035  PRINT "     1 =PAGE1   2 =PAGE2"
6040  PRINT "     Z =FLIP TEXT/GRAPHICS"
6050  PRINT "     X =FLIP PAGE 1/2"
6051  PRINT
6053  PRINT "     ANY OTHER KEY TO CONTINUE"
6100  RETURN
10000  REM  INITIALIZE VARIABLES
10010 D$ =  CHR$ (4):NP = 220
10020 MEMMOV = 96 * 256:SUBTRCT = 97 * 256
10030 DT = 99 * 256
10040 DS = 100 * 256
10050 SB = 98 * 256
10060 ID = 1
10999  RETURN
11000  REM
11001  REM LOAD MACH.LANG.ROUTINES
11010  PRINT D$;"BLOAD MEMMOV, A";MEMMOV;",D1"
11020  PRINT D$;"BLOAD SUBTRCT,A";SUBTRCT
11030  RETURN
12000  REM
12001  REM  END
12010  TEXT : HOME
12013  PRINT
12015  PRINT "VOID DETECTION PROGRAM
12016  PRINT " "
12017  PRINT "ENDED: ";DA$
12100  END
```

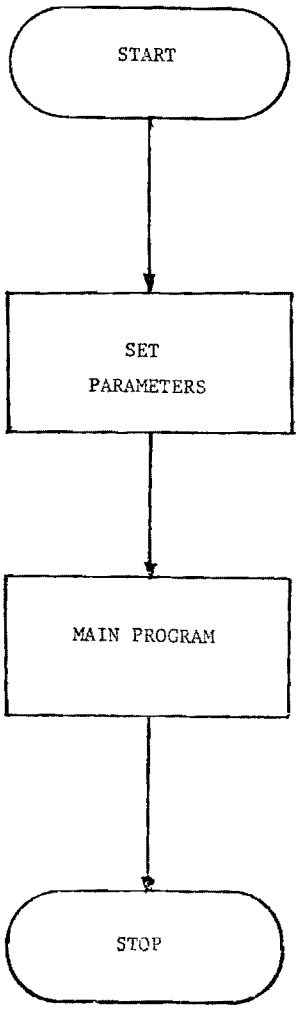

FIGURE F-1. BASIC DIAGRAM

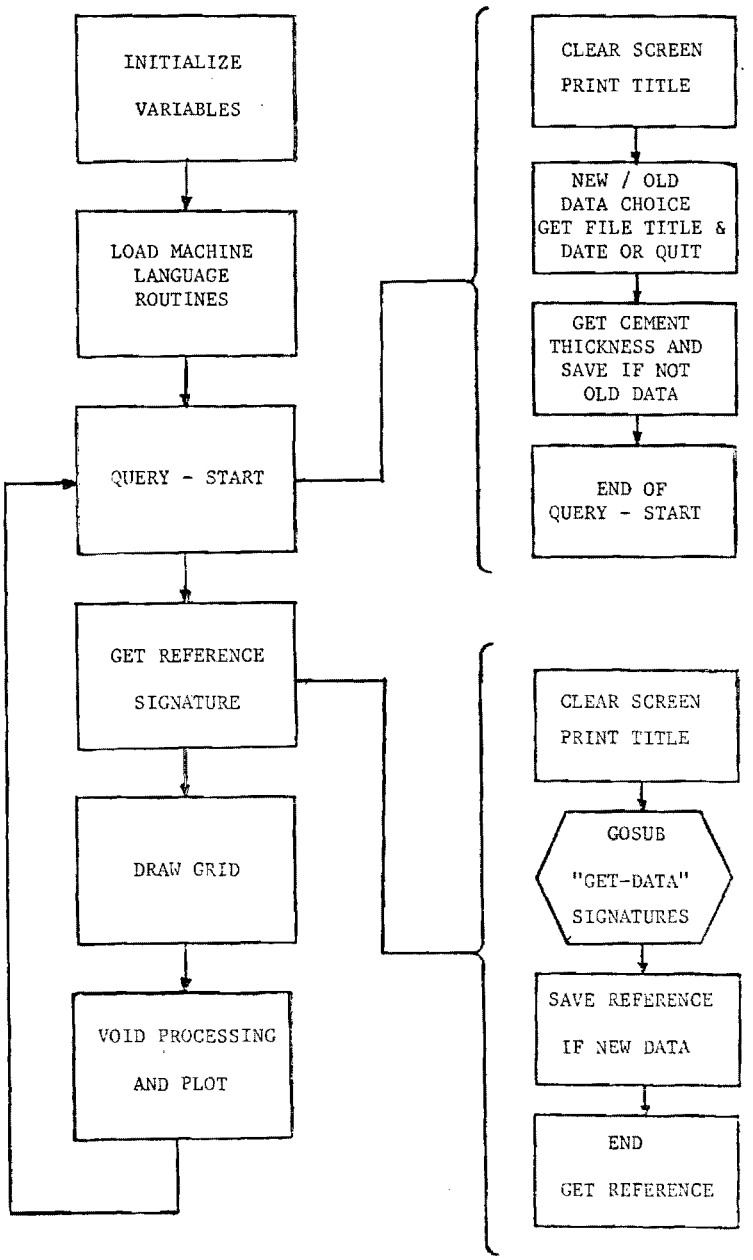

FIGURE F-2. MAIN PROGRAM

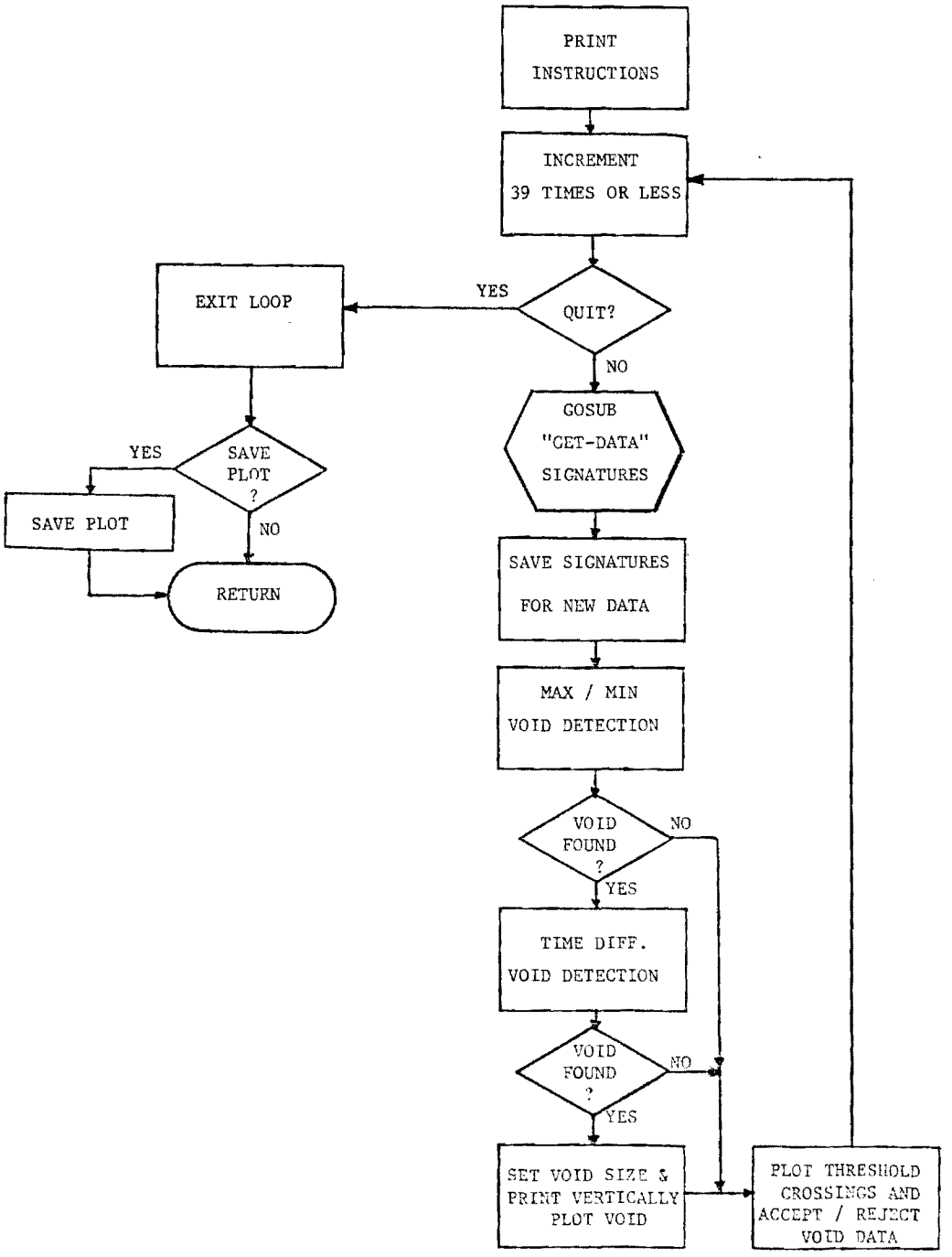

FIGURE F-3. VOID PROCESSING AND PLOT

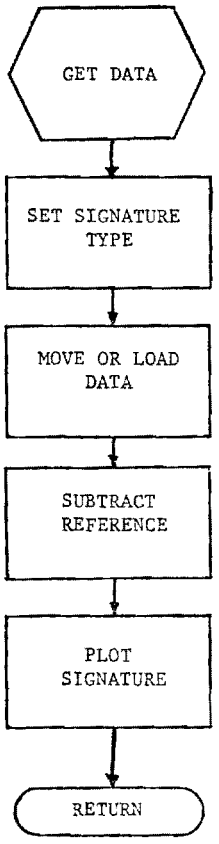

FIGURE F-4. GET DATA

TABLE F-2

VARIABLES AND MEMORY LOCATIONS

LOMEM:102*256	:	SET LOMEN TO PROTECT DATA FROM VARIABLES	
(ME)MMOV = 96*256	:	LOC OF MEMORY MOVER MACHINE LANG. ROUTINE	
(SU)TRCT = 97*256	:	LOC OF SUTRCI (SUBTRACTION)	DATA AND
SB = 98*256	:	LOC OF SUBTRACTED DATA	MACHINE
DT = 99*256	:	LOC OF A/D DATA (AFTER MOVE)	LANGUAGE
BS =100*256	:	LOC OF REFERENCE DATA	ROUTINES
NP =220	:	NUMBER OF DATA POINTS PER SIGNATURE	
D$ = CHR$(4)	:	CNTRL-D FOR DOS COMMANDS	FILE
FL$ = (1- 20 CHAR)	:	DATA FILE NAME STRING	CONTROL
DA$ = MM/DD/YY	:	DATA STRING FOR FILE NAME	VARIABLES
T1, T2	:	TEXT/GRAPHICS TOGGLING VARIABLES	
A$,A,A1,I,J,DA,AG	:	TEMPORARY VARIABLES (SEVERAL USES)	
DS	:	DISK RETRIEVAL (0 = use A/D, 1 = get data from disk)	
TB	:	TABBING VARIABLE	GENERAL
MM	:	HOLDS MEMORY LOCATIONS; A TEMPORARY VARIABLE	USES
AD	:	A/D CONVERSION VARIABLE → SET AD = 0,1 (0 = REF, 1 = DATA)	
PX, PY	:	HOLD X,Y VALUES FOR HIRES PLOT OF SIGNATURE	
DM, DN	:	MAX/MIN COMPARISON VALUES	
NN	:	NP-20, END POINT OF MAX/MIN SEARCH	
TH	:	MAX/MIN TEST THRESHOLD	VOID
XF, NF	:	MAX,MIN BOOLEAN (0 = NOT FOUND, 1 = FOUND)	DETECTION VARIABLES
DA%	:	INTEGER VARIABLE USED TO SCAN SIGNATURE	
VD	:	VOID FOUDN BOOLEAN (0 = NO, 1 = YES)	
IM, IE	:	LOCATIONS (0 → NP) OF MAX AND MIN	
DC	:	COUNT OF SIGNATURES READ IN	
CL	:	CEMENT THICKNESS	

TABLE F-3

CODE LOCATIONS

ROUTINES:

(Machine Language)

MEMMOV, moves data from A/D Loc. ($CIFF) to regular memory

SUBTRCT, subtracts ref. data (BS) from A/D (DT) and stores in subtracted area (SB)

BASIC:

Line			
	100	-	OPEN TEXT FILE
	110	-	CLOSE TEXT FILE
	120	-	READ TEXT FILE
	130	-	WRITE TEXT FILE
	140	-	OPEN AND READ TEXT FILE
	141	-	OPEN AND WRITE TEXT FILE
	150	-	TEXT/GRAPHICS PAGE TOGGLE
	200	-	PRINT VERTICAL NUMBER (##.#)
	300	-	GET DATA SIGNATURES
	400	-	WAIT FOR KEYSTROKE (OBSOLETE)
	500	-	PLOT SIGNATURE
	600	-	MIN/MAX VOID DETECTOR
	800	-	BSAVE SIGNATURES
	900	-	TIME DIFFERENCE VOID DETECTOR
	1000	-	QUERY-START
	1300	-	GET REFERENCE SIGNATURE
	1500	-	DRAW GRID
	[1505	-	SAME MINUS INITIALIZATION]
	1600	-	GET VOID DATA
	1800	-	EXIT PROGRAM
	1900	-	PLOT
	2000	-	MAIN PROGRAM
	3000	-	VOID-SIZE, AMPLITUDE
	4000	-	ACCEPT/REJECT VOID DATA

6000	-	INSTRUCTIONS (TEXT PAGE 1)
10000	-	INITIALIZE VARIABLES
11000	-	LOAD MACHINE LANG. ROUTINES
12000	-	END PROGRAM

NATIONAL COOPERATIVE HIGHWAY RESEARCH PROGRAM REPORT 237

LOCATING VOIDS BENEATH PAVEMENT USING PULSED ELECTROMAGNETIC WAVES

W. J. STEINWAY, J. D. ECHARD, AND C. M. LUKE
Georgia Institute of Technology
Atlanta, Georgia

RESEARCH SPONSORED BY THE AMERICAN ASSOCIATION OF STATE HIGHWAY AND TRANSPORTATION OFFICIALS IN COOPERATION WITH THE FEDERAL HIGHWAY ADMINISTRATION

AREAS OF INTEREST:

MAINTENANCE
CONSTRUCTION AND MAINTENANCE EQUIPMENT
SOIL EXPLORATION AND CLASSIFICATION
SOIL FOUNDATIONS
(HIGHWAY TRANSPORTATION)
(PUBLIC TRANSIT)
(RAIL TRANSPORTATION)
(AIR TRANSPORTATION)
(OTHER)

'RANSPORTATION RESEARCH BOARD
ATIONAL RESEARCH COUNCIL
'ASHINGTON, D.C.
NOVEMBER 1981

NATIONAL COOPERATIVE HIGHWAY RESEARCH PROGRAM

Systematic, well-designed research provides the most effective approach to the solution of many problems facing highway administrators and engineers. Often, highway problems are of local interest and can best be studied by highway departments individually or in cooperation with their state universities and others. However, the accelerating growth of highway transportation develops increasingly complex problems of wide interest to highway authorities. These problems are best studied through a coordinated program of cooperative research.

In recognition of these needs, the highway administrators of the American Association of State Highway and Transportation Officials initiated in 1962 an objective national highway research program employing modern scientific techniques. This program is supported on a continuing basis by funds from participating member states of the Association and it receives the full cooperation and support of the Federal Highway Administration, United States Department of Transportation.

The Transportation Research Board of the National Research Council was requested by the Association to administer the research program because of the Board's recognized objectivity and understanding of modern research practices. The Board is uniquely suited for this purpose as: it maintains an extensive committee structure from which authorities on any highway transportation subject may be drawn; it possesses avenues of communications and cooperation with federal, state, and local governmental agencies, universities, and industry; its relationship to its parent organization, the National Academy of Sciences, a private, nonprofit institution, is an insurance of objectivity; it maintains a full-time research correlation staff of specialists in highway transportation matters to bring the findings of research directly to those who are in a position to use them.

The program is developed on the basis of research needs identified by chief administrators of the highway and transportation departments and by committees of AASHTO. Each year, specific areas of research needs to be included in the program are proposed to the Academy and the Board by the American Association of State Highway and Transportation Officials. Research projects to fulfill these needs are defined by the Board, and qualified research agencies are selected from those that have submitted proposals. Administration and surveillance of research contracts are the responsibilities of the Academy and its Transportation Research Board.

The needs for highway research are many, and the National Cooperative Highway Research Program can make significant contributions to the solution of highway transportation problems of mutual concern to many responsible groups. The program, however, is intended to complement rather than to substitute for or duplicate other highway research programs.

NCHRP REPORT 237

Project 10-14 FY '79
ISSN 0077-5614
ISBN 0-309-03169-9
L. C. Catalog Card No. 81-85314

Price: $6.80

NOTICE

Published reports of the

NATIONAL COOPERATIVE HIGHWAY RESEARCH PROGRAM

are available from:

Transportation Research Board
National Academy of Sciences
2101 Constitution Avenue, N.W.
Washington, D.C. 20418

Printed in the United States of America.

FOREWORD

By Staff
Transportation
Research Board

This report presents the results of a study that determined the feasibility of using pulsed electromagnetic wave (radar) technology for locating and measuring voids beneath reinforced and nonreinforced concrete pavements. The radar equipment provides return signals from voids that have unique characteristics by which determination can be made of the location, depth, and shape of the voids. A microcomputer, directly connected to the radar equipment, provides a means of real-time processing to extract information from the radar return signal and record the results. Although the technology and equipment have been shown to be feasible for locating and measuring voids, the influence of high temperatures and moisture contents on return signals needs further study, and equipment development should be pursued to provide the basis for units that are practical for field use. The findings of the study will be of particular interest to researchers of agencies involved in the construction and maintenance of pavements. The findings are also useful to individuals engaged in the electromagnetic wave technology field.

Voids often develop over a period of years beneath portland cement concrete pavements and approaches to bridges, and at other locations such as joints, because of pumping, consolidation, subsidence, and erosion of the support material from beneath the pavement. An ability to locate voids by nondestructive surveys would permit replacement of support material before the development of pavement distress and loss of structural qualities. The objectives of this research were to determine the feasibility and practicality of pulsed electromagnetic wave (radar) technology for locating and measuring voids beneath reinforced and nonreinforced concrete pavements and to identify or develop techniques for processing the radar's return signals.

The Georgia Institute of Technology researchers adapted available radar equipment, originally developed for the detection of nonmetalic mines, for the location of voids beneath pavements. Mathematical models and algorithms were developed for analyzing return signals from pavements, base materials, and voids; and a microcomputer was selected for processing the data. The radar equipment and data processing system were then evaluated by laboratory controlled measurements and field measurements conducted on a specially constructed outdoor test lane 72 ft long by 8 ft wide of 9-in. thick portland cement concrete, with and without steel, reinforcing over a dense-graded aggregate base.

The findings of this study indicate that it is feasible and practical to use radar technology for locating and measuring voids beneath pavements, both reinforced and nonreinforced. It has also shown that the signal returns can be processed in the field by microcomputer with the resulting capability of longitudinal void location within 6 in. and void depth determinations up to 8.5 in. with a standard deviation of less than 0.5 in. Temperatures above 70F limit the measurement capability of the equipment used in the study. Prior to extensive field use, the influence of environmental conditions, such as high temperatures, should be documented, and the equipment should be designed and built to withstand normal field handling and transportation conditions.

CONTENTS

1 SUMMARY

PART I

2 CHAPTER ONE Introduction and Research Approach

2 CHAPTER TWO Findings and Interpretation
- Measurement and Processing Equipment
- Theoretical Modeling
- Signal Processing
- Laboratory Measurements
- Test Lane Measurements
- Operational Equipment Considerations

9 CHAPTER THREE Conclusions and Suggested Research

PART II

9 APPENDIX A Measurement and Processing Equipment

12 APPENDIX B Theoretical Modeling

19 APPENDIX C Signal Processing

21 APPENDIX D Laboratory Measurements

29 APPENDIX E Test Lane Measurements

33 APPENDIX F Software

CHAPTER ONE

INTRODUCTION AND RESEARCH APPROACH

An ability to locate voids beneath portland cement concrete (PCC) pavements by periodic nondestructive surveys would permit replacement of support material before the development of pavement distress and loss of structural qualities. The primary objective of NCHRP Project 10-14 is to determine the practicality of using pulsed electromagnetic wave technology for locating voids beneath reinforced and nonreinforced PCC pavements up to 18 in. thick. A secondary objective is the identification or development of data processing techniques suitable for use with equipment that can be operated by field personnel and provide information on the parameters of voids beneath the pavement.

Initial work on this project was directed towards obtaining the pulsed electromagnetic wave equipment that showed promise for accuracy, reliability, and economical application for locating and defining voids beneath pavement slabs. The research approach included an examination of existing pulsed electromagnetic wave equipment, signal processing hardware, and recording devices.

After this initial work, attention was concentrated on the development of data analysis algorithms for processing the response signals from the pulsed electromagnetic wave equipment to enable identification of the location, depth, and shape of voids beneath pavements. The first step was to construct a mathematical model for the pavement/void/base configuration and a mathematical model for the electromagnetic wave equipment. The two models were then combined and used to predict response signal characteristics. This theoretical model was used as an aid to developing data processing algorithms that can be used to locate and identify void shape and depth beneath pavements.

The final task on this project was the experimental evaluation of the void detection pulsed electromagnetic wave equipment and data analysis procedures with regard to accuracy, precision, reliability, limitations, operational characteristics, and environmental effects. Measurements were made in two phases. The first measurement phase was conducted under laboratory controlled conditions using sections of PCC pavement, 9 in. thick with and without reinforcing steel, over various types of base materials, with both low and high moisture levels. In addition, voids were of various depths, both empty and filled with water. The second measurement phase was conducted using a specially constructed outdoor test lane, 72 ft long and 8 ft wide, of 9-in. thick portland cement concrete over a dense-graded aggregate base. Calibrated voids of various sizes were surveyed in-place before PCC was poured and reinforcing steel was placed in one-half of the test lane.

The remaining chapters of this report include a brief description of the electromagnetic wave equipment, the data analysis procedures, and the results and interpretation of the measurements made in the laboratory and on the specially constructed outdoor test lane. The appendixes contain details of the work covering the electromagnetic wave equipment selected, the theoretical modeling, the signal processing algorithms, the laboratory measurements and results, and the test lane construction, measurements, and results.

CHAPTER TWO

FINDINGS AND INTERPRETATION

MEASUREMENT AND PROCESSING EQUIPMENT

The electromagnetic wave equipment chosen for measurements on this project was a very short pulse radar. This radar has the required accuracy and reliability and can be constructed economically. The characteristics of the radar signal response from pavement containing voids will allow signal processing algorithms to recognize small variations related to void detection and identification.

The equipment is mounted on a movable platform and includes output devices that clearly display results in easily interpreted symbols. The system is totally portable and can be operated by a semiskilled person. A microcomputer is used to control two output devices: a video-screen display and a line printer. The radar signal response from the pavement void is processed in an "on-line" fashion by the microcomputer to extract information usable by the field personnel in determining void location, depth, and shape. Permanent recording of the radar signals is available automatically via magnetic disks attached to the microcomputer. Measure-

ment results for void detection are presented on the video monitor and the line printer.

The radar system and the microcomputer were mounted on a cart that could be pushed to most locations for measurement purposes. A complete description of the radar hardware and the microcomputer is given in Appendix A. Figure 1 is a block diagram of the system, and Figure 2 is a photograph of the equipment mounted on the chart.

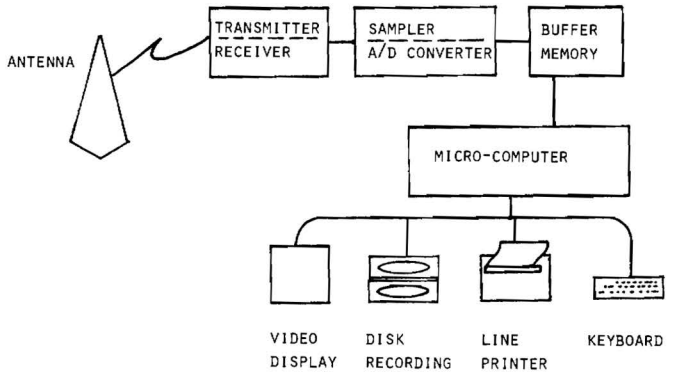

Figure 1. Block diagram of measurement system.

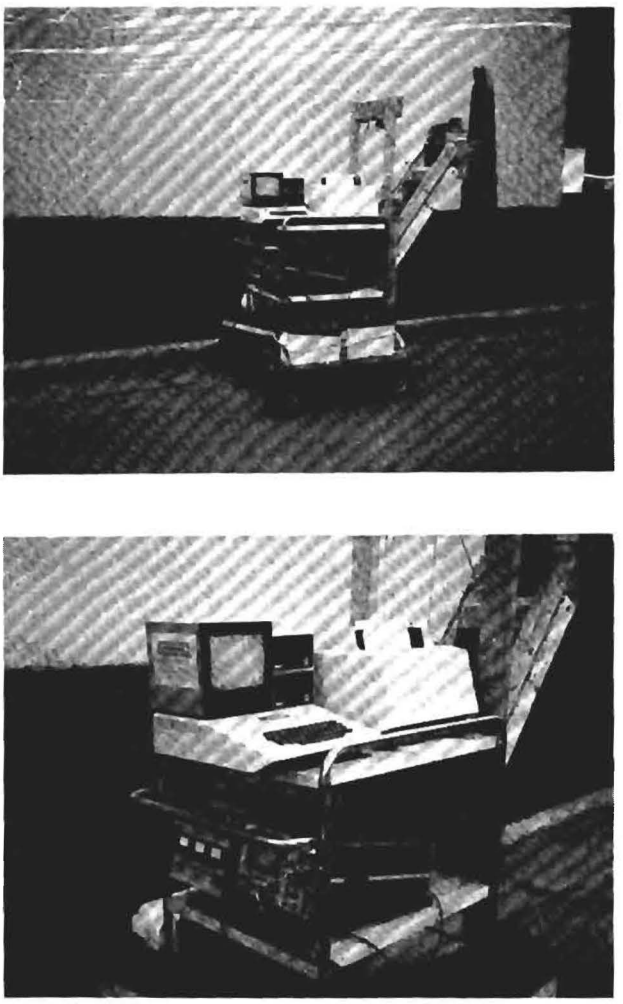

Figure 2. Photograph of measurement system.

It is emphasized that the system described and used by the researchers for this study is not a fully operational highway version in that the equipment has not been exposed to the rigors of actual highway use. However, measurements provided by the radar equipment and the algorithms programmed on the microcomputer are identical to those desired in an operational system.

A typical return signal waveform from PCC pavement with a void beneath is shown in Figure 3. The transmitted pulse is a single sinewave cycle of approximately 1 nanosecond (nsec) in time. It travels through a coaxial cable and is connected to the antenna. The connector on the antenna causes a small reflection to be observed in the signal return. The signal travels through the horn-type antenna cavity and enters the air medium. The antenna itself is not perfectly matched to the air; thus, another reflection occurs at the end of the antenna. This reflection tends to be very distorted and large in amplitude. The signal that is propagated in air strikes the surface of the concrete, and only a very small amount penetrates. The majority is reflected, and appears as a replica of the transmitted pulse. Of the signal that does penetrate, some energy will be reflected by each subsequent interface. In the case of a "no void" situation a single small return will be present from the pavement–base interface. In the case of a void existing, two signals will be present. The time of occurrence and amplitude of those signals are the important parameters for void location and size determination.

In the data measurements presented in this report only the time interval of the signal return around which a void typically will occur is processed and displayed (or plotted).

THEORETICAL MODELING

The development of a theoretical signal model was essential to the understanding of the problem of making measurements of voids under pavement via radar. Transmission line theory provided the means for the model solution; the details are given in Appendix B. The mathematical algorithms derived from the study were programmed on the microprocessor, and many simulated data sets were generated.

The simulated data sets were anlyzed to extract signal characteristics unique to the void detection and identification process. In this process two important discriminants were identified, and they provide the theoretical basis for the signal processing techniques. For voids less than 2.5 to 3 in., there is primarily a change in the amplitude of the return signal. For voids larger than this a time difference measurement is used; that is, measuring the time difference between the negative and positive peaks of the return signals from the void interfaces.

Figure 4 shows a set of simulated waveforms from voids ranging in depth from 0 in. to 8.5 in. in 0.5-in increments for PCC pavement thickness of 5 in.

The set of waveforms is plotted only around the actual time of void occurrence. Time $t=0$ signifies the surface of the pavement. The waveform that occurs at approximtely 2 nsec in the 0.5-in. to 8.5-in. traces is the reflection from the bottom of the pavement and top-of-void air-space interface and is an inverted version of the transmitted signal. The part of the signal that occurs at a varying time from 2.3 nsec. to 3.5 nsec is the return from the bottom of void air-space and base

interface. Where two signals interfere with each other, void depths 0.5 in. to approximately 3 in., an amplitude variation is visible. Beyond 3 in. the time difference is the key indicator of void depth.

The time scale for the data is linearly related to depth, but will be segmented dependent on the dielectric constant, ϵ, through which the signal is propagating. In Figure 4, a depth scale is indicated at the top of the plot and is divided into two parts. The first part represents the time–depth scale through 5-in. PCC pavement medium with $\epsilon=6$. The second part is scaled with respect to air, $\epsilon=1$ for the void. Thus, concrete thickness can be read directly as can void depth, with the two readings added to give depth to the bottom of void air-space. Beyond the bottom of void air-space reflection the air–time calibration is not valid. With this segmented time–depth relation in mind the plots in this report will be simply labeled in time only (nanoseconds), with the realization that in air-void areas, 1 nsec=5.9 in.

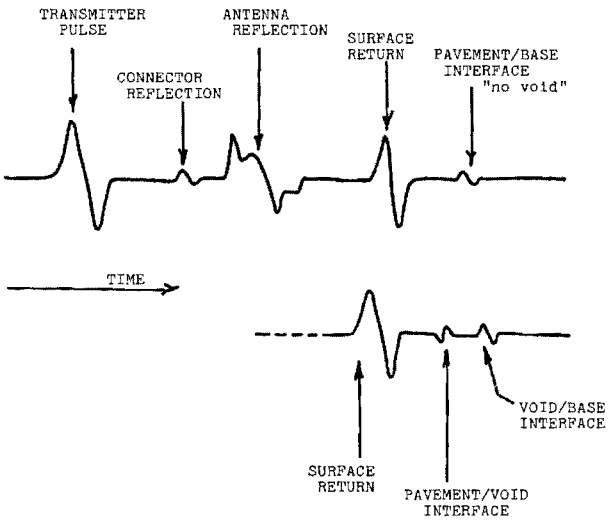

Figure 3. Illustrative signal return.

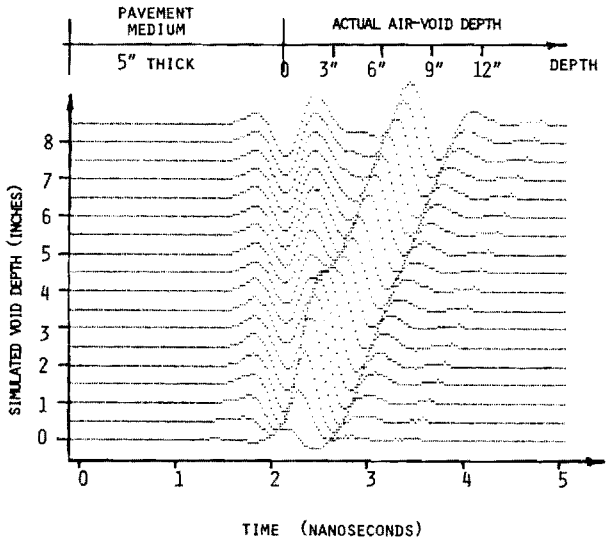

Figure 4. Simulated waveforms—void sizes 0 in. to 8.5 in.

If the variations of the time and amplitude are plotted versus void size, Figures 5 and 6 result. In Figure 5 the important area of the amplitude variation occurs between 0 in. and 2.5 in. where a monotonically increasing relationship is evident. The time difference plot of Figure 6 shows a linear relationship with void size from approximately 3 in. and greater.

SIGNAL PROCESSING

The analog signal processing begins with detection of the large signal waveform from the top surface of the concrete.

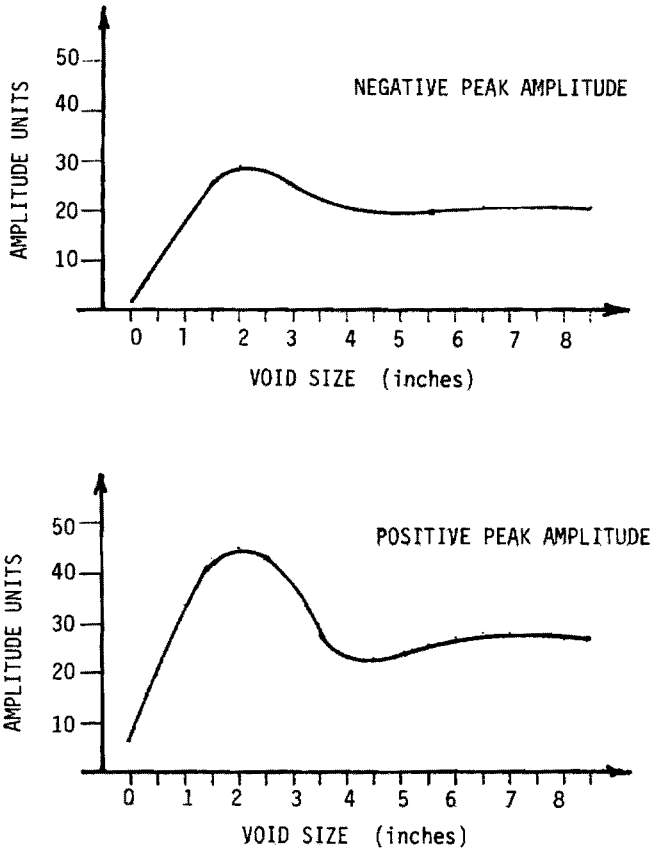

Figure 5. Amplitude variation of waveforms.

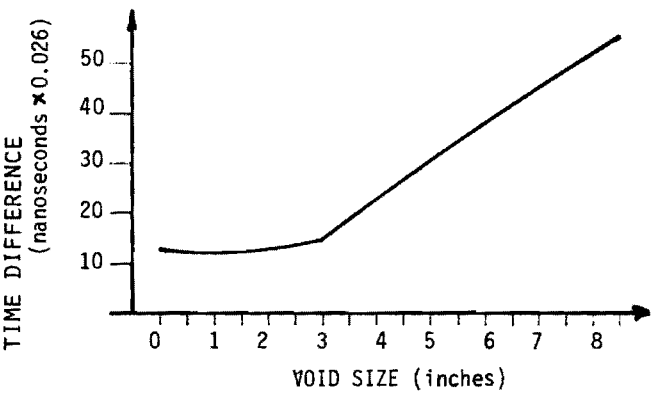

Figure 6. Time difference variation of waveforms.

A timing window is started when the top surface of the concrete is detected and stopped after approximately 20 nsec has elasped. The signal response during the timing window represents the return from typical PCC pavement and the base material to a depth of at least 24 in. A portion of this signal, from the pavement surface to approximately 12-in. depth, is then digitized by an analog-to-digital converter and stored in a digital buffer that is accessible by the microprocessor. The actual measurement process is controlled by the operator via microprocessor commands; the operator can position the equipment over the area to be tested and designate when a measurement is to be made.

The digital signal processing algorithms were synthesized from information provided by the theoretical modeling study. The specific discriminants used are the time between the negative and positive peaks and the amplitudes of those peaks. The computer algorithms search through the electromagnetic return signal and identify minimum and maximum values and their time of occurrence. If the amplitude exceeds a minimum threshold and time differences fall within prescribed bounds, a void is said to exist. The time discriminant is then examined to determine if the void depth is greater or less than 3 in. If the void is less than 3 in., the amplitude is employed to obtain the void depth estimate. If the void depth is greater than 3 in., a time difference is used to directly gauge void size.

A graphical representation of the void sizing algorithm is shown in Figure 7. In the first part of the algorithm the void size is based on the ratio of the negative peak to a calibration number. This number is determined by the operator during a set of preliminary calibration measurements. The procedure for calibration involves finding sections of pavement where voids are not likely to exist and making measurements. The signal return accepted for calibration at that time is used as a reference during the remainder of the measurements. The second part of the void sizing algorithm makes use of the time difference between the negative and positive peak signal returns from the concrete–void interface and void–base interface, respectively. At approximately 3 in. and greater these signals have a time difference that is directly proportional to the void size. Appendix C covers the details of the signal processing.

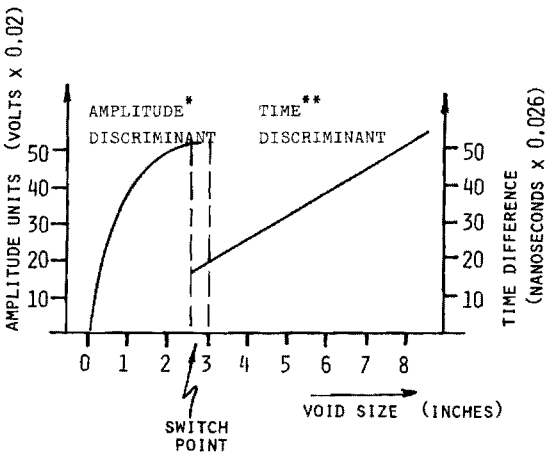

*AMPLITUDE: void size = $(6/\pi)\ \sin^{-1}\left(\frac{\text{amplitude peak}}{\text{calibration \#}}\right)$

**TIME: void size = 0.026 x 5.9014402 x time units

Figure 7. Graphical representation of discrimination algorithm.

The next step in the signal processing is to present the results on the visual display. Microcomputer software was developed to display the signal return from a particular measurement, whether or not a void exists, and the size of the void if it exists. The information is also automatically saved for future use and can be typed out on a line printer for permanent recording. Various options were also incorporated to permit permanent visual recording of the signal waveform on magnetic disk. Post-processing software was developed to display a sequence of measurements and send the plot to the line printer for permanent recording. All of the plots of signal waveforms in this report were generated or processed by the microcomputer and subsequently plotted on the line printer.

LABORATORY MEASUREMENTS

The experimental evaluation of the void detection pulsed electromagnetic wave equipment and signal processing algorithms was accomplished in two phases. The objective was to evaluate the accuracy, precision, reliability, limitations, operational characteristics, and environmental characteristics of the equipment and processing algorithms. The first phase was conducted inside a laboratory under controlled environmental conditions. Test sections of PCC pavement approximately 43 in. by 43 in. by 9 in. thick, both reinforced and nonreinforced, were used. These test sections were placed over base materials of PCC, asphaltic concrete, dense-graded aggregate, and portland cement stabilized clay. Measurements were made as the moisture levels for the pavement section and the base material were varied. Voids were simulated by elevating the pavement section a measured amount above the base material. Figure 8 is a photograph of a pavement section over the clay base; a 4-in. void is visible. Measurements were made for void depths ranging from 0 in. to 8.5 in. in 0.5-in. increments. These measurements are shown in Appendix D. Some measurements were made for simulated voids partially filled with water. The findings indicate a definite agreement with the theory as to the variation in amplitude of the positive and negative peaks and in the time differential of the peaks. Thus, the discriminant from the theoretical considerations were verified. In addition, the measurements provided the basis for verifying and refining the theoretical model.

As an example of the results achieved, Figure 9 is a representation of what the operator will see on the visual display after processing a set of measurements as given by Figure 4. A brief explanation of this figure is given here; the reader is referred to Appendix C for details. The horizontal axis represents a series of sequential measurements; in the case illustrated, 18 measurements were made. The vertical axis is calibrated in inches and information about the signal return and a void, if detected and sized, is represented. The estimated size for the void is represented two ways: (1) by the length of a vertical bar, and (2) by the numbers read vertically downward at the bottom of the plot. The distance from the top of the plot to the horizontal line where the void bars begin

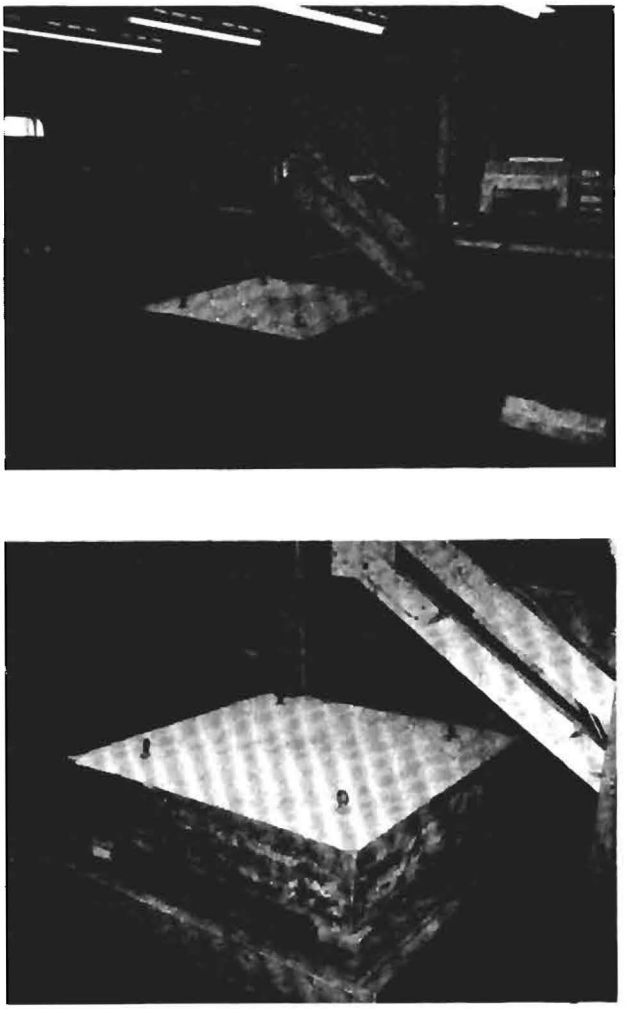

Figure 8. Laboratory measurement configuration.

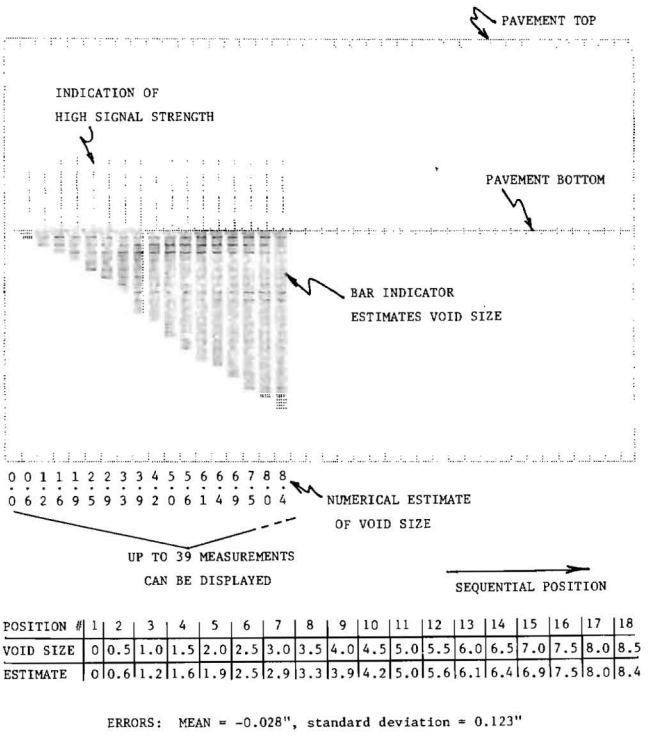

POSITION #	1	2	3	4	5	6	7	8	9	10	11	12	13	14	15	16	17	18
VOID SIZE	0	0.5	1.0	1.5	2.0	2.5	3.0	3.5	4.0	4.5	5.0	5.5	6.0	6.5	7.0	7.5	8.0	8.5
ESTIMATE	0	0.6	1.2	1.6	1.9	2.5	2.9	3.3	3.9	4.2	5.0	5.6	6.1	6.4	6.9	7.5	8.0	8.4

ERRORS: MEAN = -0.028", standard deviation = 0.123"

Figure 9. Synthetic display of measurement results.

represents the concrete pavement, and below the line is base material. The narrow vertical lines visible above the void size bars represent areas of the signal return where the amplitude exceeds a threshold value. Currently this value is set just above the clutter or noise in the signal return, thus only the strongest signals are displayed.

As indicated by the void bars, this is a sequence of increasing size voids, and follows the signal sequence given in Figure 4. The signals were generated by simulation for voids of 0 in. to 8.5 in. in 0.5-in. increments. The estimated depths, via the algorithms, are summarized below the plot. The mean and standard deviation for these estimates is $\mu = -0.028$ in., $\sigma = 0.123$ in. Additional plots are given in Appendix D for actual measurements on several base types.

TEST LANE MEASUREMENTS

The second phase of the experimental evaluation was conducted on a specially constructed outdoor test lane representative of a section of concrete highway. The test lane measures 72 ft long, 8 ft wide, and 9 in. thick. The test lane was constructed according to the Georgia Department of Transportation specifications using portland cement concrete over a dense-graded aggregate base. Calibrated voids of various depths and shapes were surveyed in place before the concrete was poured. In one-half of the test lane, reinforcing steel was used. The voids were created by shaped pieces of lightweight foam, the foam itself being virtually invisible to the electromagnetic signal.

Figure 10 is a photograph of the measurement equipment on the test lane, and Figure 11 gives an approximate layout for the voids beneath the pavement and the reinforcing bars in the pavement. Exact measurements resulting from the survey of the test lane are given in Appendix E. Measurements on the test lane were made over the wide temperature range of 32 F to 100 F, which had a definite influence on the results of the signal processing algorithms. Moisture is also a critical element that can affect performance. Initially when measurements were made during the summer at temperatures around 90 F, void indications were visible only to a trained operator. The microprocessor processing algorithms were not capable of the performance desired. Measurements subsequently made during the fall and winter seasons at temperatures down to 32 F produced excellent results.

Figure 12, presented in the format of Figure 9, is the result of a set of processed measurements taken every 6 in. along a path through the center of voids as indicated in Figure 11. The void sizes that were estimated by the processing algorithms are given both on the figure, as would be seen by the operator, and in Table 1. The results in Table 1 indicate void-size estimates with a $\mu = 0.09$ in. and $\sigma = 0.46$ in.

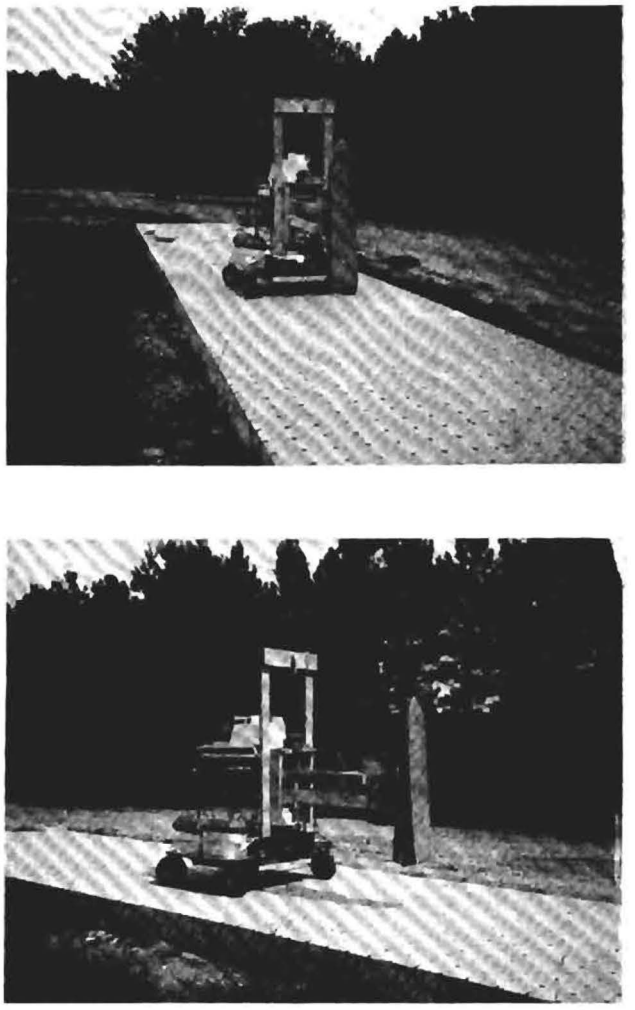

Figure 10. Test lane and measurement equipment.

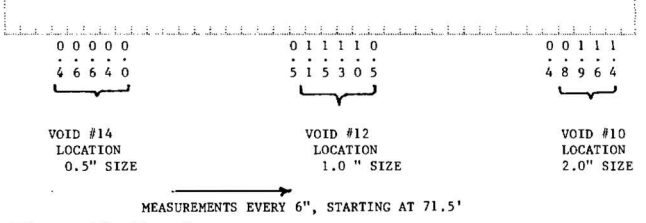

Figure 12. Test lane measurements.

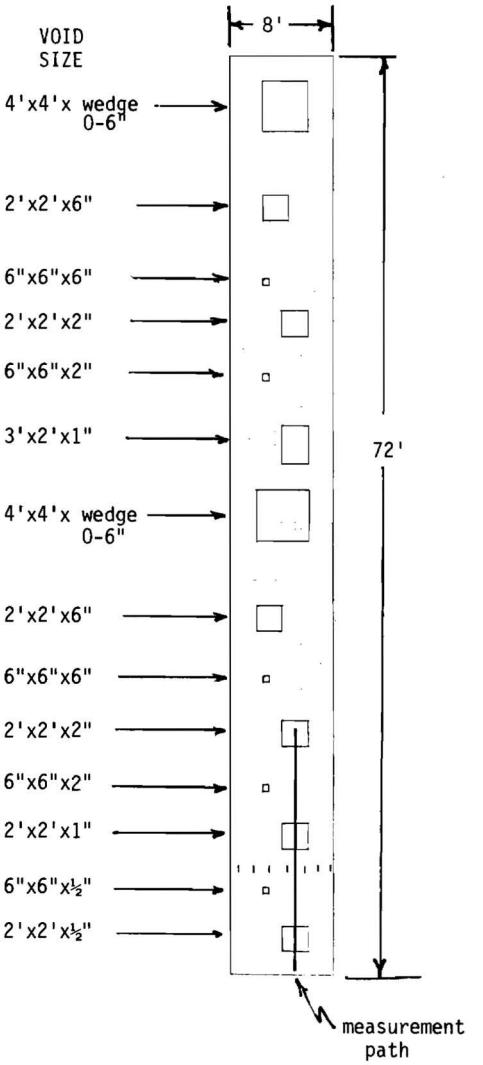

Figure 11. Test lane void layout.

OPERATIONAL EQUIPMENT CONSIDERATIONS

Several factors must be considered if this system is to be built for field operation. They include the efficient coverage over an actual highway and modifications for environmental conditions.

Highway Coverage

Speed

The current radar unit has an effective signal (or pulse) per second output of 50 PPS. If one reading every 6 in. is used as a criterion, the unit has the capability of covering 25 ft/sec or 17.1 mph. Thus, the radar unit itself has a reasonable coverage/speed capability. The microprocessor is currently configured as a demonstration unit and processes only about one signal return every 5 sec. Indeed, even if efficiently written software codes were used, it is doubtful that any acceptable speed could be produced. Thus, a new, faster processor unit must be implemented. Identical operations to that used by the researchers would be programmed; the only difference would be speed of processing. Processors exist on the market today that have the desired capability.

Table 1. Void size estimates (except for columns 1 and 2, the data are in inches).

VOID #	TEST LANE POSITION	ACTUAL VOID SIZE	VOID SIZE ESTIMATE	SIZE ERROR	POSITION ERROR
14	70.'	0.5	.4	-.1	0
14	69.5'	0.5	.6	+.1	0
14	69.'	0.5	.6	+.1	0
14	68.5'	0.5	.4	-.1	0
14	68.0'	0.5	.0	-.5	.0
12	62.5'	0.	.5	+.5	-6.
12	62.'	1.0	1.1	+.1	0
12	61.5'	1.0	1.5	+.5	0
12	61.'	1.0	1.3	+.3	0
12	60.5'	1.0	1.0	0.	0
12	60.'	1.0	0.5	-.5	0
10	54.5'	0.	.4	+.4	-6
10	54.'	2.	.8	-1.2	0
10	53.5'	2.	1.9	-.1	0
10	53.'	2.	1.6	-.4	0
10	52.5'	2.	1.4	-.6	0

SUMMARY: $\bar{X}$ = -0.09"
σ = 0.46"

Width

Currently the antenna in use is effective over not more than a 2-ft width (±1, 1 ft). It is noted that the characteristics are slightly different in the length direction for an effective coverage of ±6 in. To completely cover a single highway lane at one time would require the use of multiple antennas. There appears to be no mechanical equipment problem posed by the mounting of multiple antennas in a side-by-side configuration. There would be electrical considerations. The antennas would have to be sequentially pulsed with energy, and some of the signal background characteristics might change because of coupling of energy into adjacent antennas. At this time the researchers believe that the electrical changes pose no problem in interpreting the signal return from a void. The speed of highway coverage would remain the same (17.1 mph maximum) with multiple antennas.

Environmental Factors

Operational Equipment Configuration

As currently configured the equipment is an experimental measurements system. None of the hardware has been exposed to (nor was it expected to be) the rigors of highway use day after day. Both the radar unit and the microprocessor must be repackaged for that purpose. The actual repackaging of the equipment to withstand highway conditions, including environmental factors such as rain, snow, heat, and so on, does not pose any technical challenges. With the presupposition of this type of equipment availability the electrical characteristics remain unchanged. The basic signal representation would be identical to what is presented in this report. It has been indicated by the researchers that spurious reflections from objects within 6 ft of the antenna can be a problem and must be minimized. The operational equipment configuration, especially if multiple antennas are used, is critical if minimum reflection is to be realized. Techniques for this task exist and make the final operational hardware realizable with a minimum of additional experimentation.

With the existing experimental measurements system some attempt was made to minimize these spurious reflections by simply eliminating causes. That is, objects were not allowed in the vicinity (± 6 ft) of the antenna while measurements were being made.

As a proof of concept demonstration, absorbing material was placed around the antenna at a standoff distance of 2 ft. This simple technique provided a significant reduction of unwarranted reflections, and would definitely be used in an operational system.

Temperature and Moisture

Although temperature and moisture are considered environmental factors, they have been singled out as having a critical effect on the signal characteristics. In fact, it appears at this time that if the temperature–moisture levels are too high, the equipment cannot be operated. This is the prime area that requires more study if an operational system is desired. Theoretical analysis indicates that attenuation of the electromagnetic signal varies with total moisture content and temperature. From the curves given in the theoretical material in Appendix B, for 75 F temperature and 10 percent moisture, the attenuation is about 5 to 10 times as great as it would be for a temperature of 140 F and the same moisture level. Specific attenuation measurements were made both in the laboratory and on the test lane to verify that high temperature measurement problems on the test lane are related to the moisture–temperature combination. Under the same moisture conditions, attenuation for measurements on the outdoor test lane at 100 F was a factor of 4 greater than attenuation for laboratory measurements at 78 F. Clearly, the effects of high temperature are a higher attenuation level and a decrease in signal strength to a point where the microprocessor algorithms cannot detect and size the void.

Reliability

Over the period of this research effort, the radar and microcomputer have been extremely reliable. Only minimal repairs and maintenance have been necessary. Highway use would require fastening components firmly to support structures that would be shock-mounted to maintain high reliability.

CHAPTER THREE

CONCLUSIONS AND SUGGESTED RESEARCH

The electromagnetic wave equipment chosen for the void detection and size measurement program provides excellent results. The signal response from the radar has the sensitivity and accuracy to allow application of signal processing algorithms and to identify small variations related to the void detection problem. The equipment itself can be economically constructed and is suitable for highway operation with a minimum of modifications.

The microcomputer connected to the radar processes the signal returns in an on-line mode and presents the results on a video monitor as well as on a line printer for a permanent copy. Magnetic disk provides permanent recording of the actual signal returns.

The system, mounted on a movable cart, provides the portability needed for this research project. Its configuration permits operation by field personnel with a minimum amount of skill required.

Further research concerning the equipment should consist of methods of protection from the environment and shock and vibration mounting. The microcomputer for application to rapid highway measurements should be updated for faster processing.

The theoretical modeling affords a complete understanding of the void detection and sizing problem. It provides the basis for development of the discriminants necessary for the algorithm development. The theory also provides a preliminary background for the attenuation effects of moisture and temperature.

A combination of analog and digital signal processing gives the timing signals necessary for the extraction of the portion of the radar signal return corresponding to the possible locations of a void. Digital signal processing algorithms developed for detecting and sizing the voids provide the capability for spatial void location to ±6 in. and depth sizing up to 8.5 in. with a standard deviation of the error of less than 0.5 in. Calibration of the measurement process is easily accomplished by field personnel.

The laboratory measurements afford a controlled environment for studying the radar signal interactions with voids. The controlled measurements also enable verification of the discriminants developed in the theoretical modeling. Several typical base materials under various moisture levels can be measured. Void depths from 0 in. to 8.5 in. in 0.5-in. increments were measured, and an extensive data base was accumulated for future use. Suggested future measurements should include special processing to show that the thickness of the concrete pavement and its dielectric constant can be estimated. Present measurements give an indication that this can be accomplished.

The test lane measurements provided an opportunity to obtain data from a set of known calibrated voids under PCC pavement that closely simulated an actual highway situation. Measurements were made over a wide temperature range and results indicate that at high temperatures (e.g. 100 F) a large attenuation of the electromagnetic signal occurs. Measurements made at less than 70 F resulted in excellent void location and sizing estimates. This result definitely indicates that environmental conditions, especially high temperature, limit the measurement capability. Thus, the optimum time to make measurements could be during the winter season, at low temperatures, when the attenuation is minimized. Further research is suggested into the effects of temperature on the signal strength. Both laboratory and actual highway measurements should be made to more fully substantiate currently available measurements and modeling information.

Overall suggestions for additional research include preliminary design of an operational high-speed processing system, measurements in the laboratory and on the test lane on a continuing basis to completely document the effects of temperature, and actual highway measurements to verify effectiveness of the processing algorithms.

APPENDIX A

MEASUREMENT AND PROCESSING EQUIPMENT

As a result of research, the electromagnetic wave equipment chosen most suitable for measurements on this project was a very short pulse radar. This radar has the required accuracy and reliability and can be economically constructed. The signal response from the radar has the characteristics that will allow signal processing algorithms to recognize small variations related to void detection and identification.

In order to have a totally portable system capable of being operated by a semiskilled person the equipment must have output devices that clearly display results in easily interpreted symbols and be mounted on a movable platform. To satisfy the first requirement, a microcomputer was used with video-screen display and a line printer for output. The signal response from the radar equipment is processed "on-line" by the microcomputer and provides information to field personnel for void location, depth, and shape. Permanent recording of the radar signals is available automatically via magnetic disks attached to the microcomputer. Results for void detection are not only available on the video monitor but can be printed on the line printer.

To satisfy the portable requirement, the radar system and the microcomputer are mounted on a cart that can be pushed to most locations for measurement purposes. A complete description of the radar hardware and the microcomputer is given in the following.

RADAR HARDWARE

Electromagnetic Wave Equipment

The requirements for void detection and sizing necessitate the use of equipment of very high time resolution and usability at short distances from the medium being measured. This translates into a requirement for an extremely short pulse of energy to be generated by the equipment. In order to actually transmit this energy into the medium a wide bandwidth, low loss, matched antenna must be used. The return signal from the medium being measured enters the antenna and must be detected. This requires a sensitive wide bandwidth receiver.

The radar that satisfies these requirements and is used in these tests is an adaptation of the vehicle-mounted mine detection radar developed by the Calspan Corporation, Buffalo, N.Y., for the U.S. Army (MERADCOM, Ft. Belvoir, Va.) (*A-1, A-2*). The radar transmits pulses consisting of one cycle at 1 gigahertz (GHz) (i.e., a 1-nsec pulse width). Because 1 cycle of 1 GHz is a transient type of signal, a bandwidth as much as 2 GHz is needed to prevent distortions of the signal. For the system in this project, this bandwidth is required only in the transmitter, antenna, and sampler. The wide bandwidth is not needed for the video sections because the periodic, real-time return signal is sampled and reconstructed at a much lower frequency. Figure A-1 is a block diagram of the system, and the following paragraphs describe the figure in detail.

Timing Generator

The timing for the system is derived from a 15-megahertz (MHz) crystal controlled oscillator. This signal is divided down to produce all gating and trigger waveforms needed in the radar. In particulr, the timing generator produces the 5-MHz signal that establishes the radar pulse repetition frequency (the number of pulses per second that are transmitted).

Transmitter

The transmitter can be divided into a short-pulse driver and avalanche pulse generator. The drive consists of a snap-off step-recovery diode that generates a transition across a coaxial pulse forming network, thereby generating a short transition pulse. Amplification is achieved by a transistor operated in the avalanche mode for high-speed switching. The transistor output goes directly to the antenna.

Antenna

The antenna is of broadband design, working over the range from 200 MHz to 2 GHz in frequency. To obtain the low-frequency response, a transverse electromagnetic (TEM) horn was used which was not limited by low frequency. To maintain the required wide bandwidth, the plates of the horn are flared and exponentially tapered with resistive card loading on the ends. Because of this, there is little reflection of energy from the antenna into the receiver. In other words, the antenna has a very low-voltage standing wave ratio and most of the energy is transmitted into the medium.

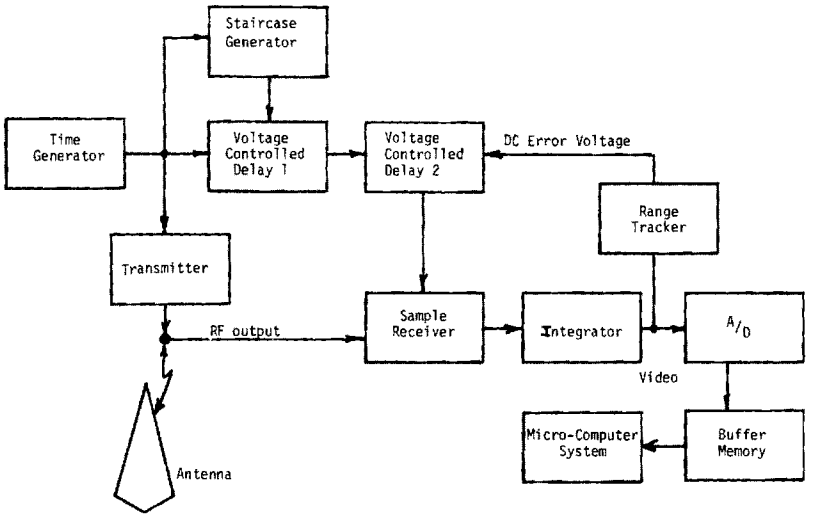

Figure A-1. Radar block diagram.

Sample Receiver

The returning signal is sampled by a Schottky barrier diode that is strobed by a snap-off step-recovery diode at a 5-MHz rate. The periodicity of the received waveforms allows one to take individual samples from pulse-to-pulse in order to reconstruct the waveform over a longer time period, thereby decreasing the bandwidth requirements on the video and digital subsystems as shown in Figure A-2. To have samples at times differing from the transmit pulse, the 5-MHz signal to the sampler is delayed by voltage-controlled delay lines 1 and 2. The control voltage for delay line 1 is a staircase waveform of 200 steps. Each voltage step causes the sample strobe to occur later on the waveform than the previous sample strobe. Because there are 200 steps, a sample is taken at 200 positions across the real-time waveform. At each of these 200 positions, 450 samples are taken and an integration is performed to increase the signal-to-noise ratio. Each voltage step moves the sample strobe out 92.5 picoseconds (psec) in range. Because there are 200 steps, the width of the sample window is 200 × 92.5 psec = 18.5 nsec. Comparing real-time waveforms to reconstructed waveforms, 18.5 nsec of real time corresponds to 18 milliseconds (msec) in reconstructed time. The position of the sample window in range is controlled by delay line 2 via a voltage from the range tracker.

Range Tracker

The main function of the range tracker is to establish a fixed-time reference position for the surface return. Once this is established, all other video is referenced to this time. Video cannot be referenced to the transmit pulse because of the varying antenna height above the ground. If it were, the position in time of the void return would vary making detection difficult. The range tracker locks on the surface by applying an error voltage to delay line 2 that keeps the leading edge of the sample window locked to a point slightly behind the surface return. The void always remains at the same position within the window regardless of antenna height.

Analog-to-Digital Converter with Buffer Storage

The video information must first be converted into a digital format before it can be processed by the computer. That is the purpose of the analog-to-digital converter. Figure A-3 shows sequential sampling that is used with the converter. The waveform can be represented by samples taken over 1 cycle of the video waveform. The video is sampled and in real time, and each sample is converted to a digital word and stored in a buffer memory. Both loading and unloading of the buffer are under computer software control.

MICROCOMPUTER

The microcomputer chosen for the void detection system was built by APPLE Computer, Inc., Cupertino, Calif., and consists of the following components.

Main Computer
48,000 words of random access memory
Keyboard interface
BASIC and PASCAL language systems
Video Display
9-in. black and white
Text and graphics modes of display
Two Mini-Floppy Disk Drives
5-in. floppy diskettes
102,000 words of storage each diskette

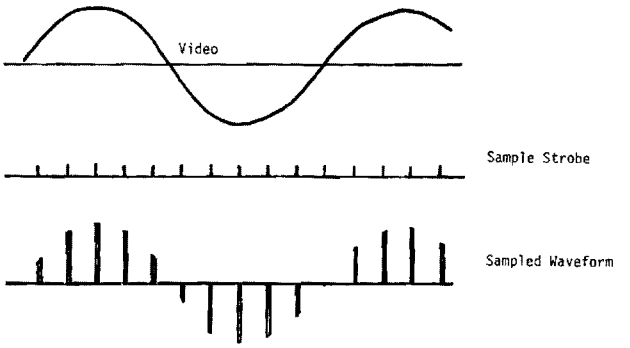

Figure A-3. Sequential sampling.

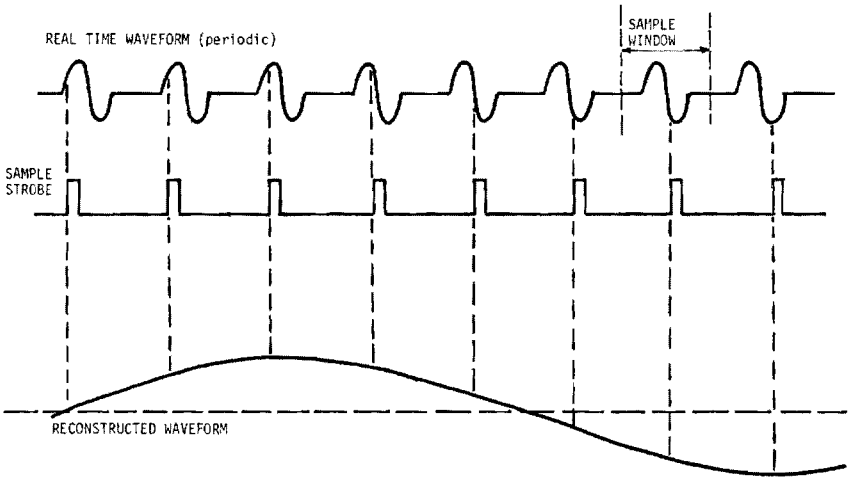

Figure A-2. Periodic sampling (single sample/position).

3 Interface Cards

Radar interface—digitizes radar data

Communications interface—transfers data to/from the CYBER Facility printer interface—line printer communication

Printer

Capable of printing out data/program listings or graphics (plots); all the plots of actual or simulated data presented in this report were generated on the printer.

REFERENCES

A-1. BECHTEL, M. E., and ALONGI, A. V., "Antennas and Pulsers for a Vehicular-Mounted Mine Detector (U)." CALSPAN Report *MA-5366-E-1* (Sept. 1974).

A-2. BECHTEL, M. E., and ALONGI, A. V., Discriminator and Display for Vehicular-Mounted Mine-Detector Radar (U)." CALSPAN Report *MA-5366-E-2* (June 1976).

APPENDIX B

THEORETICAL MODELING

A theoretical mathematical model was developed for a concrete slab, an air void, and an underlying base material to evaluate their effect on impinging radar electromagnetic (EM) waves. These theoretical results can then be compared to the measurements taken with the short-pulse radar to assist in interpreting the measured results. This appendix describes the details of the mathematical model development and the theoretical effects of void depth, spurious reflections, and concrete attenuation on the reflected EM waves.

MATHEMATICAL MODEL

The model of a concrete slab and its surrounding environment is shown in Figure B-1. The model was deliberately kept simplistic so that describing mathematics would be tractable. The source and receiver of the electromagnetic (EM) waves are located above the slab, and the waves are directed into the slab by an appropriate antenna. The EM waves are reflected by the slab surface and dielectric discontinuities beneath the slab surface. If there is no void beneath the slab, the only dielectric discontinuity beneath the slab surface will be at the concrete–soil interface and the incident EM waves will be reflected from it. If a void does exist, there will be two dielectric discontinuities beneath the slab surface: the concrete–void interface and the void–soil boundary. Each of these boundaries will reflect the incident EM waves.

Consider for a moment the behavior of electromagnetic waves at the boundary between two media as shown in Figure B-2. The reflection coefficient, ρ, at the boundary is given by

$$\rho = \frac{n_2 - n_1}{n_2 + n_1} \tag{B-1}$$

where n_1 and n_2 are the wave impedance of medium 1 and 2, respectively. For a perfect conductor, the wave impedance is zero; for a nonconducting, nonferrous medium such as dry soil or concrete, the wave impedance is

$$n = \sqrt{\frac{\mu_0}{\epsilon}} \tag{B-2}$$

where μ_o is the magnetic permittivity of space, and ϵ is the dielectric constant of the medium. If the wave impedance for free space (air) is denoted by

$$n_0 = \sqrt{\frac{\mu_0}{\epsilon_0}} \tag{B-3}$$

Eqs, 1 and 2 may be written as

$$n = \frac{n_0}{\sqrt{\epsilon_r}} \tag{B-4}$$

and

$$\rho = \frac{\sqrt{\epsilon_{r1}} - \sqrt{\epsilon_{r2}}}{\sqrt{\epsilon_{r1}} + \sqrt{\epsilon_{r2}}} \tag{B-5}$$

where ϵ_r is the relative dielectric constant of the medium. Note that if medium 1 has a smaller relative dielectric constant than medium 2, ρ has a negative value. On the other hand, if medium 1 has a larger relative dielectric constant than medium 2, ρ is positive.

Consider the situation where a void is not present beneath the concrete slab, as shown in Figure B-3. Also, assume the transmitted pulse (the amplitude variation of the EM waves with time) is of the shape shown in the same figure. How should the radar returns from the air–concrete and the concrete–soil interfaces appear? The concrete has a dielectric constant greater than that of air; thus, ρ at the air–concrete interface has a negative value. If the soil is moist, its dielectric constant will be greater than that of concrete and ρ at the concrete–soil interface will also be nega-

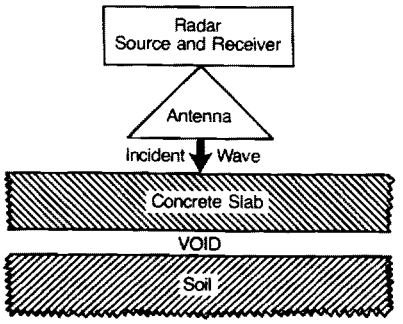

Figure B-1. Concrete slab and environment.

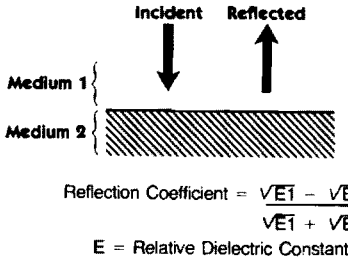

Figure B-2. Behavior of EM waves at a dielectric boundary.

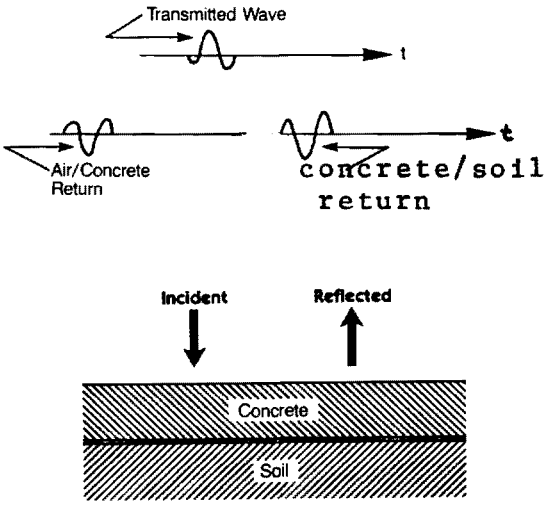

Figure B-3. Behavior of EM waves at air–concrete and concrete–soil boundaries.

tive. Thus, the radar return will appear as shown in Figure B-3. Assuming the concrete–soil boundary is far enough below the slab surface so the two reflected pulses do not overlap, each of the returns should appear as the inverse of the transmitted waveform as illustrated. If the soil is very dry, its dielectric constant may be smaller than that of concrete. Then the radar return from the concrete–soil boundary will be the same polarity as the transmitted waveform.

Extending this simplified analysis to the case where a void (air gap) between the concrete slab and the soil base does exist, the reflected EM waves (radar returns) are as shown in Figure B-4. Because the dielectric constant of concrete is greater than that of air, the reflection coefficient at the concrete–void interface is positive. However, the reflection coefficient at the void–soil interface is negative. Thus, the reflected pulses from these two boundaries are of different polarities as shown.

The time separation between the pulses from the top and bottom of the void is proportional to the depth of the void in the direction of the incident EM wave propagation. Because the radar is positioned so the incident EM waves travel perpendicular to the concrete slab surface, the time separation between pulses is proportional to the void thickness. The relationship between an air–void depth, d, and pulse separation is as follows:

$$\text{pulse separation} = \frac{2d}{C}$$

$$\text{PS (nanoseconds)} = \frac{d \text{ (inches)}}{5.9} \qquad \text{(B-6)}$$

where $C = 118.0288 \times 10^8$ in./sec.

The radar that was used in this measurement program has a pulse length of about 1 nsec. Thus, the void depth must be greater than 5.9 in. if the reflected radar pulses from the concrete–void and void–soil interfaces are not to overlap in time. Most of the voids expected are much smaller than 5.9 in. Thus, the radar returns from the top and bottom of the void will overlap. Because the two pulses are of different polarities, they will tend to subtract, producing a particular pulse shape that may be much different from the ones shown in Figure B-4. In addition, the amplitude of the composite pulse will vary depending on the time separation between the two pulses. The amplitude will tend to be proportional to the time separation and, hence, the void depth. This is one property of the radar return that can be used to estimate void size.

Another consideration that complicates the prediction of what one should expect the radar return to be is multiple reflections, as shown in Figure B-5. In Figure B-5(a), multiple reflection of the EM waves between the top and bottom faces of the concrete slab is shown. Some of the incident radar energy is reflected back and forth between faces. Each time, some of the energy is returned towards the radar receiver, yielding a returning pulse of energy. However, if the distance between the concrete slab faces is greater than $^{5.9}/\sqrt{\epsilon_{\text{concrete}}}$ in., or approximately 2.4 in. for dry concrete, the pulses do not overlap and each reflection is easily identifiable.

Multiple reflections between the air–void faces, as shown in Figure B-5(b), combine and must be considered, however. Because the distance between air–void faces is much less than 5.9 in., the pulse returns resulting from multiple reflections do overlap and each contributes to the composite pulse return. The individual contribution can be calculated. Also, each succeeding reflection is smaller than the preceding one. Thus, only a finite number of reflections need to be considered.

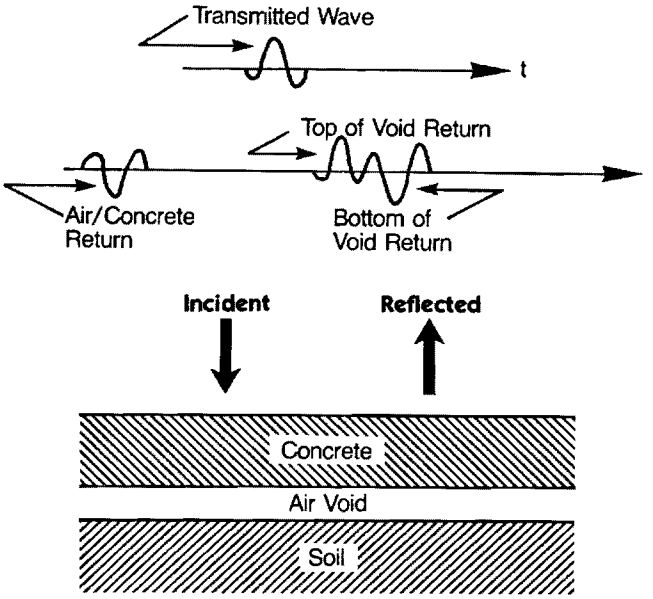

Figure B-4. Behavior of EM waves at concrete–air and air–soil boundaries.

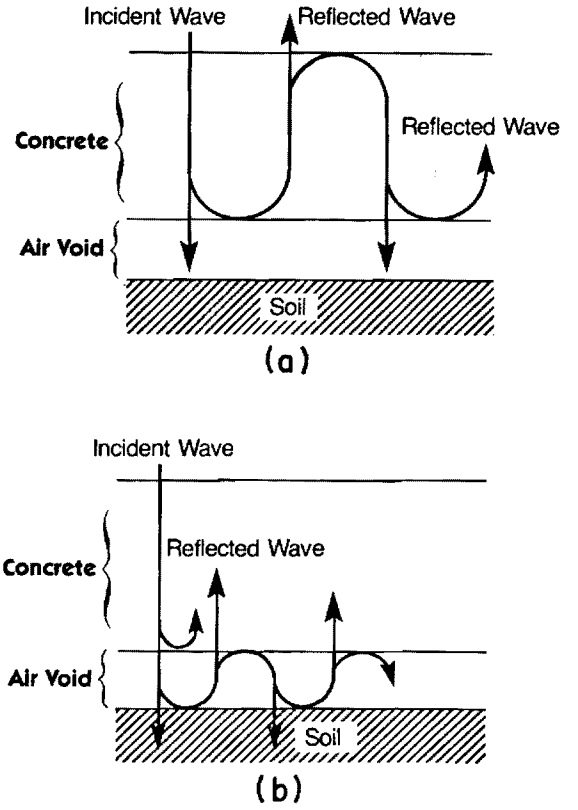

Figure B-5. Multiple reflections between (a) slab faces and (b) void faces.

EFFECT OF VOID SIZE

An approximate mathematical expression for the composite radar return, $s(t)$, due to single and multiple (3) bounces between void faces is as follows:

$$s(t) = \rho_1 X(t) + \rho_2 \left[1-\rho_1^2\right] X(t+\tau) + \rho_1 \rho_2^2 \left[1-\rho_1^2\right] X(t+2\tau) + \rho_1^2 \rho_2^3 \left[1-\rho_1^2\right] X(t+\tau) \quad \text{(B-7)}$$

Where:

$X(t)$ = transmitted pulse;
ρ_1 = reflection coefficient at the concrete–void interface;
ρ_2 = reflection coefficient at the void–soil interface; and
τ = time delay the radar pulse experiences in traveling across the void and back.

This expression was programmed on a digital computer and the composite reflected waveform calculated and plotted. The radar return pulses are shown in Figure B-6. In this figure, void depth was varied and soil dielectric constant was selected to approximately match the measured data. The concrete relative dielectric constant for dry concrete was determined by radar measurements to be about 6.0 and the road base approximately 12.

On examining the plots shown in Figure B-6, one notes that both the negative and positive peaks of the reflected EM wave increase in magnitude as the void depth increases. However, when the void depth is larger than about 2 in., the peak amplitude of the returning EM wave starts to diminish. For void depths of 3 in. and larger, the pulse amplitude appears to be independent of void size. This behavior of the returning EM waves can be explained by realizing that void depths of 3 in. or greater produce returning pulses that tend to be nonoverlapping and, thus, signal interference does not occur. The amplitude of the positive peak is plotted in Figure B-7 as a function of void size in inches. Note that the amplitude of the positive peak varies in almost linear fashion for void depths less than 2 in. For void depths between 2 and 3 in., the amplitude of the peak starts to decrease, and for void depths 3 in. or larger the amplitude is somewhat independent of void size. The amplitude of the negative peak as a function of void size is plotted in Figure B-8. Note that the behavior of the negative peak is very similar to that of the positive peak just described.

Another measure of void size is the time separation between the EM reflection from the top of the air void and the EM reflection from the bottom of the air void. A plot of the separation between the largest positive going peak and the largest negative going peak as a function of void size is shown in Figure B-9. In this figure, note that the time separation between these two pulses varies linearly with void size only for void depths of 3 in. or larger. For void depths less than 3 in., there is virtually no change in the time difference as a function of void size. Thus one concludes from Figures B-7 through B-9 that the pulse amplitude can be used to

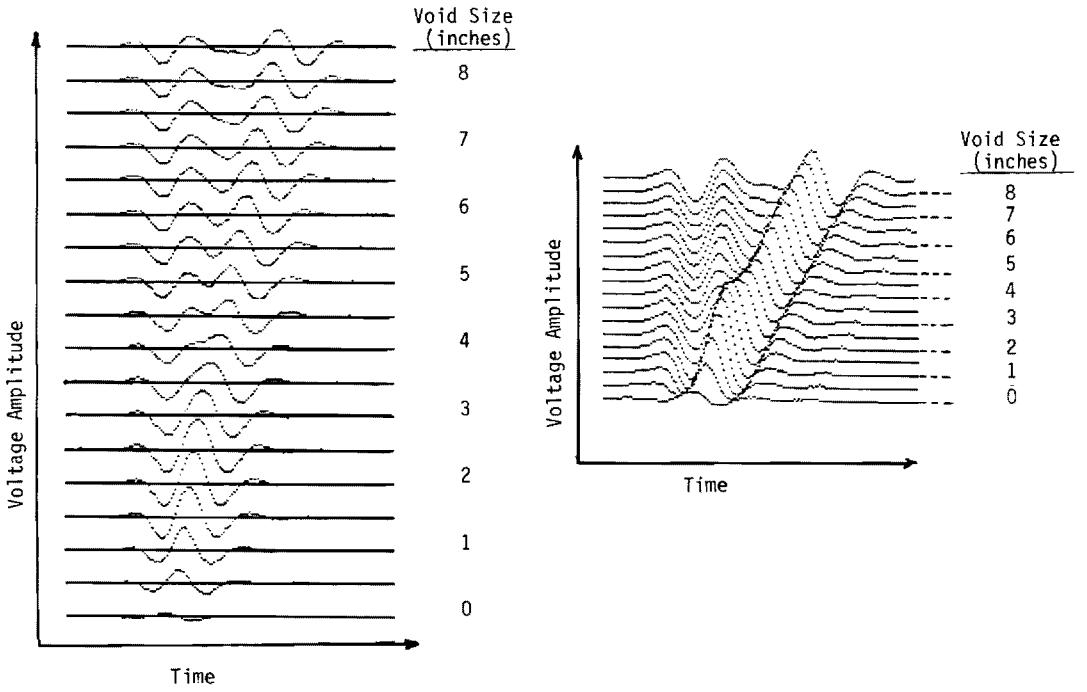

Figure B-6. Theoretical radar time responses (identical time responses shown in two plot formats).

estimate void size for voids of 2 in. or less and that the time separation between returning pulses can be used to estimate void sizes of 3 in. or more. However, it appears that void depths between 2 and 3 in. present a problem. There is a slight slope to the curve in Figure B-9 for void depths less than 3 in. It may be that one can use the combination of the curve in Figure B-9 with the curves in Figures B-7 and B-8 to estimate void sizes between 2 and 3 in.

The initial value of the amplitude plots shown in Figures B-7 and B-8 changes with the type of road base. This variation or change is shown in Figure B-10 for three different types of road bases (dense-graded aggregate, portland cement stabilized clay, and asphaltic concrete). Note that only the portion of the curve for void depths of 2 in. or less changes with road base type. The net effect is that the proportionality constant between the pulse amplitude and the void size changes with road base type. If the road base type is known a priori, one can select the proper proportionality constant and estimate void size based on the amplitude of the returning EM pulse. Road base type does not have any effect on the estimation of void sizes of larger than 3 in. because the time separation between the returning pulses is not a function of this variable, but is dependent only on the air–void size.

EFFECTS OF SPURIOUS REFLECTIONS

In any radar system, there are spurious reflections that can mask the signals of interest. In the short-pulse radar system used in this project, the interference resulting from spurious reflections limits the performance of the system. To recognize radar returns from air voids underneath concrete slabs, the returns must be large enough to exceed the interference level caused by reflections. To understand this limitation, it is important to know why these spurious reflections are generated and what steps one may take to reduce them. In Figure B-11, the short-pulse radar is shown in its environment. As indicated, the transmitter/receiver is attached to an antenna that is suspended in the air above a highway concrete slab. The transmitter/receiver is connected to a cable via a connector, and the cable is attached to the antenna via a connector. Connector joints in this cable create spurious reflections. Also, the interface between the antenna and the air represents a discontinuity and radar reflections are generated. In addition to the concrete slab and road base, other discontinuities generating reflections are obstacles that are laterally displaced from the radar; for example, the mobile cart on which the radar is mounted. Other obstacles that may generate spurious reflections are personnel in the vicinity of the radar or perhaps nearby vehicles and other such obstacles.

The time that it takes an electromagnetic pulse to traverse an electrical circuit, such as a cable or antenna, is equal to the physical length of the circuit divided by the velocity of the electromagnetic wave within the circuit. For microwave cables with air dielectric, the velocity of EM waves is approximately the speed of light. Thus the time it takes waves to travel from one end of the cable to the other is its physical length divided by the speed of light. The velocity of EM waves through an antenna structure, such as the one used with the short-pulse radar, is much slower than the speed of light. The exact delay time through the antenna is not known, but is considerably more than that associated with its length. Of course, the transit time of EM waves through air is equal to the distance they travel divided by the speed of light. The transit time through concrete depends on the amount of moisture in the concrete. The dielectric constant of dry concrete at these frequencies is approximately six. Thus, the time it takes electromagnetic waves to traverse one direction

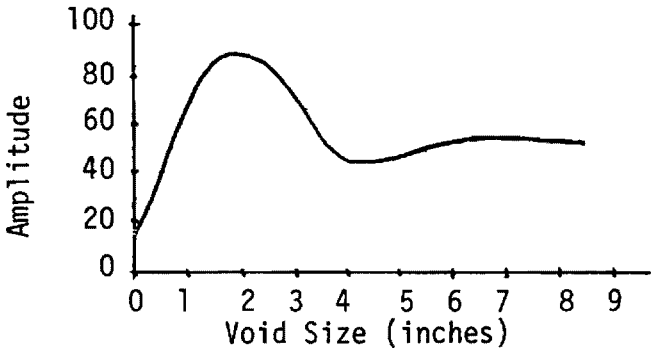

Figure B-7. Amplitude of positive peak versus void depth.

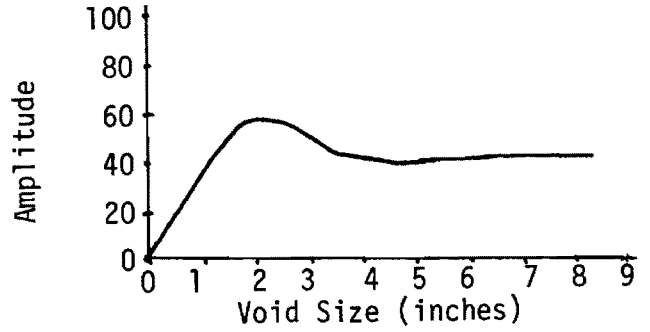

Figure B-8. Amplitude of negative peak versus void depth.

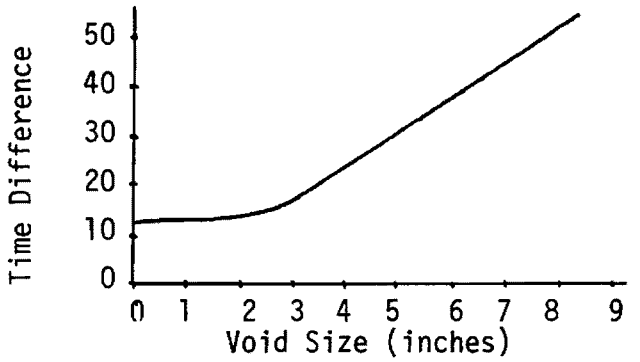

Figure B-9. Time difference versus void depth.

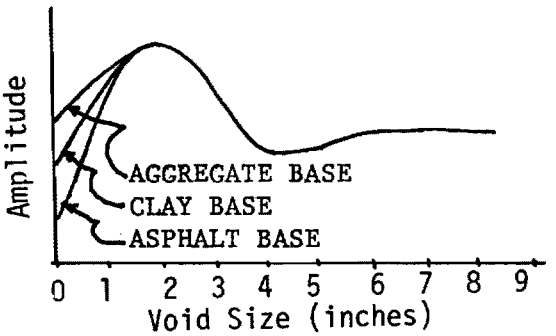

Figure B-10. Amplitude of peak for various types of road bases.

in the concrete slab is the thickness of the slab divided by the velocity of the waves through the slab. The velocity of EM waves through concrete is approximately the speed of light divided by the square root of the relative dielectric constant.

The reflections in the antenna cable place an attenuated replica of the slab return at about the same time as the void return, thus interfering with the void return. Other paths that provide interfering signals in the time period of interest are suggested in Figure B-12. In Figure B-12, the presence of interference caused by spurious reflections is shown by the solid curve and the signal that one may expect from a void is indicated by the dashed line. It is fairly obvious that if the void return is attenuated and is small, one may have difficulty in distinguishing it from the interference signals. Thus, it is necessary that the void amplitude be several times larger than the largest interference signal amplitude in order to differentiate between the two. The ratio of these two signals is called the signal-to-interference ratio (SIR). The SIR should be at least 4 or greater in order to properly detect the presence of an air void. In the next section of this appendix the sources of signal attenuation will be addressed. As indicated in that section, the major source of attenuation only attenuates the void signal and does not have much of an effect on the interference level. Thus the void signal may be reduced in size comparable to that of the interference level.

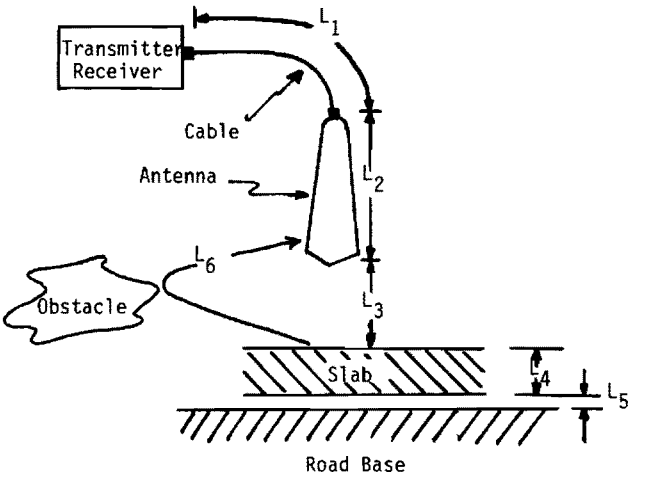

Figure B-11. Radar environment—electrical lengths of various EM wave paths.

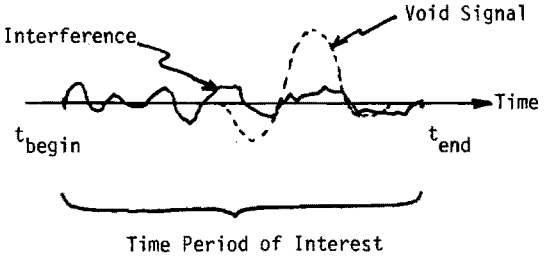

Figure B-12. Void signal in the presence of interference caused by spurious reflections.

EFFECTS OF ATTENUATION

The effects of attenuation on the void return signal is threefold. As mentioned previously, the attenuation reduces the returning signal relative to the interference level and thus the SIR may be insufficient for proper void detection. Another effect of attenuation is to lengthen the pulse so as to distort the return signal. A third effect is to reduce the peak-to-peak amplitude of the returning signal and thus make it difficult to estimate the size of the void based on amplitude. Because of these reasons, it is important to understand the effects of attenuation and how it comes about and under what conditions it exists. In this section attenuation factors for various types of materials as a function of moisture will be reviewed and presented.

The major source of attenuation in this application is the concrete slab positioned on the road base. Radar return signals from beneath the road base are not of interest. Thus, in this discussion, attenuation characteristics of the concrete block is of paramount importance. Unfortunately, very little information on the attenuation characteristics of concrete at the frequency of the short-pulse radar seems to be available. However, some inferences can be made based on existing data.

Attenuation characteristics of materials are very much dependent on the frequency of the electromagnetic energy impinging on it. Therefore, a discussion of the radar frequency of operation is necessary. The temporal signal generated by the radar transmitter is approximately that shown in Figure B-13 (a). The frequency spectrum of this transmitted signal is calculated to be that shown in Figure B-13 (b). The antenna frequency characteristics will modify this spectrum somewhat. However, because the antenna is very wideband, it does not significantly alter the spectrum shown. Most of the energy in the transmitted signal is located between the "one-half power" frequencies. These frequencies are defined where the voltage spectrum is down 0.707 from the peak value. For the spectrum shown, these frequencies are approximately 0.4 and 1.2 GHz with a mean of about 0.8 GHz. Thus, the attenuation characteristics of concrete over this frequency band are of major interest.

The attenuation of EM waves in a dielectric material is given by

$$\text{Attn} = e^{-\alpha x} \tag{B-8}$$

where

α = $(2\pi f/c)\sqrt{\epsilon_r}\tan\eta\,\delta$;
f = frequency;
c = velocity of light;
ϵ_r = the relative dielectric constant;
$\tan\delta$ = the loss tangent; and
x = the distance EM waves travel through the dielectric material.

The attenuation in decibels (dB) per inch of two-way travel is given by

$$\text{Attn (dB/in.)} = 2.31 \times 10^{-9} f \epsilon_r \tan\delta \tag{B-9}$$

with the terms as previously defined. Thus, there are two

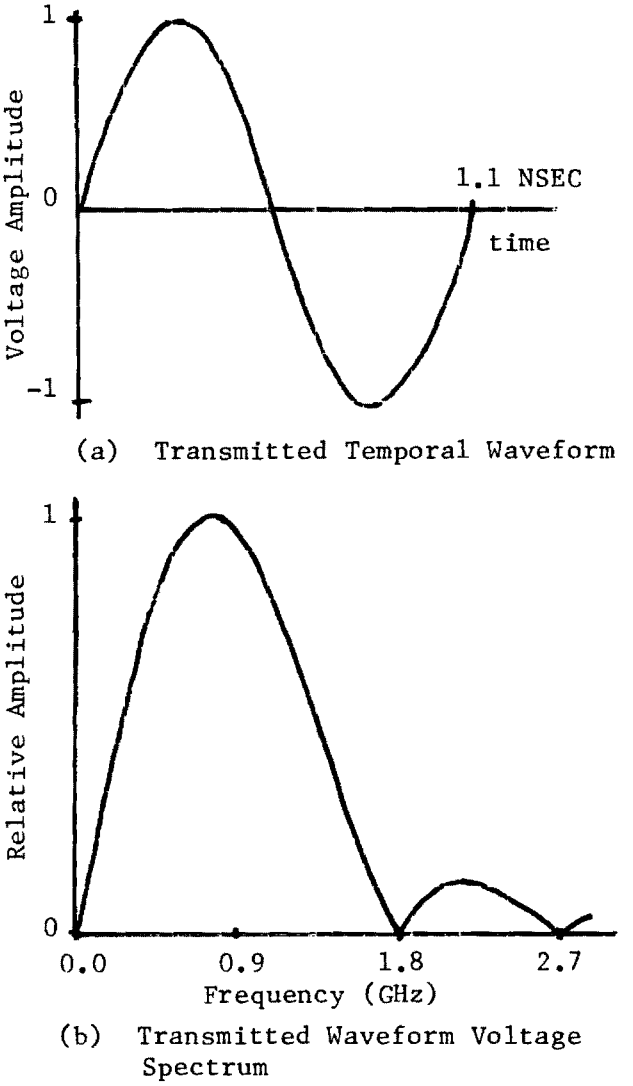

Figure B-13. Temporal and spectral responses of transmitted waveform.

dielectric properties that contribute to a material's attenuation characteristics: the relative dielectric constant and the loss tangent. Tables of these two characteristics for a large variety of materials exist (*B-2, B-3, B-4*). However, usually they are given for widely separated discrete frequencies (e.g., 0.3 and 3.0 GHz). The value of these parameters between these frequencies appears not to be available for many materials. Dielectric properties for a few materials have been measured in the frequency range of interest over a continuous range of frequencies. For example, the relative dielectric constant and loss tangent of Goodrich clay has been measured and is given in Figures B-14 and B-15 for two different temperatures. Similar information for concrete over a range of temperatures and moisture conditions is highly desirable, but apparently not available. One paper (*B-4*) discusses concrete but not in the frequency range of interest for this application. The dielectric constant and loss tangent for a frequency of 3.0 GHz (λ = 10cm) is indicated in Figures B-14 and B-15 by an asterisk. The corresponding two-way

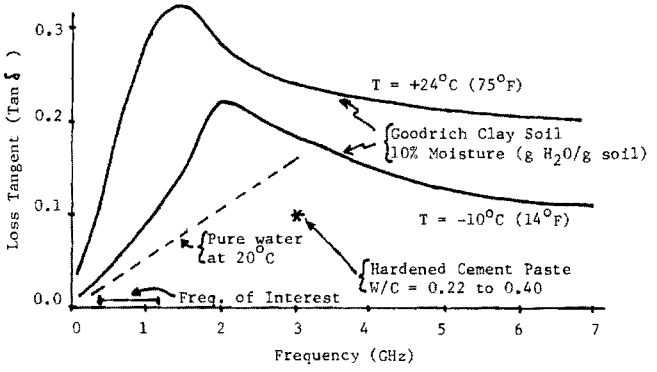

Figure B-14. Loss tangent of Goodrich clay, water, and hardened cement paste.

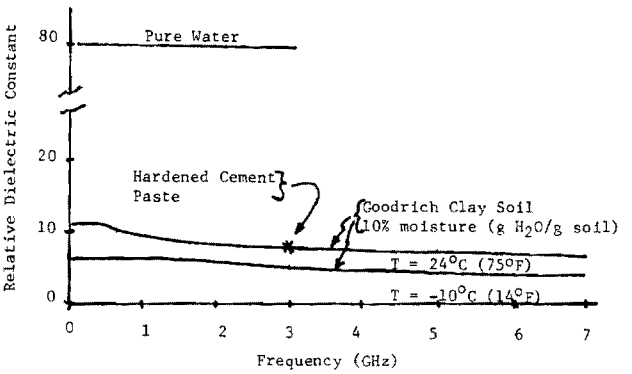

Figure B-15. Relative dielectric constant of Goodrich clay, water, and hardened cement paste.

attenuation has been calculated using the information in Figures B-14 and B-15 and is shown in Figure B-16. Note that the signal attenuation value shown for hardened cement is about half that of clay at 3.0 GHz. Whether this is true at all frequencies is not known.

Hoekstra and Delaney (*B-3*) indicate that many types of soils are characterized by a "dielectric relaxation" at certain frequencies. The dielectric constant decreases with increasing frequency and the dielectric loss factor (loss tangent) goes through a maximum at a certain frequency. They indicate that the relaxation observed can be attributed to the presence of bound water in soils. In comparing the relaxation of water in bulk and soil water, it is observed that the frequency of maximum dielectric loss in soils is displaced to a much lower frequency than in bulk water; typically between 0.3 to 1 GHz for soil water compared to 22 GHz for bulk water. Also, the frequency of maximum loss is dependent on temperature. These effects are clearly illustrated by the curves shown in Figures B-14 and B-15 for the Goodrich clay. In general, lower temperature yields a lower attenuation and a higher frequency of maximum loss. Apparently, the so-called "bound water" consists of a thin layer of water molecules intimately bonded to polar sites in the host medium. This bonding reduces the rotational polarizability of the water molecules and thus lowers their relaxation frequency (*B-5*).

It is suspected by the authors of this report that the same effects of moisture on concrete can be observed. In summary, there is more information on moist soils than on moist concrete at the frequencies of interest. For the purpose of this discussion on theory, it will henceforth be assumed that moist concrete behaves in the same manner as moist Goodrich clay. It is also postulated that concrete at lower temperatures (e.g. freezing) will exhibit considerably lower attenuation in the same manner as moist Goodrich clay. This observation becomes significant when trying to interpret some of the measured data collected on this project.

The effect of the attenuation on the radar return from an air void under a concrete slab is threefold as indicated earlier. First, the signal-to-interference ratio (SIR) is reduced. For example, the signal attenuation through a 10-in. slab of concrete with the loss characteristic postulated in Figure B-16 is about 8 dB at 24C (one-half the value for clay at 0.8 GHz). If the moisture content or the temperature is reduced, this loss decreases dramatically. For example, if the temperature is below freezing, the attenuation through 10 in. of material is about 2 dB. If the concrete is relatively dry, the attenuation has been observed by the authors at much smaller values. As indicated earlier, most of the interference signals do not travel through the concrete slab and, therefore, do not experience this attenuation. Thus, the attenuation being discussed directly reduces the SIR, and thereby reduces the ability to distinguish void signals from interference signals.

Another effect of attenuation is to corrupt the estimation of void size if the void is less than 3 in. where peak signal values are used in the estimation. For larger void sizes, the attenuation does not directly affect the estimation.

A third effect of attenuation on the radar return from an air void is to distort the shape of the returning signal, making it more difficult to recognize. In Figure B-16, note that high frequencies in the band of interest are attenuated more than the low frequencies are attenuated. Thus, the spectrum of the radar return is distorted causing the radar signal itself to be changed. The general effect is to make the spectrum narrower in bandwidth and, thus, make the radar returning signal of longer time duration. However, this effect is not as serious as the attenuation of signal amplitude. The signal is likely to be attenuated below the interference level before any major distortion of signal shape can be observed.

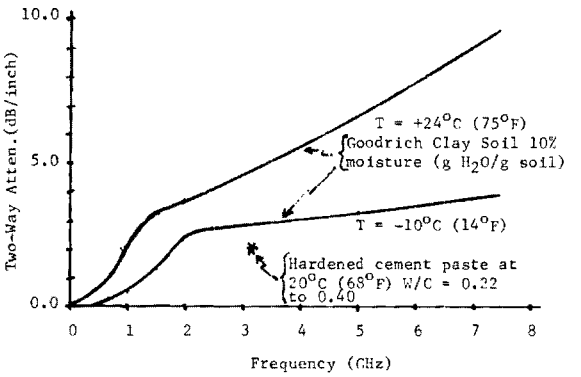

Figure B-16. Two-way attenuation vs. frequency for Goodrich clay soil with 10% moisture at two temperatures. Attenuation for hardened cement paste at 3 GHz is indicated by an asterisk.

REFERENCES

B-1. RAMO, S., and WHINNEY, J. R., *Fields and Waves in Modern Radio*. John Wiley and Sons, Inc., N.Y. (1960) pp. 270-292.

B-2. VON HIPPEL, A. R., Editor, *Dielectric Materials and Applications*, The M.I.T. Press, Cambridge, Mass. (1954).

B-3. HOEKSTRA, P., and DELANEY, A., "Dielectric Properties of Soils at UHF and Microwave Frequencies." *J. Geophys. Res.*, Vol. 79, No. 11 (Apr. 10, 1974) pp. 1699-1708.

B-4. HASTED, J. B., and SHAH, M. A., "Microwave Absorption by Water in Building Materials." *Brit. J. Appl. Phys.*, Vol. 15 (1964) pp. 825-836.

B-5. HERRICK, D. L., *An Intrusive Slotted Cylinder Antenna Array for Subsurface Moisture Profiling*. Ph.D. Dissertation, Montana State University, 1979. Univ. Microfilms International, Ann Arbor, Mich.

APPENDIX C

SIGNAL PROCESSING

ANALOG/DIGITAL HARDWARE PROCESSING

The analog signal processing involves the detection of the large signal return from the top of the surface of the pavement. This is accomplished by an electronic hardware section called the "range tracker." Once the time of the surface return is established, all other video timing is referenced to that point for the hardware functions. This has been done so that small random movements of antenna height above the ground do not affect the signal return timing for void detection. With the top of the pavement surface established as a fixed-time reference, voids will appear within a fixed-time interval after the reference time.

From this reference point a timing "window" is initiated. The signal is allowed to pass through for subsequent processing for approximately 20 nsec (20×10^{-9} sec), relating to an equivalent distance in air of approximately 10 ft. This time (20 nsec) in a medium such as concrete, $\epsilon = 6$, is modified by the dielectric constant so that approximately 4 ft are available for processing. It is noted that this is only a result of timing conditions in the analog processor. The radar signal return before application of the window represents a distance of approximately 100 ft in air, or 30 ft in average soil. With the analog signal windowing applied, the available depth is limited.

A portion of the analog signal in this timing window is then digitized by an analog-to-digital converter and stored in a digital buffer memory. The buffer memory is accessed by the microcomputer under program control, and, thus, the signal return is now represented by a set of numbers that can be further processed by the software program in the microcomputer. The actual time at which a set of samples is digitized and put into the microcomputer memory is under direct operator control. A command is issued to the microcomputer by the operator and the sampling process is initiated. Thus, the operator can position the radar equipment over the specific area to be tested and designate when a measurement is to be made. The amount of signal currently digitized and stored is approximately equivalent to a 2-ft depth.

DIGITAL SOFTWARE SIGNAL PROCESSING

Any manipulation of the radar signal return can be construed as "signal processing." Therefore, everything that occurs within the microcomputer related to the signal falls in this category and needs explanation. For this reason this section has been divided into two parts: the first detailing the signal processing related to the theory of finding and sizing voids; and the second describing secondary manipulations of the signal return. These secondary manipulations do not extract information but include such processing functions as display and storage of the signal.

Signal Processing Related to Theory of Finding and Sizing Voids

Listing of Processing

1. Calibrate signal return using reference waveform.
2. Identify local minimums and maximums in the signal return.
3. Locate the smallest minimum and largest maximum and test for "threshold" crossing.
4. Test for time difference between the selected smallest/largest peaks; estimate void size if time discriminant is applicable.
5. Test for amplitude values; estimate void size using amplitude.

Description

1. The signal return from the concrete–base media has a significant amount of interference or clutter amplitude perturbations. In an attempt to "normalize" or remove the interference a "reference" signal return is recorded from an area where no void is likely to exist. This reference is subtracted directly from all subsequent measurements. Only perturbations from the reference signal are thus processed for void location and sizing. The clutter perturbations remain essentially fixed over the extent of the concrete pavement. Changes occur in going from a nonreinforced section to a

reinforced section if thickness changes drastically or temperature–moisture content varies significantly. In these cases, a new reference signal must be recorded.

2. The identification of the minimum and maximum peaks of the signal return is the first step in void detection. As indicated in the theoretical modeling there is a reflection from the bottom of the pavement–void interface and another reflection from the void–base interface. The size of the void determines the timing of the two signal reflections. Even under no void conditions there will exist a signal reflection if the base material is not identical to the pavement material, but this should be minimal because of the subtraction of the reference. A sequential search is made through the signal and all local minimum and maximum values are stored along with their time of occurrence.

3. From the theoretical modeling it is known that if a void is present, a large negative amplitude peak occurs first followed by a large positive amplitude peak. As a result, the algorithm initially searches through the list of minimum values and picks the largest negative amplitude as the candidate. Then the algorithm searches for the largest positive peak occurring after the negative amplitude occurrence. The resulting output is now the amplitude and time of occurrence for the largest negative peak and the largest positive peak following the negative peak occurrence. The amplitudes are then compared to a minimum acceptable amplitude called the "threshold." If the values fall below this threshold there is a high probability that the minimum and maximum pair chosen does not represent the location of a void. This threshold value has been computed based on laboratory measurements to give reliable void detection and identification of size.

4. As described in the theoretical modeling, the time differential between the identified peaks is a measure of void size, especially for voids larger than 3 in. Thus the algorithm checks this time differential. If the value exceeds the nominal value for a 3-in. void, the void is sized by that time differential. If the time is less than the nominal value for a 3- in. void, the determination of void size is passed on to the amplitude discrimination. For actual signal returns from voids there is a minimum value for the time differential, and the algorithm checks to see that the minimum is exceeded. This prevents random noise spikes from being detected as voids.

The time between data samples being processed is 0.026 nsec. In terms of the time difference in these units, the void size is estimated by

$$\text{Void size (inches)} = (0.026)\cdot(5.9014402)\cdot\text{Time difference}$$

with the constraint that the time difference is greater than 19 time units or data samples. This establishes the switch point at 3 in.

5. On the basis of the theoretical modeling and with calibration biases developed during laboratory measurements, the amplitude discrimination algorithm looks at the negative peak values to size a void less than 3 in. Experience with laboratory measurements has shown that the negative peak value yields the best results.

In terms of the amplitude units in the microcomputer for the data samples, the void size is estimated by

$$\text{Void size (inches)} = \frac{6}{\pi}\sin^{-1}\left[\frac{\text{Peak negative amplitude}}{\text{Calibration number}}\right]$$

with the constraint that the time difference is less than or equal to 19 time units.

Secondary Manipulations of Signal Return

Listing of Processing

1. Transfer data from buffer memory to microcomputer memory.
2. Transfer data from microcomputer memory to magnetic disk memory.
3. Display data and plot on the video unit.
4. Print data out on the line printer.

Description

1. The signal return that has been digitized by the analog-to-digital converters is stored in a temporary buffer memory. The digitizer samples the signal return every 0.013 nsec. In concrete, this is approximately equivalent to 0.03 in. This memory is not easily used for normal microcomputer operations, and a special retrieval algorithm was written so that the signal data are accessible. The algorithm transfers up to 512 8-bit binary words from the buffer memory to the computer memory.

2. At the option of the operator, signal returns can be automatically transferred from microcomputer memory and stored on permanent magnetic diskettes. The algorithm transfers up to 512 8-bit binary words from microcomputer memory to disk.

For the detection and sizing of voids it was determined that only a sampling of every other point was needed to accurately represent the signal return. In addition, the total length of 512 points was deemed unnecessary because the area or time for a signal return from a void should appear much sooner than the 400th point. Thus, every other point, for the first 440 points, was chosen for transfer, making the total of 220 points available. This represents approximately 1.15 ft of depth in concrete. When 9 in. of concrete is assumed, the signal return is composed of a portion through the concrete and the remainder through the void (air). The resulting signal return processed (220 points) thus represents 9 in. of concrete and approximately 12 in. of void possible below the concrete—a total depth of just under 2 ft. It is important to realize that this is simply a function of user chosen parameters. If thicker concrete pavement is involved or more depth is desired, only timing parameter changes are necessary. No limitations are placed on the signal processing or void sizing algorithms because of the chosen timing parameters.

3. Several display options are available to the operator at any time during the data processing sequence. The first is the actual digitized signal return. The second is the numerical information about the minimum and maximum amplitudes and time difference values of the signal. The third is the "synthetic" void location and sizing display, which is the primary information display for the operator. This display illustrates both numerically and graphically the void location and size results for each measurement. The display is labeled

"synthetic" because of the representative graphical indications of concrete pavement thickness and void size. Figure C-1 shows the display with annotations for explanation. The results obtained from the signal processing through the amplitude–time discriminant algorithms are directly shown on the display.

4. At any point in the measurement process, a permanent hard-copy of the results can be obtained. All the necessary data have been stored on magnetic disk and can also be printed at any time in the future. The software programs involved can plot 220 points for a single return, and the multiple option can plot up to 17 returns on the same video display and obtain a hard-copy.

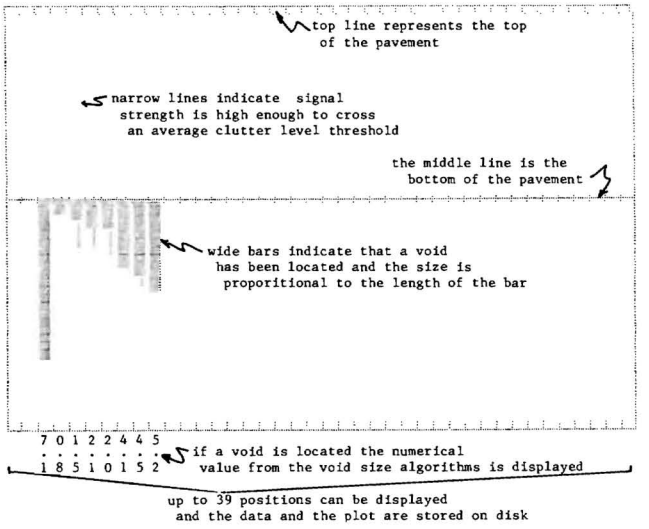

Figure C-1. Synthetic display for measurements.

APPENDIX D

LABORATORY MEASUREMENTS

The experimental evaluation of the void detection pulsed electromagnetic wave equipment and signal processing algorithms was accomplished in two phases—the objective of the experimental evaluation being to quantify the accuracy, precision, reliability, limitations, operational characteristics and environmental characteristics of the equipment and processing algorithms. The first phase was conducted inside a laboratory under controlled environmental conditions. (The second phase was conducted on a specially constructed outdoor test lane, and is discussed in Appendix E.)

Test sections of portland cement concrete (PCC) pavement approximately 43 in. by 43 in. by 9 in. thick, both reinforced and nonreinforced, were used. These test sections were placed over base materials of PCC, asphaltic concrete, dense-graded aggregate, and portland cement stabilized clay; and measurements were made. Moisture levels were varied both for the concrete top section as well as the base material. Voids were simulated by elevating the top concrete section a measured amount above the base material.

Actual measurements were made for void depths 0 in. to 8.5 in. in 0.5-in. increments. Some measurements were made simulating voids filled with water. The findings indicate a definite agreement with the theory as to the variation in amplitude of the positive and negative peaks and in the time differential of the peaks. Thus, the discriminants from the theoretical considerations were verified. In addition, the measurements provided the basis for calibration of the theoretical modeling. The calibration involves a bias for differing base materials.

In the following discussion the details of the laboratory measurements and results are given. The design and construction of the test sections of concrete pavement, base sections, the methods used to obtain voids between the pavement and base sections, and methods for calibration are detailed. Extensive plots are included covering all measurements made, including nonreinforced and reinforced concrete sections. The analysis of the measurements and the resulting tables for void sizing are included.

PAVEMENT AND BASE DESCRIPTION

Four base forms were constructed from wood, all with dimensions of 43 in. by 43 in. by 12 in. The base forms were filled with portland cement concrete (12 in. deep), asphaltic concrete (8 in. deep), dense-graded aggregate (10 in. deep), and portland cement stabilized clay (12 in. deep). Three pavement forms were constructed from wood, all with inside dimensions of 43 in. by 43 in. by 9 in. These forms were all filled with portland cement concrete, one having reinforcing steel. So that the pavement sections could be moved easily, eye bolts were included in the corners. A hoist was also constructed to accommodate the movement of the concrete pavement sections. All materials and construction methods followed as close as possible State of Georgia Construction specifications.

VOID SIMULATION

Measurements were made by placing one of the PCC pave-

ment sections on top of a selected base section. Voids were created by elevating the top section using exact-sized wood blocks. The wooden blocks themselves do not interfere with the radar signal return from the voids. Complete sets of wooden blocks were made such that voids from 0 in. to 8.5 in. in 0.5-in. increments could be created.

CALIBRATION

The pulsed electromagnetic wave equipment must be adjusted at the beginning of each day to ensure that a consistent set of measurements can be obtained from day to day. In addition, fine tuning may be required if there are large temperature changes during the measurement time period. To make this calibration as easy as possible a calibration test fixture was constructed. Figure D-1 shows the configuration for this fixture. The fixture contains special light weight absorbing foam and a metal plate. The foam absorbs some of the electromagnetic energy, thus decreasing the return from the metal plate. This calibration fixture is very light weight and provides a consistent reference for the equipment. So that a very consistent set of measurements could be obtained in the laboratory controlled conditions, the calibration fixture was used as a check between each void size change. This procedure is not necessary under normal operating conditions; only an initial calibration is needed.

PLOTTED MEASUREMENTS

Figures D-2 to D-5 show the results of measurements for void depths 0 in. to 8.5 in. in 0.5-in. increments over all four types of base materials. The PCC pavement section used did not contain reinforcing steel. Figures D-6 to D-9 show the same measurements of voids using the steel reinforced pavement section.

Each figure has four associated plots. The first in each is a sequence of signal returns for void depths 0 in. to 8.5 in., in 0.5-in. increments, with each signal return sequentially offset for clarity. This type of plot facilitates comparisons between signals as the void size increases. By examining this figure the differences in the signals become evident, especially the time deviation of the most positive amplitude peak. The second plot is of the time difference actually measured by the microcomputer between the largest negative amplitude peak and the largest positive amplitude peak. By examining this figure it can be seen that this curve follows the theoretical modeling quite accurately. Similarly it can be seen that in the neighborhood of 3 in. a slope change occurs. It is in this area of a steeper slope that reliable void sizing can be accomplished. The remaining two plots illustrate the largest negative amplitude peak value and the largest positive amplitude peak value respectively. These plots also follow the theory very closely, the steepest slope occurring in the void size areas less than 3 in.

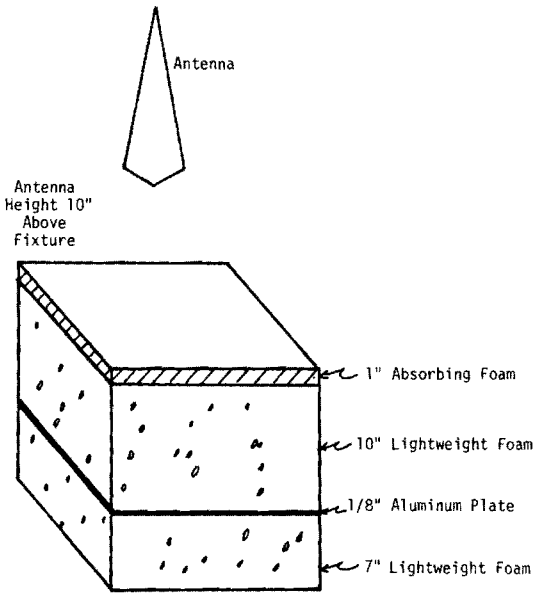

Figure D-1. Calibration fixture.

In all cases, the plots with and without reinforcing steel can be compared in the area of the void and be found to be almost identical. This clearly indicates that the reinforcing steel has only a minimal effect on the signal response from the void and is not a potential problem area. There is a difference in the signal returns in the area where the steel rod occurs. This result indicates that the electromagnetic wave equipment can definitely detect and locate reinforcing steel.

In all of the foregoing measurements the pavement sections and the base material were kept as dry as possible, being exposed only to inside laboratory temperatures and humidity levels. Voids themselves were kept empty. This set of measurements represents an excellent verification of the theoretical modeling. The data for the cases of PCC and asphaltic concrete, dense-graded aggregate, and stabilized clay base materials were put through the signal processing software for void location and sizing. The results for the PCC base are shown in Figure D-10 for the synthetic displays; they are also given in Table D-1 along with a mean and standard deviation computation for the error in estimation of void size. The results for the other base materials are not shown because they were almost identical to that of the PCC base.

Figures D-11 and D-12 are plots of signal returns from selected void sizes for wet PCC and stabilized clay base sections. Two moisture levels were used, the second being considered very wet, and by comparison no significant signal changes are observed. In addition, comparison with the dry measurements yielded no significant differences. For this set of measurements it is important to remember that only the base materials were wet. When the top pavement sections have a higher moisture level attenuation of the signal results. It is concluded that as long as the high moisture levels are confined to the base materials no degradation in performance for locating and sizing voids beneath pavement occurs.

Figure D-13 plots signal returns for the situation indicated in the diagram. For this case, the void was represented by a 12 in. by 12 in. by 2 in. thick piece of foam set in the aggregate base material under soaking wet conditions. The pavement section on top did not have reinforcing steel. The measurements plotted were made by sequentially moving the equipment across the block in 2-in. increments. This situation simulates the location of a typical void under highway pave-

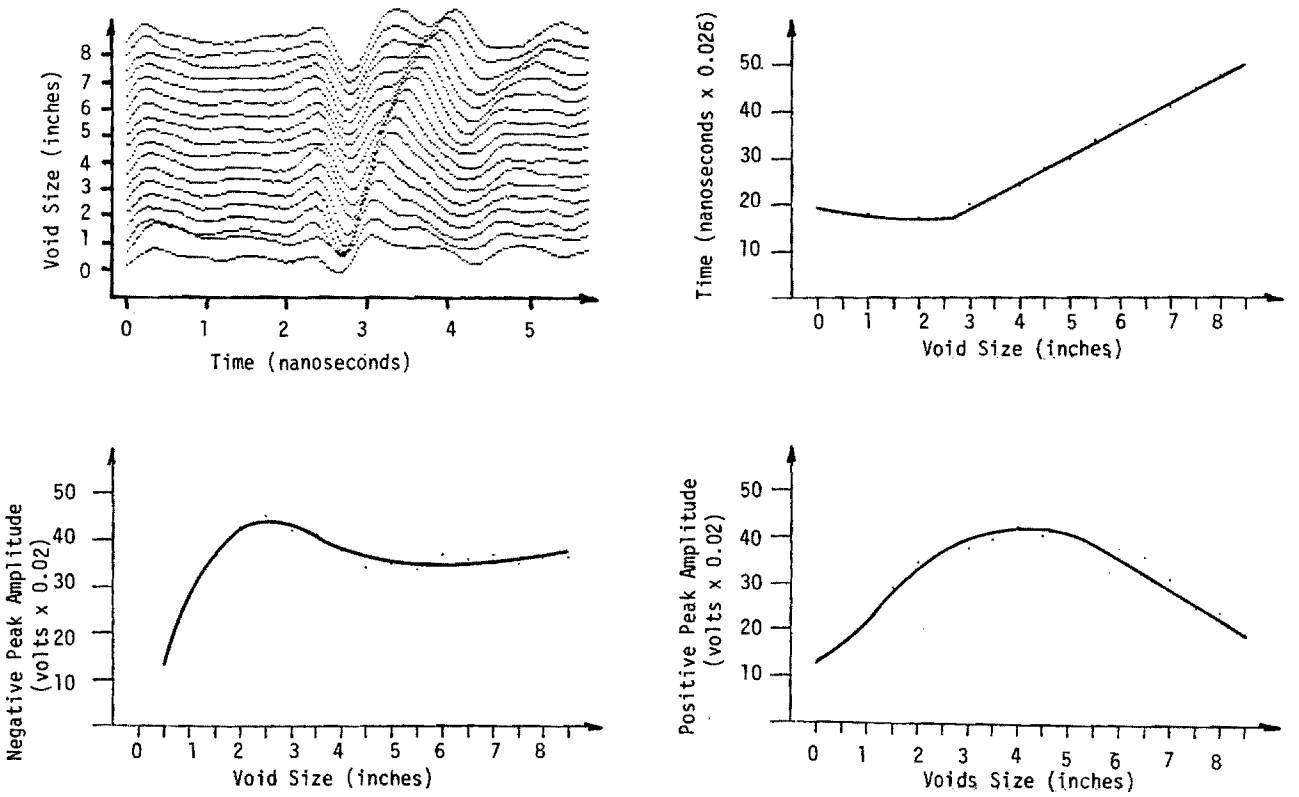

Figure D-2. Laboratory measurements, nonreinforced pavement, portland cement concrete base.

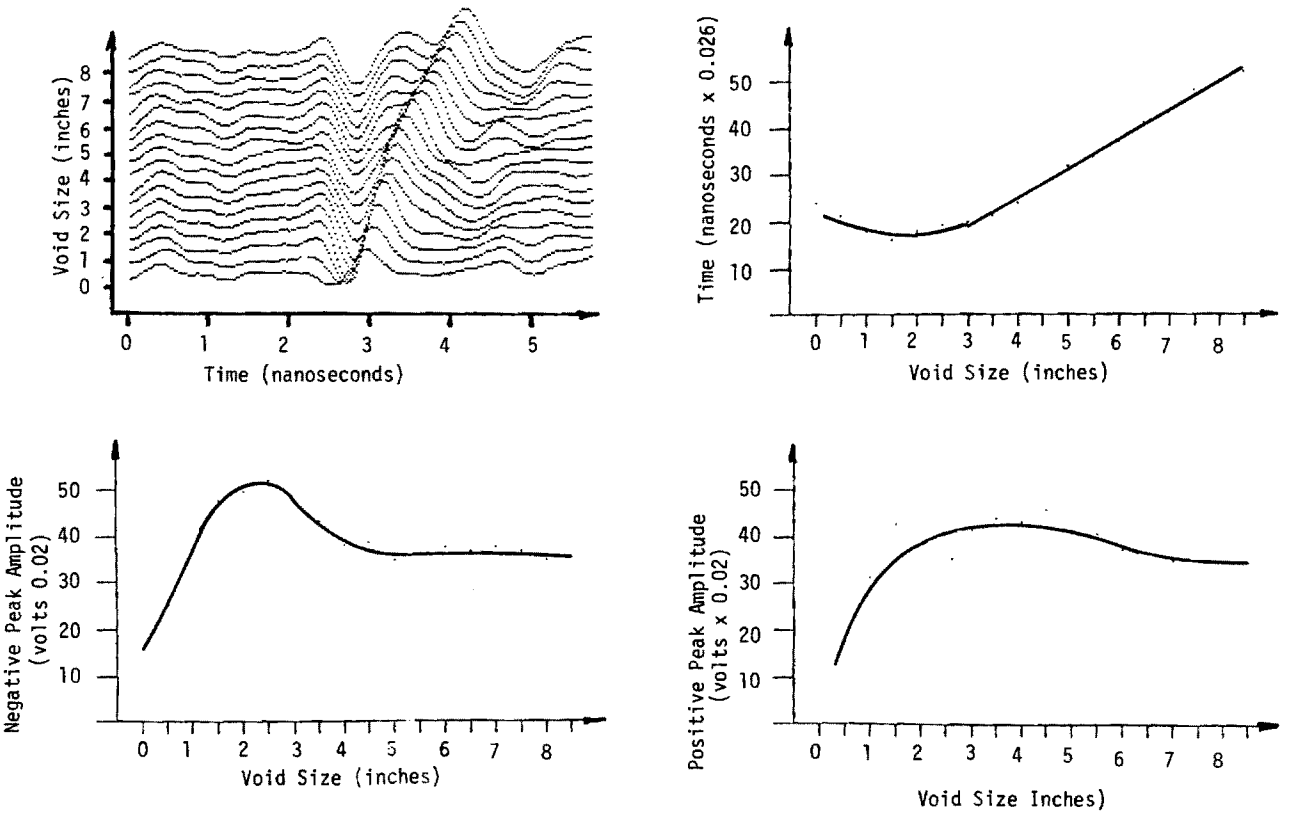

Figure D-3. Laboratory measurements, nonreinforced pavement, portland cement stabilized clay base.

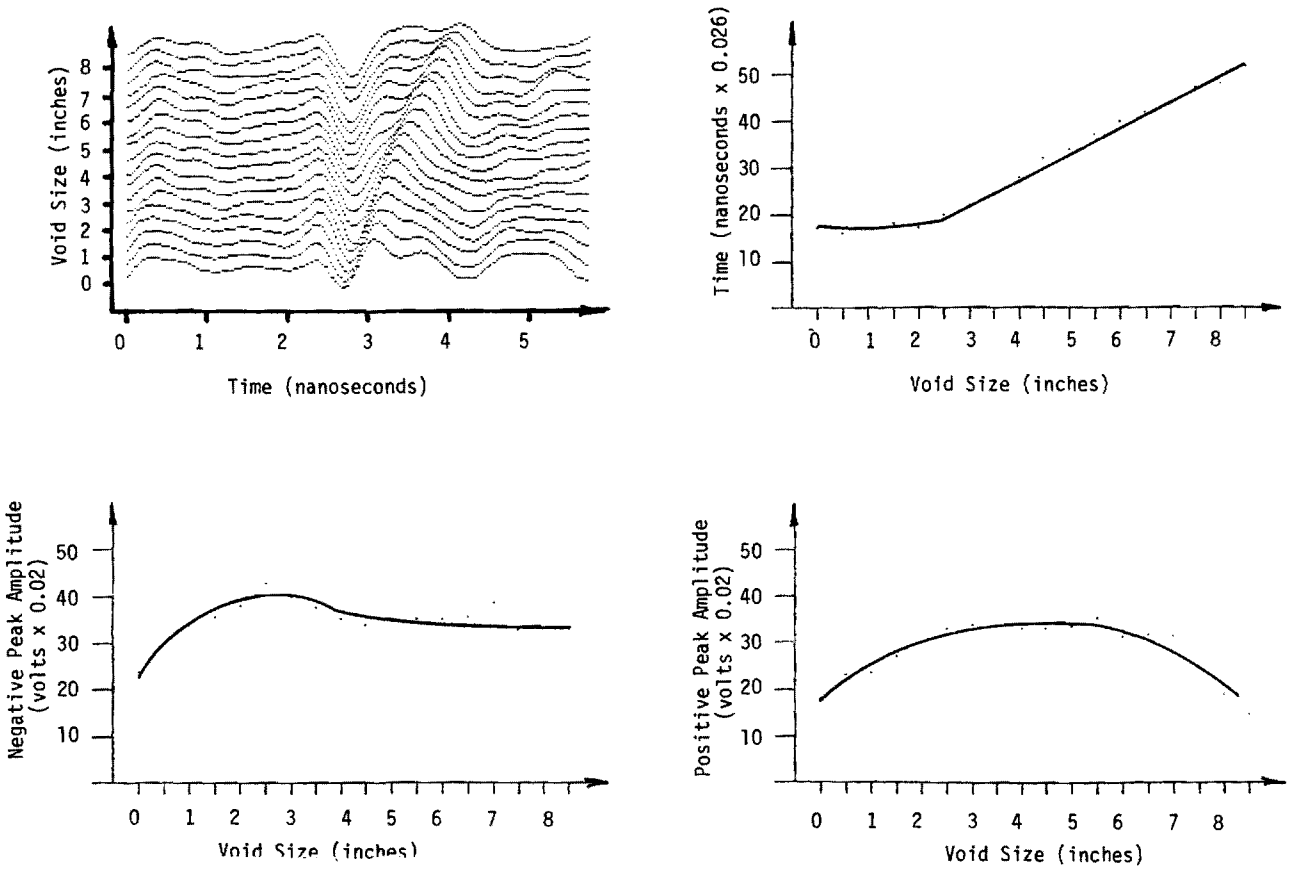

Figure D-4. Laboratory measurements, nonreinforced pavement, dense-graded aggregate base.

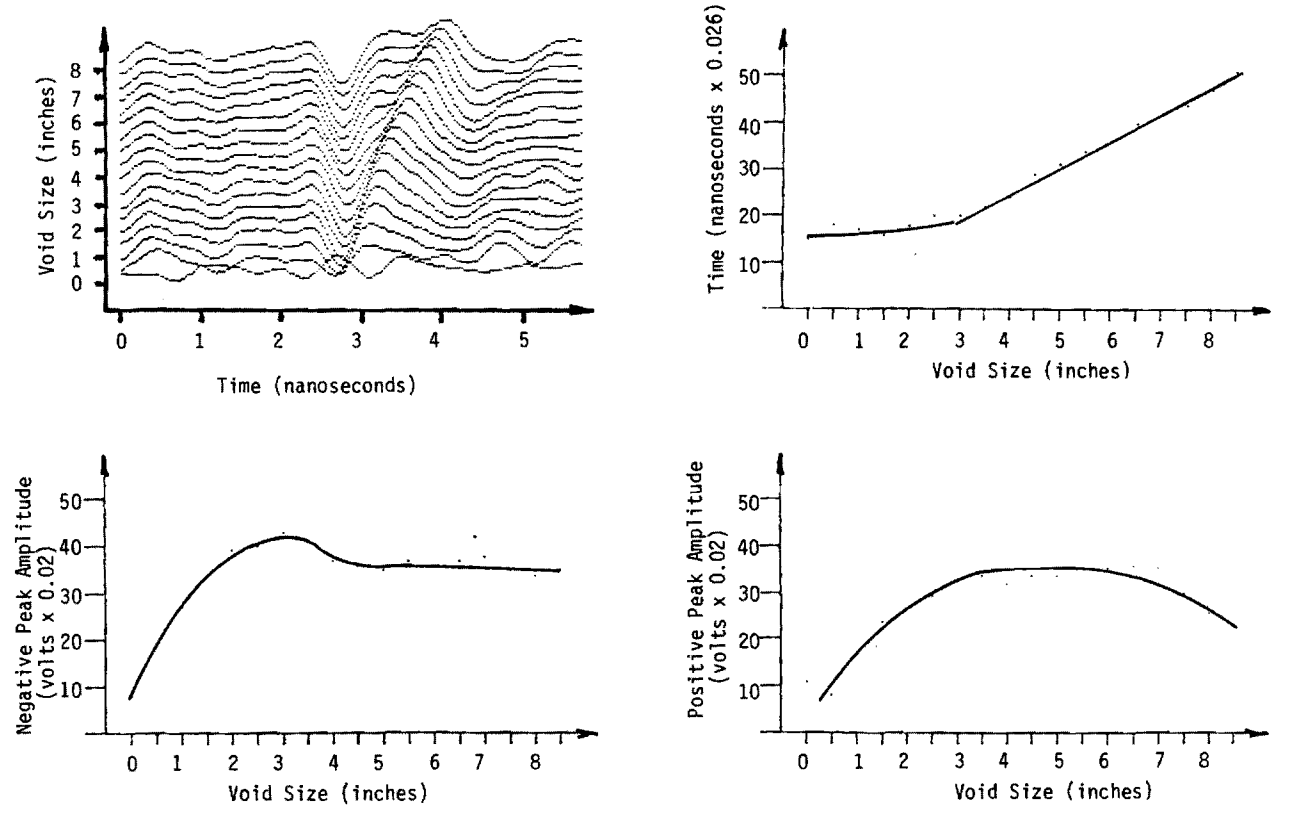

Figure D-5. Laboratory measurements, nonreinforced pavement, asphaltic concrete base.

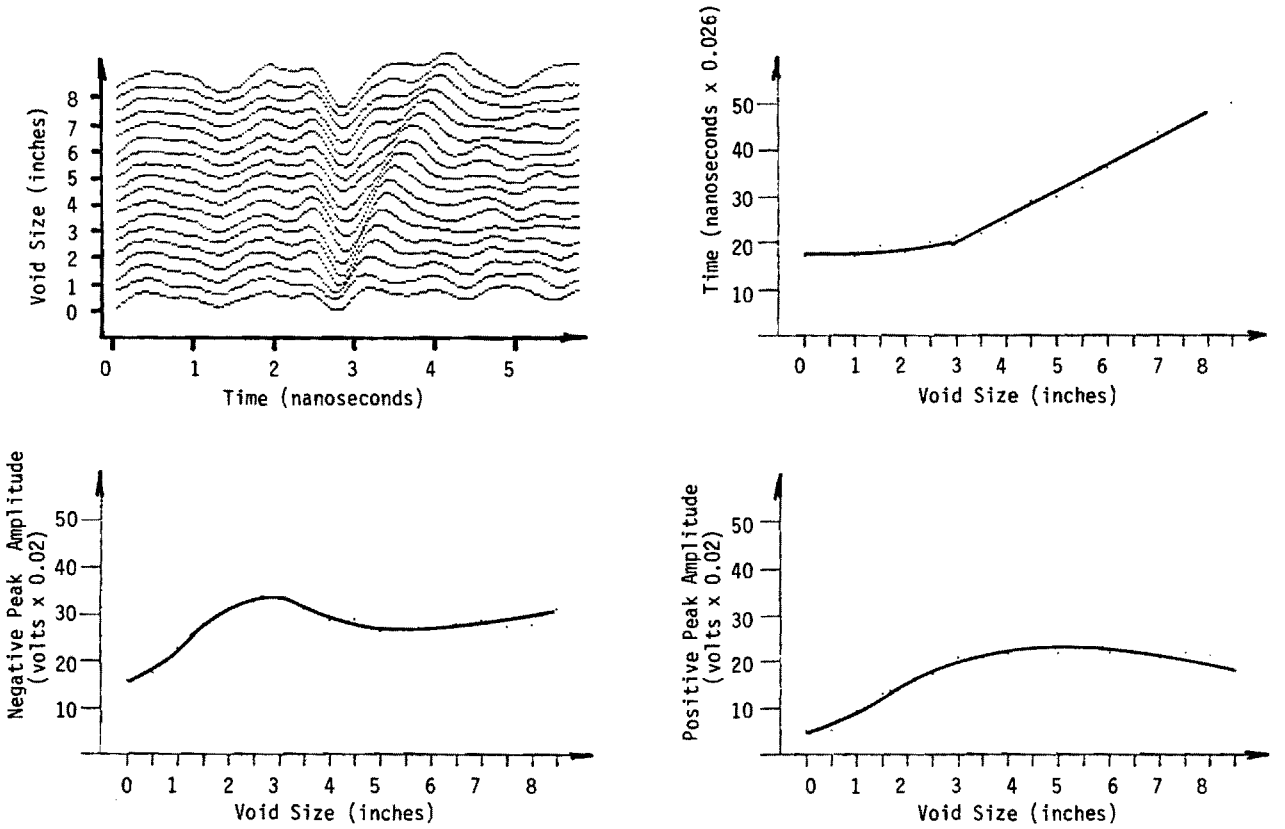

Figure D-6. Laboratory measurements, reinforced pavement, portland cement concrete base.

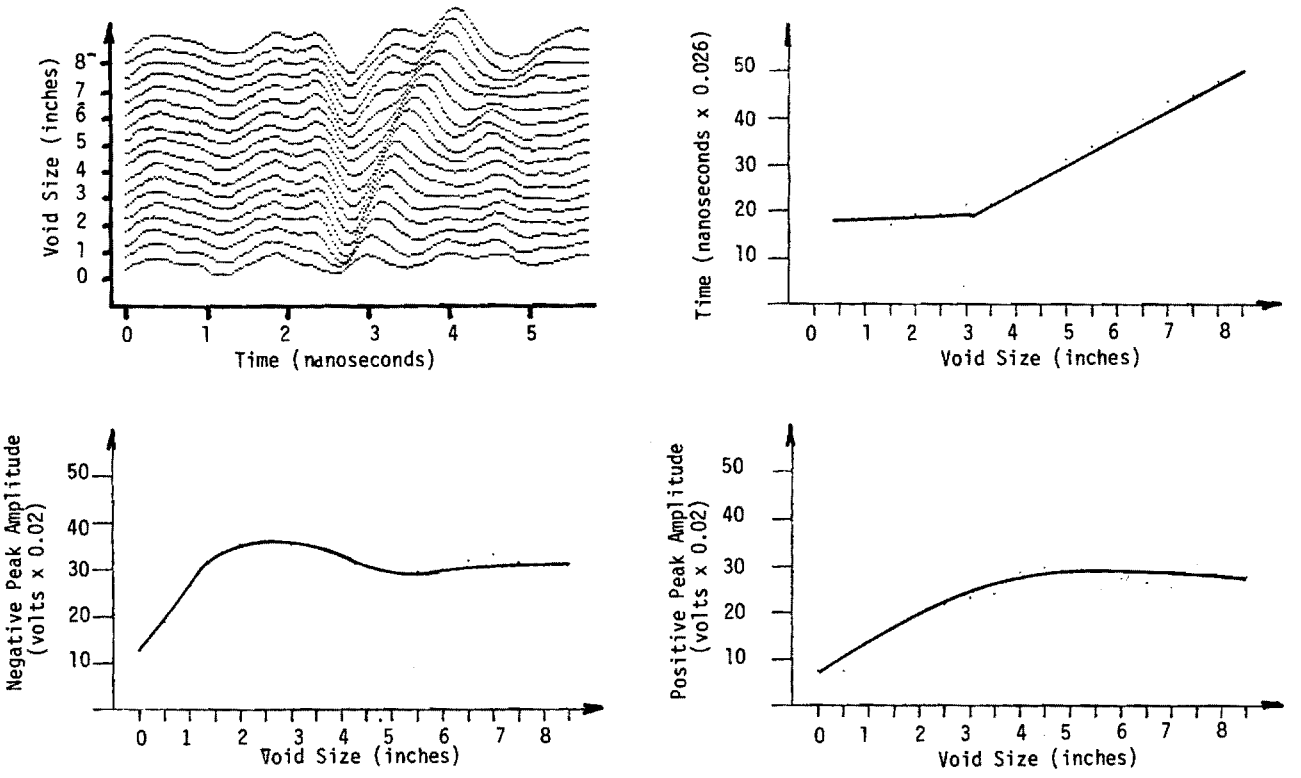

Figure D-7. Laboratory measurements, reinforced pavement, portland cement stabilized clay base.

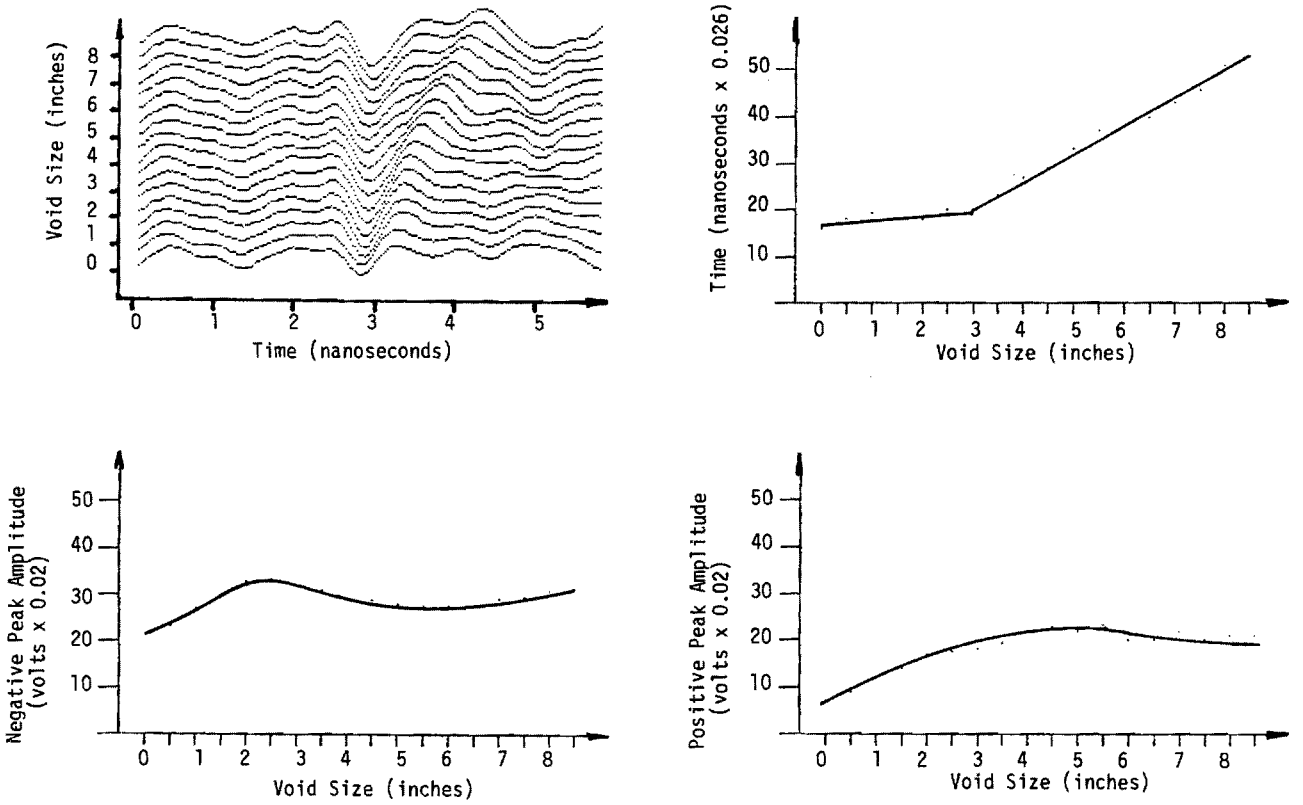

Figure D-8. Laboratory measurements, reinforced pavement, dense-graded aggregate base.

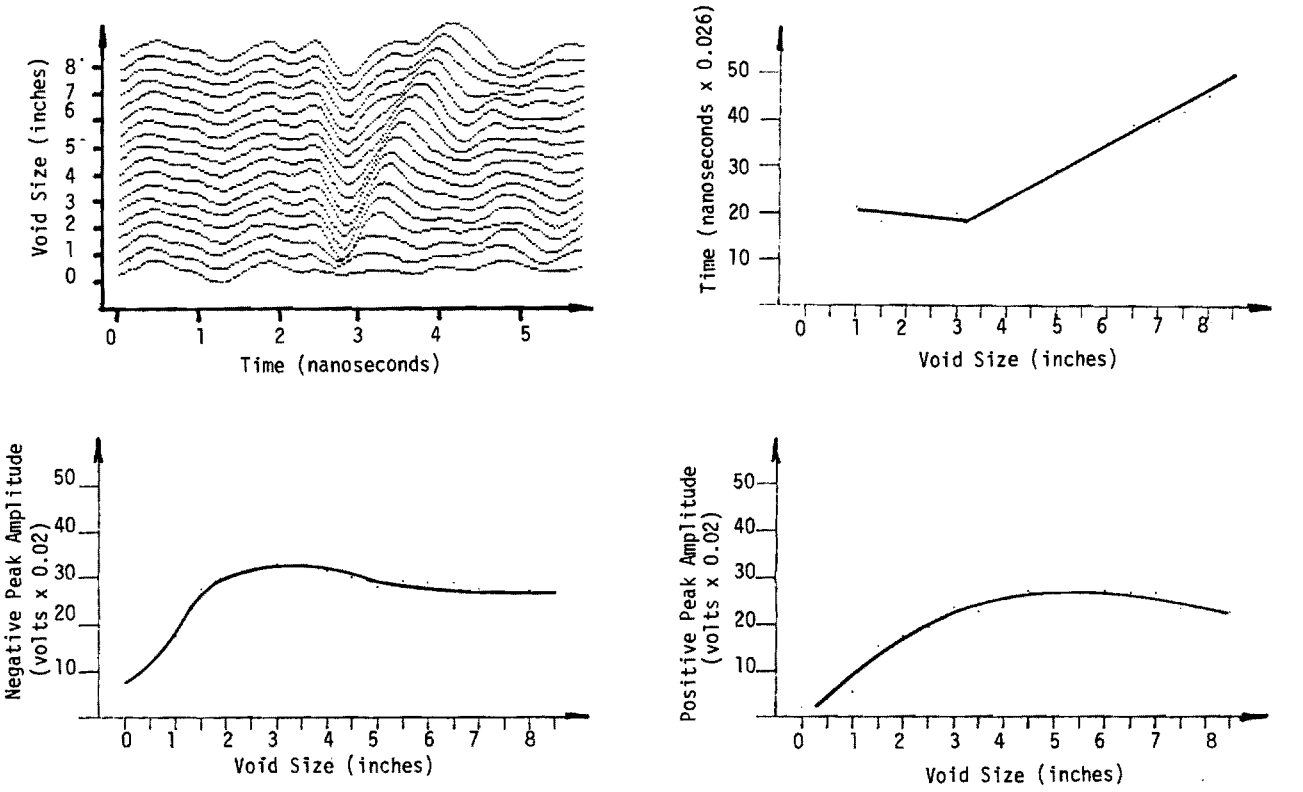

Figure D-9. Laboratory measurements, reinforced pavement, asphaltic concrete base.

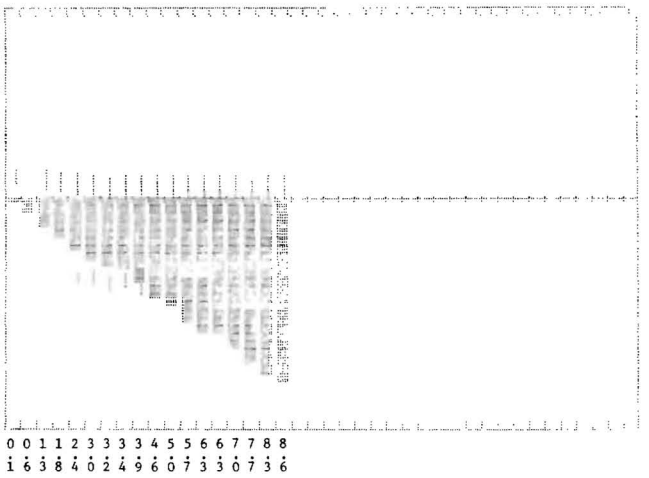

Figure D-10. Synthetic display measurements for PCC base.

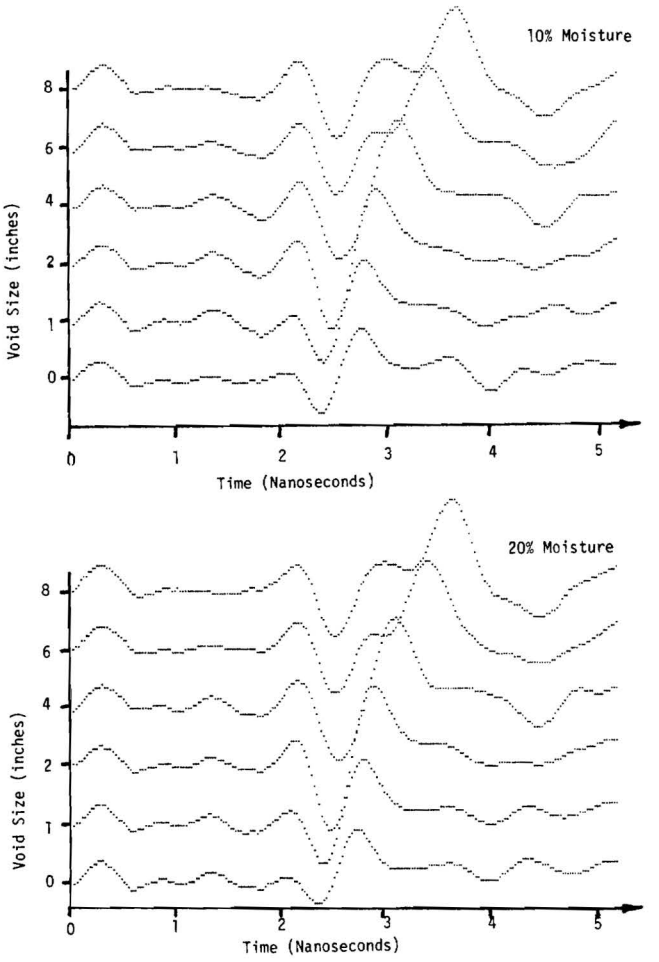

Figure D-11. Measurements with wet PCC base.

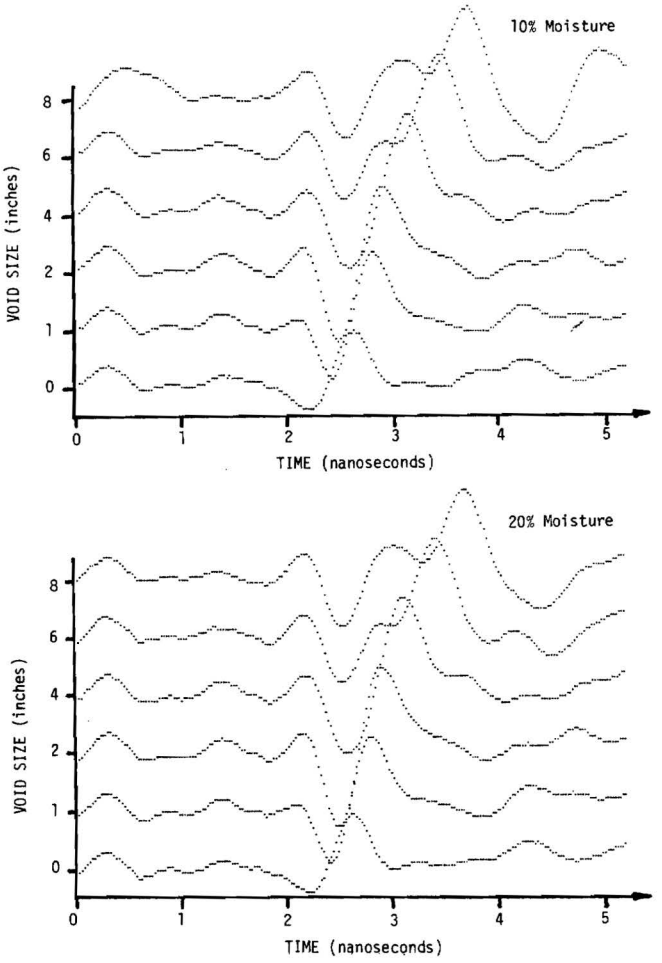

Figure D-12. Measurements with wet stabilized clay base.

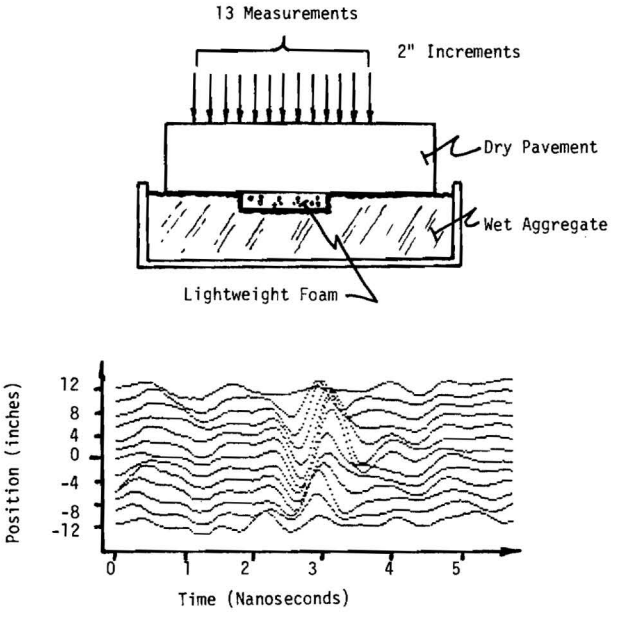

Figure D-13. Void location simulation—wet base.

Table D-1. Results summary for PCC base.

	Error: μ = 0.14", σ = 0.18"		
POSITION #	VOID SIZE	ESTIMATE	ERROR
1	0.0	0.1	+.1
2	0.5	0.6	+.1
3	1.0	1.3	+.3
4	1.5	1.8	+.3
5	2.0	2.4	+.4
6	2.5	3.0	+.5
7	3.0	3.2	+.2
8	3.5	3.4	-.1
9	4.0	3.9	-.1
10	4.5	4.6	+.1
11	5.0	5.0	+.0
12	5.5	5.7	+.2
13	6.0	6.3	+.3
14	6.5	6.3	-.2
15	7.0	7.0	+.0
16	7.5	7.7	+.2
17	8.0	8.3	+.3
18	8.5	8.6	+.1

Table D-2. Laboratory attenuation measurements (78°F).

PAVEMENT	MOISTURE	ATTENUATION	SIGNAL-TO-INTERFERENCE RATIO
Dry Non-reinforced	5%	14 dB	12 dB
Dry Reinforced	5%	15 dB	10 dB
Wet Non-reinforced	11%	20 dB	7 dB

ment with wet base conditions. The indication is that the signal returns decrease in strength at the edges of the void. At greater than 4 in. from the edge of the void, the signal no longer indicates a void.

Figure D-14 shows measurements of a selected set of void sizes with 0.5 in. of water filling the bottom of the void. The base material was clay and the pavement section did not contain reinforcing steel. The water itself has a very high reflection coefficient, thus a larger magnitude return is observed for the positive peak. Also, because more energy is reflected, less is transmitted through the water and the top of the clay base is not obviously visible. The table included in Figure D-14 lists the time and amplitude discrimination results for these measurements. As indicated by the table, the discrimination algorithm was in error by −0.5 in. for void size, exactly the depth of the water. This result is expected because the large return from the water masks the true void bottom. Only if a void is totally filled with water is it possible to obtain a return from the bottom, thus making a void size estimate possible.

All measurements inside the laboratory thus far have been with dry portland cement concrete (PCC) pavement sections. In order to obtain background data on the effects of moist pavement conditions, one of the sections was heavily soaked with water. Table D-2 summarizes the results of attenuation measurements made for both wet and dry pavement sections. The units of comparison are decibels; if a value of 10 dB attenuation is observed, only one-tenth of the signal strength is available. The wet block clearly attenuates the signal a significant amount, and in some cases will eliminate the possibility of seeing voids. Another measure of system performance is the amount of signal strength returned from a void as compared to the noise or miscellaneous signal returns. Such measurements have indicated a ratio of 20 dB or approximately 100 times greater signal than noise is possible under dry conditions. Significant attenuation will decrease this ratio, and the minimum ratio with which the microcomputer signal processing algorithms can produce reliable results is approximately 8 to 10 dB.

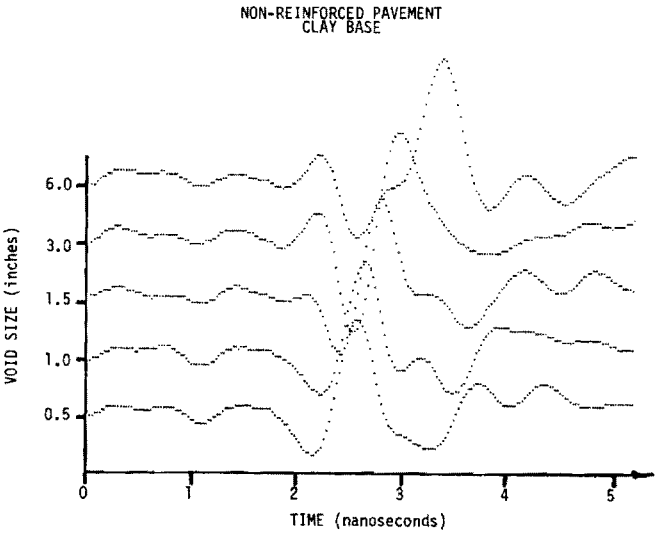

VOID FILLED WITH 0.5 INCHES WATER

ACTUAL VOID SIZE	DISCRIMINATION ALGORITHM RESULT
0.5"	0.1"
1.0"	0.55"
1.5"	1.3"
3.0"	2.6"
6.0"	5.4"

Figure D-14. Measurements —void partially filled with water.

APPENDIX E

TEST LANE MEASUREMENTS

The second phase of the experimental evaluation was conducted on a specially constructed outdoor "test lane" which is representative of a section of concrete highway. The test lane measures 72 ft long, 8 ft wide, and 9 in. thick. Georgia Department of Transportation specifications were used in its construction; portland cement concrete over dense-graded aggregate base. Surveyed in-place before concrete was poured were calibrated voids of various depths and shapes. In one-half of the test lane, reinforcing steel was used. The voids were created by shaped pieces of light weight foam, the foam itself being virtually invisible to the electromagnetic signal emitted.

Several sets of measurements were made over the test lane with the main variable being temperature. Initial measurements were made at 100F and results were very poor. Voids were visible; that is they could be located, but only by the trained operator. The magnitude of the signal return was not large enough for the microprocessor to be able to positively detect. This lack of signal strength is directly attributable to the moisture content in the concrete. The attenuation of the electromagnetic signal varies with total moisture content and temperature.

Later measurements made at temperatures from 32F to 70F produced signal levels that resulted in void location and sizing via the microprocessor algorithms. Results verify the discriminants developed.

In the following, the details of the test lane construction, which include a description of the voids and how they were created, is given. The measurements made on the test lane are illustrated and results discussed. Conclusions regarding the effects of moisture and temperature are given, and future research and measurements are suggested.

TEST LANE CONSTRUCTION

The test lane pavement is 72 ft long by 8 ft wide by 9 in. thick portland cement concrete, built in accordance with Section 430 of the State of Georgia Specification for Concrete Highways. The base material is dense-graded aggregate, 8 in. thick, again following the Georgia Specification. Reinforcing steel bars were included in one-half of the test lane pavement and small dowel bars were placed in the pavement section without reinforcing steel. Figures E-1 to E-3 are drawings of the reinforcing steel bar and dowel bar positions; the method used to support the bars and locations for all steel bars are as indicated.

To create the voids under the pavement surface, calibrated holes were dug and pieces of light weight foam were laid into the aggregate. The foam itself is invisible to the electromagnetic energy, and is used to keep the void areas intact during the pouring of the slab. The top surface of the foam was level with the top surface of the aggregate. Figure E-4 shows the results of a survey of the void layout and Table E-1 gives the details of the void sizes. Figures E-5 and E-6 are photographs taken during the construction phases of the test lane.

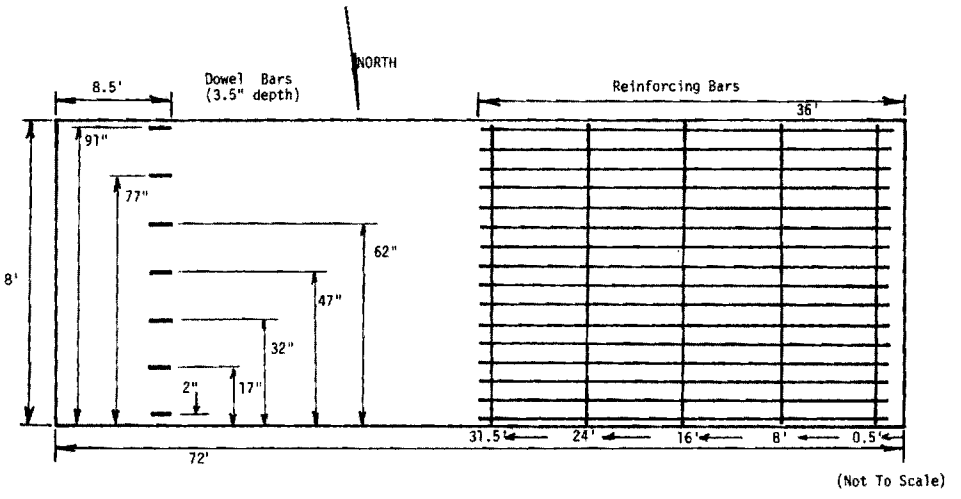

Figure E-1. Plan of reinforcing bars and dowel bars.

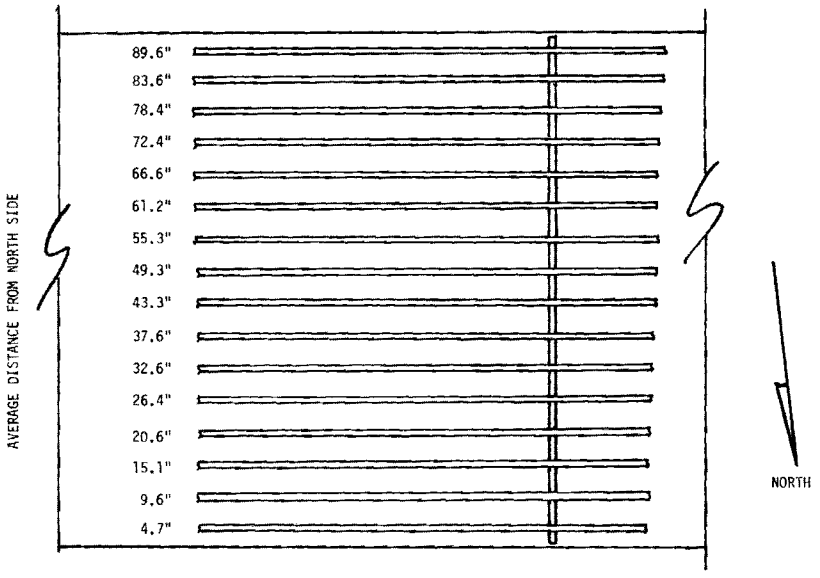

Figure E-2. Reinforcing bar layout.

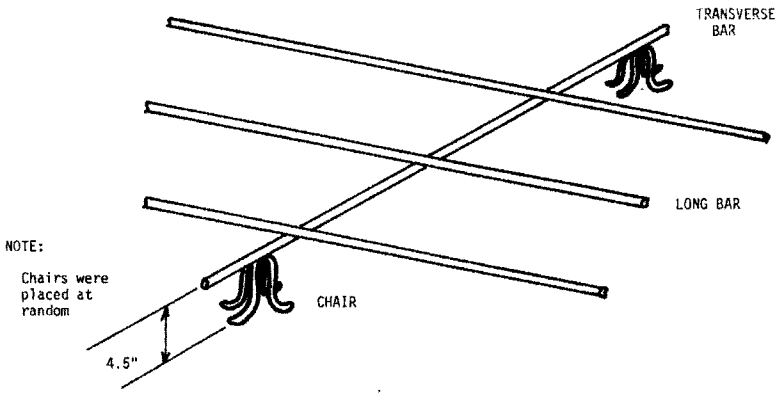

Figure E-3. Chair supports.

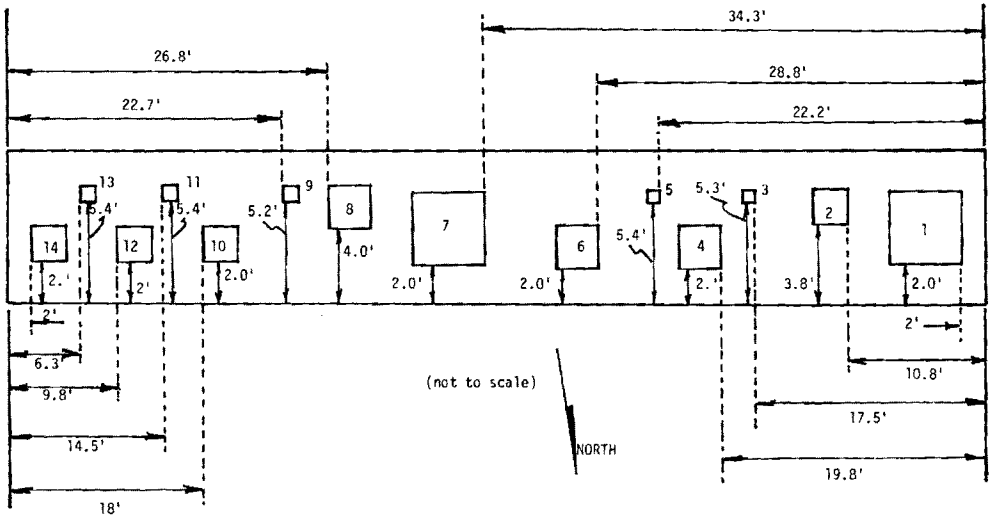

Figure E-4. Void layout.

Table E-1. Void sizes.

VOID NUMBER	LENGTH (in.)	WIDTH (in.)	VOID SIZE (in)
1	48	48	wedge, 0-6
2	24	24	6
3	6	6	6
4	24	24	2
5	6	6	2
6	36	24	1
7	48	48	wedge, 0-6
8	24	24	6
9	6	6	6
10	24	24	2
11	6	6	2
12	24	24	1
13	6	6	½
14	24	24	½

Figure E-5. Photograph of test lane layout.

Figure E-6. Photograph of test lane during concrete pouring.

TEST LANE MEASUREMENTS

Markings (small dots) were painted over the entire surface of the pavement in a 6-in. square grid to ensure the repeatability of positioning of the measurements as well as to serve as a method for cataloging measurement positions.

Figure E-7 is a schematic diagram of measurements shown in Figures E-8, E-9, and E-10. Figure E-8 is a plot of a sequential set of measurements for the position set 1 indicated on the schematic diagram. These measurements were made at a temperature of 90F. The void areas can be located by visual inspection. It is noted that the large return, approximately one-third of the distance up the plot and close to the surface point in time, is the signal return from a saw-cut/dowel bar combination in the pavement. The saw-cut over the dowel bars was made so that its effect on the signal return could be gaged. Although the void areas can be located by the trained operator, the microcomputer algorithm has difficulty recognizing the signal response. The lack of signal strength reduces the probability of detecting and correctly sizing a void. Many sets of measurements such as these were made at temperatures from 85F to 100F with the same results.

The lack of signal strength returned from the void is directly attributable to the moisture content in the concrete. But the moisture itself is not the key factor in the signal attenuation problem. More important is the temperature–moisture combination. From the information given in Appendix B with respect to attenuation, there can be a factor of 10 difference in the attenuation between temperatures of 40F and 90F.

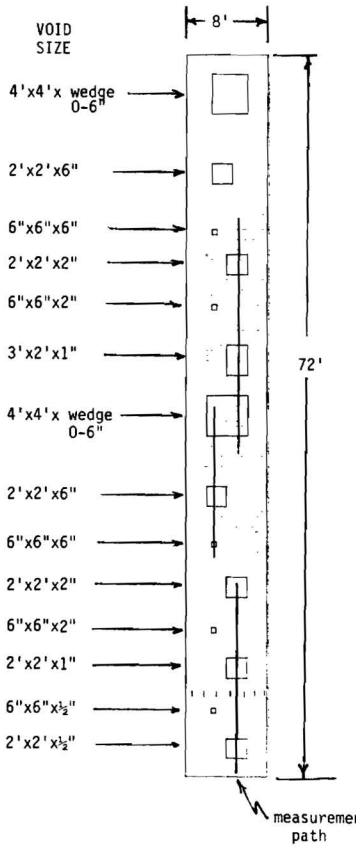

Figure E-7. Schematic diagram of measurements path.

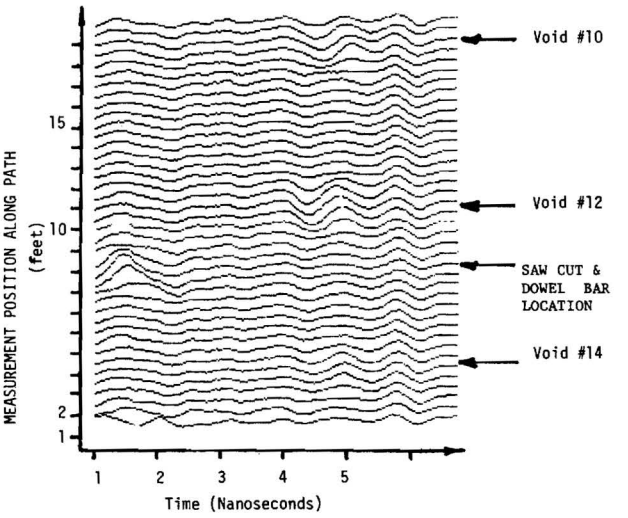

Figure E-8. Test lane measurements, set 1, 90F.

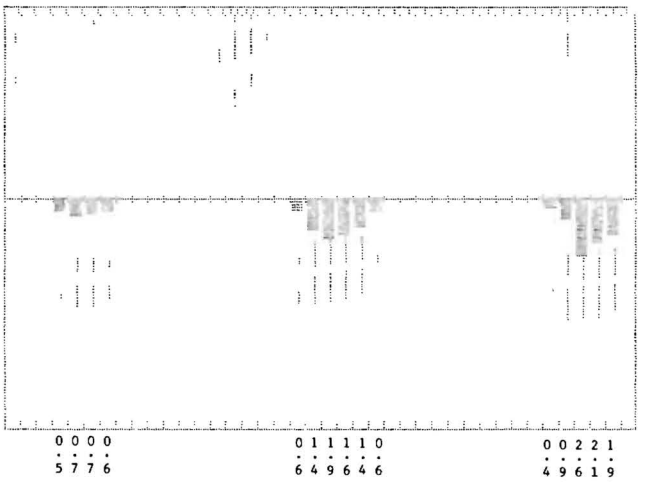

Figure E-9. Test lane measurements, set 1, 32F.

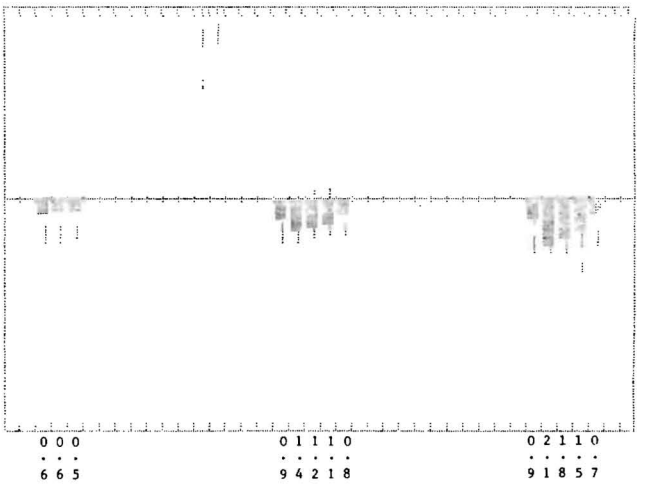

Figure E-10. Test lane measurements, set 1, 50F.

In order to verify that the problem with the test lane measurements was related to the moisture–temperature combination, specific attenuation measurements were made. Table E-2 shows the measurement configuration with the accompanying results. The return signals from a metal plate with and without a section of pavement over the metal plate were compared. The difference in signal levels relates directly to the attenuation of the pavement. Laboratory measurements were made using a dry reinforced block, a dry nonreinforced block, and a wet nonreinforced block—all at a temperature of 78F. Outdoor test lane measurements were made at a temperature of 100F. The metal plate was inserted under the edge of the test lane by first digging out the base material slightly. As indicted in the table, there is a 12 dB (factor of ~ 16) increase in attenuation for the outside test lane measurements over that of the dry nonreinforced laboratory measurements. A better comparison of the effects of temperature only is to compare the wet laboratory measurement with the outdoor test lane measurement. For this case the moisture levels in both pavement sections were very close. The resulting attenuation difference is 6 dB (factor of 4). Clearly the effects of a high temperature is a higher attenuation level and decrease in signal strength to a point where the microcomputer algorithms cannot detect and size the void.

Figures E-9 and E-10 show the results for processing measurements made at temperatures of 32F and 50F. As is clearly indicated, a much different conclusion is drawn with respect to the validity of the location and sizing algorithms. Summary statistics are given in Table E-3.

Further research is suggested into the effects of temperature on signal strength. Both laboratory and outdoor measurements should be made to more fully substantiate currently available measurements and modeling information. Actual highway measurements should be made to verify the signal processing discrimination algorithms effectiveness under typically varying road conditions.

Table E-2. Attenuation comparison.

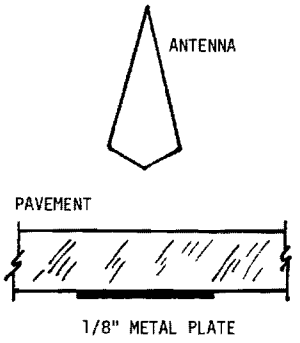

PAVEMENT	TEMPERATURE	MOISTURE	ATTENUATION*	SIR*
Dry non-reinforced	78°F	5%	14 dB	12 dB
Dry reinforced	78°F	5%	15 dB	10 dB
Wet non-reinforced	78°F	11%	20 dB	7 dB
TEST LANE	92°F	9%	26 dB	1 dB

* dB = 10 x LOG_{10}(signal ratio)

Table E-3. Results summary for test lane, 32F, 50F.

Void Size	32° Estimate	50° Estimate
0.5"	0.5	0.0
0.5"	0.7	0.6
0.5"	0.7	0.6
0.5"	0.6	0.5
0.5"	0.	0.0
0.0"	0.6	0.0
1.0	1.4	0.9
1.0	1.9	1.4
1.0	1.6	1.2
1.0	1.4	1.1
1.0	0.6	0.8
0.0	0.4	0.9
2.0	0.9	2.1
2.0	2.6	1.8
2.0	2.1	1.5
2.0	1.9	0.7

32°F, mean error = 0.2", standard deviation = 0.38"

50°F, mean error = -.1", standard deviation = 0.48"

APPENDIX F

SOFTWARE

This appendix contains a listing (Table F-1) of the software code implemented in the APPLE II PLUS microprocessor. The code is written in BASIC language for the most part, interspersed with machine language commands. It must be noted that this code is processor specific. Following the code are flow charts linking identified pieces of code (Figs. F-1 through F-4). Definitions of the variables are included in Tables F-2 and F-3.

Table F-1. Software code listing.

```
21  POKE 33,40
25  LOMEM: 102 * 256
40  PRINT  CHR$ (4);"NOMON C,I,O": TEXT : HOME
50  GOTO 2000: REM  MAIN PROGRAM
99  REM DISK I/O
100  PRINT D$;"OPEN ";FL$;DA$;SI;",D2": RETURN : REM OPEN-FILE
110  PRINT D$;"CLOSE ";FL$;DA$;SI: RETURN : REM  CLOSE-FILE
120  PRINT D$;"READ ";FL$;DA$;SI: RETURN : REM  READ-FILE
130  PRINT D$;"WRITE ";FL$;DA$;SI: RETURN : REM  WRITE-FILE
140  GOSUB 100: GOSUB 120: RETURN : REM  OPEN-READ
141  GOSUB 100: GOSUB 130: RETURN : REM  OPEN-WRITE
148  REM
149  REM TEXT/HIRES, PG 1/2 TOGGLES
150 T1 = 0:T2 = 0
152  GET A$:A =  ASC (A$)
153 A1 =  NOT (A = 88 OR A = 90 OR A = 84 OR A = 71 OR A = 49 OR A = 50)
154  IF A = 90 THEN T1 = T1 + 1
155  IF A = 88 THEN T2 = T2 + 1
156  IF A = 71 THEN T1 = 1
157  IF A = 84 THEN T1 = 0
158  IF A = 49 OR A = 50 THEN T2 = A - 49
159  IF A1 THEN T1 = 0:T2 = 0
170 T1 = (T1 / 2 -  INT (T1 / 2)) * 2
171 T2 = (T2 / 2 -  INT (T2 / 2)) * 2
175  POKE  - 16304 + (1 - T1),0
180  POKE  - 16302 + (1 - T2),0
185  POKE  - 16300 + T2,0
190  POKE  - 16298 + T1,0
195  IF  NOT A1 THEN 152
197  RETURN
198  REM
199  REM  VERTICAL #,LINES 21-24
200  IF A < 0 THEN  INVERSE
205 A =  ABS (A): POKE  - 16300,0
210  HTAB TB: VTAB 21: PRINT  INT (A / 10)
220  HTAB TB: PRINT  INT (A -  INT (A / 10) * 10)
230  HTAB TB: PRINT "."
240  HTAB TB: PRINT  INT ((A -  INT (A)) * 10);: VTAB 20: PRINT
245  NORMAL
250  RETURN
299  REM
300  REM GET A/D, AD=-1,0,1
305 MM = DT: IF AD = 0 THEN MM = BS
310  IF DS THEN  PRINT : PRINT D$;"BLOAD ";FL$;DA$;SI;",A";MM
315  IF DS THEN 330
325 I =  PEEK (49328): REM  A/D
330  POKE MEMMOV + 9,MM / 256: POKE MEMMOV + 24,MM / 256
340  CALL MEMMOV
350  POKE SUBTRCT + 4,DT / 256: POKE SUBTRCT + 7,BS / 256: POKE SUBTRCT + 12,SB /
 256
355  IF AD = 1 THEN  CALL SUBTRCT
360 MM = SB: IF AD = 0 THEN MM = BS
365  GOSUB 500: REM PLOT REF
375  IF A$ = "N" THEN 1300
385  RETURN
399  REM
400  REM  WAIT FOR KEY
```

Table F-1 Continued

```
401  POKE  - 16368,0
402  IF  PEEK ( - 16384) < 128 THEN 402
403  RETURN
498  REM
499  REM SIG-PLOT
500  HCOLOR= 3:C1 = 220 / NP:C2 = 150 / 255
505  HGR2
520  FOR I = 1 TO NP
530 PX = C1 * (I - 1)
535 PY = C2 *  PEEK (MM + I)
540  HPLOT PX,PY
550  NEXT I
560 PX = 240
565  HPLOT PX,1 TO PX,150
580 PY = 75
585  HPLOT 230,PY TO 250,PY
587  GOSUB 150
590  RETURN
598  REM
599  REM MIN/MAX VOID-DET.
600 DM =  - 1000:DN = 1000:NN = NP - 20:TH = 10
605 XF = 0:NF = 1
610  FOR I = 50 TO NN
620 DA% = 127 -  PEEK (SB + I)
630  IF DN < DA% THEN 650
640 DN = DA%:IE = I
650  NEXT I
655  IF  ABS (127 -  PEEK (SB + IE)) < TH THEN NF = 0
660  FOR I = IE TO NN
670 DA% = 127 -  PEEK (SB + I)
675  IF DM > DA% THEN 690
680 DM = DA%:IM = I:XF = 1
690  NEXT I
700  IF  ABS (127 -  PEEK (SB + IM)) < TH THEN XF = 0
710 VD = NF AND XF
713  VTAB 15: PRINT  SPC( 75)
715  VTAB 15: HTAB 1: PRINT "MIN=";DN;"MAX=";DM;"   DELTA=";IM - IE
716  HTAB 1: PRINT "AT  ";IE;"AT  ";IM
720  RETURN
799  REM
800  REM SAVE SIGNATURES
805  VTAB 1: PRINT
810  PRINT D$;"BSAVE ";FL$;DA$;SI$;",A";SB;",L";NP + 1
820  RETURN
898  REM
899  REM TIME-DIFF DET.
900 VD = 0
910  IF ((IM - IE) > 10 AND (IM - IE) < 70) THEN VD = 1
920  RETURN
999  REM
1000  REM QUERY-START
1010  TEXT : HOME
1011  PRINT "  VOID DETECTION PROGRAM"
1012  PRINT " "
1013  PRINT "  GEORGIA INSTITUTE OF TECHNOLOGY"
1014  PRINT " "
1015  PRINT "  ENGINEERING EXPERIMENT STATION"
1016  PRINT " ": PRINT " "
1020  PRINT "OLD,NEW DATA OR QUIT? (O,N,Q) ": GET A$: PRINT
1025  IF A$ = "Q" THEN  GOTO 12000
1030  IF  NOT (A$ = "O" OR A$ = "N") THEN 1010
1040 DS = 0: IF A$ = "O" THEN DS = 1
1050  PRINT "WHAT FILE NAME FOR DATA SETS?"
1051  INPUT "(UP TO 15 CHARS)-";FL$: PRINT
1052  IF FL$ = "" THEN  GOTO 1010
1060  IF DS THEN  INPUT "DATE DATA WAS SAVED? ";DA$
```

Table F-1 Continued

```
4056  VTAB 18: PRINT
4060 DC = DC - 1
4100  RETURN
6000  VTAB 1
6001  INVERSE : PRINT "CAL. DATA";
6005  NORMAL : PRINT " N = NO"
6006  PRINT "           ANY OTHER = ACCEPT": PRINT
6010  INVERSE : PRINT "VOID DATA"
6015  NORMAL : PRINT " COMANDS:"
6020  PRINT "     Q =QUIT    N =DO NOT ACCEPT"
6030  PRINT "     T =TEXT    G =GRAPHICS"
6035  PRINT "     1 =PAGE1   2 =PAGE2"
6040  PRINT "     Z =FLIP TEXT/GRAPHICS"
6050  PRINT "     X =FLIP PAGE 1/2"
6051  PRINT
6053  PRINT "     ANY OTHER KEY TO CONTINUE"
6100  RETURN
10000  REM  INITIALIZE VARIABLES
10010 D$ =  CHR$ (4):NP = 220
10020 MEMMOV = 96 * 256:SUBTRCT = 97 * 256
10030 DT = 99 * 256
10040 BS = 100 * 256
10050 SB = 98 * 256
10060 ID = 1
10999  RETURN
11000  REM
11001  REM LOAD MACH.LANG.ROUTINES
11010  PRINT D$;"BLOAD MEMMOV, A";MEMMOV;",D1"
11020  PRINT D$;"BLOAD SUBTRCT,A";SUBTRCT
11030  RETURN
12000  REM
12001  REM  END
12010  TEXT : HOME
12013  PRINT
12015  PRINT "VOID DETECTION PROGRAM
12016  PRINT " "
12017  PRINT "ENDED: ";DA$
12100  END
```

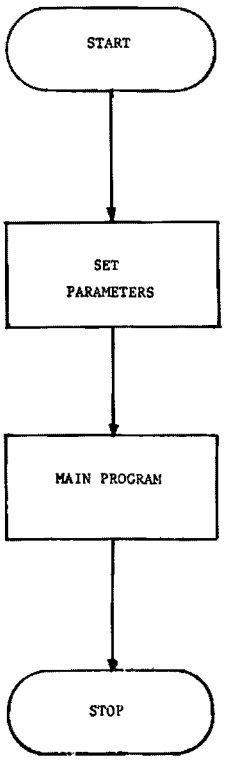

Figure F-1. Basic diagram.

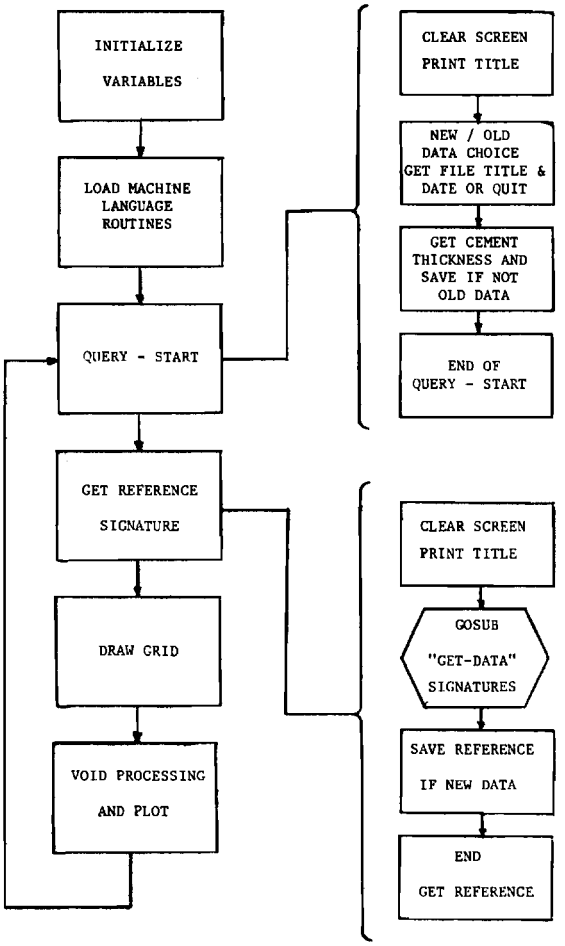

Figure F-2. Main program.

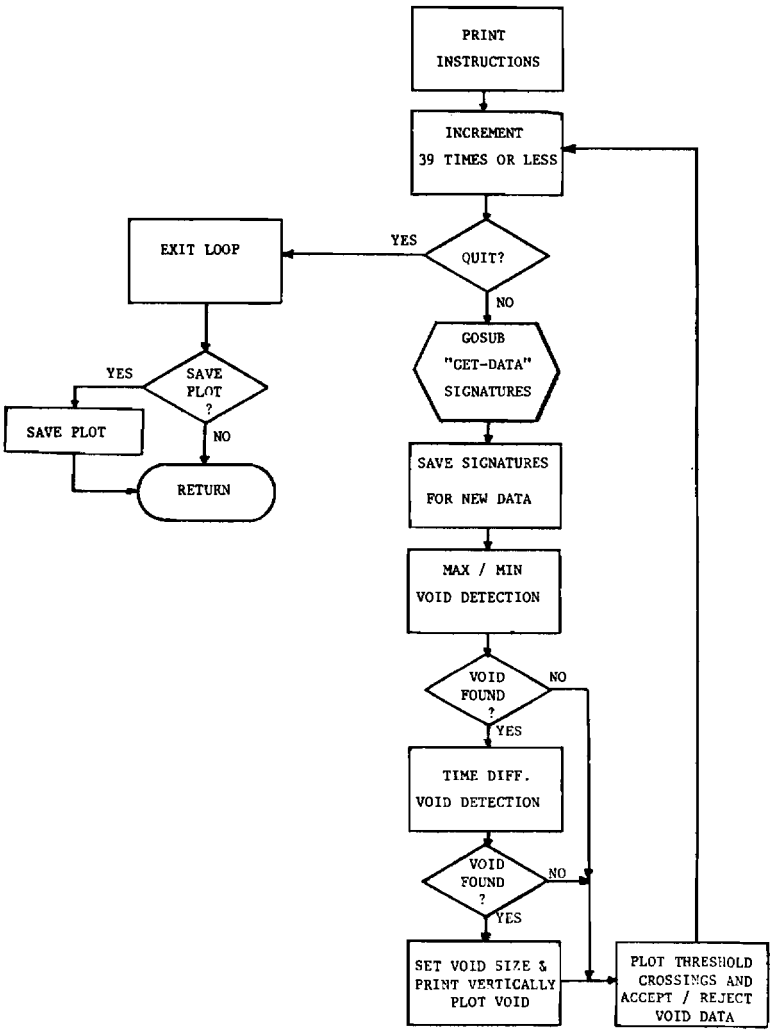

Figure F-3. Void processing and plot.

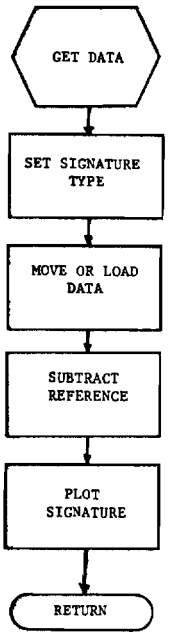

Figure F-4. Get data.